UNIVERSITÀ DEGLI STUDI DI MILANO

Corso di Dottorato in Ricerca Biomedica Integrata
XXXII Ciclo

Dipartimento di Scienze Biomediche per la Salute
Dipartimento di Bioscienze

NEURONAL NICOTINIC RECEPTORS AND EPILEPSY: A MORPHO-FUNCTIONAL STUDY ON A CONDITIONAL MURINE MODEL

Tesi di Dottorato di:
Debora MODENA
Matricola R11595

Tutor Scientifico: *Dott.ssa Alida AMADEO*

Coordinatore del Corso di Dottorato: *Prof.ssa Chiarella SFORZA*

Anno Accademico 2018-2019

TABLE OF CONTENTS

Abstract

Autosomal Dominant Nocturnal Frontal Lobe Epilepsy (ADNFLE) is a focal epilepsy characterized by hyperkinetic seizures frequently arising in the frontal lobe during sleep. The ADNFLE families often bear mutations on genes coding for subunits of the nicotinic cerebral acetylcholine receptors (nAChRs), that regulate excitability and neurotransmitter release. By regulating arousal, the cholinergic system modulates the sleep-waking cycle and is implicated in cognitive processes, besides exerting a crucial role during synaptogenesis. A widespread cerebral nAChR subtype is α4β2, and the first ADNFLE-linked mutation found on the β2 subunit was β2-V287L. In this study, we applied immunohistochemical and electrophysiological methods to a murine model of ADNFLE conditionally expressing β2-V287L, which develops spontaneous seizures during slow-wave sleep, only when the transgene is expressed during brain development (Manfredi *et al.*, 2009). First, we studied whether the expression of β2-V287L could alter the maturation of the GABAergic system, which is known to regulate synaptogenesis during early postnatal stages. We focused on the most important Cl^- cotransporter, the K^+/Cl^- cotransporter-2 (KCC2), that sets the transmembrane Cl^- gradient in the brain. The balance of abundance and activity of KCC2 is implicated in epileptogenesis as well as in the compensatory responses observed in hyperexcitable networks. Hence, we studied the postnatal distribution of this protein in wild-type (WT) and β2-V287L mice by means of immunohistochemical staining and densitometric analysis. In β2-V287L mice, the KCC2 amount in layer V of prefrontal cortex (PFC) was lower than in the control littermates at postnatal day 8 (P8). Consistently, electrophysiological recordings on pyramidal neurons showed that the GABAergic excitatory to inhibitory switch was delayed in PFC layer V of mice carrying the transgene. At later stages, however (P60), the amount of KCC2 in PFC layer V was instead higher in transgenic mice, accompanied by a decreased KCC2 expression in the reticular thalamic nucleus (RT). These data suggest that β2-V287L could produce stable alterations of the PFC synaptic network, by delaying the GABAergic switch, whereas the late reversal of KCC2 expression in β2-V287L could be a compensatory response to hyperexcitability or a direct contribution to seizure facilitation in the adult thalamocortical network (**Chapter 2**).

In PFC, layer V is the most prone to develop seizures. In normal conditions, layer V pyramidal cell activity is tightly controlled by parvalbumin-positive (PV+) fast-spiking (FS) cells and somatostatin-positive (SOM+) regular-spiking non-pyramidal (RSNP) cells, the two

most abundant GABAergic interneuron populations in this region. We thus studied the spontaneous excitatory (EPSC) and inhibitory (IPSC) postsynaptic currents by applying patch-clamp methods to pyramidal, FS and RSNP neurons in murine brain slices. In mice expressing β2-V287L, the ratio between the basal frequencies of EPSCs and IPSCs increased in pyramidal neurons, whereas an opposite effect was observed in FS (but not in RSNP) cells. This suggests that i) a higher basal excitatory input is present in mice carrying the transgene, and ii) this effect could be due to an impairment of the normal inhibitory feedback produced by FS interneurons on pyramidal cells. To better determine the cellular basis of these observations, we estimated the number of both PV+ and SOM+ neurons and of the GABAergic and glutamatergic synaptic terminals contacting these neurons. To this purpose, we used immunohistochemical staining and 3D reconstruction of neurons and terminals. We found no significant changes in the GABAergic cell populations, nor in the GABAergic terminals. However, PV+ cells displayed a significant increase of glutamatergic terminals, suggesting that the functional decrease of glutamatergic input onto FS cells was not caused by a decreased synaptic density, but by a decreased efficacy of glutamatergic transmission onto FS cells (**Chapter 3**). A parallel analysis was focused on the main cerebral cholinergic nuclei and thalamic RT showing no significant differences in mice bearing the transgene **(Chapter 4).** Our chronic model of hyperexcitability opens the way to future studies on the role of β2-V287L on synapse formation and how it can be pharmacologically modulated to attempt preventive therapeutic approaches in epilepsy.

In the secondary project of my work, we carried out a preliminary study of the protein α-synuclein in both WT and β2-V287L mice. The physiological role of α-synuclein and the reason of its accumulation in neurodegenerative pathologies, such as Parkinson's disease (PD) and dementia with Lewy bodies (DLB), is unknown. Both PD and DLB also show non-motor manifestations, such as sleep dysfunction and EEG alterations, which in DLB became frequently epileptic seizures. We thus hypothesize a functional link between α-synuclein and the cholinergic system. We quantified α-synuclein in CTRL and β2-V287L mice, using immunofluorescence methods on the *corpus striatum* (CS) and the somatosensory cortex. Moreover, a colocalization analysis was done for GABA and glutamate vesicular transporters with α-synuclein, to check if the colocalization index was altered in epileptic mice. We found a significant decrease of α-synuclein expression in the dorsolateral CS of the epileptic mice, and an increase of the colocalization ratio in GABAergic synapses of the dorsomedial CS. These preliminary results suggest the existence of a functional relationship between α-synuclein and nAChRs (**Chapter 5**).

Chapter 1

General Introduction

THE CENTRAL CHOLINERGIC SYSTEM

Acetylcholine (ACh) is a neurotransmitter widely distributed in both peripheral nervous system and central nervous system (CNS), where it mainly initiates muscle contraction and acts primarily as a neuromodulator, respectively. In the mammalian brain, ACh not only appears to play important roles in cognitive functions regulation (as learning, memory, attention and cognition) but also in the physiological sleep-wake cycle control (Abreu-Villaça *et al.*, 2011; Zaborszky *et al.*, 2012).

ACh is a small molecule, synthesized in the presynaptic terminal by the choline acetyltransferase (ChAT). ChAT is a single-strand globular protein that transfers an acetyl group from acetyl coenzyme A (AcetylCoA) to choline in the synaptic endings of cholinergic neurons. AcetylCoA is produced from glucose in the mitochondrial compartment while choline is reuptaken from the extracellular fluid by a choline trasporter (CHT) (Oda, 1999). After its synthesis, ACh is loaded into presynaptic vesicles by the vesicular acetylcholine transporter (VAChT). ACh transportation into synaptic vesicles is an active process made possible by the action of a vesicular protonic pump which transports H^+ in the internal space of vesicles from cytoplasm. This protonic gradient is exploited by VAChT which is thought to exchange one molecule of ACh with 2 H^+ (Bravo *et al.*, 2004). The increase of intracytoplasmatic Ca^{2+} concentration is the signal for vesicular fusion with the presynaptic membrane and ACh release. In the synaptic cleft, ACh can bind both to postsynaptic nicotinic (nAChRs) or muscarinic receptors (mAChRs), generally leading to an excitatory effect on postsynaptic cells. mAChRs are metabotropic receptors coupled to a G-protein that are composed of seven transmembrane domains. Five subtypes of mAChRs have been described: M2 and M4, which produce inhibition; and M1, M3 and M5, which have excitatory effects. These differential roles depend on which G-protein mediates their intracellular signalling pathways. When compared to nAChRs, much less is known about what the activation of M1-M5 receptors does in the brain (Abreu-Villaça *et al.*,

2011). Nicotinic receptors are pentameric ligand-gated cationic channels that belong to the CysLoop superfamily. They are made up of various combinations of five subunits arranged symmetrically around a central pore permeable to cations (Na^+, K^+ and, in some cases, Ca^{2+}) (Abreu-Villaça *et al.*, 2011; Ghasemi *et al.*, 2015). In the mammalian brain, nine subunits have been described: α subunits (α2-α7) and β subunits (β2-β4), each one encoded respectively by the *CHRNA2-CHRNA7* and the *CHRNB2-CHRNB4* genes. Various combinations of subunits assemble to build multiple subtypes of nAChRs, which can be classified into two groups regarding their differential subunit composition: the homopentameric and the heteropentameric receptors (Becchetti *et al.*, 2015). Nevertheless, ACh can also play an inhibitory role in a lesser extent when targeting GABAergic neurons. In the cleft, once ACh has bound to its receptors, it is hydrolysed by acetylcholinesterase (AChE) into acetate and choline (Oda, 1999). The latter is almost recovered by CHT, so continued ACh production is guaranteed (Abreu-Villaça *et al.*, 2011; Zaborszky *et al.*, 2012) (**Fig. 1**).

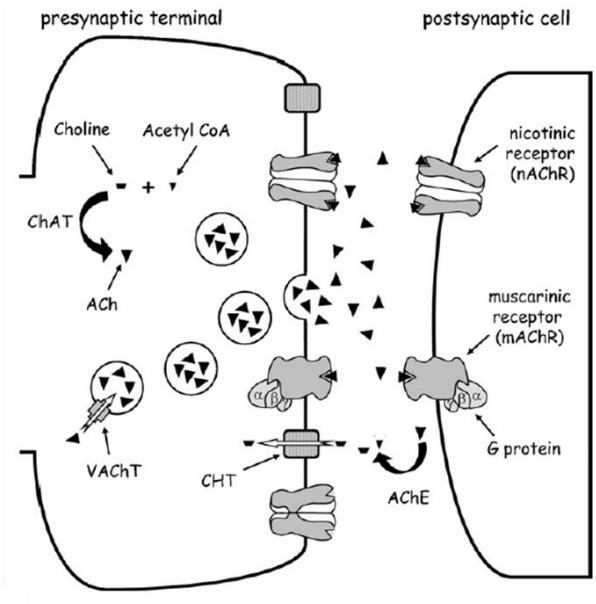

Fig. 1. The cholinergic synapse. *Schematic representation of acetylcholine biosynthesis, storage and degradation by ChAT, VAChT and AChE, respectively (Abreu-Villaça et al., 2011).*

Antibodies against VAChT are particularly useful to highlight the terminal field of cholinergic innervation (Arvidsson *et al.*, 1997), whereas antibodies against ChAT also mark cholinergic neuronal soma. Surprisingly, the gene sequences encoding for

VAChT were discovered within the first intron of ChAT gene (Oda, 1999). This organization called 'cholinergic locus' suggests a coregulation and coexpression of ChAT and VAChT proteins (Arvidsson *et al.*, 1997).

Immunocytochemical studies of cat and rodent brains have demonstrated that ChAT immunoreactive neurons are aggregated into six major groups: Ch1-Ch6 (**Table 1**). These cholinergic cell groups project to a wide range of cortical and subcortical sites (Newman *et al.*, 2012).

System	Cholinergic cell group	Containing nuclei	Target
Basal forebrain	Ch1	Medial septum (MS)	Hippocampus
Basal forebrain	Ch2	Vertical limb of the diagonal band of Broca (DBv)	Hippocampus
Basal forebrain	Ch3	Horizontal limb of the diagonal band of Broca (DBh)	Olfactory bulb
Basal forebrain	Ch4	Basal magnocellular nucleus or nucleus basalis of Meynert (nBM)	Neocortex, Basolateral amygdala
Brainstem	Ch5	Pedunculopontine tegmental nucleus (PPT)	Thalamus, Basal ganglia and Basal forebrain
Brainstem	Ch6	Laterodorsal tegmental nucleus (LDT)	Thalamus, Basal ganglia and Basal forebrain

Table 1. Location, nomenclature (Ch1-6), nuclei and connections of the main cholinergic cell groups in the Central Nervous System (CNS). *The cholinergic cell groups Ch1-4 constitute the basal forebrain cholinergic system (green) whereas cell groups Ch5-6 are part of the brainstem cholinergic system (red).*

Moreover, cholinergic neurons are distributed in the striatum, in several nuclei of encephalic nerves and in the posterior horn of the spinal cord.

Ch5 e Ch6 belong to the reticular system of the brainstem and send their prolongations to thalamus and cerebral cortex (CC) with a prevalent excitatory effect. Ch5 and Ch6 in mammals are mainly formed respectively by the pedunculopontine nucleus (PPT) and the laterodorsal tegmental nucleus (LDT). They indirectly project to CC through two ascending pathways: a dorsal one relayed by the thalamus and a ventral one which bypasses the thalamus and projects to the hypothalamus and basal

telencephalon. Some of the ventral fibers activate hypothalamic and subthalamic neurons which themselves stimulate CC. The other fibers of the ventral ascending bundle are relayed by the basal forebrain to the CC. Cholinergic fibers from PPT and LDT represent an important contingent of the ascendant pathways (Hallanger *et al.*, 1987; Jourdain *et al.*, 1989), taking part in cortical arousal, locomotion and muscle tone control (Abreu-Villaça *et al.*, 2011; Newman *et al.*, 2012).

Cholinergic neurons in basal magnocellular nucleus (Ch4) possess very long and branching dendrites in strict relationship with other prosencephalic neurons (Butcher, 1992; Woolf, 1991).

The major projection to CC originates from basal magnocellular nucleus while the other prosencephalic nuclei project to very restricted telencephalic zones (Butcher, 1992).

The CC is extensively and homogenously innervated by cholinergic fibers, in particular, somatosensory, visual, motor and prefrontal cortices present a broadly homogeneous laminar distribution of cholinergic innervation, especially in prefrontal cortex (Aracri *et al.*, 2010; Henny and Jones, 2008; Mechawar *et al.*, 2000). Many authors assume that a diffuse and non-synaptic cholinergic transmission prevails in CC (Descarries *et al.*, 1997, 2004). This observation rises from immunocytochemical experiments using antibodies against ChAT, in rats (Mechawar *et al.*, 2002; Umbriaco *et al.*, 1994), cats (De Lima and Singer, 1986), macaque (Mrzljak *et al.*, 1995) and humans (Smiley *et al.*, 1997). Cholinergic terminals appear like an intricate network of fine axons presenting numerous varicose buttons containing the neurotransmitter. ACh seems to be released by an '*en-passant*' mechanism and operates on sites distant from the releasing zone (Descarries *et al.*, 1997; 2004). '*En-passant*' release or volume transmission implies diffusion of chemical signals at relevant concentration in the extracellular fluid for distances larger than the synaptic cleft. Volume transmission is a relatively slow manner of communication if compared to fast synaptic classical transmission and may influences a large population of neurons (Steriade, 2001). ACh concentration is in fact maintained at a constant level in the extraneuronal space (Descarries *et al.*, 1995). The ultrastructural evidence of volume transmission was suggested by Umbriaco *et al.* (1994). They analyzed the parietal cortex of adult rats and found that synaptic junctions of cholinergic terminals were a minority in every layer concluding that the great majority of cholinergic terminals in the rat neocortex is endowed with varicosities. Other lines of evidence support the notion that ACh exerts

important modulatory roles through nonsynaptic transmission. The distribution of acetylcholinesterase does not fully overlap the one of nAChRs, and low tonic ACh concentrations are measured in the cerebrospinal fluid, even in the absence of cholinesterase inhibitors (Dani and Bertrand, 2007; Lendvai and Vizi, 2008; Pepeu and Giovannini, 2008).

The concept of volume cholinergic transmission is in accordance with the cholinergic regulation of cerebral cognitive function and with the hypothesis that some neurological disorders could result, directly or indirectly, from alterations in the extraneuronal level of ACh, rather than the cessation of its action at synaptic or non-synaptic sites (Descarries *et al.*, 1997).

However, there is some controversy about cholinergic transmission in CC. Rodents show a low synaptic incidence (10-15%), while the synaptic specialization increases in human (67%; Smiley *et al.*, 1997). In addition, immunohistochemistry analyses on murine cerebral cortex showed the presence of ChAT positive cells, that appeared at the end of the first postnatal week and their density dramatically increased at the beginning of the second postnatal week and remained high in adulthood (Consonni *et al.*, 2009). Therefore, alterations in cholinergic transmission may have subtle effects on the circuits of the CNS.

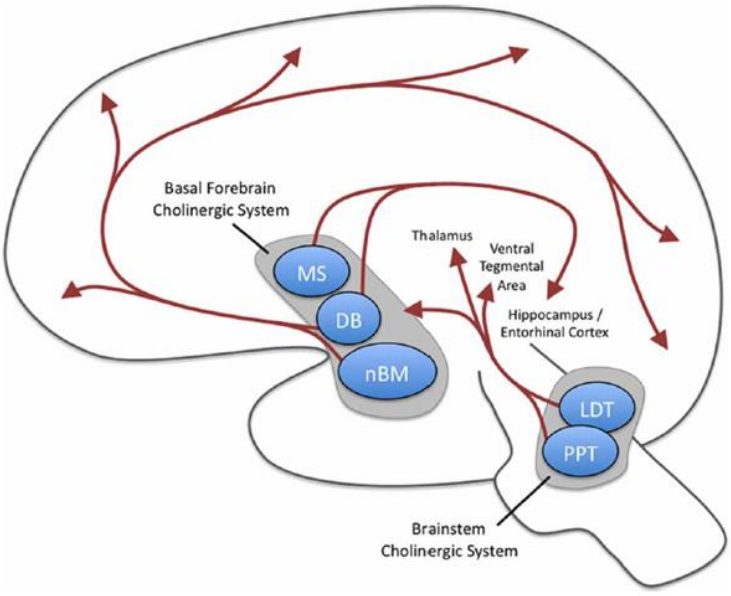

***Fig. 2. Schematic illustration of the main cholinergic projections of the CNS**. (A) Brainstem nuclei PPT and LDT project to the thalamus which is connected to the entire cortex (not shown). (B) Basal forebrain nuclei MS, DB (containing DBv and DBh) and nBM project directly to the cortex (Newman et al., 2012).*

The cholinergic system, as said before, is involved in neuropsychic functions, such as learning, memory, arousal, sleep and movement control. It appears to be the one of the regulatory systems that show more alterations in neurodegenerative disorders like Alzheimer's disease (AD), Parkinson's disease (PD), schizophrenia (SCH), depression (D), senile dementia (SD), amyotrophic lateral sclerosis (ASL), Huntington's disease (HD) and sudden infant death syndrome (SIDS; Oda, 1999). Although cholinergic neurons are only 10-15% of the total, about 50% of the degenerated cells are cholinergic (Hu et al., 2003; Wong *et al.*, 1999).

Both AD and SD are progressive neurodegenerative disorders and predominantly impair memory and cognitive functions. There is a general consensus that they are accompanied by a loss and dysfunction of the basal forebrain cholinergic neurons and decreased expression of brain nAChRs (Gotti and Clementi, 2004; Oda, 1999).

ASL selectively affects motoneurons in the brain and spinal cord and results in loss of these neurons, resulting in progressive weakness and wasting of muscles. The remaining motoneurons furthermore present a lower ChAT immunoreactivity attesting a loss of function in ASL spinal cord (Clark *et al.*, 1990).

HD is a neurodegenerative disorder characterized by choreic involuntary movements, cognitive decline and variable psychiatric symptoms. The morphological hallmark of HD is a marked symmetric atrophy of the neostriatum. Although the numbers of cholinergic neurons in this zone is preserved, ChAT activity is significantly decreased (Ferrante *et al.*, 1987).

SCH is a neuropsychiatric disorder characterized by hallucinations, emotional withdrawal and attention impairment. A prevalent hypothesis indicates that the symptoms of this disease are due to dopaminergic overactivity (Harrison, 1999). Karson *et al.* (1993) have demonstrated that the tissue concentration of ChAT is significantly lower in the mesopontine tegmentum of schizophrenic subjects.

SIDS remains unexplained, despite investigations. A decreased activity of ChAT has been demonstrated in striatum (Kalaria *et al.*, 1993) and hypothalamus (Sparks and Hunsaker, 1991); furthermore, the number of ChAT immunoreactive neurons is lower in the hypoglossal nucleus and the dorsal motor nucleus of the vagus (Mallard *et al.*, 1999).

Despite the important alterations of the cholinergic system in these diseases, it is not clear if cholinergic dysfunction is cause or effect of the mentioned pathologies. On the other hand, a strict causative role of cholinergic system impairment seems clear

for certain forms of sleep-related partial epilepsy, linked to mutations of several genes coding for subunits of the neuronal nicotinic receptors.

THE SLEEP-WAKE CYCLE

The cholinergic system is well known to regulate the transitions between the brain states with distinct level of attention. In particular, it is involved in the transition between the different sleep stages and in the shift from sleep to wakefulness (and vice versa).

Sleep is a vital biological process that can be defined as a readily reversible state of immobility, unconsciousness and reduced responsiveness and interaction with the environment (Bear *et al.*, 2007; McCarley, 2012). Its functions are still unclear, but it is known to be essential for all vertebrates as sleep deprivation leads to important impairments (Bear *et al.*, 2007).

The sleep-wake cycle is regulated by different neuronal groups, that constitute the ascending reticular activating system (ARAS). The ARAS is formed by the so-called “awake centres” that include a handful of cell groups located in the forebrain, brainstem and hypothalamus (**Fig. 3**): the noradrenergic *locus coeruleus*, the serotonergic raphe nuclei, the histaminergic tuberomammillary nucleus, the cholinergic cells from the basal forebrain (BF) and the cholinergic mesopontine tegmental nuclei (LDT and PPT). These areas are reciprocally connected and send widespread and diffuse direct projections to the cortex (or indirect through the thalamus) that promote wakefulness and alertness. Thus, sleep occurs when these centres are shut down. The responsible for switching off the *awake centres* is the ventrolateral preoptic nucleus (VLPO) in the hypothalamus. Inputs from the visual pathways when it is dark lead to the activation of the VLPO, which inhibits all the “awake centres” through the inhibitory connections between them. Moreover, this system is stabilized by the dorsomedial nucleus of the hypothalamus (DMH) avoiding a tendency to flip unpredictably between sleeping and waking (Bear *et al.*, 2007; McCarley *et al.*, 2012).

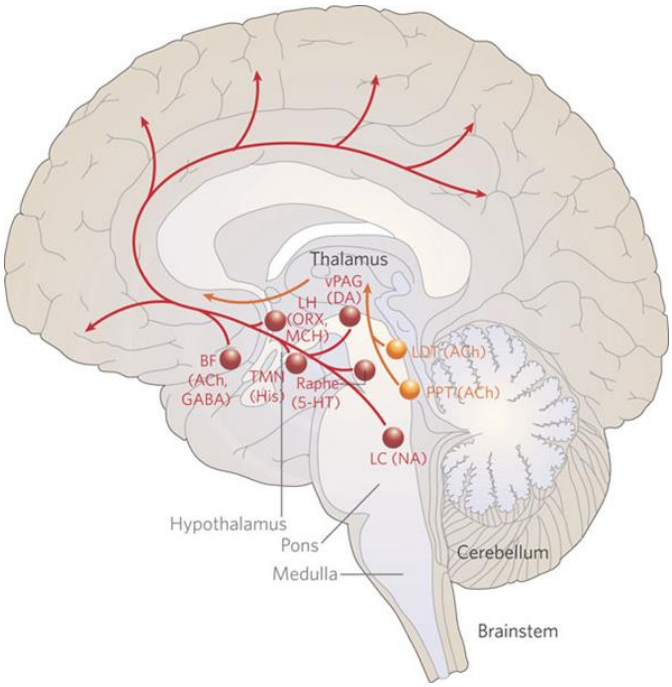

Fig. 3. Schematic representation of the main nuclei with ascending projections that constitute the Ascending Reticular Activating System (ARAS)*: the noradrenergic (NA) locus coeruleus (LC), the serotonergic (5-HT) raphe nuclei (Raphe), the histaminergic (His) tuberomammillary nucleus (TMN) and the cholinergic (ACh) pedunculopontine tegmental nucleus (PPT), laterodorsal tegmental nucleus (LDT) and basal forebrain nuclei (BF). Nuclei from the hypothalamus (LH) and tegmentum (vPAG) are also shown (Reichert et al., 2016).*

Sleep is not a uniform process, as it can be divided into two different states: the rapid eye movement sleep (REM sleep), in which rapid horizontal movements of the eyes can take place; and the non-rapid eye movement sleep (NREM sleep), where these movements are absent.

ACh release is high in wakefulness, strongly decreases during NREM sleep, and rises again in REM sleep, suggesting that in REM sleep the neocortical tone is sustained mainly by the excitatory effects of ACh (**Fig. 4**) (Becchetti *et al.*, 2015). Thus, increased activity of both brainstem and BF cholinergic systems is associated with states when cortical activation and conscious awareness occur (Becchetti and Amadeo, 2016). Furthermore, accumulating evidence reveals that nAChRs are important mediators of the arousing effects of ACh and the NREM sleep stability (Becchetti *et al.*, 2015).

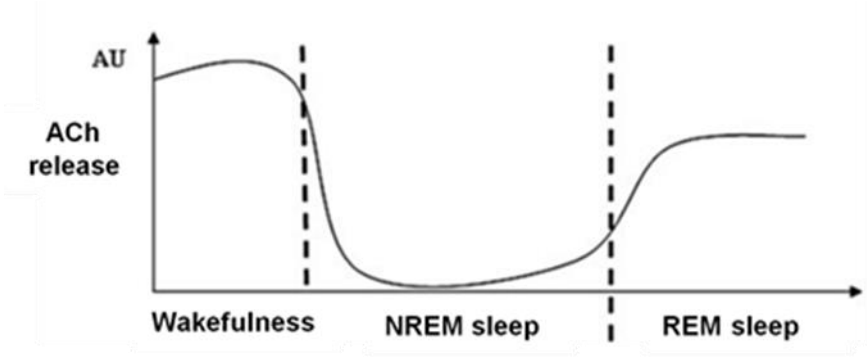

Fig. 4. Schematic graphic representation of the Ach release during the sleep-wake cycle stages. *AU: arbitrary units (Becchetti and Amadeo, 2016).*

NREM sleep is characterized by limited metabolic rate, low brain temperature and decreased sympathetic activity. On the other hand, there is an increased parasympathetic activity as evidenced by constriction of the pupils. Muscle tone and reflexes are intact. NREM sleep is divided into four characteristic stages:

- stage 1: represents the transition from wakefulness to sleep and is characterized by a slight slowing of the EEG (10-30 μV and 16-25 Hz). During this stage and throughout the NREM sleep, there is some activity of skeletal muscles, but not rapid eye movements;
- stage 2: is characterized by bursts of sinusoidal waves called 'sleep spindles' (12-14 Hz) and high biphasic waves called 'K complexes';
- stage 3: shows high amplitude, slow delta waves (0,5-2 Hz) in EEG activity;
- stage 4: is characterized by the same slow wave activity typical of stage 3 (**Fig. 5**).

On the other hand, REM sleep shows an EEG activity similar to that observed in wakefulness. REM sleep has also been called 'paradoxical sleep'. However certain neurons, located in pons, lateral geniculate nucleus and occipital cortex, fire in more intense bursts during REM sleep than during wakefulness. This activity generates high-voltage spike potentials in the EEG called 'ponto-geniculo occipital spikes' (PGO spikes). PGO spikes originate in the pontine reticular formation and propagate through the lateral geniculate nucleus to occipital cortex, they are correlated with rapid eye movements during REM sleep which is associated with dreaming. In contrast with this phenomenon almost all skeletal muscles tone is lost (atonia) during REM stage, in fact

the pons also sends signals to shut off the neurons in the spinal cord. REM sleep plays a major role in the processing of new information and the cholinergic system is active during this stage.

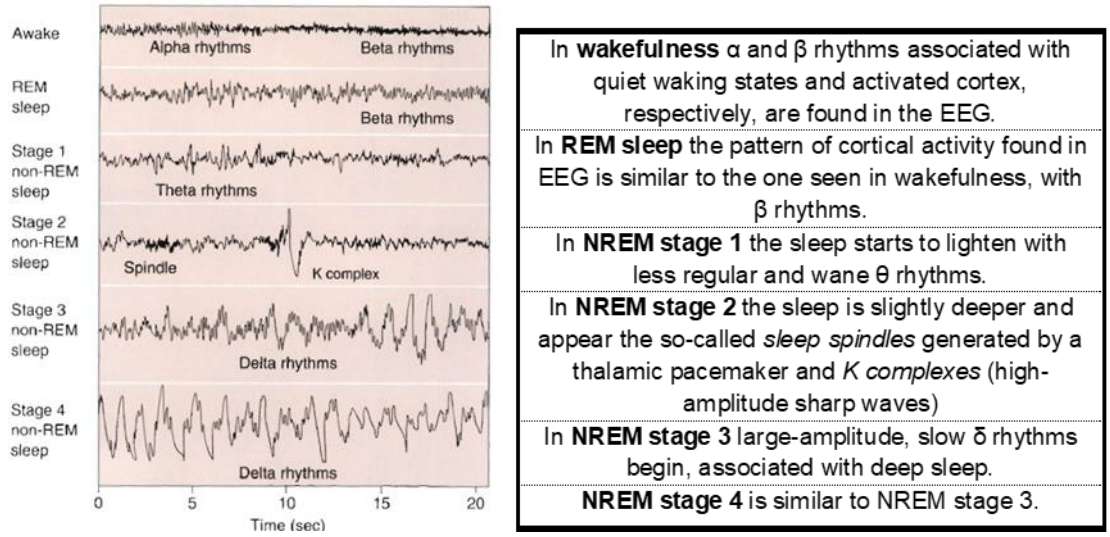

Fig. 5. Cortical excitability patterns observed in EEG during wakefulness and sleep *(Bear et al., 2007).*

The NREM and REM phases alternate cyclically during sleep. Human adults usually begin sleep by progressing from stage 1 through stage 4 of NREM sleep. After about 70-80 minutes the sleeper usually returns briefly to stage 3 or stage 2 and then enters in the first part of REM phase of the night, which lasts about 5-10 minutes. In humans the length of the cycle from the start of NREM sleep to the end of the first end phase is 90-110 minutes. This cycle of NREM and REM sleep is typically repeated four or six times a night. In successive cycle the duration of NREM phases 3 and 4 decreases while the length of the REM phases increases (**Fig. 6**) (Becchetti *et al.*, 2015).

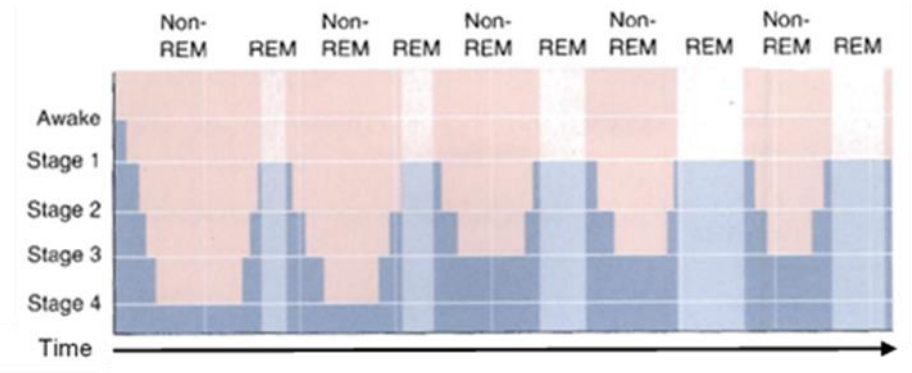

Fig. 6. Graphic representation of the sleep cycle during a normal night. *The cycle starts with NREM sleep stage 1 (a transition from wakefulness and sleep). The cycle progresses through NREM sleep stages 2, 3 and 4, reaching deep sleep. Then reverts to NREM sleep stages again until REM sleep. This sequence is repeated several times, but each cycle has shorter NREM periods and longer REM periods (Bear et al., 2007).*

The transition between REM and NREM stages is regulated by different neuronal groups. These neurons are divided into two classes: REM-off and REM-on cells, which respectively stimulate (REM-on) or inhibit (REM-off) REM activity.

NREM sleep is regulated by the activation of mainly two REM-off cell groups, from *locus coeruleus* (LC) and dorsal raphe (DR).

LC cells produce noradrenaline, while DR neurons mainly use serotonin as neurotransmitter. Their activity is high during NREM sleep and wakefulness and decreases during REM stage. Slow waves activity during NREM stage is generated through thalamocortical interaction. This pattern is caused by GABAergic reticular thalamic neurons which inhibit the thalamocortical neurons. This inhibition deactivates low thresholds Ca^{2+} currents, which produce a rebound low threshold Ca^{2+} spike burst when inhibition ceases. After the burst, membrane currents return the cell to the hyperpolarized state, restarting the process. This cycle of calcium influx followed by hyperpolarization results in rhythmic firing. Reticular thalamic neurons release GABA when they fire and thereby hyperpolarize thalamocortical neurons. This hyperpolarization results in a rebound low threshold calcium spike in these thalamocortical cells. The rhythmic firing of thalamocortical cells produces synchronized postsynaptic potentials in cortical neurons that cause the spindle waves seen in the sleep EEG. These cells generate a rhythmic discharge that blocks the transmission of sensorial information and the irregular impulse flow of information processing, thus preserving sleep (Steriade, 2003).

During REM sleep and waking, spindle waves are blocked as the cholinergic neurons of the ARAS depolarize the GABAergic cells in the reticular thalamic nucleus, thus preventing the hyperpolarization that initiates the rhythmic firing of reticular cells. In the absence of this rhythmic input, asynchronous and higher frequency background activity in thalamic cells projecting to the cortex results in the low-voltage EEG and correlated brain activation characteristic of waking and REM sleep. The REM-on cells responsible for this stage of sleep are mainly located in PPT and LDT.

Cholinergic transmission is thus fundamental not only for the transition between wakefulness and sleep, but also for the different stages of sleep, in particular during the stage 2 of NREM phase, in which, as we will see, alterations are associated with a sleep-related form of epilepsy.

AUTOSOMAL DOMINANT NOCTURNAL FRONTAL LOBE EPILEPSY (ADNFLE)

Epilepsy is a neurological disorder caused by an alteration in brain neuronal excitability. Epilepsies are usually classified on the base of aetiological criteria: primary or idiopathic epilepsies in which there are no known causes except hereditary factors; secondary or symptomatic epilepsies that are associated with brain lesions (e.g. malformation, tumour and perinatal asphyxia). Seizures can be clinically classified into two categories:

1. generalized seizures, beginning without a preceding aura and involving both brain hemispheres from the onset. They can be further divided into convulsive or non-convulsive type. The latter is the typical absence seizure found in children and consists in cessation of all motor activity, resulting in loss of consciousness. The convulsive type is the most common epileptic manifestation and consists in generalized stiffening, jerking or twitching and loss of consciousness;
2. focal or partial seizures originating in a small group of neurons. Partial seizures, whose main symptom is a localized jerking, can be either simple (without alteration of consciousness) or complex (with alteration of consciousness). A peculiar characteristic is the presence of ‘auras’ (for example anomalous feelings or sensations) preceding the onset of a seizure. Sometimes focal seizures can be secondarily generalized.

The pathogenesis of epilepsy is, in the majority of the cases, still controversial, but it is however known that epileptic seizures are induced by abnormal focal or generalized synchronized electrical discharges within the CNS. The equilibrium in communication between neurons is regulated by a network of excitatory and inhibitory circuits. Both alterations of excitatory and inhibitory mechanisms can disturb this balance, which may result in epileptic discharges. The excitability and the communication between neurons are mediated by action potential conduction and synaptic transmission. Since ion channels provide the basis for these processes, any mutation causing channel dysfunction may directly alter brain excitability and induce epileptic seizures.

Definitive proof of a causative pathological role of ion channels and, in particular, of the neuronal nAChRs has been found for Autosomal Dominant Nocturnal Frontal Lobe Epilepsy (ADNFLE), a rare idiopathic epilepsy with monogenic inheritance, the first idiopathic epilepsy for which specific mutations have been found (Steinlein *et al.*, 1995). The large majority of these mutations reside on genes coding for subunits of the neuronal nAChRs.

ADNFLE is characterized by clustered attacks of brief motor seizures originating from the frontal lobe mostly during light sleep and, especially, during stage 2 of NREM sleep (Sheffer *et al.*, 1995). The age of onset of this epilepsy is usually childhood or early adolescence (Provini *et al.*, 2000), with a penetrance in ADNFLE families of about 70-80%, but exceptions with much lower penetrance have been described (Leniger *et al.*, 2003). The mean seizure frequency in the absence of treatment is about 20 per month and decreases with age. Often an arousal event occurs before or during the early stage of the seizures. Seizures are mostly stereotyped and can consist of brief stiffening of the limbs, accompanied by gradual turning of the head and dystonic movements of arms or legs. Sleepwalking has been repeatedly reported, as well as grunting sounds, screaming and difficulty with breathing. As in many focal epilepsies, interictal electroencephalogram (EEG) tracings are normal in most patients and even in ictal EEG typical epileptic activity is rarely found. Thus, to establish diagnosis, simultaneous video and polygraphic recordings of the seizures are commonly used. Ictal EEG can show bifrontal slowing that might be more pronounced at one side. Carbamazepine can control or significantly reduce seizures in about two third of the patients. The remaining third of the cases is mostly drug resistant, but some patients might benefit from a combination of two or more antiepileptic drugs (Combi *et al.*,

2004). To date, hundreds of ADNFLE families have been identified. Nonetheless, because the genetic analysis is incomplete and because misdiagnosis is still frequent (Nobili *et al.*, 2014), the exact incidence of the disease is unknown. Ten to fifteen percent of the ADNFLE families bear mutations on genes coding for subunits of the neuronal nicotinic receptor (Ferini-Strambi *et al.*, 2012; Picard and Brodtkorb, 2008).

Eight mutations on genes coding for subunits of neuronal nAChRs have been found to be linked to ADNFLE in independent families. Four mutations have been found in exon 5 encoding for the M2 transmembrane domain of the α4 subunit (*CHRNA4* gene): a substitution of a serine with a phenylalanine in 248 position (S248F; Steinlein *et al*., 1995); a substitution of a serine with a leucine in 252 position (S252L; Hirose *et al.*, 1999); a substitution of a isoleucine with a threonine in 265 position (T265I; Leniger *et al.*, 2003); an insertion of three nucleotides in 766 position (766ins3; Steinlein *et al.*, 1997). Three mutations have been found on *CHRNB2* coding for β2: a substitution of a valine with a leucine in 287 position (V287L; De Fusco *et al.*, 2000); a substitution of a valine with a methionine in 287 position (V287M; Phillips *et al.*, 2001); a substitution of a isoleucine with a methionine in 312 position (I312M; Bertrand *et al.*, 2005). Finally, a mutation has been found on *CHRNA2* coding for α2: a substitution of an isoleucine with an asparagine in 279 position (I279N; Aridon *et al.*, 2006).

All these ADNFLE related mutations, except for β2-I312M and α2-I279N, are located within or close to the second transmembrane region (M2) of the interested nAChR subunit. The M2 region builds the wall of the ion channel, thus it seems that only mutations that have a direct effect on the ion pore could cause ADNFLE. Coexpression of the control and mutated *CHRNA4* and *CHRNB2* alleles harbouring the known ADNFLE mutations yields ACh-evoked currents of amplitude comparable to control receptors with a higher agonist sensitivity. Some mutations display alterations in the desensitization kinetics. In addition, a reduction of calcium permeability, was observed for two of the mutants (α4-S248F and α4-L776ins3). Hence, increase in ACh sensitivity is the only common characteristic so far been observed between the ADNFLE mutations in the *CHRNA4* and *CHRNB2* genes. It can be therefore concluded that a gain of function mutation could be the origin of neuronal network dysfunction that might lead to the epileptic seizures in ADNFLE patients (Dani and Bertrand, 2007; Hurst *et al.*, 2013; Indurthi *et al.*, 2019).

In agreement with the increasingly recognized importance of the cholinergic system in higher brain functions, works have shown that nAChR mutations in ADNFLE families not only cause epilepsy but can also be associated with additional neurological or psychiatric features (Cho *et al.*, 2003; Hirose *et al.*, 1999; Magnusson *et al.*, 2003).

MURINE MODELS OF ADNFLE

Since 2006, several murine models of ADNFLE have become available. Klaassen *et al.* (2006) used C57BL/6J mice to generate knock-in strains expressing either α4-S252F or α4-+L264, respectively homologous to the human α4-S248F and α4-(776ins3). Heterozygous mice present recurrent seizures accompanied by increased nicotine-dependent GABA release in layer II/III of the PFC (Klaassen *et al.*, 2006) and layer V of the motor cortex (Mann and Mody, 2008). On the other hand, in a different genetic background (CD1-129/Sv), expression of α4-S248F was found to confer a nicotine-induced dystonic arousal complex similar to the motor features of human ADNFLE, but no spontaneous seizures (Teper *et al.*, 2007).

The other mutant subunit that has been widely studied in mice is β2-V287L. A knock-in strain expressing β2-V287L in C57BL/6 background displays a disturbed sleep pattern, abnormal excitability in response to nicotine, but no overt seizure phenotype (Xu *et al.*, 2011; O'Neill *et al.*, 2013). Moreover, conditional strains were generated expressing β2-V287L in FVB background, under control of the tetracycline promoter (TET-off system; Manfredi *et al.*, 2009) (**Fig. 7**). Expression of β2-V287L does not alter the surface expression level of heteromeric nAChRs, but causes spontaneous seizures, generally during periods of increased delta wave activity. The epileptic phenotype is not reversed when β2-V287L is silenced by administering doxycycline in adult mice. Conversely, when the transgene is silenced between the embryonic day 1 and the postnatal day 15, no seizures are observed, even if the transgene is expressed at a later stage. Finally, in transgenic rats expressing α4-S284L, epileptic seizures are observed during slow-wave sleep (SWS). These are accompanied by attenuation of synaptic and extrasynaptic GABAergic transmission before the onset of the epileptic phenotype and abnormal glutamate release at the onset of seizures (Zhu *et al.*, 2008). In summary, these murine models of ADNFLE do not display gross morphological alteration in their brains, but tend to show abnormal

excitability, generally accompanied by disturbed sleep. The presence of spontaneous seizures is strain-dependent. The physiological analysis is incomplete, but points to altered GABAergic transmission in PFC. Furthermore, the only conditional model presently available suggests that critical stages of synaptic stabilization are implicated in the pathogenesis of ADNFLE (Manfredi *et al.*, 2009).

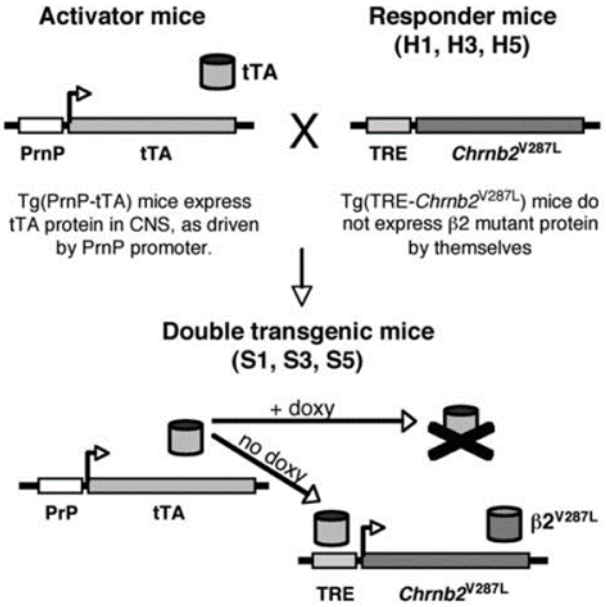

Fig. 7. Schematic representation of the TET-off conditional expression system controlling CHRNB2 mutated gene expression. *Double-transgenic mice express modified β2 subunit in CNS. The administration of doxycycline (doxy) prevents tTA binding to TRE promoter, and thus silencing the expression of β2 mutant protein (Manfredi et al., 2009).*

THE ROLE OF NICOTINIC ACETYLCHOLINE RECEPTORS IN ADNFLE

In the past few decades, a large number of studies have demonstrated that nAChRs can play an important role in the pathophysiology of a wide variety of neurological diseases, such as autism, schizophrenia, Alzheimer's disease and some epileptic disorders. In particular, nAChRs have a clear causative role in the sleep-related epilepsy ADNFLE (Becchetti *et al.*, 2015; Ghasemi *et al.*, 2015).

Nicotinic acetylcholine receptors (nAChRs) are pentameric ligand-gated cationic channels that belong to the CysLoop superfamily. They are made up of various combinations of five subunits arranged symmetrically around a central pore permeable to cations (**Fig. 8A**) (Abreu-Villaça *et al.*, 2011; Ghasemi and Hadipour-Niktarash,

2015). In the mammalian brain, nine subunits have been described: α subunits (α2-α7) and β subunits (β2-β4), each one encoded respectively by the *CHRNA2-CHRNA7* and the *CHRNB2-CHRNB4* genes. Various combinations of subunits assemble to build multiple subtypes of nAChRs. The nAChRs family has been divided into two classes:

a) Receptors binding α-bungarotoxin (αBgTx), which may be homomeric (made up of α7-α9 subunit homopentamers) or heteromeric pentamers (containing α7, α8 or α9, α10);

b) Receptors that do not bind αBgTx, which contain the α2-α6 and β2-β4 subunits, and only form heteromeric receptors that bind agonist with high affinity (Lindstrom, 2000).

The homopentamers have five ACh binding sites (one on each subunit) located at the interface between two adjacent subunits, whereas the prevalent heteropentamers probably contain two α subunits and three β subunits and therefore have two binding sites, located at the interface between the α and the β subunits. The ACh binding site has a principal and a complementary component. In heteromeric nAChRs the principal component is carried by α2-α4 or α6 subunits and the complementary component is carried by β2 or β4. In the homomeric receptors each subunit contributes to both the principal and the complementary parts of ACh binding site (Changeux and Edelstein, 1998; Corringer *et al.*, 2000). In the brain, the heteropentameric α4β2 and the homopentameric (α7)5 appear to be the most predominant subtypes (**Fig. 8B**) (Abreu-Villaça *et al.*, 2011; Becchetti *et al.*, 2015; Ghasemi and Hadipour-Niktarash 2015; Noebels *et al.*, 2012).

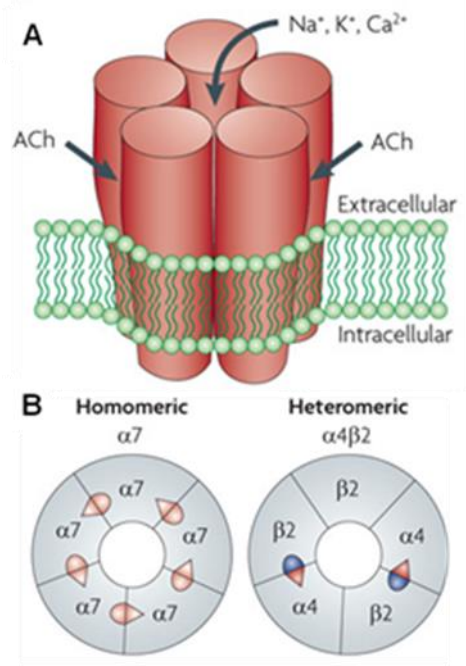

Fig. 8 (A) Pentameric structure of nAChRs. (B) Schematic representation of the two most predominant nAChRs subtypes, α7 and α4β2, respectively *(Changeux, 2010).*

Functionally, the different nAChR subtypes can exist in four distinct conformations: a resting closed conformation (no ligand), open (after ligand binding), and two 'desensitised' closed channel states: inactive (I) or desensitised (D) that are refractory to activation on a timescale of millisecond (I) or minutes (D), but have a high affinity (pM-nM) for agonist (Paterson and Nordberg, 2000; Gotti and Clementi, 2004). Ligand binding to the neurotransmitter binding site or any of the allosteric sites can modify the equilibrium between the different conformational states of the receptors. Moreover, the transition between the different receptor states can also be regulated by phosphorylation (Changeux and Edelstein, 1998).

Each nAChR subunit is made up of an extracellular N-terminal domain, three transmembrane domains (M1-M3), a large intracellular loop and a final hydrophobic transmembrane domain (M4) followed by a short extracellular C-terminal sequence (Rush *et al.*, 2000). Consensus sequences for phosphorylation sites are located on the loop between M3 and M4 (Paterson and Norberg, 2000). The pore is lined by the terminal portion of M1 domain and by M2. This region is directly involved in ion permeability and gating (opening and closing) and is also involved in channel desensitization (Hogg *et al.*, 2003). The N-terminal domain contains, near the ACh binding site, a Ca^{2+} binding domain involved in potentiation of the receptor. Ca^{2+} is

released during neurotransmitter release in the synaptic cleft. The concentration of this ion could increase from 1mM to 10 mM and this could affect ACh affinity of the receptor (Hogg *et al.*, 2003).

The distribution of the receptors could be different among species, brain regions and even cortical layers. In murine brains α7 expression prevails in the hippocampus. α2β2 and α4β2 receptors are widely distributed throughout the brain, although they are particularly abundant in the thalamus. α2β4 and α4β4 receptors are located in the inferior colliculus, interpeduncular nucleus, habenula and medulla. α3β4 nAChRs are found in the interpeduncular nucleus, habenula, fasciculus retroflexus and area postrema. In general, both in mice and rats, the most common receptor subtype in the brain is α4β2, nevertheless other subunits are significantly represented (Marubio and Changeux, 2000; Muramatsu *et al.*, 2018; Zoli *et al.*, 2018). Neuronal staining (for both pyramidal cells and interneurons) prevails in layers II/III and V. Neuropilar signal is denser in the upper layers (Aracri *et al.*, 2013; Nakayama *et al.*, 1995; Zoli *et al.*, 2018).

Receptor distribution is broadly similar among primates (Han *et al.*, 2003), although there appear to be important differences that are difficult to analyze in detail because the number of subjects is limited and the used techniques are not always comparable. Based on the results of *in situ* hybridization studies, it seems that the most important and widespread receptor subtypes in the human brain are the heteropentamer α4β2 and the homopentamer α7 (Gotti *et al.*, 2007). α4β4/β2 subtype is present in striatum, hippocampus habenula and cortex. The α6β3 subtype is expressed in the mesencephalic nuclei, particularly in the monoaminergic neurons. The α9/10 subtypes are mainly expressed in the cochlea. α2 is widely expressed in human (Aridon *et al.*, 2006). In human post-mortem brain samples there is a high α2 expression in the thalamus, widespread expression at intermediate levels in the isocortex and lower expression in hippocampus and subcortical nuclei. This pattern broadly overlaps with the one observed for α4 (which is less expressed in the thalamus). α7 receptors are present in the autonomic ganglia, hippocampus and thalamic nuclei (reticular, geniculate), cerebellum, pituitary and pineal glands, and cortex. β2 is homogeneously expressed while β4 is equally distributed in foeti and aged samples (Hellstrom-Lindahl, 1999).

nAChRs may be expressed at postsynaptic, presynaptic and nonsynaptic sites (Ghasemi *et al.*, 2015). The different location has different functional meaning:

- presynaptic nAChRs autoreceptors mediate the feedback modulation of transmitter release and represent the simplest concept of presynaptic receptor. Nicotinic autoreceptors are present both on motor nerve terminals and in the brain on cholinergic terminals in CC and hippocampus (Dani and Bertrand, 2007);
- presynaptic nicotinic heteroreceptors modulate the release of other neurotransmitters such as GABA, glutamate and serotonin (Paterson and Nordberg, 2000);
- post-synaptic receptors mediate a classical excitatory synaptic transmission. They are located on neuronal soma and dendrites (Hogg *et al.*, 2003);
- the function of nAChRs expressed in extrasynaptic sites is unclear. These receptors are probably activated by '*en-passant'* release of ACh by axonal varicosities (Hogg *et al.*, 2003).

nAChRs CONTRIBUTION TO SYNAPTOGENESIS DURING THE DEVELOPMENT

As is also indicated by conditional expression of β2-V287L (Manfredi *et al.*, 2009), the subtle prefrontal circuit alterations that cause ADNFLE seizures are likely to be produced during the developmental phases of network stabilization. In mammals, a "brain growth spurt" occurs around birth, characterized by neurite outgrowth, synaptogenesis, myelinisation and circuit pruning (Eriksson *et al.*, 2000). In rodents, this phase spans the first 2-3 postnatal weeks and is accompanied by maturation of the cholinergic system and a transient increase of nAChR subunit expression.

In rat forebrain, β2 appears in mid-gestation and peaks in the second postnatal week, along with α4 and α7 (Mansvelder and Role, 2006). A similar pattern is observed in mouse (Bailey *et al.*, 2012; Kassam *et al.*, 2008), although evidences are less extensive. At this stage, the density of extrinsic cholinergic innervation (Mechawar *et al.*, 2002) and cortical cholinergic cells (Consonni *et al.*, 2009) increases dramatically. Treatment with nicotinic ligands in the second postnatal week produces persistent behavioral and morphological alterations (Eriksson *et al.*, 2000) and mice lacking β2 show region-specific changes in cortical structure (Cordero-Erausquin *et al.*, 2000).

Nonetheless, the specific nAChR roles during neural circuit wiring are still largely unknown. The spontaneous nAChR activity was reported to regulate the developmental switch, the so-called “switch of GABA”, between the excitatory and inhibitory roles of γ-aminobutyric acid (Liu *et al.*, 2006; GABA). The latter transition depends on the progressive substitution of the transporter NKCC1, which absorbs Cl^- and is mainly expressed in early stages, with KCC2, which extrudes Cl^- and is expressed at later stages (Ben-Ari *et al.*, 2012; Rivera *et al.*, 1999). Both homo- and heteromeric nAChR activities seem to regulate the expression of these transporters (Liu *et al.*, 2006). In particular, KCC2 appears after postnatal day 3 in layer V pyramidal neurons. Its expression accompanies the formation of GABAergic synapses and KCC2 variants have been associated to epilepsy (Kaila *et al.*, 2014; Puskarjov *et al.*, 2014). Precise timing of early GABAergic excitation is important for early neuronal development and integration into circuits (Ben-Ari *et al.*, 2012; Ge *et al.*, 2006). A work in transgenic rats expressing α4-S284L (Zhu *et al.*, 2008) suggests that this mechanism may also be active at a later stage. In these rodents, the onset of the epileptic seizures (around 8 weeks after birth) is accompanied by a decrease of the expression ratio of KCC2 and NKCC1, with a consequent depolarizing shift of the $GABA_A$ reversal potential, which could explain the observed alterations in GABAergic transmission (Yamada *et al.*, 2013).

Findings suggest a possible interplay even between cholinergic and GABAergic signalling in regulating the formation and remodelling of synaptic connections (Liu *et al.*, 2006). Releasing GABA onto different neuronal population, GABAergic interneurons can regulate cells excitability giving rise to networks oscillations which are supposed to allow distinct brain states transition and high cognitive functions (Klausberger and Somogyi, 2008). The GABAergic excitatory period plays a key role in neuronal maturation and integration into circuits during embryonic development and after adult neurogenesis (Ben-Ari, 2002). Further evidences suggest that GABA-mediated membrane depolarization provides the first excitatory drive necessary for promoting neurite outgrowth and synapse formation (Cherubini and Zacchi, 2013). Therefore, the “switch of GABA” is associated with a complex timing of events that lead the formation of functional neuronal units (Ben-Ari, 2014). Pharmacological nAChRs blockade *in vivo* revealed the effects of spontaneous nicotinic cholinergic activity on GABAergic maturation: when nAChR activation is prevented by antagonist

administration, GABA administration remains excitatory. GABA application on acute dissociated chick ciliary ganglion neurons induced a depolarization even in advanced developmental stages (E14 when this kind of response is usually loss). Also α7-nAChRs knock-out prevents the “switch of GABA”. The depolarizing chloride gradient, resulting from an immature expression pattern of chloride transporters (NKCC1/KCC2) in pyramidal cells, appears to be responsible for the extended period of GABAergic excitation. Morphological analysis revealed reduced spines density and dendritic arborization in treated neurons. Also nAChRs genetic knock-out exerts a similar effect (Liu *et al.*, 2006). Cholinergic signaling was thus proposed to cooperate with GABAergic ones in regulating neurogenesis probably affecting gene expression.

In the murine cortex, the majority of nAChR subunits show a transient peak of expression at early postnatal life (P7–P14). This is associated with dendrite outgrowth and synapses formation that leads to the development of a proper neuronal network (Lin and Koleske, 2010). Shortly afterwards (P14–P21), a drop in some nAChR genes expression is observed. This temporal window is focal for the shaping of excitatory glutamatergic system by affecting dendrites and synapses maturation and pruning (Lai and Ip, 2013). These findings suggest that the down-regulation of some nAChR genes may be required for brain circuits development. As the brain matures (P21–P60), the expression of most nAChR genes is relatively low as compared to developmental stages. In the adult brain, nAChRs have been involved in the maintenance and plasticity of hippocampal and cortical excitatory systems (Poorthuis and Mansvelder, 2013; Proulx *et al.*, 2013; Yakel, 2013).

Dendritic spines provide critical postsynaptic compartments for excitatory glutamatergic transmission in the mammalian brain. Spines facilitate the transmission of the excitatory signal to the dendrites and they are focal for intracellular signalling compartmentalization. For example, they limit calcium influx to specific cellular compartments, therefore mediating synapse-specific effects (Lozada *et al.*, 2012). Heteromeric nAChRs alterations have been found to deeply affect dendritic spines formation and glutamatergic synapses localization in CNS: β2 KOs mice ($\beta2^{-/-}$) or mice pharmacologically treated in order to reduce β2 nAChRs expression (with RNA interference) do not show any reduction in glutamatergic synapses number; synapses functionality seems not to be affected (Lozada *et al.*, 2012). Adopting the same genetic and pharmacological manipulations other studies have revealed a reduction in the

number of dendritic spines. The spine loss in β2 KOs is observed in CA1 hippocampal and cortical pyramidal neurons at early postnatal stages (P4) and persists until adulthood (P40–P60). When the β2 subunit expression is silenced, glutamatergic synapses appear to shift their localization to dendritic shafts (Lozada *et al.*, 2012). Synapses localization plays an extremely important role in signal integration and transmission (Yuste and Bonhoeffer, 2001): therefore the redistribution of synapses in the absence of β2 subunit induces significant alterations on network connectivity and plasticity.

Size and complexity of the pyramidal dendritic trees appear to be reduced in the adult β2 KOs mice cortex (P60). Not all areas are equally affected, probably due to different nAChR subunit expression in different cortical areas (Ballesteros-Yanez *et al.*, 2010). β2 nAChRs may thus represent a central component that controls spine-based synapses and, subsequently, circuitry refinement.

In addition, heteromeric nAChRs can affect the glutamatergic system development by directly modulating neurotransmitter release: presynaptic nAChRs have been found to promote both glutamate and GABA release on layer V prefrontal cortex pyramidal neurons (Aracri *et al.*, 2010). Maintenance of synaptic input is critical for dendritic stabilization (Cline and Haas, 2008; Trachtenberg *et al.*, 2002). nAChRs located on presynaptic glutamatergic terminals are known to facilitate the release of glutamate that help to convert “silent” synapses to functional ones in developing hippocampal and cortical neurons (Molas and Dierssen, 2014). Conversion of silent synapses into functional ones constitutes an efficient mechanism for enhancing synaptic efficacy in the immature brain; it is commonly accepted that this conversion occurs mainly at a postsynaptic site with the insertion of new α-amino-3-hydroxy-5-methyl-4-isoxazole propionate receptors (AMPARs) on the subsynaptic membrane. Nicotine administration has been found to elicit persistent changes in synaptic efficacy in immature glutamatergic synapses. (Maggi *et al.*, 2003).

Mutation in nAChRs are therefore very likely to alter the synchronized neuronal firing which drives the formation of coherent neuronal network.

THE CHOLINERGIC SYSTEM AND ITS INTERPLAY WITH GABAERGIC AND GLUTAMATERGIC SYSTEMS

Both nicotine and endogenously released acetylcholine (ACh) increase the probability of neurotransmitter release. Several mechanisms may account for the nicotine-promoted glutamatergic synapse activation: calcium influx through nAChRs and voltage gated Ca^{2+} channels may directly promote neurotransmitter vesicular release or affect synaptic efficiency through the activation of several intracellular signalling cascade. The activity of nAChRs seems also to enhance postsynaptic responses mediated by *N*-methyl-D-aspartate receptors (NMDARs) thus participating in the induction of synaptic plasticity both in the hippocampus and cortex. A recent hypothesis is that nAChRs and NMDARs have complementary roles in synaptic plasticity: both nAChRs and NMDARs show relatively high Ca^{2+} permeability, and activation of these receptors modulates intracellular Ca^{2+} concentrations. However, nAChRs can conduct Ca^{2+} at resting membrane potentials, whereas NMDARs cannot, due to the Mg^{2+} blockade. Mansvelder and McGehee (2000) proposed that nAChRs and NMDARs can fulfill complementary excitatory system long-term enhancement (Mansvelder and McGehee,2000; Feduccia *et al.*, 2014). Evidence also suggests that nAChRs control excitatory transmission and plasticity indirectly, through GABAergic interneurons: nAChRs location on inhibitory populations provide these receptors with a broad range of possible modulation of glutamatergic system being able to inhibit or stimulate pyramidal neurons (Griguoli and Cherubini, 2012; Gu and Yakel, 2011; Poorthuis and Mansvelder, 2013). In addition, nAChRs can also modulate the excitatory system via non-neuronal cells: astrocytic nAChRs enhance synaptic plasticity in the hippocampus (Lopez-Hidalgo *et al.*, 2012) and can trigger the recruitment of AMPARs on postsynaptic sites (Wang *et al.*, 2013). nAChRs are found both presynaptically and postsynaptically at most glutamatergic synapses in cortex and hippocampus (Bertrand *et al.*, 1993; Fabian-Fine *et al.*, 2001). The activation of these receptors facilitates glutamate release and can promote long-term potentiation in a synapse-specific manner requiring coincident glutamatergic transmission at the synapse (Yakel, 2012). An elegant work from Halff and colleagues highlighted a novel mechanism by which nicotinic activity can drive synaptic potentiation independent of fast excitatory transmission. The enhancement can be induced by α7 nAChRs acting in a cell autonomous manner on the postsynaptic cell. The enhancement results from

a stabilization and accumulation of GluA1-containing AMPARs (GluA1s) at synaptic sites on dendritic spines. The nicotine-induced entrapment of GluA1s depends on intracellular free calcium, the availability of PDZ [postsynaptic density-95(PSD-95/Discs large (Dlg)/zona occludens-1 (ZO-1)]-binding scaffold proteins, and the lateral mobility of surface GluA1s (Halff *et al.*, 2014). Cell-autonomous actions have been proposed for nAChRs in regulating network integration and synapse formation of developing neurons (Campbell *et al.*, 2010; Lozada *et al.*, 2012). Both acute and chronic nicotine administration led to stabilization of GluA1s on spines (Pepeu and Giovannini, 2004; Umbriaco *et al.*, 1995). This mechanism could be relevant not only for nicotine exposure, but also for endogenous nicotinic cholinergic signalling through ACh and can therefore play a focal role in neuronal network development and stabilization.

In general, β2 nAChRs regulate glutamate release from thalamocortical fibers (Gioanni *et al.*, 1999; Lambe *et al.*, 2003). The expression and roles of nAChRs on pyramidal cell somata and terminals are more variable, depending on species, layer and cerebral region (Aracri *et al.*, 2013; Dickinson *et al.*, 2008; Marchi and Grilli, 2010; Poorthuis *et al.*, 2012). Nonetheless, the global effect of ACh release in deep layers is thought to be excitatory and dominated by β2 receptors (Poorthuis *et al.*, 2012). This is relevant in the present context, as layer V is particularly prone to develop seizures (Richardson *et al.*, 2008). During NREM sleep, the cholinergic tone is low, but hyperfunctional nAChRs could maintain abnormal glutamate release, even in the face of low ACh levels, thus increasing sleep fragmentation. In fact, the rat strain expressing α4-S284L shows higher nicotine-dependent glutamate release during slow-wave sleep (Zhu *et al.*, 2008). It seems however unlikely that hyperfunctional nAChRs can produce paroxystic hyperexcitability by a moderate stimulation of glutamate release in the neocortex. Because the pyramidal neuron activity is potently regulated by the feedback control exerted by GABAergic neurons, some degree of circuit disinhibition is generally required to lead to seizure-like activity (Richardson *et al.*, 2008). This is confirmed by theoretical modeling showing that altering the “weight” of inhibitory connections is the most effective way of modulating the excitability of recurrent networks (Murphy and Miller, 2009; Ozeki *et al.*, 2009). Therefore, to understand the nAChR-dependent hyperexcitability it is necessary to also consider the nicotinic regulation of neocortical GABAergic transmission. In fact, expression of heteromeric nAChRs on the soma of

different interneuronal populations is established in rats (Christophe *et al.*, 2002), humans (Alkondon *et al.*, 2000) and mice (Aracri *et al.*, 2010). Heteromeric nAChRs also exert presynaptic control of GABA release onto pyramidal cells (Klaassen *et al.*, 2006; Aracri *et al.*, 2010).

THE ORIGIN OF SEIZURES IN ADNFLE

In the light of the above evidences, ADNFLE seizures could be triggered by several mechanisms. (1) During slow-wave sleep (SWS), thalamocortical neurons tend to be inhibited (Steriade and McCarley, 2005). In these conditions, an upsurge of ACh in the presence of hyperfunctional nAChRs could cause excessive GABA release in the prefrontal cortex (PFC) and thus abnormal hyperpolarization of pyramidal neurons. This would deinactivate low-threshold, voltage-gated Ca^{2+} channels and activate pacemaker H-type currents, thus making pyramidal cells more sensitive to post-inhibitory rebound (Klaassen *et al.*, 2006). (2) Alternatively, nAChR activation could stimulate reciprocal inhibition between GABAergic interneurons, thus producing pyramidal cell disinhibition. This latter mechanism has been excluded in Klaassen's work (2006), but may explain Zhu's results (2008). (3) Another possible mechanism considers thalamocortical interplay. In stage 2 of NREM sleep, spindle waves are generated in the thalamus by the regulatory action of RT cells onto thalamocortical cells (Lüthi, 2014), but cortical neurons are essential in synchronizing their appearance in wide thalamocortical regions. Sleep spindles can turn into epileptiform activity and could be promoted by nAChR-dependent stimulation of glutamate release onto RT cells and the release of GABA from RT cells onto thalamocortical cells (Sutor and Zolles, 2001). A more detailed interpretation is made difficult because of the current uncertainties about the GABAergic cell populations and their physiological roles in the neocortex. The classification of GABAergic interneurons must take into account a number of factors, such as morphology, axonal and dendritic connectivity, efficacy and dynamics of input and output synapses, intrinsic electrophysiological properties, combinations of molecular markers, such as Ca^{2+}-binding proteins and neuropeptides, and developmental origin (Cauli *et al.*, 2014; DeFelipe *et al.*, 2013). The role of different GABAergic populations in the cortical microcircuit is unclear, and differences occur between layers, brain areas and species. A simplified classification, which covers more

than 85% of cortical interneurons, is based on expression of parvalbumin (PV), somatostatin (SOM) and serotonin 5-HT_3 receptor (Lee *et al.*, 2010; Tasic *et al.*, 2016; Zeisel *et al.*, 2015). The last group can be subdivided in neurons that express vasoactive intestinal peptide (VIP) or not (non-VIP) (Kepecs and Fishell, 2014; Rudy *et al.*, 2011). PV neurons are generally fast- spiking (FS) cells (Hu *et al.*, 2014), which are thought to be the main responsible of surround inhibition, particularly in layer V. Models of interactions between the GABAergic populations were proposed based on studies on hippocampus and sensory, but not associative, cortices (Pfeffer *et al.*, 2013). While PV-cells mainly inhibit the perisomatic compartments of pyramidal cells, SOM-cells form synapses onto dendrites of pyramidal neurons and inhibit PV interneurons (but not vice versa). SOM-cells would thus not only increase inhibition in the dendrites but also decrease the perisomatic inhibition mediated by PV-cells (Pfeffer *et al.*, 2013). In contrast, VIP-cells produce scarce inhibition of pyramidal cells, but seem to specifically target SOM-cells. In this way, VIP-cells may indirectly stimulate PV-cells. This simplified picture is complicated by the presence of chandelier cells, a subtype of PV-cells that mainly targets the axon hillock of pyramidal cells. Their function seems critical in PFC (Hardwick *et al.*, 2005) and shows species-specific characteristics possibly related to neurologic disorders (Woodruff and Yuste, 2008). The study of how nAChRs regulate GABAergic populations is in its infancy. Nonetheless, the non-FS cells (mainly SOM, probably) that form GABAergic synapses onto FS-PV cells (Pfeffer *et al.*, 2013) express α7, α4, and β2 nAChR subunits (Armstrong and Soltesz, 2012). Therefore, mechanism (2- “The origin of seizures in ADNFLE”) above could be facilitated in SWS, when glutamatergic transmission weakens. In these conditions, inhibition between interneurons may prevail because of nicotinic excitation of the cell bodies of the non-FS cells that innervate the FS-PV-cells. Moreover, FS-cells also present reciprocal inhibitory connections (Gibson *et al.*, 1999; Galarreta and Hestrin, 2002). Because FS-cell terminals express α4β2 nAChRs, it is possible that when the overall glutamatergic input decreases, the action of hyperfunctional nAChRs on presynaptic terminals shifts the synaptic balance toward interneuronal inhibition.

nAChRs, ADNFLE and α-SYNUCLEIN: COULD THERE BE A POSSIBLE LINK BETWEEN EPILEPSY AND PARKINSON'S DISEASE?

As stated before, the cholinergic system appears to be the one of the regulatory systems that show more alterations in neurodegenerative disorders like Alzheimer's disease (AD), Parkinson's disease (PD), amyotrophic lateral sclerosis (ASL) and Huntington's disease (HD) (Oda, 1999). Further works have also highlighted that nAChRs mutations in ADNFLE families not only cause epilepsy but can also be associated with additional neurological or psychiatric features (Cho *et al.*, 2003; Hirose *et al.*, 1999; Magnusson *et al.*, 2003). Moreover, PD and dementia with Lewy bodies (DLB) show sleep dysfunction and EEG alterations (McDowell *et al.*, 2014; Morris *et al.*, 2015), which in DLB became frequently epileptic seizures.

Parkinson's disease, in particular, is accompanied by loss of dopaminergic neurons in the nigrostriatal pathway, and nAChRs are very important in regulating dopamine release in this pathway through α6β3β2 and α4β2 nicotinic receptors (Champtiaux *et al.*, 2003; Quik and Kulak, 2002). Other neuronal systems that contribute to the proper function of the nigrostriatal pathway contain nAChRs (for example, α7 on glutamatergic nerve endings, α4β2 on cholinergic and GABAergic interneurons, α6α4β2 on GABAergic neurons of the *substantia nigra*). In rodent and monkey models of PD, there is a selective decrease in the number of α6, α4 and β2 containing receptors as detected by means of specific ligand binding or immunoprecipitation experiments (Champtiaux *et al.*, 2003, Lai *et al.*, 2004; Quik *et al.*, 2004). Moreover, a decrease in nAChRs similar to the one reported in AD has been found in the cerebral cortex of Parkinson's disease patients, which is mainly due to a decrease in α4 and α7 containing receptors (Burghaus *et al.*, 2003). These latter findings are in agreement with the impaired cognitive functions presented by some patients.

Furthermore, recent studies, focused on the neuropathological features and the proteomic profiling of epileptic tissues, unraveled the presence of lipofuscin and tau aggregates (Liu *et al.*, 2016; Sànchez *et al.*, 2018) other than the alteration of α-synuclein expression both in human and in animal model epileptic brains (Hu *et al.*, 2015; Li *et al.*, 2010; Yang *et al.*, 2006). Moreover, novel findings highlighted the interplay between α-synuclein and synaptic neuronal activity (Yamada and Iwatsubo, 2018), in particular its role in the modulation of cholinergic signaling through interaction with nAchRs (Liu *et al.*, 2013).

α-Synuclein is encoded by the *SNCA* gene and it can be divided into three different domains: the N-terminal domain, the non-amyloid- domain (NAC) and the C-terminal domain. The NAC domain is considered to be responsible of synuclein accumulation and all the identified mutations associated with synucleinopathies occur in this domain (Burré, 2015; Ueda *et al.*, 1993). In normal conditions, α-synuclein is highly soluble and has a random coil conformation *in vitro*, however, when studied in presence of lipidic membranes, lipid binding is accompanied with an increase of α-helicity, which suggests that it may be membrane associated (McLean *et al.*, 2002). Many interactions with other proteins like synapsin or SNARE proteins have been proven and the list is still increasing (Benskey *et al.*, 2016; Burré, 2015), inflecting its structure and function. Physicochemical conditions can alter its normal structure promoting its aggregation (**Fig. 9**), like temperature or pH. In some cases, the monomeric, soluble and unstructured protein takes an insoluble and very ordinated conformation with fibrillar shape, the β-sheet conformation.

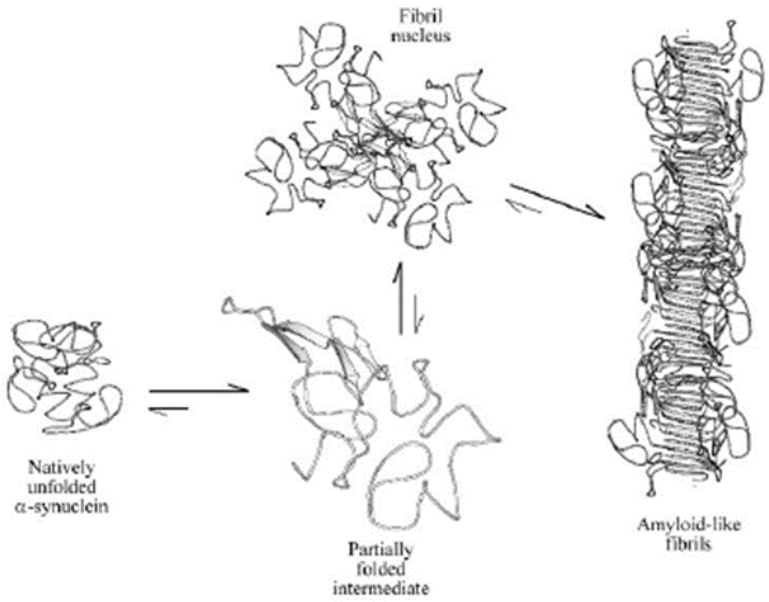

Fig. 9. Model of β-sheet aggregation for α-synuclein *(Uversky et al., 2001).*

As discussed before, α-synuclein is basically found through all the nervous system, mainly in the synapses and, in a smaller amount, in the nuclei (McLean *et al.*, 2000; Yu *et al.*, 2007). Despite decades of intensive investigation, the neuronal function still remains elusive, even if its interactions and localization suggest a regulatory synapse-

related function. α-Synuclein has been shown to induce membrane curvature and vesicle formation (Burré, 2015). In addition, its interactions to assemble the SNARE complex (Davidson *et al.*, 1998) and to organise membrane components like vesicular transporters (Guo *et al.*, 2008), suggest a crucial role in synaptic transmission. Studies regarding α-synuclein overexpression have reported a decrease in synaptic vesicle trafficking and docking, corresponding to a decrement of neurotransmitter release (Gaugler *et al.*, 2012; Lundblad *et al.*, 2012). On the other hand, a decreased expression has shown a reversal response with a decrement of vesicle endocytosis (Vargas *et al.*, 2014). Some studies have hypothesized that α-synuclein levels depend on neuronal activity, showing that the latter modulates the release of the protein from neurons (Yamada and Iwatsubo, 2018) and that synaptic dysfunction might cause α-synuclein accumulation (Nakata *et al.*, 2012). Particularly, dopaminergic neurons seem to have higher susceptibility to α-synuclein alterations. Knock-down α-synuclein mice showed increased density of VMAT2 molecules per vesicle, while an overexpression of α-synuclein brought an inhibition of VMAT2 function (Guo *et al.*, 2008). Furthermore, it seems to regulate monoamines homeostasis in synapses interacting with the serotonin transporter or dopamine transporter DAT (Butler *et al.*, 2015; Wersinger *et al.*, 2006), although its mechanism of action is still controversial. Particularly, on dopaminergic terminals, it has been reported to inhibit the expression and activity of tyrosine hydroxylase (Masliah *et al.*, 2000; Perez *et al.*, 2002; TH), a key enzyme in the dopamine synthesis pathway. It has been tested that α-synuclein is highly mobile within presynaptic terminals: it disperses from vesicles upon stimulation, while during inactivity it is present in high concentrations (Fortin *et al.*, 2010). Consequently, after the depolarization, the low α-synuclein concentration allows a quick vesicular traffic facilitating neurotransmission. This way, it also permits a higher activity of TH and amino acid decarboxylase, required for dopamine replacing in the synaptic terminal. On the other hand, the increase of α-synuclein after stimulation facilitates vesicular recycling and dopamine reuptake and packaging done by DAT and VMAT, with also an inhibition of exocytosis.

α-Synuclein started to gain interest from the scientific community in the 1997, when a mutation in the *SNCA* gene was discovered in some families with hereditary PD and when it was discovered that it is the major constituent of the histopathological lesions occurring in some specific neurodegenerative disorders (Polymeropoulos *et al.*, 1997;

Spillantini *et al.*, 1998). For this reason, these diseases were classified as synucleinopathies (PD, DLB and multiple system atrophy). Synucleinopathies are characterized by an abnormal accumulation of α-synuclein aggregates in neurons and nerve fibers. Anyway, around 10% of neurologically normal elder people above 60 years of age presents also an abnormal accumulation of the protein in the nervous system, but their levels are much lower (McCann *et al.*, 2013). All these diseases have the following shared symptoms: parkinsonism (tremor, rigidity, postural instability and bradykinesia), impaired cognition, visual hallucinations and sleep disorders. Patients who suffer from synucleinopathies often present EEG alterations and the sleep dysfunctions can precede the onset of parkinsonism by many years (McDowell *et al.*, 2014). Indeed, excessive day-time sleepiness and REM behavioural disorder (RBD) have been linked to an increased risk of developing PD (Abbott *et al.*, 2005; Arnulf *et al.*, 2002).

α-Synuclein filaments are the major ultrastructural component of pathological inclusions in synucleinopathies (Goedert, 2001; Spillantini *et al.*, 1998). The aggregation of this protein mostly occurs in the soma and neurites, and the resulting deposits are called Lewy bodies (or Lewy neurites) because they were initially identified by Heinrich Lewy in 1912. The initial sites displaying aggregation of α-Synuclein in the CNS are the olfactory bulb and the dorsal nucleus of the vagus, in the brainstem (Benskey *et al.*, 2016). Together with the synaptic dysfunction, α-synuclein aggregates have been proven to be neurotoxic. The formation of oligomers is shown to increase the permeability of synthetic lipidic vesicles (Volles *et al.*, 2001). Two mechanisms have been proposed to explain this: (1) α-synuclein oligomers may integrate into the membrane forming a channel-like structure causing an uncontrolled membrane permeability (Ding *et al.*, 2002; Kostka *et al.*, 2008); (2) oligomers enhance the ability of ions to pass through the lipidic membrane but without the formation of any pore (Kayed *et al.*, 2004). In PD, it has been found that *substantia nigra pars compacta* is one of the most affected areas of the brain. Dopamine neurons are extremely affected by synuclein aggregation, probably because it has a higher density of α-synuclein in physiological conditions (Taguchi *et al.*, 2016). In any case, not only neurons of the *substantia nigra pars compacta* are affected, but also other regions of the CNS, including the cerebral cortex (Farrell *et al.*, 2014; Fleming *et al.*, 2008).

On these bases, unraveling the involvement of α-synuclein imbalance in the pathogenesis of both neurodegenerative diseases, such as PD, and epilepsy is still a challenging matter.

AIM OF THE WORK

Despite the involvement of the cholinergic system in several neurologic disorders, ADNFLE is the only pathology for which a causative role of cholinergic transmission seems established. Several mutations in neuronal nAChRs subunits have been found to be linked to this disease and, in 2009, Manfredi and colleagues generated a β2-V287L double-transgenic mouse that recapitulates several features of the human pathology. However, the functional alterations observed in the mutant channels associated with ADNFLE are not sufficient to determine the epileptic pathogenesis. This also applies to the features of transgenic murine lines expressing such mutant subunits. We thus aimed at improving our understanding on the role of nAChRs mutations in the pathogenesis of ADNFLE.

Chapter 2 shows the effect of β2-V287L subunit on the expression of chloride cotransporters NKCC1 and KCC2 in both neocortex and thalamus at different developmental stages and on the “switch of the GABA” during the development.

Chapter 3 describes the microcircuits of the adult β2-V287L double-transgenic mouse prefrontal cortex by means of electrophysiological recordings and morphological analyses. The work is focused on the cholinergic, GABAergic and glutamatergic systems.

Chapter 4 deals with the main cerebral cholinergic nuclei and with the morphological aspects of cholinergic and GABAergic systems in the thalamus, with a main focus on the thalamic reticular nucleus.

Chapter 5 is focused on the preliminary study of α-synuclein in different brain regions of wild-type and β2-V287L double-transgenic mice, to underline the possible link between Parkinson’s disease and epilepsy.

REFERENCES

Abbott RD, Ross GW, White LR, Tanner CM, Masaki KH, Nelson JS … Petrovitch H (2005) *Excessive daytime sleepiness and subsequent development of Parkinson disease.* Neurology, 65(9), 1442-1446.

Abreu-Villaça Y, Filgueiras CC and Manhães AC (2011) *Developmental aspects of the cholinergic system.* Behavioural brain research. 221: 367-378.

Alkondon M, Pereira EF, Eisenberg HM and Albuquerque EX (2000) *Nicotinic receptor activation in human cerebral cortical interneurons: a mechanism for inhibition and disinhibition of neuronal networks.* J. Neurosci. 20, 66–75.

Aracri P, Consonni S, Morini R, Perrella M, Rodighiero S, Amadeo A and Becchetti A (2010) *Tonic modulation of GABA release by nicotinic acetylcholine receptors in layer V of the murine prefrontal cortex.* Cerebral Cortex 20: 1539-1555.

Aracri P, Amadeo A, Pasini ME, Fascio U, and Becchetti A (2013) *Regulation of glutamate release by heteromeric nicotinic receptors in layer V of the secondary motor region (Fr2) in the dorsomedial shoulder of prefrontal cortex in mouse.* Synapse 67, 338-357.

Aridon P, Marini C, Di Resta C, Brilli E, De Fusco M, Politi F, Parrini E, Manfredi I, Pisano T, Pruna D, Curia G, Cianchetti C, Pasqualetti M, Becchetti A, Guerrini R and Casari G (2006) *Increased sensitivity of the neuronal nicotinic receptor alpha2 subunit causes familial epilespy with nocturnal wandering and ictal fear.* Am. J. Hum. Genet. 79: 342-350.

Armstrong C and Soltesz I (2012) *Basket cell dichotomy in microcircuit function*. J. Physiol. (Lond.) 590, 683-694.

Arnulf I, Konofal E, Merino-Andreu M, Houeto JL, Mesnage V, Welter ML … Agid Y (2002) *Parkinson's disease and sleepiness: an integral part of PD.* Neurology, 58(7), 1019-1024.

Arvidsson U, Riedl M, Elde R and Meister B (1997) *Vescicular acetylcholine transporter (VAChT) protein: a novel and unique marker for cholinergic neurons in the central and peripheral nervous systems.* J. Comp. Neurol. 378: 454-467.

Bailey CD, Alves NC, Nashmi R, De Biasi M and Lambe EK (2012). *Nicotinic α5 subunits drive developmental changes in the activation and morphology of prefrontal cortex layer VI neurons.* Biol. Psychiatry 71, 120-128.

Ballesteros-Yáñez I, Benavides-Piccione R, Bourgeois JP, Changeux JP and De Felipe J (2010) *Alterations of cortical pyramidal neurons in mice lacking high-affinity nicotinic receptors*. Proceedings of the National Academy of Sciences 107: 11567-11572.

Bear MF (2007) *Neuroscience: Exploring the Brain.* 3rd edition. USA: Lippincott Williams & Wilkins. ISBN: 9780781760034.

Becchetti A, Aracri P, Meneghini S, Brusco S and Amadeo A (2015) *The role of nicotinic acetylcholine receptors in autosomal dominant nocturnal frontal lobe epilepsy.* Frontiers in Physiology. 6(22):1-12.

Becchetti A and Amadeo A (2016) *Why we forget our dreams: acetylcholine and norepinephrine in wakefulness and REM sleep.* Behavioral and brain sciences. (39):20-21.

Ben-Ari Y (2002) *Excitatory actions of GABA during development: the nature of the nurture.* Nat Rev Neurosci. 3(9):728-39.

Ben-Ari Y, Woodin MA, Sernagor E, Cancedda L, Vinay L, Rivera C *et al.* (2012) *Refuting the challenges of the developmental shift of polarity of GABA actions: GABA more exciting than ever!* Front. Cell. Neurosci. 6:35.

Ben-Ari Y (2014) *The GABA excitatory/inhibitory developmental sequence: a personal journey. Neuroscience.* 279:187-219.

Benskey MJ, Perez RG and Manfredsson FP (2016) *The contribution of alpha synuclein to neuronal survival and function - Implications for Parkinson's disease.* Journal of Neurochemistry, 137(3), 331-359.

Bertrand D, Galzi JL, Devillers-Thiery A, Bertrand S and Changeux JP (1993) *Mutations at two distinct sites within the channel domain M2 alter calcium permeability of neuronal alpha 7 nicotinic receptor.* Proceedings of the National Academy of Sciences 90: 6971-6975.

Bertrand D, Picard F, Le Hellard S, Weiland S, Favre I, Phillips H, Bertrand S, Berkovic SF, Malafosse A and Mulley J (2002) *How mutations in the nAChRs can cause epilepsy.* Epilepsia 43 (Suppl 5): 112-122.

Bertrand D, Elmslie F, Hughes E, Trounce J, Sander T, Bertrand S and Steinlein OK (2005) *The CHRNB2 mutation I312M is associated with epilepsy and distinct memory deficits.* Neurobiol. Dis. 20 (3): 799-804.

Bravo DT, Kolmakova NG and Parsone SM (2004) *Transmembrane Reorientation of the Substrate-Binding Site in Vescicular Acetylcoline Transporter.* Biochemistry 43: 8787-8793.

Burghaus L, Schutz U, Krempel U, Lindstrom J, Schroder H (2003) *Loss of nicotinic acetylcholine receptor subunits alpha4 and alpha7 in the cerebral cortex of Parkinson patients*. Parkinsonism. Relat. Disord. 9: 243-246.

Burré J (2015). *The synaptic function of α-synuclein.* Journal of Parkinson's Disease, 5(4), 699-713.

Butcher L (1992) *The cholinergic basal forebrain and its telencephalic targets: interrelations and implication for cognitive function.* Neurotransmitter Interactions and Cognitive Function: 15-26.

Butler B, Saha K, Rana T, Becker JP, Sambo D, Davari P … Khoshbouei H (2015) *Dopamine transporter activity is modulated by -synuclein. Journal* of Biological Chemistry, 290(49), 29542-29554.

Campbell NR, Fernandes CC, Halff AW and Berg DK (2010) *Endogenous signaling through α7-containing nicotinic receptors promotes maturation and integration of adult-born neurons in the hippocampus.* The Journal of Neuroscience 30: 8734-8744.

Cauli B, Zhou X, Tricoire L, Toussay X and Staiger JF (2014) *Revisiting enigmatic cortical calretinin-expressing interneurons.* Front. Neuroanat. 8:52.

Champtiaux N, Gotti C, Cordero-ErausquinM, David DJ, Przybylski C, Lena C, Clementi F, Moretti M, Rossi FM, Le Novere N, McIntosh JM, Gardier AM and Changeux JP (2003) *Subunit composition of functional nicotinic receptors in dopaminergic neurons investigated with knock-out mice*. J. Neurosci. 23: 7820-7829.

Changeux JP and Eldestein SJ (1998) *Allosteric receptors after 30 years.* Neuron. 21: 959-980.

Cherubini E and Zacchi P (2013) *Building up the inhibitory synapse.* Front Cell Neurosci. 6:62.

Cho YW, Motamedi GK, Laufenberg I, Sohn SI, Lim JG, Lee H, Yi SD, Lee JH, Kim DK, Reba R, Gaillard WD, Theodore WH, Lesser RP and Steinlein OK (2003) *Korean kindred with autosomal dominant nocturnal frontal lobe epilepsy and mental retardation.* Archives of Neurology 60 (11): 1625-1632.

Christophe E, Roebuck A, Staiger JF, Lavery DJ, Charpak S and Audinat E (2002) *Two types of nicotinic receptors mediate an excitation of neocortical layer I interneurons.* J. Neurophysiol. 88, 1318–1327.

Clark AW, Tran PM, Parhad IM, Krekoski CA and Julien JP (1990) *Neuronal gene expression in amyotrophic lateral sclerosis.* Mol. Brain Res. 7: 75-83.

Cline H and Haas K (2008) *The regulation of dendritic arbor development and plasticity by glutamatergic synaptic input: a review of the synaptotrophic hypothesis.* The Journal of physiology 586: 1509-1517.

Combi R, Dalpra L, Tenchini ML and Ferrini-Strambi L (2004) *Autosomal dominant noctunal frontal lobe epilepsy- A critical overview.* Journal of Neurology 251 (8): 923-934.

Consonni S, Leone S, Becchetti A and Amadeo A (2009). *Developmental and neurochemical features of cholinergic neurons in the murine cerebral cortex*. BMC Neurosci. 10:18.

Cordero-Erausquin M, Marubio LM, Klink R and Changeux JP (2000) *Nicotinic receptor function: new perspectives from knockout mice.* Trends Pharmacol. Sci. 21, 211-217.

Corringer PJ, Le Novere N and Changeux JP (2000) *Nicotinic receptors at the amino acid levels.* Annu. Rev. Pharmacol. Toxicol: 40: 431-458.

Dani JA and Bertrand D (2007) *Nicotinic acetylcholine receptors and nicotinic cholinergic mechanisms of the central nervous system.* Annu Rev Pharmacol Toxicol. 47:699--729.

Davidson WS, Jonas A, Clayton DF and George JM (1998) *Stabilization of Synuclein secondary structure upon binding to synthetic membranes.* Journal of Biological Chemistry, 273(16), 9443-9449.

DeFelipe J, López-Cruz PL, Benavides-Piccione R, Bielza C, Larrañaga, P, Anderson S *et al.* (2013) *New insights into the classification and nomenclature of cortical GABAergic interneurons.* Nat. Rev. Neurosci. 14, 202-216.

De Fusco M, Becchetti A, Patrignani A, Annesi G, Gambardella A, Quattrone A, Ballabio A, Wanke E and Casari G (2000) *The nicotinic receptor beta2 subunit is mutant in nocturnal frontal lobe epilepsy.* Nature Genetics 26 (3), 275-276.

De Lima AD and Singer W (1986) *Cholinergic innervation of the cat striate cortex: a choline acetyltransferase immunocytochemical analysis.* The Journal of Comparative Neurology 250: 324-338.

Descarries L, Umbriaco D, Contant C and Watkins KC (1995) *Nonjunctional relationships of monoamine axon terminals in the cerebral cortex of adult rat.* In: Volume Transmission in The Brain: Novel Mechanism for Neuronal Transmission: 53-62. Eds Fuxe K and Agnati LF. Raven Press, New York.

Descarries L, Gisiger V and Steriade M (1997) *Diffuse transmission by acetylcholine in the Central Nervous System.* Progr. Neurobiol. 53: 603-625.

Descarries L, Mechawar N, Aznavour N and Watkins KC (2004) *Structural determinants of the roles of acetylcholine in cerebral cortex.* Progress in Brain Research 145 (2): 45-58.

Dickinson JA, Kew JN and Wonnacott S (2008). *Presynaptic α7- and β2- containing nicotinic acetylcholine receptors modulate excitatory amino acid release from rat prefrontal cortex nerve terminals via distinct cellular mechanisms.* Mol. Pharmacol. 74, 348-359.

Ding TT, Lee SJ, Rochet JC and Lansbury PT (2002) *Annular α-synuclein protofibrils are produced when spherical protofibrils are incubated in solution or bound to brain-derived membranes.* Biochemistry, 41(32), 10209-10217.

Eriksson P, Ankarberg E and Fredriksson A (2000) *Exposure to nicotine during a defined period in neonatal life induces permanent changes in brain nicotinic receptors and in behaviour of adult mice.* Brain research 853: 41-48.

Fabian-Fine R, Skehel P, Errington ML, Davies HA, Sher E, Stewart MG and Fine A (2001) *Ultrastructural distribution of the α7 nicotinic acetylcholine receptor subunit in rat hippocampus.* The Journal of Neuroscience 21: 7993-8003.

Farrell KF, Krishnamachari S, Villanueva E, Lou H, Alerte TNM, Peet E … Perez RG (2014) *Non-motor parkinsonian pathology in aging A53T α-Synuclein mice is associated with progressive synucleinopathy and altered enzymatic function.* Journal of Neurochemistry, 128(4), 536-546.

Feduccia AA, Chatterjee S and Bartlett SE (2014) *Neuronal nicotinic acetylcholine receptors: neuroplastic changes underlying alcohol and nicotine addictions.* Frontiers in Molecular Neuroscience 3: 6521-6527.

Ferini-Strambi L, Sansoni V and Combi R (2012) *Nocturnal frontal lobe epilepsy and the acetylcholine receptor.* Neurologist 18, 343–349.

Ferrante RJ, Beal MF, Kowall NW, Richardson EP Jr, Martin JB (1987) *Sparing of acetylcholinesterase-containing striatal neurons in Huntington's disease.* Brain Res. 411: 162-167.

Fleming SM, Tetreault NA, Mulligan CK, Hutson CB, Masliah E and Chesselet MF (2008) *Olfactory deficits in mice overexpressing human wildtype α-synuclein.* 28(2), 247-256.

Fortin DL, Nemani VM, Nakamura K and Edwards RH (2010) *The behavior of α-synuclein in neurons.* Movement Disorders, 25(SUPPL. 1).

Galarreta M and Hestrin S (2002) *Electrical and chemical synapses among parvalbumin fast-spiking GABAergic interneurons in adult mouse neocortex.* Proc. Natl. Acad. Sci. U.S.A. 99, 12438-12443.

Gaugler MN, Genc O, Bobela W, Mohanna S, Ardah MT, El-Agnaf OM … Schneider BL (2012) *Nigrostriatal overabundance of α-synuclein leads to decreased vesicle density and deficits in dopamine release that correlate with reduced motor activity.* Acta Neuropathologica, 123(5), 653-669.

Ge S, Goh ELK, Sailor KA, Kitabatake Y, Ming G and Song H (2006) *GABA regulates synaptic integration of newly generated neurons in the adult brain.* Nature 439, 589-593.

Ghasemi M and Hadipour-Niktarash A (2015) *Pathologic role of neuronal nicotinic acetylcholine receptors in epileptic disorders: implication for pharmacological interventions.* Reviews in the Neurosciences. 26(2), 199-223.

Gibson JR, Beierlein M and Connors BW (1999) *Two networks of electrically coupled inhibitory neurons in neocortex.* Nature 402, 75-79.

Gioanni Y, Rougeot C, Clarke PB, Lepousé C, Thierry AM, Vidal C (1999) *Nicotinic receptors in the rat prefrontal cortex: increase in glutamate release and facilitation of mediodorsal thalamo-cortical transmission.* Eur J Neurosci. 11(1):18-30.

Goedert M (2001) Alpha-Synuclein And Neurodegenerative Diseases. 2(July), 492-501.

Gotti C and Clementi F (2004) *Neuronal nicotinic receptors: from structure to pathology.* Progress in Neurobiology 74: 363-396.

Gotti C, Moretti M, Gaimarri A, Zanardi A, Clementi F and Zoli M (2007) *Heterogeneity and complexity of native brain nicotinic receptors.* Bioche. Pharmacol. 74: 1102-1111.

Griguoli M and Cherubini E (2012) *Regulation of hippocampal inhibitory circuits by nicotinic acetylcholine receptors.* The Journal of physiology 590: 655-666.

Gu Z and Yakel LJ (2011) *Timing-dependent septal cholinergic induction of dynamic hippocampal synaptic plasticity.* Neuron 71: 155-165.

Guo JT, Chen AQ, Kong Q, Zhu H, Ma CM and Qin C (2008) *Inhibition of vesicular monoamine transporter-2 activity in -synuclein stably transfected SHSY5Y cells.* Cellular and Molecular Neurobiology, 28(1), 35-47

Halff AW, Gómez-Varela D, John D and Berg DK (2014) *A novel mechanism for nicotinic potentiation of glutamatergic synapses.* The Journal of Neuroscience 34: 2051-2064.

Hallanger AE, Levey AI, Lee HJ, Rye DB and Wainer BH (1987) *The origins of cholinergic and other subcortical afferents to the thalamus in the rat.* J. Comp. Neurol. 262: 105-124.

Han ZY, Zoli M, Cardona A, Bourgeois JP, Changeux JP, Le Novere N (2003) *Localization of [3 H]nicotine, [3 H]cytisine, [3 H]epibatidine, and [125 I]alpha-Bungarotoxin binding sites in the brain of Macaca mulatta.* Journal of Comparative. Neurology 461: 49-60.

Hardwick C, French SJ, Southam E and Totterdell S (2005) *A comparison of possible markers for chandelier cartridges in rat medial prefrontal cortex and hippocampus.* Brain Res. 1031, 238-244.

Harrison PJ (1999) *The neuropathology of schizophrenia: A critical review of the data and their interpretation.* Brain 150: 454-459.

Hellstrom-Lindahl E, Gorbounova O, Seiger A, Mousavi M and Nordberg A (1998) *Regional distribution of nicotinic receptors during prenatal development of human brain and spinal cord.* Brain Res. Dev. Brain Res. 108: 147-160.

Henny P and Jones BE (2008) *Projections from basal forebrain to prefrontal cortex comprise cholinergic, GABAergic and glutamatergic inputs to pyramidal cells or interneurons.* Eur. J. Neurosci. 27, 654–670.

Hirose S, Iwata H, Akiyoshi H, Kobayashi K, Ito M, Wada K, Kaneko S and Mitsudome A (1999) *A novel mutation of CHRNA4 responsible for autosomal dominant nocturnal frontal lobe epilepsy.* Neurology 53 (8): 1749-1753.

Hogg RC, Raggenbass M and Bertrand D (2003) *Nicotinic acetylcholine receptors: from structure to brain function.* Reviews of Physiology, Biochemistry and Pharmacology 147: 1-46.

Hu C, Wong TP, Cotè SL, Bell KFS and Cuello AC (2003) *The impact of Aβ-plaques on cortical cholinergic and non-cholinergic presynaptic boutons in Alzheimer's disease-like transgenic mice.* Neuroscience 12: 421-432.

Hu H, Gan J and Jonas P (2014) *Interneurons. Fast-spiking, parvalbumin+ GABAergic interneurons: from cellular design to microcircuit function.* Science 345:1255263.

Hu R, Luo J, Wang W, Wang X, Xi Z (2015) *Alpha-Synuclein Is A Potential Biomarker In The Serum And Csf Of Patients With Intractable Epilepsy.* Seizure, 27:6-9.

Hurst R, Rollema H and Bertrand D (2013) *Nicotinic acetylcholine receptors: from basic science to therapeutics.* Pharmacol Ther. 137(1):22-54.

Indurthi DC, Qudah T, Liao VW, Ahring PK, Lewis TM, Balle T, Chebib M and Absalom NL (2019) *Revisiting autosomal dominant nocturnal frontal lobe epilepsy (ADNFLE) mutations in the nicotinic acetylcholine receptor reveal an increase in efficacy regardless of stochiometry.* Pharmacol Res. 139:215-227.

Jourdain A, Semba K and Fibiger HC (1989) *Basal forebrain and mesopontine tegmental projections to the reticular thalamic nucleus: an axonal collateralization and immunohistochemical study in the rat.* Brain Research 505: 55-65.

Kaila K, Price TJ, Payne JA, Puskarjov M and Voipio J (2014) *Cationchloride cotransporters in neuronal development, plasticity and disease.* Nat. Rev. Neurosci. 15, 637-654.

Kalaria RN, Fiedler C, Hunsaker III JC and Sparks DL (1993) *Synaptic neurochemistry of human striatum during development: Changes in sudden death infant syndrome.* J. Neurochem. 60: 2098-2105.

Karson CN, Casanova MF, Kleinman JE and Griffin WST (1993) *Choline acetyltransferase in schizophrenia.* Am. J. Psychiatry 150: 454-459.

Kassam SM, Herman PM, Goodfellow NM, Alves NC and Lambe EK (2008) *Developmental excitation of corticothalamic neurons by nicotinic acetylcholine receptors.* J. Neurosci. 28, 8756-8764.

Kayed R, Sokolov Y, Edmonds B, McIntire TM, Milton SC, Hall JE and Glabe CG (2004) *Permeabilization of lipid bilayers is a common conformation-dependent activity of soluble amyloid oligomers in protein misfolding diseases.* Journal of Biological Chemistry, 279(45), 46363-46366.

Kepecs A and Fishell G (2014) *Interneurons cell types are fit to function.* Nature 505, 318-326.

Klaassen A, Glykys J, Maguire J, Labarca C, Mody I and Boulter J (2006) *Seizures and enhanced cortical GABAergic inhibition in two mouse models of human autosomal dominant nocturnal frontal lobe epilepsy.* Proc. Natl. Acad. Sci. U.S.A. 103, 19152-19157.

Klausberger T and Somogyi P (2008*) Neuronal diversity and temporal dynamics: the unity of hippocampal circuit operations.* Science 321: 53-57.

Kostka M, Högen T, Danzer KM, Levin J, Habeck M, Wirth A … Giese A (2008) *Single particle characterization of iron-induced pore-forming α-synuclein oligomers.* Journal of Biological Chemistry, 283(16), 10992-11003.

Lai A, Sum J, Fan H, McIntosh JM, Quik M (2004) *Selective recovery of striatal 125I-alpha-conotoxinmii nicotinic receptors after nigrostriatal damage in monkeys.* Neuroscience 127:399-408.

Lai KO and Ip NY (2013) *Structural plasticity of dendritic spines: the underlying mechanisms and its dysregulation in brain disorders.* Biochimica et Biophysica Acta (BBA)-Molecular Basis of Disease 1832: 2257-2263.

Lambe EK, Picciotto MR, Aghajanian GK (2003) *Nicotine induces glutamate release from thalamocortical terminals in prefrontal cortex.* Neuropsychopharmacology. 28(2):216-25.

Lee S, Hjerling-Leffler J, Zagha E, Fishell G and Rudy B (2010) *The largest group of superficial neocortical GABAergic interneurons expresses ionotropic serotonin receptors.* J. Neurosci. 30, 16796–16808.

Lendvai B and Vizi ES (2008) *Nonsynaptic chemical transmission through nicotinic acetylcholine receptors.* Physiol Rev. 88:333--340.

Leniger T, Kananura C, Hufnagel A, Bertrand S, Bertrand D and Steinlein OK (2003) *A new Chrna4 mutation with low penetrance in nocturnal frontal lobe epilepsy.* Epilepsia 44 (7): 981-985.

Li A, Choi YS, Dziema H, Cao R, Cho HY, Jung YJ, Obrietan K (2010) *Proteomic Profiling Of The Epileptic Dentate Gyrus.* Brain Pathol. 20(6):1077-89.

Lin YC and Koleske AJ (2010) *Mechanisms of synapse and dendrite maintenance and their disruption in psychiatric and neurodegenerative disorders.* Annual review of neuroscience 33: 349-353.

Lindstrom J (2000) *The structures of neuronal nicotinic receptors.* In: Clementi F, Fornasari D, Gotti C (Eds) Handbook of Experimental Pharmacology Vol. Neuronal Nicotinic Receptors. Springer, Berlin: 101-162.

Liu Z, Neff RA and Berg DK (2006) *Sequential interplay of nicotinic and GABAergic signaling guides neuronal development.* Science 314, 1610-1613.

Liu Q, Emadi S, Shen JX, Sierks MR, Wu J (2013) *Human α4β2 Nicotinic Acetylcholine Receptor As A Novel Target Of Oligomeric α-Synuclein.* Plos One. 8(2):E55886.

Liu JY, Reeves C, Diehl B, Coppola A, Al-Hajri A, Hoskote C, Mughairy SA,Tachrount M, Groves M, Michalak Z, Mills K, Mcevoy AW, Miserocchi A, Sisodiya SM, Thom M (2016) *Early Lipofuscin Accumulation In Frontal Lobe Epilepsy.* Ann Neurol. 80(6):882-895.

López-Hidalgo M, Salgado-Puga K, Alvarado-Martínez R, Medina AC, Prado-Alcalá RA and García-Colunga J (2012) *Nicotine uses neuron-glia communication to enhance hippocampal synaptic transmission and long-term memory*. PloS one 7 (2012): e49998.

Lozada AF, Wang X, Gounko NV, Massey KA, Duan J, Liu Z and Berg DK (2012) *Induction of dendritic spines by β2-containing nicotinic receptors.* The Journal of Neuroscience 32: 8391-8400.

Lundblad M, Decressac M, Mattsson B and Bjorklund A (2012) *Impaired neurotransmission caused by overexpression of α-synuclein in nigral dopamine neurons.* Proceedings of the National Academy of Sciences, 109(9), 3213-3219.

Lüthi A (2014) *Sleep spindles: where they come from, what they do.* Neuroscientist 20, 243-256.

Maggi L, Le Magueresse C, Changeux JP and Cherubini E (2003) *Nicotine activates immature "silent" connections in the developing hippocampus.* Proceedings of the National Academy of Sciences 100: 2059-2064.

Magnusson A, Stordal E, Brodtkorb E and Steinlein O (2003) *Schizophrenia, psychotic illness and other psychiatric symptoms in families with autosomal dominant nocturnal frontal lobe epilepsy caused by different mutations.* Psychiatric Genetics 13 (2): 91-95.

Mallard C, Tolcos M, Leditschke J, Campbell P and Rees S (1999) *Reduction in Choline acetyltransferase immunoreactivity but not muscarinic-m2 immunoreactivity receptor in the brainstem of SIDS infants.* J. Neuropathol. Exp. Neurol. 58: 255-264.

Manfredi I, Zani AD, Rampoldi L, Pegorini S, Bernascone I, Moretti M *et al.* (2009) *Expression of mutant β2 nicotinic receptors during development is crucial for epileptogenesis.* Hum. Mol. Genet. 18, 1075-1088.

Mann E O and Mody I (2008) *The multifaceted role of inhibition in epilepsy: seizure-genesis through excessive GABAergic inhibition in autosomal dominant nocturnal frontal lobe epilepsy.* Curr. Opin. Neurol. 21, 155-160.

Mansvelder HD and McGehee DS (2000) *Long-term potentiation of excitatory inputs to brain reward areas by nicotine.* Neuron 27: 349-357.

Mansvelder HD and Role LW (2006) *Neuronal receptors for nicotine: functional diversity and developmental changes.* Brain Development, ed M. W. Miller (Oxford: Oxford University Press), 341-362.

Marchi M, and Grilli M (2010) *Presynaptic nicotinic receptors modulating neurotransmitter release in the central nervous system: functional interactions with other coexisting receptors*. Prog. Neurobiol. 92, 105-111.

Marubio LM and Changeux JP (2000) *Nicotinic acetylcholine receptor knockout mice as animal models for studying receptor function.* European Journal of Pharmacology 393: 113-121.

Masliah E, Rockenstein E, Veinbergs I, Mallory M, Hashimoto M, Takeda A … Mucke L (2000) *Dopaminergic loss and inclusion body formation in alphasynuclein mice.* Science, 287(February), 1265-1269.

McCann H, Stevens CH, Cartwright H and Halliday GM (2013) *α-Synucleinopathy phenotypes.* 1–17.

McCarley RW, Brown RE, Basheer VA, McKenna JY and Strecker RE (2012) *Control of sleep and wakefulness.* Physiological Reviews. 92(3): 1087-1187.

McDowell KA, Shin D, Roos KP and Chesselet MF (2014) *Sleep dysfunction and EEG alterations in mice overexpressing alpha-synuclein.* J Parkinsons Dis. 4(3):531-539.

McLean PJ, Kawamata H, Ribich S and Hyman BT (2000) *Membrane Association and Protein Conformation of α-Synuclein in Intact Neurons.* Journal of Biological Chemistry, 275(12), 8812-8816.

Mechawar N, Cozzari C and Descarries L (2000) *Cholinergic innervation in adult rat cerebral cortex: a quantitative immunocytochemical description.* J. Comp. Neurol. 428, 305–318.

Mechawar N, Watkins KC and Descarries L (2002) *Ultrastructural features of the acetylcholine innervation in the developing parietal cortex of rat.* The Journal of Comparative Neurology 443: 250-258.

Molas S and Dierssen M (2014) *The role of nicotinic receptors in shaping and functioning of the glutamatergic system: A window into cognitive pathology.* Neuroscience & Biobehavioral Reviews 46: 315-325.

Morris M, Sanchez PE, Verret L, Beagle AJ, Guo W, Dubal D, Ranasinghe KG, Koyama A, Ho K, Yu GQ, Vossel KQ, Mucke L (2015) *Network Dysfunction In α-Synuclein Transgenic Mice And Human Lewy Body Dementia.* Ann Clin Transl Neurol. 2(11):1012-28.

Mrzljak L, Pappy M, Leranth C and Goldman-Rakic PS (1995) *Cholinergic synaptic circuitry in the macaque prefrontal cortex.* The Journal of Comparative Neurology 357: 603-617.

Muramatsu I, Masuoka T, Uwada J, Yoshiki H, Yazama T, Lee KS, Sada K, Nishio M, Ishibashi T and Taniguchi T (2018) *A New Aspect of Cholinergic Transmission in the Central Nervous System.* In: Akaike A, Shimohama S, Misu Y, editors. Nicotinic Acetylcholine Receptor Signaling in Neuroprotection. Singapore: Springer; 2018. Chapter 3.

Murphy BK and Miller KD (2009) *Balanced amplification: a new mechanism of selective amplification of neural activity patterns.* Neuron 61, 635–648.

Nakata Y, Yasuda T, Fukaya M, Yamamori S, Itakura M, Nihira T … Mochizuki H (2012) *Accumulation of α-Synuclein Triggered by Presynaptic Dysfunction.* Journal of Neuroscience, 32(48), 17186-17196.

Nakayama H, Shioda S, Okuda H, Nakashima T and Nakai Y (1995) *Immunocytochemical localization of nicotinic acetylcholine receptor in rat cerebral cortex.* Brain Res Mol Brain Res. 32:321-8.

Neupane K, Solanki A, Sosova I, Belov M and Woodside MT (2014) *Diverse metastable structures formed by small oligomers of -synuclein probed by force spectroscopy.* PloS One, 9(1), e86495.

Newman EL, Gupta K, Climer, JR, Monaghan JK and Hasselmo ME (2012) *Cholinergic modulation of cognitive processing: insights drawn from computational models.* Frontiers In Behavioural Neuroscience. 13:6-24.

Nobili L, Proserpio P, Combi R, Provini F, Plazzi G, Bisulli F *et al.* (2014) *Nocturnal frontal lobe epilepsy.* Curr. Neurol. Neurosci. Rep. 14, 424.

Noebels JL, Avoli M, Rogawski MA et al. (2012) *Jasper's Basic Mechanisms of the Epilepsies.* 4th edition. National Center for Biotechnology Information (US).

Oda Y (1999) *Choline acetyltransferase: the structure, distribution and pathologic changes in the central nervous system.* Pathology International 49: 921-937.

Ozeki H, Finn IM, Schaffer ES, Miller KD and Ferster D (2009) *Inhibitory stabilization of the cortical network underlies visual surround suppression.* Neuron 62, 578-592.

Smiley JF, Morrell F, Mesulam MM (1997) *Cholinergic synapses in human cerebral cortex: an ultrastructural study in serial sections.* Experimental Neurology 144: 361-368.

O'Neill HC, Laverty DC, Patzlaff NE, Cohen BN, Fonck C, McKinney S *et al.* (2013) *Mice expressing the ADNFLE valine 287 leucine mutation of the β2 nicotinic acetylcholine receptor subunit display increased sensitivity to acute nicotine administration and altered presynaptic nicotinic receptor function.* Pharmacol. Biochem. Behav.

Paterson D and Nordberg A (2000) *Neuronal nicotinic receptors in the human brain.* Progress in Neurobiology 61:75-111.

Paxinos G (2015) *The Rat Nervous System.* 4th ed. Elsevier. ISBN: 978-0-12374245-2.

Pepeu G and Giovannini MG (2004) *Changes in acetylcholine extracellular levels during cognitive processes.* Learning & Memory 11: 21-27.

Pepeu G and Giovannini MG (2008) *Changes in acetylcholine extracellular levels during cognitive processes.* Learn Mem. 11:21--27.

Perez RG, Waymire JC, Lin E, Liu JJ, Guo F and Zigmond MJ (2002) *A role for alpha-synuclein in the regulation of dopamine biosynthesis.* The Journal of Neuroscience: The Official Journal of the Society for Neuroscience, 22(8), 3090-3099.

Pfeffer CK, Xue M, He M, Huang ZJ and Scanziani M (2013) *Inhibition of inhibition in visual cortex: the logic of connections between molecularly distinct interneurons.* Nat. Neurosci. 16, 1068-1076.

Phillips HA, Favre I, Kirkpatrick M, Zuberi SM, Goudie D, Heron SE, Sheffer IE, Sutherland GR, Berkovic SF, Bertrand D and Mulley JC (2001) *CHRNB2 is the second acetylcholine receptor subunit associated with autosomal dominant nocturnal frontal lobe epilepsy.* American Journal of Human Genetics 68 (1): 225-231.

Picard F and Brodtkorb E (2008) *Familial frontal lobe epilepsy* in Epilepsy. A Comprehensive Textbook, ed J. Engel and T. A. Pedley (Philadelphia, PA: Lippincott Williams and Wilkins), 2495–2502.

Polymeropoulos MH, Lavedan C, Leroy E, Ide SE, Dehejia A, Dutra A … Nussbaum RL (1997) *Mutation in the α-synuclein gene identified in families with Parkinson's disease.* Science, 276(5321), 2045-2047.

Poorthuis RB, Bloem B, Schak B, Wester J, de Kock CP and Mansvelder HD (2012). *Layer-specific modulation of the prefrontal cortex by nicotinic acetylcholine receptors.* Cereb. Cortex 23, 148-161.

Poorthuis RB and Mansvelder HD (2013) *Nicotinic acetylcholine receptors controlling attention: behavior, circuits and sensitivity to disruption by nicotine.* Biochemical pharmacology 86: 1089-1098.

Proulx E, Piva M, Tian MK, Bailey CD and Lambe EK (2014) *Nicotinic acetylcholine receptors in attention circuitry: the role of layer VI neurons of prefrontal cortex.* Cellular and Molecular Life Sciences 71: 1225-1244.

Provini F, Plazzi G, Montagna P and Lugaresi E (2000) *The wide clinical spectrum of nocturnal frontal lobe epilepsy.* Sleep Medicine Review 4 (4): 375-386.

Puskarjov M, Seja P, Heron SE, Williams TC, Ahmad F, Iona X et al. (2014) *A variant of KCC2 from patients with febrile seizures impairs neuronal Cl^- extrusion and dendritic spine formation.* EMBO Rep. 15, 723-729.

Quik M and Kulak JM (2002) *Nicotine and nicotinic receptors; relevance to Parkinson's disease*. Neurotoxicology 23: 581-594.

Quik M, Bordia T, Forno L, McIntosh JM (2004) *Loss of alphaconotoxinMII- and A85380-sensitive nicotinic receptors in Parkinson's disease striatum.* J. Neurochem. 88: 668–679.

Richardson KA, Fanselow EE and Connors BW (2008). *Neocortical anatomy and physiology.* In Epilepsy. A Comprehensive Textbook, eds J. Engel and T. A. Pedley (Philadelphia, PA: Lippincott Williams and Wilkins), 323–335.

Rivera C, Voipio J, Payne JA, Ruusuvuori E, Lahtinen H, Lamsa K et al. (1999) *The K^+/Cl^- co-transporter KCC2 renders GABA hyperpolarizing during neuronal maturation.* Nature 397, 251-255.

Rudy B, Fishell G, Lee S and Hjerling-Leffler J (2011) *Three groups of interneurons account for nearly 100% of neocortical GABAergic neurons.* Dev. Neurobiol. 71, 45-61.

Rush R, Kuryatov A, Nelson ME and Lindstrom J (2002) *First and second transmembrane segments of α_3, α_4, β_2 and β_4 nicotinic acetylcholine receptor subunits influence the efficacy and potency of nicotine.* Molecular Pharmacology 61: 1416-1422.

Sánchez MP, García-Cabrero AM, Sánchez-Elexpuru G, Burgos Df, Serratosa JM (2018) *Tau-Induced Pathology In Epilepsy And Dementia: Notions From Patients And Animal Models.* Int J Mol Sci. 19(4).

Sheffer IE, Bhatia KP, Lopes-Cendes I, Fish DR, Marsden CD, Andermann E, Andermann F, Desbiens R, Keene D and Cendes F (1995) *Autosomal dominant nocturnal frontal lobe epilepsy. A distinctive clinical disorder.* Brain 118 (1): 61-73.

Sparks DL and Hunsaker JC (1991) *Sudden death infant syndrome: Altered adrenergic-cholinergic synaptic markers in hypothalamus.* J. Child Neurol. 6: 335-339.

Spillantini MG, Crowther RA, Jakes R, Hasegawa M and Goedert M (1998) *Synuclein in filamentous inclusions of Lewy bodies from Parkinson's disease and dementia with Lewy bodies.* Proceedings of the National Academy of Sciences, 95(11), 6469-6473.

Steinlein OK, Mulley JC, Propping P, Wallace RH, Phillips HA, Sutherland GR, Sheffer IE and Berkovic SF (1995) *A missense mutation in the neuronal nicotinic acetylcholine receptor alpha 4 subunit is associated with autosomal dominant nocturnal frontal lobe epilepsy.* Nature Genetics 11 (2): 201-203.

Steinlein OK, Magnusson A, Stoodt J, Bertrand S, Weiland S, Berkovic SF, Nakken KO, Propping P and Bertrand D (1997). *An insertion mutation of the CHRNA4 gene in a family with autosomal dominant nocturnal frontal lobe epilepsy.* Hum. Mol. Genet. 6: 943-947.

Steriade M (2003) *Neuronal substrates of sleep epilepsy.* Cambridge University Press.

Steriade M and McCarley RW (2005) *Brain Control of Wakefulness and Sleep.* New York, NY: Kluwer Academic/Plenum Publishers.

Sutor B and Zolles G (2001) *Neuronal nicotinic acetylcholine receptors and autosomal dominant nocturnal frontal lobe epilepsy: a critical review.* Pflügers Arch. 442, 642–651.

Taguchi K, Watanabe Y, Tsujimura A and Tanaka M (2016) *Brain region-dependent differential expression of alpha-synuclein.* Journal of Comparative Neurology, 524(6), 1236-1258.

Tasic B, Menon V, Nguyen TN, Kim TK, Jarsky T, Yao Z, Levi B, Gray LT, Sorensen SA, Dolbeare T *et al.* (2016) *Adult mouse cortical cell taxonomy revealed by single cell transcriptomics.* Nat. Neurosci. 19, 335–346.

Teper Y, Whyte D, Cahir E, Lester HA, Grady SR, Marks MJ *et al.* (2007*) Nicotine-induced dystonic arousal complex in a mouse line harboring a human autosomal-dominant nocturnal frontal lobe epilepsy mutation.* J. Neurosci. 27, 10128-10142.

Trachtenberg JT, Chen BE, Knott GW, Feng G, Sanes JR, Welker E and Svoboda K (2002) *Long-term in vivo imaging of experience-dependent synaptic plasticity in adult cortex.* Nature 420: 788-794.

Ueda K, Fukushima H, Masliah E, Xia Y, Iwai A, Yoshimoto M … Saitoh T (1993) *Molecular cloning of cDNA encoding an unrecognized component of amyloid in Alzheimer disease*. Proceedings of the National Academy of Sciences of the United States of America, 90(December), 11282-11286.

Umbriaco D, Watkins KC, Descarries L, Cozzari C and Hartman BK (1994) *Ultrastructural and morphometric features of the acetylcholine innervation in adult rat parietal cortex: an electron microscopic study in serial sections.* The Journal of Comparative Neurology 348:351-373.

Umbriaco D, Garcia S, Beaulieu C and Descarries L (1995) *Relational features of acetylcholine, noradrenaline, serotonin and GABA axon terminals in the stratum radiatum of adult rat hippocampus (CA1).* Hippocampus 5: 605-620.

Vargas KJ, Makani S, Davis T, Westphal CH, Castillo PE and Chandra SS (2014) *Synucleins Regulate the Kinetics of Synaptic Vesicle Endocytosis.* Journal of Neuroscience, 34(28), 9364-9376.

Volles MJ, Lee SJ, Rochet JC, Shtilerman MD, Ding TT, Kessler JC and Lansbury PT (2001) *Vesicle permeabilization by protofibrillar α-synuclein: Implications for the pathogenesis and treatment of Parkinson's disease. Biochemistry*, 40(26), 7812-7819.

Wang X, Lippi G, Carlson DM and Berg DK (2013) *Activation of α7-containing nicotinic receptors on astrocytes triggers AMPA receptor recruitment to glutamatergic synapses.* J Neurochem. 127(5):632-43.

Wersinger C, Rusnak M and Sidhu A (2006) *Modulation of the trafficking of the human serotonin transporter by human alpha-synuclein.* European Journal of Neuroscience, 24(1), 55-64.

Wong TP, Debeir T, Duff K and Cuello AC (1999) *Reorganization of cholinergic terminals in the coronhal cortex and hippocampus in transgenic mice carrying mutated presenilin-1 and amyloid precursor protein trangenes.* J. Neurosci. 19: 2706-2716.

Woodruff A and Yuste R (2008) *Of mice and men, and chandeliers.* PLoS Biol. 6:e243.

Woolf NJ (1991) *Cholinergic systems in mammalian brain and spinal cord.* Progress Neurobiology 37: 475-524.

Xu J, Cohen BN, Zhu Y, Dziewczapolski G, Panda S, Lester HA *et al.* (2011) *Altered activity-rest patterns in mice with a human autosomal dominant nocturnal frontal lobe epilepsy mutation in the β2 nicotinic receptor.* Mol. Psychiatry 16, 1048-1061.

Yakel JL (2013) *Cholinergic receptors: functional role of nicotinic ACh receptors in brain circuits and disease.* Pflügers Archive-European Journal of Physiology 465: 441-450.

Yamada J, Zhu G, Okada M, Hirose S, Yoshida S, Shiba Y *et al.* (2013) *A novel prophylactic effect of furosemide treatment on autosomal dominant nocturnal frontal lobe epilepsy (ADNFLE).* Epil. Res. 107, 127-137.

Yamada K and Iwatsubo T (2018) *Extracellular α-Synuclein Levels Are Regulated By Neuronal Activity.* Mol Neurodegener. 22;13(1):9.

Yang JW, Czech T, Felizardo M, Baumgartner C and Lubec G (2006) *Aberrant Expression Of Cytoskeleton Proteins In Hippocampus From Patients With Mesial Temporal Lobe Epilepsy.* Amino Acids. 30(4):477-93.

Yu S, Li X, Liu G, Han J, Zhang C, Li Y … Chan P (2007) *Extensive nuclear localization of α-synuclein in normal rat brain neurons revealed by a novel monoclonal antibody.* Neuroscience, 145(2), 539-555.

Yuste R and Bonhoeffer T (2001) *Morphological changes in dendritic spines associated with long-term synaptic plasticity.* Annual review of neuroscience 24: 1071-1089.

Zaborszky l, Van Den Pol A and Gyngesi E (2012) *The basal forebrain cholinergic projection system in mice.* In: Watson C, Paxinos G and Puelles I. The mouse nervous system (2012). USA: Elsevier Inc. 648-718.

Zeisel A, Munoz-Manchado AB, Codeluppi S, Lonnerberg P, La Manno G, Jureus A, Marques S, Munguba H, He L, Betsholtz C *et al.* (2015) *Brain structure. Cell types in the mouse cortex and hippocampus revealed by single-cell RNA-seq.* Science 347, 1138–1142

Zhu G, Okada M, Yoshida S, Ueno S, Mori F, Takahara T *et al.* (2008) *Rats harboring S284L Chrna4 mutation show attenuation of synaptic and extrasynaptic GABAergic transmission and exhibit the nocturnal frontal lobe epilepsy phenotype.* J. Neurosci. 28, 12465-12476.

Zoli M, Pucci S, Vilella A and Gotti C (2018) *Neuronal and Extraneuronal Nicotinic Acetylcholine Receptors.* Curr Neuropharmacol. 16(4):338-349.

Chapter 2

Postnatal Changes in K^+/Cl^- Cotransporter-2 Expression in the Forebrain of Mice Bearing a Mutant Nicotinic Subunit Linked to Sleep-Related Epilepsy

Alida Amadeo [a], Aurora Coatti [b], Patrizia Aracri [b], Miriam Ascagni [a], Davide Iannantuoni [a], Debora Modena [a], Laura Carraresi [d], Simone Brusco [b], Simone Meneghini [b], Annarosa Arcangeli [c], Maria Enrica Pasini [a] and Andrea Becchetti [b]

[a] *Department of Biosciences, University of Milano, Via Celoria, 26, 20133 Milano, Italy*
[b] *Department of Biotechnology and Biosciences, and NeuroMI-Milan Center of Neuroscience, University of Milano-Bicocca, Piazza della Scienza, 2, 20126 Milano, Italy*
[c] *Department of Experimental and Clinical Medicine, University of Florence, Largo Brambilla, 3, 50134 Firenze, Italy*
[d] *Dival Toscana Srl, Via Madonna del Piano, 6 – 50019 Sesto Fiorentino, Firenze, Italy*

Neuroscience 2018; 386:91-107. doi: 10.1016/j.neuroscience.2018.06.030.

ABSTRACT

The $Na^+/K^+/Cl^-$ cotransporter-1 (NKCC1) and the K^+/Cl^- cotransporter-2 (KCC2) set the transmembrane Cl^- gradient in the brain, and are implicated in epileptogenesis. We studied the postnatal distribution of NKCC1 and KCC2 in wild-type (WT) mice, and in a mouse model of sleep-related epilepsy, carrying the mutant β2-V287L subunit of the nicotinic acetylcholine receptor (nAChR). In WT neocortex, immunohistochemistry showed a wide distribution of NKCC1 in neurons and astrocytes. At birth, KCC2 was localized in neuronal somata, whereas at subsequent stages it was mainly found in the somatodendritic compartment. The cotransporters' expression was quantified by densitometry in the double-transgenic strain. KCC2 expression increased during the first postnatal weeks, while the NKCC1 amount remained stable, after birth. In mice expressing β2-V287L, the KCC2 amount in layer V of prefrontal cortex (PFC) was lower than in the control littermates at postnatal day 8 (P8), with no concomitant change in NKCC1. Consistently, the GABAergic excitatory to inhibitory switch was delayed in PFC layer V of mice carrying β2-V287L. At P60, the amount of KCC2 was instead higher in mice bearing the transgene. Irrespective of genotype, NKCC1 and KCC2 were abundantly expressed in the neuropil of most thalamic nuclei since birth. However, KCC2 expression decreased by P60 in the reticular nucleus, and more so in mice expressing β2-V287L. Therefore, a complex regulatory interplay occurs between heteromeric nAChRs and KCC2 in postnatal forebrain. The pathogenetic effect of β2-V287L may depend on altered KCC2 amounts in PFC during synaptogenesis, as well as in mature thalamocortical circuits.

INTRODUCTION

The $Na^+/K^+/Cl^-$ cotransporter-1 (NKCC1) and the K^+/Cl^- cotransporter-2 (KCC2) are major regulators of the intracellular Cl^- concentration ($[Cl^-]_i$; Kaila *et al.*, 2014a). In developing brains, the comparatively large amount of NKCC1 in neurons and astrocytes causes a high $[Cl^-]_i$, which maintains the reversal potential of the $GABA_A$ receptor currents (E_{GABA}) at depolarized values (Ben Ari *et al.*, 2007). Under these conditions, GABA release produces depolarizing effects that modulate neuronal maturation and synaptogenesis (Ben Ari *et al.*, 2007; Cancedda *et al.*, 2007). Around birth, KCC2 expression progressively increases. By lowering $[Cl^-]_i$, KCC2 leads E_{GABA} to the typical hyperpolarized values observed in the adult brain (Kaila *et al.*, 2014; Rivera *et al.*, 1999). In murine neocortex, such 'GABAergic switch' occurs during the first two postnatal weeks. Being concomitant with the formation of GABAergic synapses (Takayama and Inoue, 2010), it is thought to regulate the postnatal maturation of neuronal circuits (Ben-Ari *et al.*, 2007; Ge *et al.*, 2006).

The balance of abundance and activity of NKCC1 and KCC2 is implicated in epileptogenesis as well as in the compensatory responses observed in hyperexcitable networks (Kaila *et al.*, 2014b; Khirug *et al.*, 2010). In fact, genetic variants of these cotransporters are linked to human idiopathic epilepsy (Kahle *et al.*, 2014; Puskarjov *et al.*, 2014). Epilepsy, however, comprises a heterogeneous spectrum of disorders (Jensen, 2011). The role of NKCC1 and KCC2 has been extensively studied in parietal and temporal lobe epilepsy (Aronica *et al.*, 2007; Awad *et al.*, 2016; Dzhala *et al.*, 2005; Karlócai *et al.*, 2016; Li *et al.*, 2008; Pathak *et al.*, 2007; Talos *et al.*, 2012; Zhu *et al.*, 2008), but not in frontal epilepsy. The latter presents distinct pathophysiological features, particularly in relation to the sleep-waking cycle. In frontal lobe epilepsy, sleep favors focal seizures, but not the occurrence of secondary generalization. The opposite holds in the focal epilepsies originating in other cortical regions (Shouse and Quigg, 2008).

To address these issues, we focused on Autosomal Dominant Nocturnal Frontal Lobe Epilepsy (ADNFLE), the mendelian form of hypermotor sleep-related epilepsy, which is characterized by focal hyperkinetic seizures mainly occurring during non-rapid-eye-movement sleep (Tinuper *et al.*, 2016). ADNFLE is frequently caused by point mutations on genes coding for α or β subunits of the neuronal nicotinic

acetylcholine receptor (nAChR; Tinuper *et al.*, 2016). In the mammalian neocortex, the most widespread heteromeric nAChR is α4β2, and the first ADNFLE mutations identified on these subunits were α4-S248F (Steinlein *et al.*, 1995) and β2-V287L (De Fusco *et al.*, 2000). In heterologous expression systems, ADNFLE mutations often increase the nAChR function, at least in the heterozygous state, by augmenting its sensitivity to the agonists or causing other kinetic alterations (Becchetti *et al.*, 2015). Previous studies on the first conditional murine model of ADNFLE, expressing β2-V287L in the brain under control of a tetracycline promoter, suggest that the transgene could exert its effects during synaptogenesis (Manfredi *et al.*, 2009). Mice carrying β2-V287L develop spontaneous epileptiform seizures, mostly occurring during periods of increased delta electroencephalographic activity, which is typical of slow-wave sleep. However, for the epileptic phenotype to manifest, β2-V287L must be expressed throughout brain development, until the end of the second postnatal week (Manfredi *et al.*, 2009). These results agree with recent lines of evidence suggesting that several nAChR subunits, including β2, display a peak of expression between the second and third postnatal weeks in neocortex and hippocampus (Mansvelder and Role, 2006; Molas and Dierssen, 2014). It has thus been suggested that nAChRs regulate synaptogenesis, even though the underlying cellular mechanisms are largely unknown (Molas and Dierssen, 2014). Nonetheless, the spontaneous nAChR activity affects the developmental GABAergic switch in neuronal cultures (Liu *et al.*, 2006). In fact, both β2-containing nAChRs (Lozada *et al.*, 2012) and KCC2 (Fiumelli *et al.*, 2013; Li *et al.*, 2007; Puskarjov *et al.*, 2014) are involved in maturation and remodeling of dendritic spines. Moreover, rats expressing another nAChR mutation linked to ADNFLE (i.e. α4-S284L) display an altered KCC2/NKCC1 messenger ratio (Yamada *et al.*, 2013). Hence, we hypothesized that an early regulatory link might exist between β2-containing nAChRs and the Cl^- cotransporters, which could have long-term effects on neocortex circuits and excitability.

The timing of NKCC1 and KCC2 appearance in neocortex and thalamus (TH) was previously studied in rats (Barthó *et al.*, 2004; Clayton *et al.*, 1998; Kovács *et al.*, 2014; Wang *et al.*, 2002; Yan *et al.*, 2001), mice (Hübner *et al.*, 2001; Markkanen *et al.*, 2014; Stein *et al.*, 2004; Takayama and Inoue, 2010), and humans (Hyde *et al.*, 2011; Sedmak *et al.*, 2016). However, no detailed analysis is available in mouse for associative cortices and TH nuclei, the most relevant regions for a sleep-related frontal

epilepsy. To investigate the interplay between α4β2 nAChRs and the Cl^-/cation cotransporters, we first determined the NKCC1 and KCC2 distribution in developing neocortex and TH of wild-type (WT) mice. Next, we studied if the amount of these cotransporters was altered in mice expressing β2-V287L. The morphological analysis was coupled with a patch-clamp study of E_{GABA} time course in prefrontal cortex (PFC) layer V, which is the most susceptible to develop epileptiform activity (Telfeian and Connors, 1998). Our results show that altering the function of β2-containing nAChRs affects KCC2 expression during postnatal development, and suggest that this mechanism may contribute to epileptogenesis.

EXPERIMENTAL PROCEDURES

Animals

Mice were kept in pathogen-free conditions, with a 12 h light-dark cycle, and free access to water and food. All procedures followed the Italian law (2014/26, implementing the 2010/63/UE) and were approved by the local Ethical Committees and the Italian Ministry of Health. For the morphological analyses of WT mice, we used 33 FVB mice (Harlan) of either sex, at the following embryonic (E) or postnatal (P) days: E14-15 (n=6), P0-2 (n=8); P5 (n=2); P7 (n=4); P12-P14 (n=5); P19-21 (n=3); P40-60 (n=5). The transgenic strain we used was the S3 line of double-transgenic FVB (tTA:Chrnb2V287L) mice, which express β2-V287L under a tetracycline-controlled transcriptional activator (tTA). These mice were compared with their littermates not expressing β2-V287L, which were either WT or bearing TRE-Chrnb2V287L or PrnP-tTA genotypes (Manfredi *et al.*, 2009). For clarity, mice expressing the transgene are hereafter denoted as β2-V287L, while the control littermates are denoted as controls (CTRL). The morphological analysis was carried out on 14 animals of either sex for each experimental group (CTRL and β2-V287L), at P8 (n=6), P21 (n=6), and P60 (n=16). Patch-clamp recordings were carried out on 15 CTRL (all PrnP-tTA) and 9 β2-V287L mice, whose age distribution is detailed in the Results. No morphological or electrophysiological difference was observed between sexes.

Brain regions

For immunohistochemistry and densitometric analyses, by PFC we refer to the entire secondary motor region (also known as M2, or Fr2) in the dorsomedial shoulder of prefrontal cortex. According to Franklin and Paxinos (2008), coronal prefrontal sections were cut between +2.58 and +1.14 mm from bregma. For somatosensory cortex (SS), we sampled the extended SS region between +1.98 and +0.02 mm from bregma. Thalamic sections for reticular (RT) and ventrobasal (VB) nuclei were prepared between -0,58 and -1,82 mm from bregma. For patch-clamp experiments, coronal PFC (Fr2) slices were cut between +2.68 mm and +2.10 mm from bregma.

Chemicals and drugs

Chemicals and drugs were purchased from Sigma-Aldrich, except for D(-)-2-amino-5-phosphono-pentanoic acid (AP5), 6-cyano-7-nitroquinoxaline-2,3-dione (CNQX), and tetrodotoxin (TTX), which were purchased from Tocris Bioscience (UK). Stock solutions of gramicidin D (100 mg/ml) and CNQX (20 mM) were prepared in dimethylsulfoxide. Stock solutions of GABA, AP5, and TTX were prepared in distilled water, stored at -20°C, and diluted daily to the final concentration in our extracellular solution.

Tissue preparation for immunohistochemistry

Postnatal mice were anesthetized with isoflurane and intraperitoneal 4% chloral hydrate (4 ml/100 g, for mice younger than P14; 2 ml/100 g, for older mice), and sacrificed by intracardiac perfusion as described (Aracri et al., 2013). Embryos at E14-E15 were quickly removed from the perfused pregnant mouse (aged P40), and their heads immersed in 4% paraformaldehyde in phosphate buffer (PB), for 24 h at 4°C. Next, brains were removed and stored for 5 to 10 days in the same fresh fixative. Both embryonic and postnatal (until P14) brains were embedded in 5% agarose. Serial coronal brain sections (50 µm thick) were cut with a Leica VT1000S vibratome.

Primary antibodies

Anti-NKCC1: T4 monoclonal antibody, originated from human colonic crypt (T84 cell) NKCC1, against the carboxy-terminus M902 to S1212 (Developmental Studies Hybridoma Bank; 1:100). Anti-KCC2: polyclonal, made in rabbit, against the N-terminal His-tag fusion protein, corresponding to residues 932-1043 of rat KCC2 (Millipore; diluted 1:600). Anti-VGAT (vesicular GABA transporter): polyclonal, made in rabbit against the synthetic peptide corresponding to the N-terminal 75-87 amino acids of the rat protein (Synaptic Systems; 1:800). Anti-VGLUT1 (vesicular glutamate transporter type 1): polyclonal, made in rabbit against Strep-TagR-fusion proteins containing the amino acid residues 456–560 of the rat VGLUT1/BNPI (brain-specific Na1-dependent inorganic phosphate transporter; Synaptic Systems; 1:500). Anti-MAP2 (microtubule-associated protein 2): monoclonal, made in mouse against the rat brain MAP2 (1:1000). Anti-neurofilament H, non-phosphorylated: monoclonal, made in mouse, (SMI32; Sternberger Monoclonals; 1:1000). Anti-GAD67 (glutamic acid decarboxylase

type 1/67kDa): polyclonal, made in goat against the human recombinant glutamic acid decarboxylase type 1, rhGAD1 (aa 2-97) derived from *E. coli* (R&D Systems; 1:300).

Immunoperoxidase histochemistry for light and electron microscopy

The immunoreaction was carried out as reported (Aracri *et al.*, 2010), except that a mild pretreatment with ethanol (10%, 25%, 10% in phosphate buffered saline, PBS) was applied to increase the immunoreagent penetration. Reaction specificity was assessed by negative controls, e.g. omission of primary antiserum. In these cases, no specific staining was observed. Briefly, sections were examined on a Leica DMRB microscope, and images were acquired using a Leica DCF 480 camera coupled to a personal computer. To generate **Table 1,** two independent observers assessed the cotransporter distribution in different brain regions. At least 3 mice were examined for each developmental stage. We analyzed at least 3-4 sections for each cortical region (PFC, SS), and 5-6 sections representative of the whole rostro-caudal thalamic extension. Several images were acquired per section. For ultrastructural analysis, sections were osmicated and epoxy-embedded after completion of the immunoenzymatic procedure. After polymerization, small areas from cerebral cortex and TH were cut with a razor blade and glued to blank resin blocks for sectioning with a Reichert ultramicrotome. Ultrathin sections (50–70 nm) collected on Cu/Rh grids were counterstained with lead citrate, or left unstained, and examined with a Zeiss LEO912AB electron microscope.

Immunofluorescence histochemistry

Sections were permeabilized and blocked as described for immunoperoxidase histochemistry. They were next incubated for two nights in a mixture of one/two primary antibodies, after staining with NeuroTrace™ (1:50, Molecular Probes) and/or before staining with Hoechst (Molecular Probes), as necessary for cytoarchitecture analysis and cell counting. For NeuroTrace™ staining, sections were treated as previously described (Aracri et al., 2010). After washing the primary antibodies with PBS, sections were incubated in the following mixture of secondary fluorescent antibodies: indocarbocyanine (Cy)2 (Jackson; 1:200), or CF™488A-conjugated donkey anti-rabbit IgG (Biotium; 1:200), Cy3-conjugated donkey anti-mouse (1:200) or RedX-conjugated donkey anti-goat (Jackson; 1:200), for 75 min at room temperature. After rinsing, samples were mounted on coverslips (sometimes after nuclear staining with Hoechst)

with PBS/glycerol (1:1 v/v) and inspected with a Leica TCS-NT laser scanning confocal microscope, to visualize double or triple fluorescent labeling.

Colocalization and densitometric analysis

All confocal micrographs were collected at 40X with a Leica SP2 laser scanning confocal microscope and analyzed with ImageJ. Identical parameters were used to acquire images from cortical and TH areas, for the colocalization analysis of NKCC1 with VGAT or VGLUT1, as previously described (Aracri *et al.*, 2013). In brief, nonoverlapping pictures were acquired in at least two different sections for neocortex or TH, so that double immunolabeling was studied in 3 or 4 fields per region in each animal. For two-color colocalization analysis, tissues were excited at 488 and 568 nm. To avoid crosstalk, the fluorescent signals of Cy2 (green) and Cy3 (red) were detected sequentially. Colocalization of NKCC1 with either VGAT or VGLUT1 was determined by generating 2D cytofluorograms (Bolte and Cordeliéres, 2006) by Leica Confocal software, as shown in **Figures 2E, F**. Generation of a binary mask of image data allowed to select in each region certain intensity value pairs in the cytofluorograms, which were labeled as white signals in the original images, to represent merged antigen localization (**Fig. 2C, D**). For densitometric analysis, cortical layers and TH nuclei were identified with NeuroTrace™ and/or nuclear counterstaining; at least three/four distinct images were acquired to sample the different areas. For each animal, the mean fluorescence intensity of each image was divided by the number of neurons therein (counted with ImageJ). The values thus obtained were averaged among animals before plotting. For the densitometric analysis of NKCC1, we selected fluorescent images with low background (as shown in **Fig. 8**). The degree of colocalization of KCC2 or NKCC1 with different neuronal markers was calculated by comparing the Manders' coefficients, computed with the JACoP plug-in of ImageJ software (Bolte and Cordeliéres, 2006).

Patch-clamp in brain slices

Mice were sacrificed after deep isoflurane anesthesia, and brains extracted as reported (Aracri *et al*., 2013). Coronal sections (300 µm thick) were cut from Fr2 PFC. Experiments were performed at 33-34°. E_{GABA} was measured with the perforated patch method. The extracellular solution contained (mM): 135 NaCl, 21 $NaHCO_3$, 0.6 $CaCl_2$, 3 KCl, 1.25 NaH_2PO_4, 1.8 $MgSO_4$, 10 D-glucose, aerated with 95% O_2 and 5% CO_2

(pH 7.4). Pipette contained (mM): 140 K-Gluconate, 5 KCl, 1 $MgCl_2$, 2.5 BAPTA, 10 HEPES, pH 7.25 (adjusted with KOH). Gramicidin (up to 20 µg/mL) was only added to the solution filling the pipette shank. Borosilicate (Science Products) micropipettes (2-3 MΩ) were prepared with a P-97 Micropipette Puller (Sutter). GABA was applied onto the cell soma, by pressure ejection through a micropipette connected to a Narishige IM-3 microinjector. The recording apparatus was as described (Aracri *et al.*, 2017). The comparison of the action potential (AP) firing of pyramidal neurons in mice expressing or not β2-V287L was carried out in a separate set of experiments. The resting membrane potential (V_{rest}) was measured in open circuit mode soon after patch rupture. Spike-width was measured at half-amplitude between AP threshold and peak. After-hyperpolarization was calculated as the difference between the most negative potential reached after repolarization and the AP threshold. Capacitance and series resistance (up to ~75%) were always compensated. E_{GABA} was determined by applying five consecutive 0.5 s voltage ramps from -80 mV to -20 mV (or -85 mV to -40 mV), in either presence or absence of GABA (100 µM). The background currents were subtracted from the currents obtained in the presence of GABA. Holding potential was -68 mV. Measurements were carried out in the presence of extracellular TTX (0.5 µM), to block voltage-gated Na^+ currents, AP5 (50 µM) and CNQX (10 µM), to block ionotropic glutamate receptors. No leak subtraction procedure was ever applied. No correction for junction potentials was applied to the reported values of membrane potential. Data were analysed with Clampfit 10.6 (Molecular Devices), and OriginPro 9.1 (OriginLab).

Statistical analysis

Data are given as mean values ± standard error of the mean. The number of experiments (n) is the number of tested mice. Comparisons between two independent populations were carried out with unpaired Student's *t*-test, after testing for data normality (with a Kolmogorov-Smirnov test), and variance homogeneity (with F-test). In case of unequal variances, the Welch's correction was applied. All determinations carried out in cells from the same animal were averaged, to avoid bias from nested data (Aracri *et al.*, 2017). In the figures, p values are indicated by * ($0.01 < p \leq 0.05$) or ** ($p \leq 0.01$). Unless otherwise indicated, detailed statistics are given in the figure legends.

RESULTS

We first studied the overall pattern of postnatal expression of NKCC1 and KCC2 in WT mice, as no previous systematic study is available for mouse forebrain. Next, we investigated the effect of β2-V287L expression on the cotransporters' amounts between the second and the third postnatal week (i.e. the critical stages of synaptogenesis), and in adult mice. Because ADNFLE is a sleep-related epilepsy with frequent implication of the frontal regions, we focus our study on both PFC and TH, and use SS as the classical reference cortex.

Distribution of NKCC1 in postnatal cortex and TH of WT mice

Immunoperoxidase localization of NKCC1 is shown in **Fig. 1** for neocortex and TH, at birth (P0-P1) and P19-P21 (i.e. after completion of synaptogenesis). For PFC and SS, representative images are respectively displayed in **Fig. 1A, B** (P0-P1), and **Fig. 1C, D** (P19-P21). NKCC1 was widely distributed in neocortex since birth, with no clear differences among layers. As for TH, the NKCC1 immunoreactivity was stronger and more stable in the anterior and posterior TH nuclei (i.e. the specific nuclei). Examples at P0-P1 and P19-P21 are shown, respectively, in **Fig. 1E** and **1F**. In general, immunoreactivity resulted stable in the different nuclei up to adult stages.

In agreement with previous findings, NKCC1 was generally found in both astrocytes (labeled for GFAP; data not shown) and neurons (Hübner *et al.*, 2001; Yan *et al.*, 2001; Wang *et al.*, 2002). In the neocortex, the marked radial pattern of labeling indicates intense expression in the apical dendrites of pyramidal neurons at both P19-P21 (**Fig. 1C, D**), and P60 (**Fig. 1G**), and fainter labeling in cell bodies (**Fig. 1G**). Such pattern was confirmed by confocal analysis, as indicated by the representative images for SS shown in **Fig. 2A** (P2) and **Fig. 2B** (P60). In TH, strong immunoreactivity was also observed in thin and thick fiber bundles (such as those of internal capsule; **Fig. 1H**).

Ultrastructural analysis also revealed NKCC1+ synaptic boutons in adult neocortex and TH (an example is given in **Fig. 1I**). The neurochemical nature of these synaptic terminals was investigated by studying the colocalization of NKCC1 with either VGAT (which labels GABAergic terminals), or VGLUT1 (which labels the majority of glutamatergic terminals; Graziano *et al.*, 2008). Representative images for the neocortex at P60 are shown in **Fig. 2C** (NKCC1/VGAT), and **Fig. 2D** (NKCC1/ VGLUT1). The degree of colocalization was estimated by generating the

corresponding 2D cytofluorograms, as illustrated in **Fig. 2E** (NKCC1/VGAT), and **2F** (NKCC1/VGLUT1). The colocalization puncta are indicated as white spots in **Fig. 2C, D**. In the mature neocortex, the overlap between NKCC1 and VGAT was always weak. In particular, the calculated M2 Manders' coefficient for **Fig. 2C, E** was 0.088. A higher degree of colocalization was generally observed for NKCC1 and VGLUT1, particularly in adult PFC (**Fig. 2D, F**). The calculated M2 coefficient for **Fig. 2D, F** was 0.8, indicating that 80% of the VGLUT1+ synaptic terminals also displayed the NKCC1 signal. On the other hand, in TH nuclei, NKCC1+/VGAT + boutons were only transiently observed in the second postnatal week (data not shown).

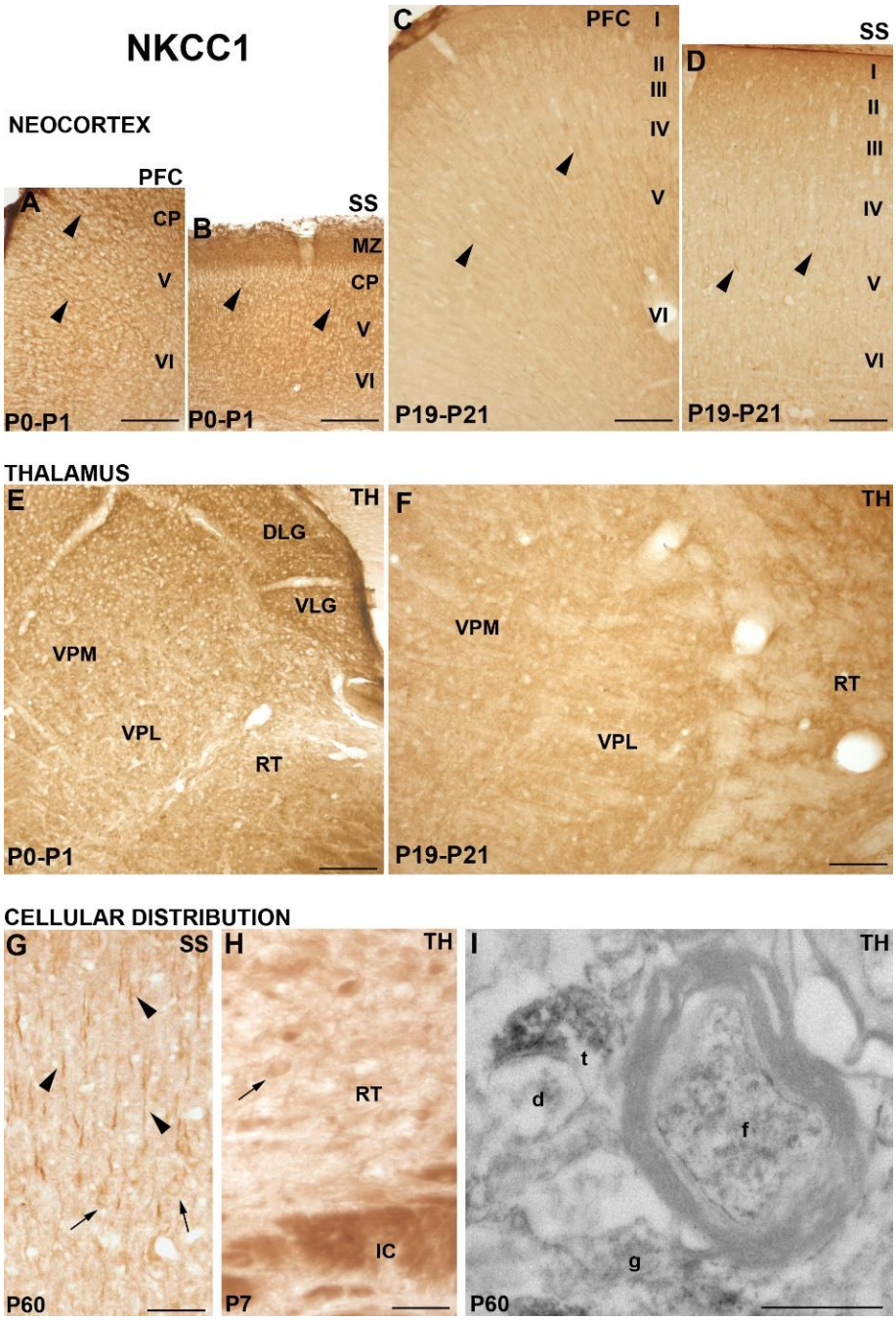

Fig. 1 Topographical and cellular distribution of NKCC1 in developing WT neocortex and thalamus (TH).

Immunohistochemical localization of NKCC1 in PFC (A, C), SS (B, D) and TH (E, F) of P0-P1 (A, B, E), and P19-P21 (C, D, F) mice. At both stages, NKCC1 was widely expressed in neocortex and TH, and mainly localized in the apical dendrites of PFC and SS pyramidal cells (arrowheads in A-D). Both in adulthood (G) and during development (H) NKCC1 was found in neurons of both neocortex and TH (arrows in G, H). NKCC1 staining was particularly intense in cortical apical dendrites (arrowheads in G), and in TH thin and thick axonal fibers, such as those of internal capsule (IC). Representative pre-embedding immunoelectron microscopy (TH at P60 in I) showed NKCC1 in the axons of myelinated fibers (f), in some glial processes (g) and in few small synaptic terminals (t) contacting distal dendrites (d). CP, cortical plate; DLG, dorsal lateral geniculate thalamic nucleus; MZ, marginal zone; I-VI, cortical layers; VLG, ventral lateral thalamic geniculate nucleus; VPM, ventral posteromedial thalamic nucleus; VPL, ventral posterolateral thalamic nucleus. Scale bars=150 µm (A-F); 50 µm (G); 40 µm (H); 0.5 µm (I).

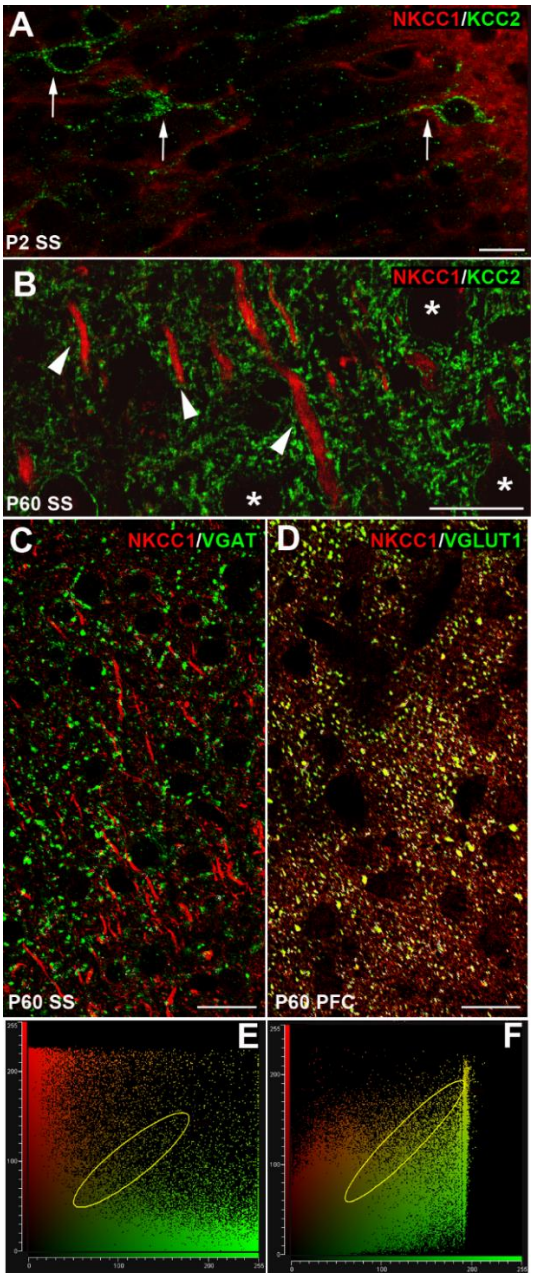

Fig. 2 Double immunofluorescence of NKCC1 with KCC2, or with synaptic markers, in WT neocortex.

Representative images (A, B) combining the NKCC1 (red) and KCC2 (green) signals, in SS. (A) At P2, NKCC1 was found ubiquitously, especially in the neuropil; KCC2 only displayed punctate labeling in the somatodendritic compartment of a fraction of neurons (arrows). (B) At P60, KCC2 and NKCC1 were found in the apical dendrites, but their distribution scarcely overlapped. KCC2 was confined to the cell surface around neuronal cell bodies (asterisks in B) and proximal dendrites (arrowheads in B); in the same dendrites, NKCC1 showed a more diffuse, cytoplasmic distribution. (C) Colocalization of NKCC1 (red) and VGAT (green), in SS at P60. (D) Colocalization of NKCC1 (red) and VGLUT1 (green), in PFC at P60. (E, F) 2D cytofluorograms showing the colocalization puncta in the region of interest (enclosed by the yellow ellipsoid) for NKCC1/VGAT (E) and NKCC1/VGLUT1 (F). These puncta are reported as yellow/white signals in the merged immunolabeling images (C, D), which represent high magnification details covering about one third of the entire fields acquired for colocalization analysis. At P60, very few terminals displayed both NKCC1 and VGAT signal colocalization (C), whereas the degree of colocalization between NKCC1 and VGLUT1 was much stronger (D). Scale bar=20 µm.

Distribution of KCC2 in developing cortex and TH of WT mice

The KCC2 distribution at different postnatal stages is illustrated in **Fig. 3**. Clusters of a few KCC2 positive (+) neurons were observed at P0-P1 in PFC layer V, and more abundantly in SS, along with an intense immunoreactivity in the marginal zone (**Fig. 3A, B**). The overall KCC2 immunoreactivity was stronger at P19-P21 (**Fig. 3C, D**). In TH, conspicuous labeling at birth was detected throughout the neuropil, except for RT (**Fig. 3E**). The anterior TH group displayed the highest labeling, followed by the posterior group and by the medial/intralaminar group. Such a distribution pattern was preserved at P19-P21 (**Fig. 3E, F**), when RT was almost devoid of KCC2 in its central region, whereas the lateral and medial borders displayed a fair labeling (**Fig. 3F**). These results suggest that KCC2 is expressed in TH earlier than in the neocortex. This was confirmed by KCC2 immunofluorescence at E14-E15, which showed a faint KCC2 signal in frontal and parietal preplate isocortices (**Fig. 4A, B**), but a more conspicuous labeling in the ventral (especially the ventral lateral geniculate nucleus, VLG, **Fig. 4D**) and dorsal TH (**Fig. 4C, D**).

Differently from NKCC1, KCC2 was only expressed in neurons and dendrites (**Fig. 3G-J**), and its distribution became increasingly polarized during development. In the neocortex, KCC2 was mainly confined to the neuronal cell bodies, during the first postnatal week (**Fig. 2A; 3A, B, G; 4E, G**). At P19-P21 (**Fig. 3C, D)**, the transporter was also found in the dendritic neuropil, and outlined the cell membranes, as can be better appreciated in **Fig. 3H,** at a higher magnification. A similar pattern was observed in the mature cortex **(Fig. 2B; 4F, H**). In TH, such distribution shift occurred before birth (**Fig. 4C, D**), and postnatal neurons showed maximal KCC2 expression in the neuropil (i.e. dendrites), even in the scarcely labeled RT (**Fig. 3J; 4I**).

As for the neurochemical nature of KCC2+ neurons in neocortex, during the first postnatal week both pyramidal neurons and GABAergic GAD67+ neurons (**Fig. 4E, G**) showed cytoplasmic immunoreactive puncta, probably vesicles, which also spread to proximal dendrites. After P7, KCC2 mainly outlined the membrane of pyramidal neurons (labeled with SMI32; **Fig. 4F**), whereas in GAD67+ structures (i.e. comprising neuronal cell bodies, processes and puncta), KCC2 was confined to the dendritic shafts (**Fig. 4H**). A different pattern was observed in TH. The GABAergic neurons, which were mainly concentrated in RT, generally showed a weak KCC2 expression. An exception was constituted by the dendrites of the GAD67+ cells located on the

medial border of RT **(Fig. 4I**). KCC2 was however intensely expressed by the dendritic neuropil of all TH neurons (**Fig. 3E, F, J; 4I**).

A semi-quantitative summary of the distribution of NKCC1 and KCC2 in PFC and TH, as obtained by immunohistochemistry at the relevant ages, is reported in **Table 1**.

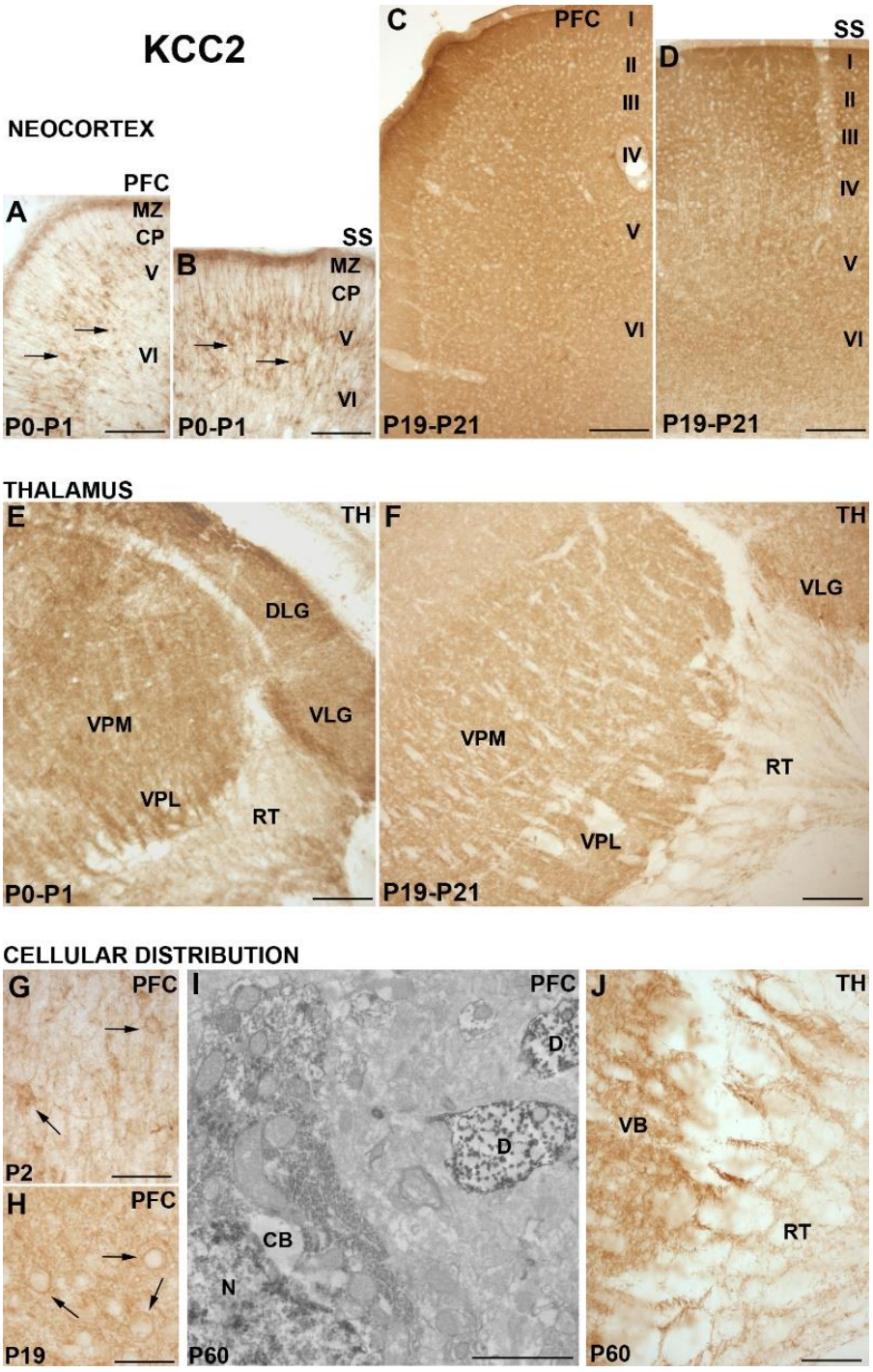

Fig. 3 Topographical and cellular distribution of KCC2 in postnatal WT neocortex and thalamus (TH).

Immunohistochemical localization of KCC2 in P0-P1 (A, B, E) and P19-P21 (C, D, F) mice. At birth, KCC2 was mainly confined to the neuronal cell bodies in PFC (A) and SS (B), and clusters of KCC2+ neurons were mainly found in layer V (arrows in A-B). At P19-P21, KCC2 was distributed throughout the neuropil in PFC (C) and SS (D). In TH nuclei, KCC2 was already present at P0-P1 in the neuropil of all regions, except RT (E). At P21, KCC2 expression in TH slightly decreased (F), and only a weak immunoreactivity was observed in the lateral and medial borders of RT (F). The immunoperoxidase localization of KCC2 showed its presence only in the neuronal cells and dendrites (G-J). At P2 in PFC, KCC2 was localized in multipolar neurons (arrows in G). Subsequently, KCC2 became distributed in the neuropil and outlined cell membranes (arrows in H), as shown also by immunoelectron microscopical localization (I), where it was exclusively observed in cell bodies (CB) and proximal dendrites (D). In TH (J)

KCC2 was mainly expressed by the dendritic neuropil, even in the scarcely labeled RT. N, nucleus; CP, cortical plate; DLG, dorsal lateral geniculate thalamic nucleus; MZ, marginal zone; I-VI, cortical layers; VLG, ventral lateral thalamic geniculate nucleus; VPL, ventral posterolateral thalamic nucleus; VPM, ventral posteromedial thalamic nucleus.
Scale bars=150 µm (A-F); 40 µm (G, H); 2 µm (I); 80 µm (J).

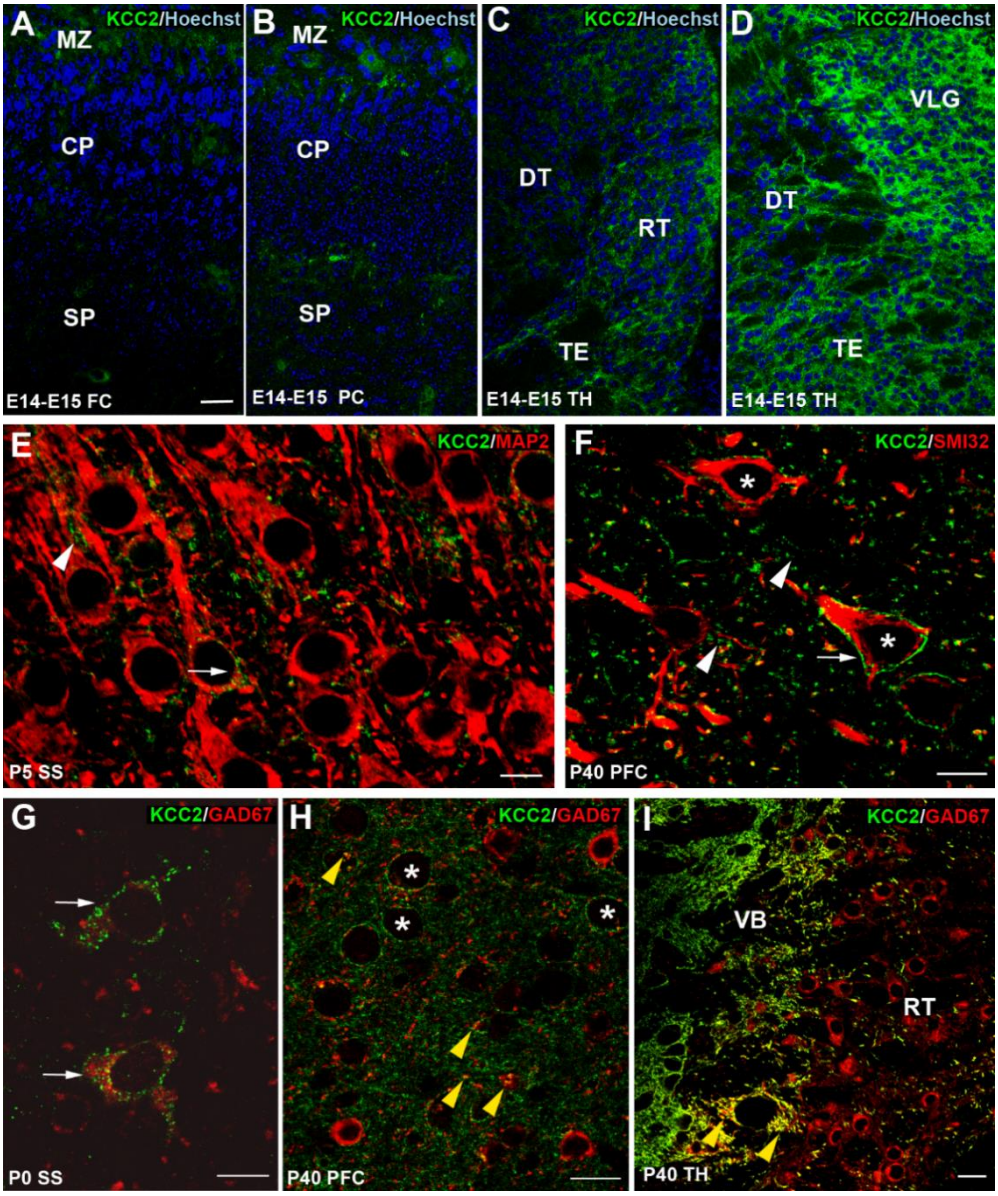

Fig. 4 Localization of KCC2 in developing WT forebrain.
A-D Topographical distribution of KCC2 in prenatal WT forebrain. Immunofluorescence staining for KCC2 (green) in embryonic (E14-E15) cortical (A, B) and thalamic (C, D) tissues; nuclei were stained with Hoechst (blue). KCC2 immunoreactivity was faint in frontal (FC) and parietal (PC) pre-plate isocortex (A, B), but strong in the rostral (C) and caudal (D) thalamic anlage.
Double immunofluorescence in SS (E, G), PFC (F, H) and TH (I). Representative images are shown for KCC2 (green) and MAP2 (red) at P5 (E), KCC2 (green) and SMI32 (red) at P40 (F), KCC2 (green) and GAD67 (red) at P0 and P40 (G-J). Around birth, KCC2 was mainly expressed in neuronal cell bodies in the neocortex (arrows in E, G). The MAP2+ pyramidal neurons and the GAD67+ interneurons showed cytoplasmic stained puncta, probably vesicles,

spreading to proximal dendrites (E, G). In P40 neocortex, KCC2 was also found in dendrites (white arrowheads in F) and outlined (arrow in F) pyramidal cell membranes (asterisks in F, H), whereas only a small fraction of the GAD67+ dendritic shafts (yellow arrowheads in D) also displayed KCC2 labeling. In TH (I), KCC2 was found in the dendritic neuropil of all TH neurons, and in the medial border of RT, where it displayed colocalization with GAD67 (yellow arrowheads in I). MZ, marginal zone; CP, cortical plate; SP, subplate; DT, dorsal thalamus; TE thalamic eminence. Scale bars=20 µm (A-D, H, I); 10 µm (E, G); 50 µm (F).

Table 1

Developmental distribution of NKCC1 and KCC2 in the forebrain of WT mouse

	E14-E15	P0-P2		P7	P19-P21		P40-P60	
	KCC2	**NKCC1**	**KCC2**	**KCC2**	**NKCC1**	**KCC2**	**NKCC1**	**KCC2**
PFC	+/-	+++	+	++	++	+++	++	+++
SS	+/-	+++	++	++	++	++	++	++
TH ant	+	+++	+++	++	+++	++	+++	++
TH me	+/-	++	+++	++	+/++	+	++	+
TH VB	+	+++	+++	+++	+++	++	+++	++
TH RT	++	+++	++	+	++	+/++	++	+/++
TH LG	+++	+++	+++	+++	+++	+++	+++	+++

Semi-quantitative analysis of the distribution of Cl^- transporters in different brain regions, at different ages, based on immunohistochemical localization, using anti-NKCC1 or anti-KCC2 antibodies, as indicated. The comparison between neonatal and P40 stages for KCC2 was also carried out by densitometric analysis, with analogous results (not shown). PFC: prefrontal cortex; SS: somatosensory cortex; TH ant: anterior thalamic area; TH me: medial thalamus, i.e. intralaminar and midline nuclei; TH VB: thalamic ventrobasal complex; TH RT: reticular thalamic nucleus; TH LG: lateral geniculate thalamic nuclei (comprising both dorsal and ventral lateral geniculate nuclei).
-: negative; +/-: scarce; +: moderately positive; ++: positive; +++: markedly positive

The β2-V287L nAChR subunit altered the timing of KCC2 expression.

To define more rigorously the spatiotemporal distribution of KCC2 at the critical postnatal stages as well as the ratio between KCC2 and NKCC1, a densitometric analysis was performed on confocal sections from mice expressing the transgene (β2-V287L) and the control littermates (CTRL). Because the maturation of synaptic circuits is accompanied by an increase in nAChR subunit expression between the second and the third postnatal weeks (Molas and Dierssen, 2014), we compared P8, P21 and adult (P60) tissue. Sections were labeled for KCC2 and NeuroTrace™, or Hoechst 33258.

The intensity of KCC2 fluorescence was divided by the number of cells identified with either marker.

Fig. 5 shows the results obtained in the neocortex at P8 (**Fig. 5A-D**), P21 (**Fig. 5E-H**) and P60 (**Fig. 5I-L**). The time course of KCC2 expression in the double-transgenic strain was consistent with the one observed in WT mice. For example, in CTRL, the densitometric values in PFC layer V increased by more than 60% between P8 (0.49 ± 0.014; n=3) and P60 (0.81 ± 0.05; n=8; $p < 0.01$ with unpaired t-test; DF=9), confirming the progressive increase of KCC2 amount after birth (cf. Table 1). The main differences between β2-V287L and CTRL mice were observed in PFC layer V, where smaller amounts of KCC2 were observed at P8 in β2-V287L mice (**Fig. 5C**). Such difference disappeared by P21 (**Fig. 5G**), and the effect was reversed at P60, when KCC2 expression was significantly higher in β2-V287L mice (**Fig. 5K**). In particular, in layer V, the ratio between the mean KCC2 fluorescence per cell in CTRL and β2-V287L decreased from ~1.32 (P8) to ~0.83 (P60). At the same ages, no differences were found in the KCC2 amounts in SS (**Fig. 5D, H, L**).

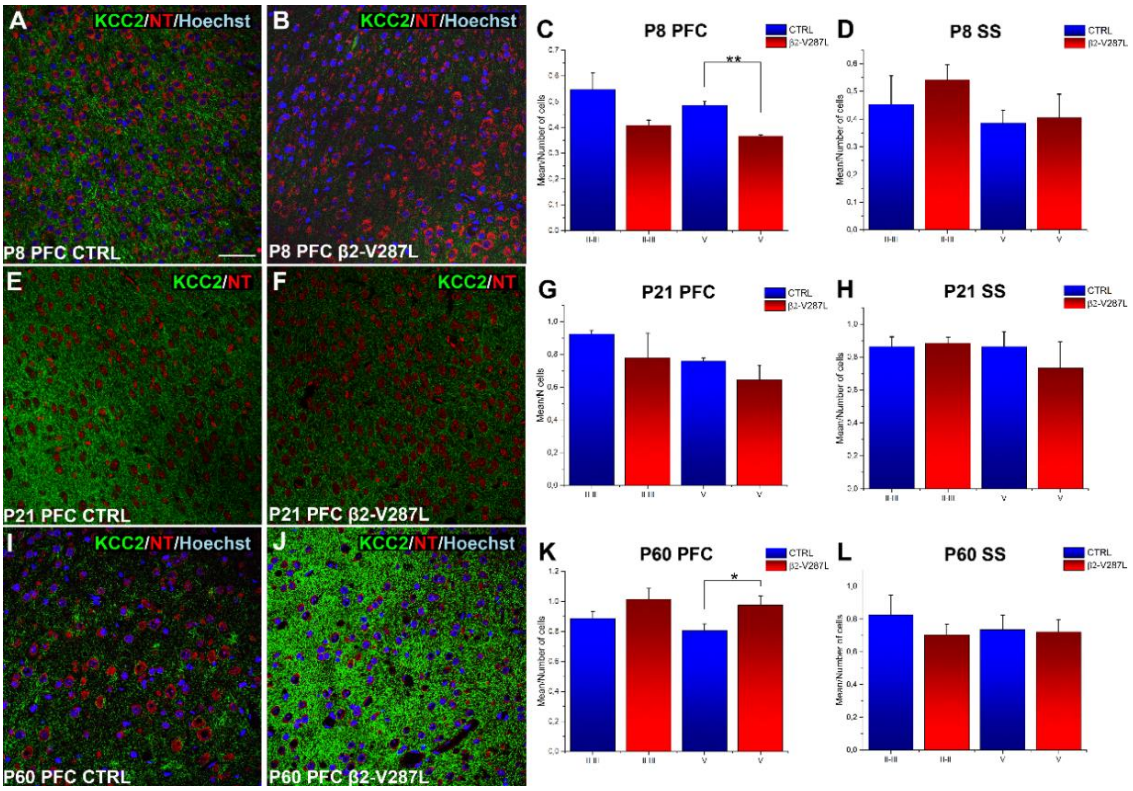

Fig. 5 Effect of β2-V287L on KCC2 expression in neocortex during postnatal development.
Immunofluorescence for KCC2 (green) counterstained with NeuroTrace™ (red; NT) and Hoechst (blue), in PFC layer V of CTRL (A, E, I) and β2-V287L (B, F, J) mice, at the indicated

ages. The corresponding densitometric analyses are summarized in the bar graphs for layers II/III and V from P8 (n=3), P21 (n=3) and P60 (n=8) mice in PFC (respectively C, G, K), and SS (respectively D, H, L). Bars give average fluorescence intensity values divided by the number of neurons. At P8, KCC2 expression in PFC layer V (C) was significantly lower in β2-V287L (0.37 ± 0.004 vs 0.49 ± 0.014 in CTRL; p < 0.01, with t-test; n=3) (C). The opposite was observed at P60, when KCC2 significantly increased in layer V of β2-V287L (0.98 ± 0.06, vs. 0.81 ± 0.05 in CTRL; p < 0.05, with t-test; n=8) (K). No statistical difference between genotypes was observed in SS (with t-test). Scale bar=20 μm.

To test whether the higher KCC2 amount observed in the PFC of adult β2-V287L mice could be partly ascribed to changes in the GABAergic neuronal populations, we analyzed the colocalization of KCC2 with GAD67. In PFC layer V, at P60 we observed the typical KCC2+ outlines around the cell bodies of pyramidal neurons (**Fig. 4F**), in WT (**Fig. 4H**), CTRL (**Fig. 6A-A'**) and β2-V287L (**Fig. 6B-B')**. In GAD67+ neurons, KCC2 expression was generally scarce (**Fig. 4H, 6A-A'**), although some colocalization was observed in β2-V287L (**Fig. 6B-B'**). Hence, the higher KCC2 amount observed in the PFC of adult β2-V287L mice could partly depend on a different expression in GABAergic neuronal subpopulation. To determine the contribution of GABAergic cells to the total KCC2 increment we quantified the overall colocalization of KCC2 and GAD67 (i.e. comprising neuronal cell bodies, processes and puncta). The degree of overlap was defined by M1 and M2 Manders' coefficients and was not significantly different between CTRL and β2-V287L mice. At P60, in PFC layer V, M1 (the fraction of colocalization on the total KCC2+ signal) was 0.17139 ± 0.00565 in CTRL, and 0.17008 ± 0.00743 in β2-V287L (p=0.895, with unpaired t-test; n=3); M2 (the fraction of colocalization on the total GAD67+ signal) was 0.36657 ± 0.00933 in CTRL, and 0.35333 ± 0.01154 in β2-V287L (p=0.423, with unpaired t-test; n=3).

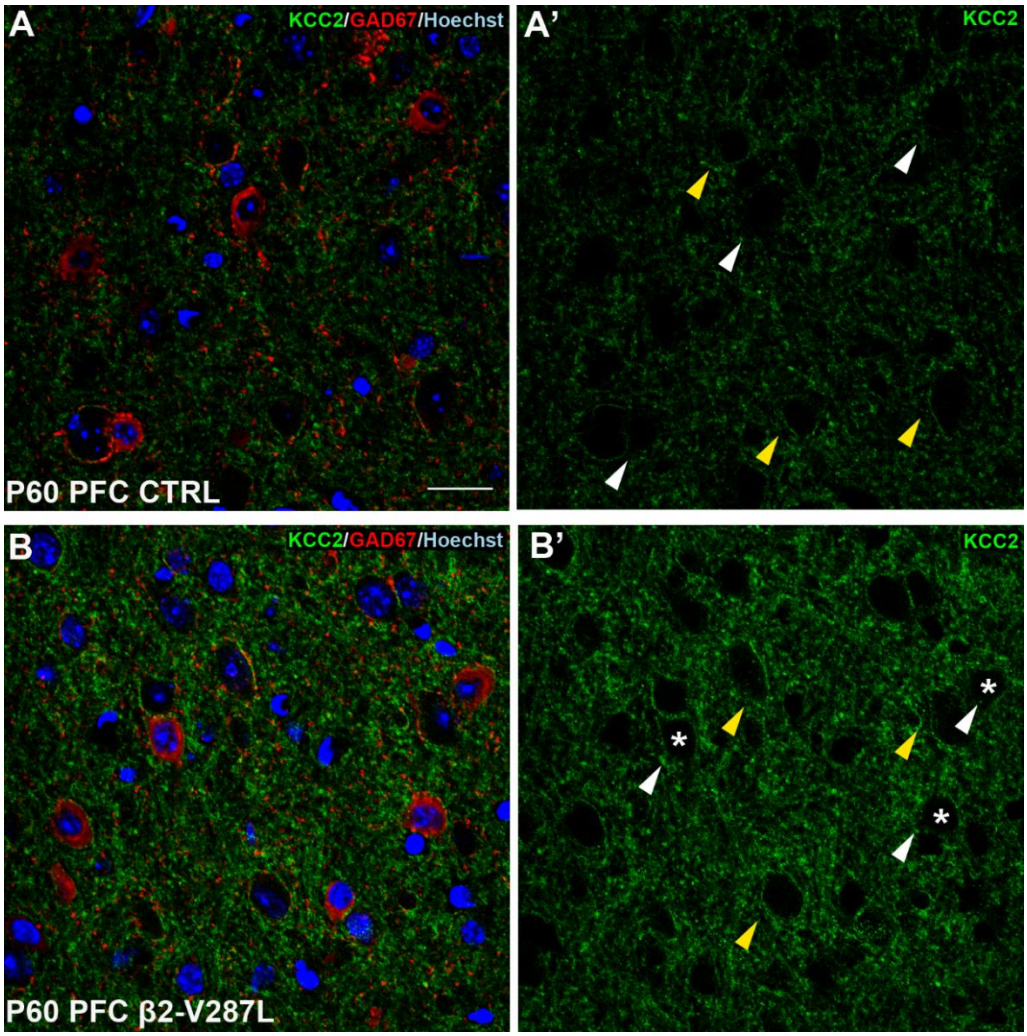

Fig. 6 Colocalization of KCC2 and GAD67 in PFC layer V of mice expressing or not β2-V287L.
Double immunofluorescence images in PFC layer V at P60, combining KCC2 (green) and GAD67 (red) localizations with nuclear staining with Hoechst (blue), for CTRL (A) and β2-V287L (B). The corresponding single labeling for KCC2 is shown in (A') for CTRL and (B') for β2-V287L. Data represent the results obtained in 3 mice for each genotype. In CTRL, GAD67+ neurons showed a weak KCC2+ staining of somatic neuronal membranes (white arrowheads) but marked KCC2+ outlines of pyramidal neurons' somata (yellow arrowheads). In β2-V287L, the KCC2 immunoreactivity pointed out somatic outlines also on some GAD67+ neurons (asterisks in B'). Scale bar=20 µm.

In TH, our densitometric analysis was focused on RT and on the main somatosensory relay nucleus VB. Once again, this analysis was consistent with the pattern observed in WT (**Table 1**). For example, in CTRL, the mean fluorescence intensity per cell in RT was 0.85 ± 0.07, at P8 (n=3), and 1.7 ± 0.04, at P60 (n=3; $p < 0.001$, with unpaired t-test; DF=4). Representative images at P60 are shown in **Fig. 7A-B**. In both nuclei, no significant differences were observed between genotypes at early postnatal stages (not shown). However, at P60, the average KCC2 amount

decreased in RT by ~20% in β2-V287L mice, compared to CTRL (**Fig. 7C**). Because in RT the KCC2+ signal was always confined to the GAD67+ dendritic neuropil (**Fig. 4I**), no analysis of overlap by Manders' coefficients was performed.

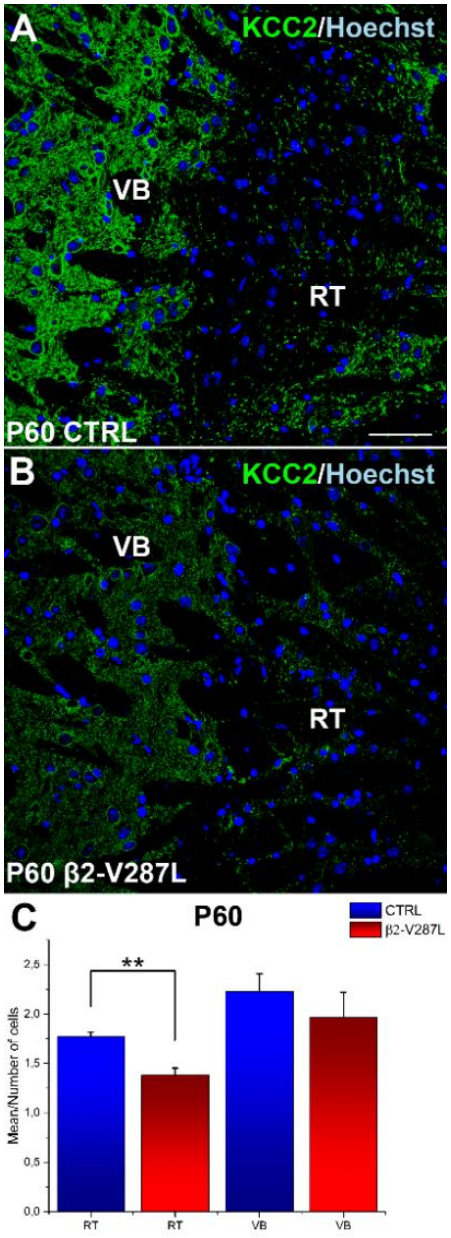

Fig. 7 Effect of β2-V287L on thalamic expression of KCC2 at P60.
Representative immunofluorescence images for KCC2 (green) counterstained with Hoechst (blue), in TH nuclei of CTRL (A) and β2-V287L (B) mice. The corresponding densitometric analyses are shown in the bar graphs (C), for RT and VB nuclei, as indicated. Data are given as mean fluorescence intensity values divided by the number of neurons. Mice bearing β2-V287L displayed a decreased KCC2 amount in RT (1.38 ± 0.07, vs. 1.77 ± 0.04 in CTRL; $p < 0.01$; DF=4; unpaired two-sample t-test with equal variance assumed; n=3). No significant difference was observed in VB (p=0.777; DF=4; unpaired two-sample t-test with equal variance assumed; n=3). Scale bar=20 µm.

β2-V287L did not change NKCC1 expression.

Because $[Cl^-]_i$ is regulated by both KCC2 and NKCC1, our densitometric analysis was extended to NKCC1, in PFC and TH, at P8 and P60 (**Fig. 8**), i.e. the regions and ages displaying altered KCC2 amounts in β2-V287L mice. To this purpose, we used the T4 antibody against NKCC1, which was also employed for the analysis of developing WT forebrain (**Fig. 1, 2)**. This antibody was previously used in rodent neocortex, hippocampus and brain stem (Ge *et al.*, 2006; Liu and Wong-Riley, 2012; Marty *et al.*, 2002; Yan *et al.*, 2001) and presents a very good specificity (Chen *et al.*, 2005). Representative images are shown in **Fig. 8A, C, E, G**. In PFC, NKCC1 expression presented no significant genotype-dependent alteration at P8 (**Fig. 8B**) and P60 (**Fig. 8D**). Similar results were obtained in TH (**Fig. 8F, H**).

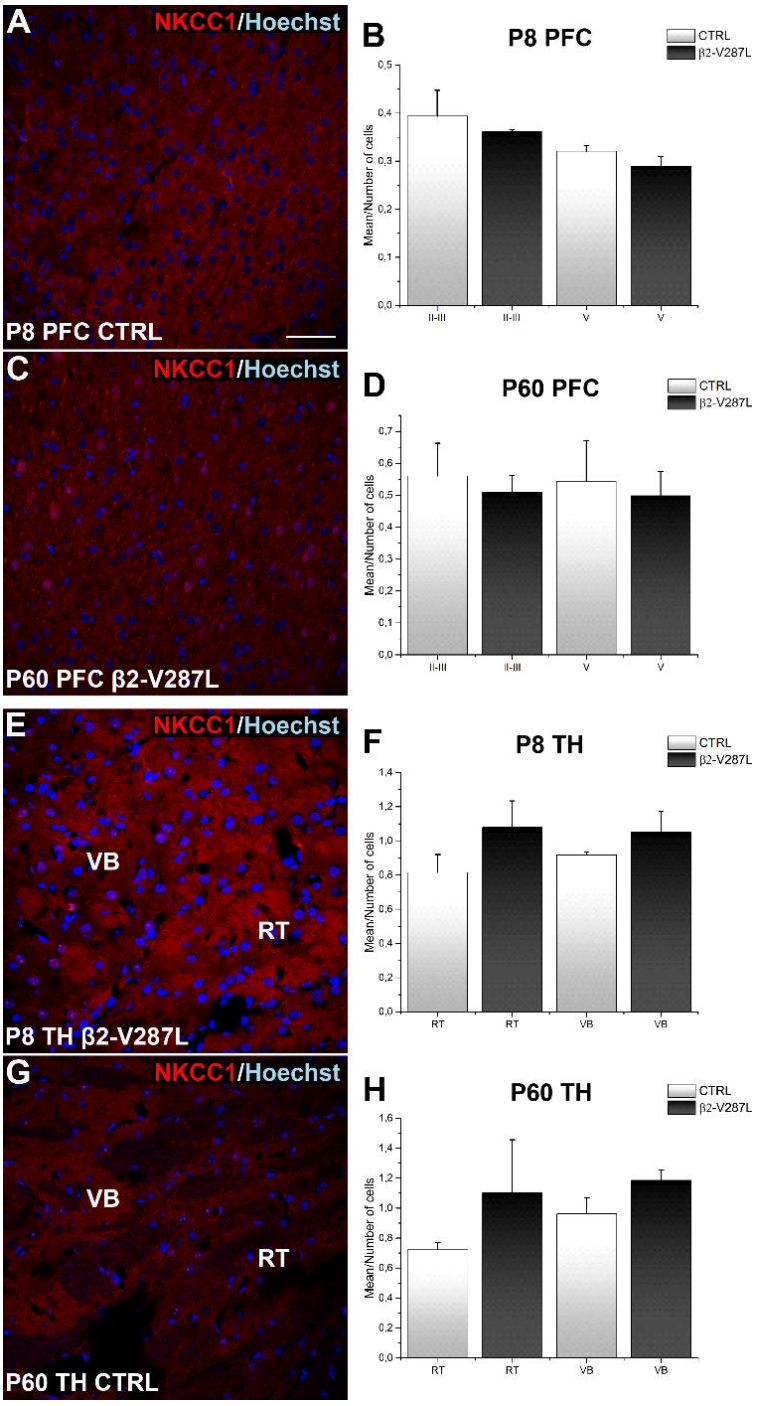

Fig. 8 Effect of β2-V287L on NKCC1 expression in developing PFC and TH. *Representative images of immunofluorescence for NKCC1 (red) counterstained with Hoechst (blue), in PFC layer V (A, C) and TH nuclei (E, G) of CTRL and β2-V287L mice, at P8 (A, E) and at P60 (C, G). The corresponding densitometric analyses are summarized in the bar graphs for layers II-III and V from P8 and P60 mice in PFC (respectively B and D) and in thalamic nuclei RT and VB (F, H), at P8 (B, F) and P60 (D, H). Data are expressed as mean fluorescence intensity divided by the number of neurons. At P8 (n=3) and P60 (n=3), no significant differences were observed in NKCC1 expression between CTRL and β2-V287L, in either PFC or TH. For example, in RT at P60, the mean fluorescence per cell was 0.73 ± 0.046 in CTRL, and 1.1 ± 0.35 in β2-V287L (p=0.396; DF=2.07; unpaired t-test, assuming unequal variances). In VB, the corresponding values were 0.96 ± 0.1 (CTRL) and 1.13 ± 0.09 (β2-V287; p=0.27; DF=4; unpaired t-test, assuming equal variances). Scale bar=20 µm.*

β2-V287L delayed the GABAergic switch in PFC layer V.

The immunofluorescence results show that the retarded expression of KCC2 in PFC layer V of β2-V287L mice was not accompanied by major changes of NKCC1. We thus hypothesized that a lower ratio between the amounts of KCC2 and NKCC1 could be associated with a delayed GABAergic switch. This was tested by measuring E_{GABA} in pyramidal cells of PFC layer V, in brain slices from P8-P9 and adult mice (older than P40). Layer V is prominent in the premotor Fr2 PFC, and presents large pyramidal neurons that are well recognizable since early postnatal stages. The morphological and electrophysiological properties of these neurons were previously described in detail (Aracri *et al.*, 2010, 2013, 2015). In brief, they display regular spiking with frequencies between 10 and 30 Hz and moderate adaptation, in the presence of depolarizing stimuli of 150 to 300 pA. The electrophysiological features of these cells are reported in **Table 2**, for a representative sample of P37-P50 mice bearing or not β2-V287L. No statistical difference was observed between CTRL and β2-V287L in V_{rest}, spike width, the ratio between the fourth and the first spike intervals, and after-hyperpolarization (with unpaired t-test). Similar values were measured in the second postnatal week (data not shown). In such pyramidal cells, we measured E_{GABA} with the perforated patch method, to avoid perturbing $[Cl^-]_i$. Representative GABAergic current traces obtained by applying voltage ramps from -85 to -40 mV (or -80 to -20 mV, at P8-P9) are displayed in **Fig. 9A**, for the indicated experimental groups. During brain maturation, E_{GABA} progressively hyperpolarized, shifting from -48.6 ± 2.03 mV at P8-P9 (15 cells were sampled from 5 mice), to -58 ± 1.7 mV in adult mice (31 cells, from 10 mice; $p < 0.01$, compared with the younger mice; unpaired t-test). A similar pattern was observed in adult β2-V287L, where E_{GABA} was -56 ± 2.5 mV (13 cells, from 5 mice; not statistically different from CTRL, with unpaired t-test). However, at P8-P9, in β2-V287L mice E_{GABA} was more depolarized than in the controls (-42 ± 1.65 mV; 11 cells from 4 mice; $p < 0.05$, compared with CTRL, with unpaired t-test). These data are summarized **Fig. 9B**. They show that, in PFC layer V, the time course of E_{GABA} hyperpolarization was delayed in β2-V287L mice, in agreement with our immunofluorescence results.

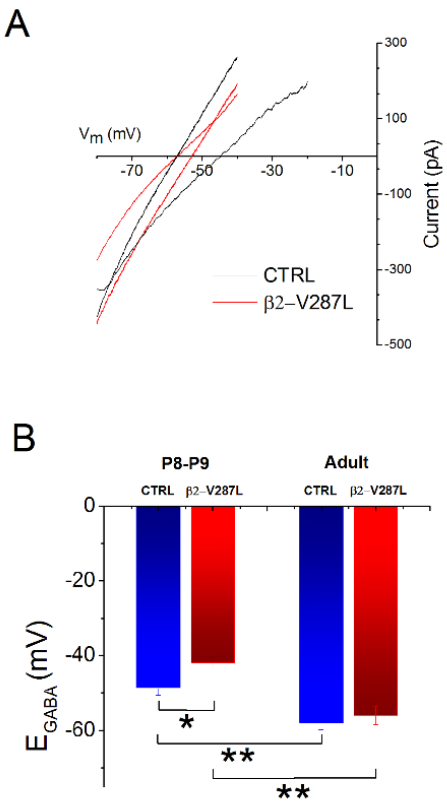

Fig. 9 The effect of β2-V287L on the GABAergic switch.
The time-course of E_{GABA} was followed by perforated-patch experiments. Layer V pyramidal neurons were studied at P8-P9 or adult stages. (A) Representative current traces (averages of 5 trials), elicited by voltage ramps (500 ms duration), in β2-V287L or CTRL mice, as indicated. The ramps between -85 and -40 mV are relative to adult mice. The ramp between -80 and -20 mV is relative to a P8 mouse. The background current was always subtracted to the current measured in the presence of GABA. (B) Average E_{GABA} values at the indicated stages, in CTRL and β2-V287L mice. Detailed statistics are given in the main text.

Table 2. Expression of β2-V287L did not alter V_{rest} and the firing properties of pyramidal cells in PFC layer V.

	V_{rest} (mV)	Spike width (ms)	4th spike interval/ 1st spike interval	AHP mV	*N*
CTRL	-69.4 ± 0.63	1.52 ± 0.08	1.8 ± 0.1	-9.3 ± 0.49	11
β2-V287L	-68.9 ± 0.52	1.51 ± 0.05	1.9 ± 0.09	-9.3 ± 0.59	9

Mice were aged P37-P50. The ratios between the fourth and the first spike interval were calculated in the presence of a 200 pA stimulation, and average firing frequency of ~15 Hz. No statistical difference was observed between mice expressing or not β2-V287L (with unpaired t-test). AHP: after-hyperpolarization.

DISCUSSION

We have analyzed the distribution of NKCC1 and KCC2 in the murine neocortex and TH, at different developmental stages. The study was carried out on both WT and a double-transgenic murine model of ADNFLE. The main finding was that mice carrying the mutant nAChR subunit β2-V287L displayed a delayed surface expression of KCC2 (but not NKCC1) in PFC layer V, during the first postnatal weeks. This led to a transient decrease in the ratio between KCC2 and NKCC1, which was accompanied by a retarded GABAergic switch. Moreover, expression of β2-V287L was also correlated to changes in KCC2 expression in adult PFC and RT thalamic nucleus.

Regional distribution of NKCC1 and KCC2 in postnatal neocortex

Previous work in rodents revealed a complex timing and cellular distribution of NKCC1 expression, in different brain regions**.** Nonetheless, our data agree with the frequent observation that the NKCC1 messenger and protein reach the highest amounts in the neocortex between P7 and P21 (Clayton *et al.*, 1998; Dzhala *et al.*, 2005; Plotkin *et al.*, 1997; Wang *et al.*, 2002; Yan *et al.*, 2001). Whether these levels of expression are retained in the adult is more controversial, as results depend on species as well as on the used antibodies and probes (Clayton *et al.*, 1998; Dzhala *et al.*, 2005; Hübner *et al.*, 2001; Plotkin *et al.*, 1997; Wang *et al.*, 2002; Yan *et al.*, 2001). Our results in both WT and double-transgenic mice suggest that the surface amount of NKCC1 remains overall stable in the mature PFC.

As for KCC2, at birth it was specifically localized in the marginal zone and infragranular layers. Its expression increased thereafter, and reached the adult distribution by the third postnatal week, in both WT and double-transgenic mice. This process paralleled the GABAergic switch, which in neocortex and hippocampus is delayed compared to the subcortical structures (Fiumelli and Woodin, 2007; Kovács *et al.*, 2014). Once again, our results broadly agree with previous results in mouse showing that KCC2 increases in postnatal stages, although regional exceptions are observed (Kovács *et al.*, 2014; Markkanen *et al.*, 2014; Wang *et al.*, 2002). They also agree with several non-systematic determinations in rat (Lacoh *et al.*, 2013), and human tissue (Hyde *et al.*, 2011). Moreover, we found KCC2 expression to be more precocious in SS. Together with other observations on more specific markers (Aracri *et al.*, 2013; Hyde *et al.*, 2011), these results support the notion that PFC matures more slowly than other brain regions, which could make it more liable to develop pathologies

related to network maturation, such as certain forms of epilepsy and schizophrenia (Hyde *et al.*, 2011; Kaila *et al.*, 2014a; Kovács *et al.*, 2014; Lacoh *et al.*, 2013).

Cotransporters' distribution in thalamic nuclei

Minor differences were observed in the postnatal amounts of NKCC1 at the tested stages, in both WT and double-transgenic mice. A more complex pattern was displayed by KCC2. In WT mice, KCC2 was found in VLG and RT as early as E14-E15, and conspicuous expression was observed at birth in all TH nuclei (**Table 1**). Its amount remained relatively stable thereafter, except in RT, where a transient KCC2 decrease was observed at the end of the first postnatal weeks, in both WT (**Table 1**) and double-transgenic mice (see text). Although no other systematic comparison of the KCC2 distribution in mouse TH is available, previous evidence also points to early KCC2 expression in TH nuclei (Horn *et al.*, 2010; Hübner *et al.*, 2001; Li *et al.*, 2002; Markkanen *et al.*, 2014; Stein *et al.*, 2004; Wang *et al.*, 2002). This likely reflects the quicker time course of thalamic circuit wiring, which is complete by P14-P15 (Amadeo et *al.*, 2001). In fact, $[Cl^-]_i$ is essentially stable by the second postnatal week in rat VB (Glykys *et al.*, 2009). More specifically, the so-called relay nuclei (comprising the anterior region), show a rapid maturation that reflects the early establishment of the connections implicated in sensory map topography (Lopez-Bendito *et al.*, 2003). By contrast, the adult RT is characterized by a weaker KCC2 immunolabeling compared with the more caudal adjacent relay nuclei (Barthò *et al.*, 2004). Our results show that such difference is not precocious, but is caused by a postnatal decrease of KCC2 in RT. Although little is known about the development of synaptic connections in RT (Amadeo *et al.*, 2001; Hou *et al.*, 2016; Nagaeva and Akhamadeev, 2006), we hypothesize that proper synaptogenesis here requires KCC2 amounts similar to those present in other TH nuclei. Subsequently, KCC2 would stabilize at lower levels in the adult RT, where E_{GABA} is more depolarized than in relay cells (Barthò *et al.*, 2004; Sun *et al.*, 2013; Ulrich and Huguenard, 1997), and the reciprocal GABAergic connections lead to excitatory effects (Sun *et al.*, 2012).

Cellular distribution of NKCC1 and KCC2 in neocortex and thalamus

In neocortex and TH, our confocal and ultrastructural analysis showed wide expression of NKCC1 in neurons, axons, synaptic terminals and astrocytes in agreement with previous results (Hübner *et al.*, 2001; Wang *et al.*, 2002; Yan *et al.*,

2001). NKCC1 was mainly found in the apical dendrites of cortical pyramidal neurons and in myelinated fiber bundles in TH, suggesting that specific mechanisms of NKCC1 regulation operate in distinct neuronal compartments (Hübner *et al.*, 2001; Yan *et al.*, 2001). Moreover, electron and confocal microscopy revealed NKCC1 in synaptic terminals. In particular, NKCC1 was found in glutamatergic (VGLUT1+) terminals, especially in adult PFC. In contrast, NKCC1 was rarely found in GABAergic (VGAT+) terminals, except in developing TH. The study of NKCC1 expression and function in presynaptic terminals is still in its infancy. Physiological evidence indicates that presynaptic NKCC1 can stimulate (Bos *et al.*, 2011) as well as inhibit (Shen *et al.*, 2013) neurotransmitter release, making it difficult to provide a general interpretation of our results. In immature rat spinal cord, NKCC1 activity enhances transmitter release from afferent fibers by favoring a GABA-dependent presynaptic depolarization (Bos *et al.*, 2011). We can hypothesize that a similar mechanism is operant in the developing TH, thus facilitating the usual depolarizing role of GABA in early stages. In contrast, NKCC1 has been found to inhibit glutamate release in photoreceptors (Shen *et al.*, 2013), a mechanism worth further investigation in the PFC VGLUT1+ terminals.

At variance with NKCC1, the cellular distribution of KCC2 was different in cortical and TH neurons. In neonatal neocortex, KCC2 was mainly localized in cell bodies of pyramidal and GABAergic neurons. During the first postnatal week, KCC2 shifted to cell membranes and dendrites, even though a significant amount of the transporter was retained on the surface of pyramidal neurons' somata. This presumably reflects the high density of GABAergic synapses around pyramidal cell bodies. Such a pattern is broadly similar to the one observed in other species (Dzhala *et al.*, 2005; Hyde *et al.*, 2011; Kovács *et al.*, 2014; Li *et al.*, 2007; Stein *et al.*, 2004). On the contrary, the KCC2 immunoreactivity of TH nuclei at birth was much closer to the adult's; this is consistent with the concept that, in rodents, KCC2 appears earlier in the TH *anlage* than in neocortex. The KCC2+ outlines observed around pyramidal cell bodies were absent or discontinuous in cortical and TH GABAergic cells, where KCC2 immunoreactivity was mainly confined to the dendrites. We attribute such difference to the relatively low average density of reciprocal GABAergic terminals among inhibitory interneurons in neocortex and TH (Aracri *et al.*, 2017; Hou *et al.*, 2016; Pi *et al.*, 2013).

The effect of β2-V287L on cotransporters' amounts and the GABAergic switch

In rodent neocortex, the nAChR subunit expression peaks in the second postnatal week, and recent lines of evidence indicate that synaptic maturation is regulated by both α7- and β2-containing nAChRs (Molas and Dierssen, 2014). Because the maximal nAChR expression is concomitant with the GABAergic switch, we studied if β2-V287L affected the Cl^- cotransporters. Between the first and the second postnatal week, the increase of KCC2 expression was delayed by β2-V287L, in PFC layer V. Since the effect was not accompanied by any alteration of NKCC1, we expected mice expressing β2-V287L to also display a more depolarized E_{GABA}, around P8. In fact, the GABAergic switch was delayed in these animals. Our data suggest that a regulatory interaction occurs between KCC2 and heteromeric nAChRs during synaptogenesis. The specific effect observed in layer V is consistent with the fact that, in this layer, the action of ACh is dominated by β2-containing nAChRs (Aracri *et al.*, 2013; Poorthuis *et al.*, 2013). Previous work also showed that expression of β2-V287L does not change the amount of heteromeric nAChRs on the plasma membrane (Manfredi *et al.*, 2009). Therefore, we attribute the action of the mutant subunit to the functional alterations it produces on nAChRs, rather than to an overall alteration of nAChR expression. Both β2-containing nAChRs (Lozada *et al.*, 2012; Molas and Dierssen, 2014) and KCC2 (Fiumelli *et al.*, 2013; Li *et al.*, 2007) regulate the formation and maturation of dendritic spines by mechanisms that are thought to involve the actin cytoskeleton. Because activating nAChRs leads to both membrane depolarization and Ca^{2+} influx, hyperfunctional mutant receptors containing β2-V287L (De Fusco *et al.*, 2000) could alter KCC2 expression by interfering with calcium signals. An alternative explanation is based on the finding that β2-V287L, as well as other ADNFLE mutations, favors the assembly of the high-affinity $(\alpha4)_2(\beta2)_3$ nAChR stoichiometry with respect to the low affinity $(\alpha4)_3(\beta2)_2$ subtype (Son *et al.*, 2009). One can hypothesize that the altered proportion of stoichiometric forms, besides altering the receptor's response to the agonist, could modify the nAChR binding to some regulatory element of the dendritic spine machinery, or possibly to KCC2 itself.

Irrespective of the molecular mechanism, the effect we observed around P8 was transient. At P60, the amount of KCC2 in PFC layer V was higher in β2-V287L mice, even though E_{GABA} was similar in adult mice carrying or not the transgene. Because layer V is highly susceptible to develop seizures (Telfeian and Connors, 1998), we

hypothesize that the steady-state increase of KCC2 in the mutant is a compensatory mechanism. A higher local Cl^- turnover would be necessary to sustain inhibition in an overactive network, and prevent a significant alteration of the steady state Cl^- levels. This explanation would be consistent with the observation that in chronic epileptic conditions (Karlocai *et al.*, 2016; Pathak *et al.*, 2007), or peritumoral tissue (Conti *et al.*, 2011), the KCC2 amounts usually increase, which points to a long-term compensation of hyperexcitability. In fact, deleting KCC2 in mice facilitates epileptiform activity (Tornberg *et al.*, 2005; Woo *et al.*, 2002), and mutations impairing KCC2 are linked to human epilepsy (Kahle *et al.*, 2014; Puskarjov *et al.*, 2014). It must be however recalled that the physiological meaning of the changes of KCC2 expression observed in epileptic networks is complex and still controversial, as the observed effects depend on the pathophysiological context and the studied region. For example, in temporal lobe, acutely induced epileptiform activity (Puskarjov *et al.*, 2012; Rivera *et al.*, 2002; Wake *et al.*, 2007), and the induction of status epilepticus (Barmashenko *et al.*, 2011; Li *et al.*, 2008; Pathak *et al.*, 2007) produce a chronic decrease of KCC2 surface expression, which is attributed to the action of higher calpain levels (Kaila *et al.*, 2014b).

As for the thalamic effects of mutant nAChRs, mice bearing β2-V287L displayed a lower KCC2 level in the mature RT nucleus. Differently from the GABAergic cells in adult PFC, in which the somatic expression of nAChRs is population-specific (Aracri *et al.*, 2017), the GABAergic RT neurons in mice express a relatively high density of postsynaptic α4β2 nAChRs. These can effectively trigger action potentials, when the cholinergic afferents are activated (Sun *et al.*, 2013). Therefore, hyperfunctional mutant nAChRs could over-stimulate RT neurons and boost calcium signaling therein. As discussed earlier, this could favor a calpain-dependent KCC2 downregulation. Such a mechanism could also be facilitated by the typical propensity of RT cells to enter into burst-like firing states (Fogerson and Huguenard, 2016).

In conclusion, the retardation of the GABAergic switch we observed in the PFC of mice carrying β2-V287L suggests that the pathogenetic mechanism in ADNFLE comprises physiological alterations during synaptogenesis that are likely to depend on the integrity of GABAergic signaling. In the adult, complex alterations of KCC2 expression were observed in the PFC and RT nucleus of mice expressing the transgene. Understanding the precise functional meaning of these alterations will require deeper studies on the thalamocortical excitability of these mice. Nonetheless,

the fact that no such alteration was observed in SS cortex and the other TH nuclei is consistent with the hypothesis that the effect of β2-V287L is specifically related to frontal hyperexcitability during sleep.

REFERENCES

Amadeo A, Ortino B, Frassoni C (2001) *Parvalbumin and GABA in the developing somatosensory thalamus of the rat: an immunocytochemical ultrastructural correlation.* Anat Embryol 203:109-119.

Aracri P, Consonni S, Morini R, Perrella M, Rodighiero S, Amadeo A, Becchetti A (2010) *Tonic modulation of GABA release by nicotinic acetylcholine receptors in layer V of the murine prefrontal cortex.* Cereb Cortex 20:1539-1555.

Aracri P, Amadeo A, Pasini ME, Fascio U, Becchetti A (2013) *Regulation of glutamate release by heteromeric nicotinic receptors in layer V of the secondary motor region (Fr2) in the dorsomedial shoulder of prefrontal cortex in mouse.* Synapse 67:338-357.

Aracri P, Banfi D, Pasini ME, Amadeo A, Becchetti A (2015) *Orexin (hypocretin) regulates glutamate input to fast-spiking interneurons in layer V of the Fr2 region of the murine prefrontal cortex.* Cereb Cortex 25:1330-1347.

Aracri P, Meneghini S, Coatti A, Amadeo A, Becchetti A (2017) *α4β2* nicotinic receptors stimulate GABA release onto fast-spiking cells in layer V of mouse prefrontal (Fr2) cortex.* Neuroscience 340:48-61.

Aronica E, Boer K, Redeker S, Spliet WG, van Rijen PC, Troost D, Gorter JA (2007) *Differential expression patterns of chloride transporters, Na^+-K^+-2Cl^--cotransporters and K^+-Cl^--cotransporter, in epilepsy-associated malformations of cortical development.* Neuroscience 145:185-196.

Awad PN, Sanon NT, Chattopadhyaya B, Carriço JN, Ouardouz M, Gagné J, Duss S, Wolf D, Desgent S, Cancedda L, Carmant L, Di Cristo G (2016) *Reducing premature KCC2 expression rescues seizure susceptibility and spine morphology in atypical febrile seizures.* Neurobiol Dis 91:10-20.

Barmashenko G, Hefft S, Aertsen A, Kirschstein T, Köhling R (2011) *Positive shifts of the $GABA_A$ receptor reversal potential due to altered chloride homeostasis is widespread after status epilepticus.* Epilepsia 52:1570-1578.

Barthó P, Payne JA, Freund TF, Acsády L (2004) *Differential distribution of the KCl cotransporter KCC2 in thalamic relay and reticular nuclei.* Eur J Neurosci 20:965-975.

Becchetti A, Aracri P, Meneghini S, Brusco S, Amadeo A (2015) *The role of neuronal nicotinic acetylcholine receptors in autosomal dominant nocturnal frontal lobe epilepsy.* Front Physiol 6:22.

Ben-Ari Y, Gaiarsa JL, Tyzio R, Khazipov R (2007) *GABA: a pioneer transmitter that excites immature neurons and generates primitive oscillations.* Physiol Rev 87:1215-1284.

Bolte S, Cordelières FP (2006) *A guided tour into subcellular colocalization analysis in light microscopy.* J Microsc 224:213-232.

Bos R, Brocard F, Vinay L (2011) *Primary afferent terminals acting as excitatory interneurons contribute to spontaneous motor activities in the immature spinal cord.* J Neurosci 31:10184-10188.

Cancedda L, Fiumelli H, Chen K, Poo MM (2007) *Excitatory GABA action is essential for morphological maturation of cortical neurons in vivo.* J Neurosci 27:5224-5235.

Chen H, Luo J, Kintner DB, Shull GE, Sun D (2005) *Na(+)-dependent chloride transporter (NKCC1)-null mice exhibit less gray and white matter damage after focal cerebral ischemia.* J Cereb Blood Flow Metab 25:54–66.

Clayton GH, Owens GC, Wolff JS, Smith RL (1998) *Ontogeny of cation-Cl^- cotransporter expression in rat neocortex.* Brain Res Dev Brain Res 109:281-292.

Conti L, Palma E, Roseti C, Lauro C, Cipriani R, de Groot M, Aronica E, Limatola C (2011) *Anomalous levels of Cl^- transporters cause a decrease of GABAergic inhibition in human peritumoral epileptic cortex.* Epilepsia 52:1635-1644.

De Fusco M, Becchetti A, Patrignani A, Annesi G, Gambardella A, Quattrone A, Ballabio A, Wanke E, Casari G (2000) *The nicotinic receptor β2 subunit is mutant in nocturnal frontal lobe epilepsy.* Nat Genet 26:275-276.

Dzhala VI, Talos DM, Sdrulla DA, Brumback AC, Mathews GC, Benke TA, Delpire E, Jensen FE, Staley KJ (2005) *NKCC1 transporter facilitates seizures in the developing brain.* Nat Med 11:1205-1213.

Fiumelli H, Woodin MA (2007) *Role of activity-dependent regulation of neuronal chloride homeostasis in development.* Curr Opin Neurobiol 17:81-86.

Fiumelli H, Briner A, Puskarjov M, Blaesse P, Belem BJ, Dayer AG, Kaila K, Martin JL, Vutskits L (2013) *An ion transport-independent role for the cation-chloride cotransporter KCC2 in dendritic spinogenesis in vivo.* Cereb Cortex 23:378-388.

Fogerson PM, Huguenard JR (2016) *Tapping the brakes: cellular and synaptic mechanisms that regulate thalamic oscillations.* Neuron 92: 687-704.

Franklin KBJ, Paxinos G (2008) *The mouse brain in stereotaxic coordinates.* 3rd ed. San Diego (CA): Academic Press. p. 256.

Ge S, Goh EL, Sailor KA, Kitabatake Y, Ming GL, Song H (2006) *GABA regulates synaptic integration of newly generated neurons in the adult brain.* Nature 439:589-593.

Glykys J, Dzhala VI, Kuchibhotla KV, Feng G, Kuner T, Augustine G, Bacskai BJ, Staley KJ (2009) *Differences in cortical versus subcortical GABAergic signaling: a candidate mechanism of electroclinical uncoupling of neonatal seizures.* Neuron 63:657-672.

Graziano A, Liu XB, Murray KD, Jones EG (2008) *Vesicular glutamate transporters define two sets of glutamatergic afferents to the somatosensory thalamus and two thalamocortical projections in the mouse.* J Comp Neurol 507:1258-1276.

Horn Z, Ringstedt T, Blaesse P, Kaila K, Herlenius E (2010) *Premature expression of KCC2 in embryonic mice perturbs neural development by an ion transport-independent mechanism.* Eur J Neurosci 31:2142-2155.

Hou G, Smith AG, Zhang ZW (2016) *Lack of intrinsic GABAergic connections in the thalamic reticular nucleus of the mouse.* J Neurosci 36:7246-7252.

Hübner CA, Lorke DE, Hermans-Borgmeyer I (2001) *Expression of the Na-K-2Cl cotransporter NKCC1 during mouse development.* Mech Dev 102:267-269.

Hyde TM, Lipska BK, Ali T, Mathew SV, Law AJ, Metitiri OE, Straub RE, Ye T, Colantuoni C, Herman MM, Bigelow LB, Weinberger DR, Kleinman JE (2011) *Expression of GABA signaling molecules KCC2, NKCC1, and GAD1 in cortical development and schizophrenia.* J Neurosci 31:11088-11095.

Jensen FE (2011) *Epilepsy as a spectrum disorder: implications from novel clinical and basic neuroscience.* Epilepsia 52(Suppl 1):1-6.

Kahle KT, Merner ND, Friedel P, Silayeva L, Liang B, Khanna A, Shang Y, Lachance-Touchette P, Bourassa C, Levert A, Dion PA, Walcott B, Spiegelman D, Dionne-Laporte A, Hodgkinson A, Awadalla P, Nikbakht H, Majewski J, Cossette P, Deeb TZ, Moss SJ, Medina I, Rouleau GA (2014) *Genetically encoded impairment of neuronal KCC2 cotransporter function in human idiopathic generalized epilepsy.* EMBO Rep 15:766-774.

Kaila K, Price TJ, Payne JA, Puskarjov M, Voipio J (2014a) *Cation-chloride cotransporters in neuronal development, plasticity and disease.* Nat Rev Neurosci 15:637-654.

Kaila K, Ruusuvuori E, Seja P, Voipio J, Puskarjov M (2014b) *GABA actions and ionic plasticity in epilepsy.* Curr Opin Neurobiol 26:34-41.

Karlócai MR, Wittner L, Tóth K, Maglóczky Z, Katarova Z, Rásonyi G, Erőss L, Czirják D, Halász P, Szabó G, Payne JA, Kaila K, Freund TF (2016) *Enhanced expression of potassium-chloride cotransporter KCC2 in human temporal lobe epilepsy.* Brain Struct Funct 221:3601-3615.

Khirug S, Ahmad F, Puskarjov M, Afzalov R, Kaila K, Blaesse P (2010) *A single seizure episode leads to rapid functional activation of KCC2 in the neonatal rat hippocampus.* J Neurosci 30:12028-12035.

Kovács K, Basu K, Rouiller I, Sík A (2014) *Regional differences in the expression of K(+)-Cl(-) 2 cotransporter in the developing rat cortex.* Brain Struct Funct 219:527-538.

Lacoh CM, Bodogan T, Kaila K, Fiumelli H, Vutskits L (2013) *General anaesthetics do not impair developmental expression of the KCC2 potassium-chloride cotransporter in neonatal rats during the brain growth spurt.* Br J Anaesth 110(Suppl 1):i10-i18.

Li H, Tornberg J, Kaila K, Airaksinen MS, Rivera C (2002) *Patterns of cation-chloride cotransporter expression during embryonic rodent CNS development.* Eur J Neurosci 16:2358-2370.

Li H, Khirug S, Cai C, Ludwig A, Blaesse P, Kolikova J, Afzalov R, Coleman SK, Lauri S, Airaksinen MS, Keinänen K, Khiroug L, Saarma M, Kaila K, Rivera C (2007*) KCC2 interacts with the dendritic cytoskeleton to promote spine development.* Neuron 56:1019-1033.

Li X, Zhou J, Chen Z, Chen S, Zhu F, Zhou L (2008) *Long-term expressional changes on Na^+-K^+-Cl^- co-transporter 1 (NKCC1) and K^+-Cl^- co-transporter 2 (KCC2) in CA1 region of hippocampus following lithium-pilocarpine induced status epilepticus (PISE).* Brain Res 1221:141-146.

Liu Q, Wong-Riley MT (2012) *Postnatal development of Na(+)-K(+)-2Cl(-) co-transporter 1 and K(+)-Cl(-) co-transporter 2 immunoreactivity in multiple brain stem respiratory nuclei of the rat.* Neuroscience 210:1-20.

Liu Z, Neff RA, Berg DK (2006) *Sequential interplay of nicotinic and GABAergic signaling guides neuronal development.* Science 314:1610-1613.

Lopez-Bendito G, Molnár Z (2003) *Thalamocortical development: how are we going to get there?* Nat Rev Neurosci 4:276-289.

Lozada AF, Wang X, Gounko NV, Massey KA, Duan J, Liu Z, Berg DK (2012) *Induction of dendritic spines by β2-containing nicotinic receptors.* J Neurosci 32:8391-8400.

Manfredi I, Zani AD, Rampoldi L, Pegorini S, Bernascone I, Moretti M, Gotti C, Croci L, Consalez GG, Ferini-Strambi L, Sala M, Pattini L, Casari G (2009) *Expression of mutant β2 nicotinic receptors during development is crucial for epileptogenesis.* Hum Mol Genet 18:1075-1088.

Mansvelder HD, Role LW (2006) *Neuronal receptors for nicotine: functional diversity and developmental changes. In: Miller MW (Ed) Brain Development. Normal Processes and the Efects of Alcohol and Nicotine.* New York: Oxford University Press. p. 404.

Markkanen M, Karhunen T, Llano O, Ludwig A, Rivera C, Uvarov P, Airaksinen MS (2014) *Distribution of neuronal KCC2a and KCC2b isoforms in mouse CNS.* J Comp Neurol 522:1897-1914.

Marty S, Wehrlé R, Alvarez-Leefmans FJ, Gasnier B, Sotelo C (2002) *Postnatal maturation of Na^+, K^+, $2Cl^-$ cotransporter expression and inhibitory synaptogenesis in the rat hippocampus: an immunocytochemical analysis.* Eur J Neurosci 15:233-245.

Molas S, Dierssen M (2014) *The role of nicotinic receptors in shaping and functioning of the glutamatergic system: a window into cognitive pathology.* Neurosci Biobehav Rev 46:315-325.

Nagaeva DV, Akhamadeev AV (2006) *Structural organization, neurochemical characteristics, and connections of the reticular nucleus of the thalamus.* Neurosci Behav Physiol 36:987-995.

Pathak HR, Weissinger F, Terunuma M, Carlson GC, Hsu FC, Moss SJ, Coulter DA (2007) *Disrupted dentate granule cell chloride regulation enhances synaptic excitability during development of temporal lobe epilepsy.* J Neurosci 27:14012-14022.

Pi HJ, Hangya B, Kvitsiani D, Sanders JI, Huang ZJ, Kepecs A (2013) *Cortical interneurons that specialize in disinhibitory control.* Nature 503:521–524.

Plotkin MD, Snyder EY, Hebert SC, Delpire E (1997) *Expression of the Na-K-2Cl cotransporter is developmentally regulated in postnatal rat brains: a possible mechanism underlying GABA's excitatory role in immature brain.* J Neurobiol 33:781-795.

Poorthuis RB, Bloem B, Schak B, Wester J, de Kock CP, Mansvelder HD (2013) *Layer-specific modulation of the prefrontal cortex by nicotinic acetylcholine receptors.* Cereb Cortex 23:148-161.

Puskarjov M, Ahmad F, Kaila K, Blaesse P (2012) *Activity-dependent cleavage of the K-Cl cotransporter KCC2 mediated by calcium-activated protease calpain.* J Neurosci 32:11356-11364.

Puskarjov M, Seja P, Heron SE, Williams TC, Ahmad F, Iona X, Oliver KL, Grinton BE, Vutskits L, Scheffer IE, Petrou S, Blaesse P, Dibbens LM, Berkovic SF, Kaila K (2014) *A variant of KCC2 from patients with febrile seizures impairs neuronal Cl^- extrusion and dendritic spine formation.* EMBO Rep 15:723-729.

Rivera C, Voipio J, Payne JA, Ruusuvuori E, Lahtinen H, Lamsa K, Pirvola U, Saarma M, Kaila K (1999) *The K^+/Cl^- co-transporter KCC2 renders GABA hyperpolarizing during neuronal maturation.* Nature 397:251-255.

Rivera C, Li H, Thomas-Crusells J, Lahtinen H, Viitanen T, Nanobashvili A, Kokaia Z, Airaksinen MS, Voipio J, Kaila K, Saarma M (2002) *BDNF-induced TrkB activation down-regulates the K^+-Cl^- cotransporter KCC2 and impairs neuronal Cl^- extrusion.* J Cell Biol 159:747-752.

Sedmak G, Jovanov-Milošević N, Puskarjov M, Ulamec M, Krušlin B, Kaila K, Judaš M (2016) *Developmental expression patterns of KCC2 and functionally associated molecules in the human brain.* Cereb Cortex 26:4574-4589.

Shen W, Purpura LA, Li B, Nan C, Chang IJ, Ripps H (2013) *Regulation of synaptic transmission at the photoreceptor terminal: a novel role for the cation–chloride co-transporter NKCC1.* J Physiol 591:133–147.

Shouse MN, Quigg MS (2008) *Chronobiology.* In: Engel JJ, Pedley TA, editors, Epilepsy: a comprehensive textbook, vol 2. Philadelphia: Lippincott Williams and Wilkins. p. 1961-1974.

Son CD, Moss FJ, Cohen BN, Lester HA (2009) *Nicotine normalizes intracellular subunit stoichiometry of nicotinic receptors carrying mutations linked to autosomal dominant nocturnal frontal lobe epilepsy.* Mol Pharmacol 75:1137-1148.

Stein V, Hermans-Borgmeyer I, Jentsch TJ, Hübner CA (2004) *Expression of the KCl cotransporter KCC2 parallels neuronal maturation and the emergence of low intracellular chloride.* J Comp Neurol 468:57-64.

Steinlein OK, Mulley JC, Propping P, Wallace RH, Phillips HA, Sutherland GR, Scheffer IE, Berkovic SF (1995) *A missense mutation in the neuronal nicotinic acetylcholine receptor α4 subunit is associated with autosomal dominant nocturnal frontal lobe epilepsy.* Nat Genet 11:201-203.

Sun YG, Wu CS, Renger JJ, Uebele VN, Lu HC, Beierlein M (2012) *GABAergic synaptic transmission triggers action potentials in thalamic reticular nucleus neurons.* J Neurosci 32:7782–7790.

Sun YG, Pita-Almenar JD, Wu CS, Renger JJ, Uebele VN, Lu HC, Beierlein M (2013) *Biphasic cholinergic synaptic transmission controls action potential activity in thalamic reticular nucleus neurons.* J Neurosci 33:2048 –2059.

Takayama C, Inoue Y (2010) *Developmental localization of potassium chloride co-transporter 2 (KCC2), GABA and vesicular GABA transporter (VGAT) in the postnatal mouse somatosensory cortex.* Neurosci Res 67:137-148.

Talos DM, Sun H, Kosaras B, Joseph A, Folkerth RD, Poduri A, Madsen JR, Black PM, Jensen FE (2012) *Altered inhibition in tuberous sclerosis and type IIb cortical dysplasia.* Ann Neurol 71:539-551.

Telfeian AE, Connors BW (1998) *Layer-specific pathways for the horizontal propagation of epileptiform discharges in neocortex*. Epilepsia 39:700-708.

Tinuper P, Bisulli F, Cross JH, Hesdorffer D, Kahane P, Nobili L, Provini F, Scheffer IE, Tassi L, Vignatelli L, Bassetti C, Cirignotta F, Derry C, Gambardella A, Guerrini R, Halasz P, Licchetta L, Mahowald M, Manni R, Marini C, Mostacci B, Naldi I, Parrino L, Picard F, Pugliatti M, Ryvlin P, Vigevano F, Zucconi M, Berkovic S, Ottman R (2016) *Definition and diagnostic criteria of sleep-related hypermotor epilepsy.* Neurology 86:1834-1842.

Tornberg J, Voikar V, Savilahti H, Rauvala H, Airaksinen MS (2005) *Behavioural phenotypes of hypomorphic KCC2-deficient mice.* Eur J Neurosci 21:1327-1337.

Ulrich D, Huguenard JR (1997) *Nucleus-specific chloride homeostasis in rat thalamus*. J Neurosci 17:2348-2354.

Wake H, Watanabe M, Moorhouse AJ, Kanematsu T, Horibe S, Matsukawa N, Asai K, Ojika K, Hirata M, Nabekura J (2007) *Early changes in KCC2 phosphorylation in response to neuronal stress result in functional downregulation*. J Neurosci 27:1642-1650.

Wang C, Shimizu-Okabe C, Watanabe K, Okabe A, Matsuzaki H, Ogawa T, Mori N, Fukuda A, Sato K (2002) *Developmental changes in KCC1, KCC2, and NKCC1 mRNA expressions in the rat brain.* Brain Res Dev Brain Res 139:59-66.

Woo NS, Lu J, England R, McClellan R, Dufour S, Mount DB, Deutch AY, Lovinger DM, Delpire E (2002) *Hyperexcitability and epilepsy associated with disruption of the mouse neuronal-specific K-Cl cotransporter gene.* Hippocampus 12:258-268.

Yamada J, Zhu G, Okada M, Hirose S, Yoshida S, Shiba Y, Migita K, Mori F, Sugawara T, Chen L, Liu F, Yoshida S, Ueno S, Kaneko S (2013) *A novel prophylactic effect of furosemide treatment on autosomal dominant nocturnal frontal lobe epilepsy (ADNFLE).* Epilepsy Res 107:127-137.

Yan Y, Dempsey RJ, Sun D (2001) Expression of Na(+)-K(+)-Cl(-) cotransporter in rat brain during development and its localization in mature astrocytes. Brain Res 911:43-55.

Zhu L, Polley N, Mathews GC, Delpire E (2008) *NKCC1 and KCC2 prevent hyperexcitability in the mouse hippocampus.* Epilepsy Res 79:201-212

Chapter 3

The Expression of Mutant β2-V287L Nicotinic Receptor Induces Alterations in the Microcircuits of the Prefrontal Cortex

Meneghini S [b], Brusco S [b], Coatti A [b], Aracri P [b], Modena D [a], Carraresi L [d], Arcangeli A [c], Amadeo A [a] and Becchetti A [b] (2017)

The role of neuronal nicotinic receptors in the pathogenesis of Autosomal Dominant Nocturnal Frontal Lobe Epilepsy: a study on wild-type and conditional transgenic mice expressing the β2-V287L subunit.

Abstract book: pp. 30, #93. XIX Scientific Convention Telethon, Riva del Garda, Italy.

Modena D [a], Meneghini S [b], Coatti A [b], Iannantuoni D [a], Corti L [b], Colombo G [b], Ascagni M [e], Madaschi L [e], Amadeo A [a] and Becchetti A [b] (2017)

Mutant nicotinic receptors linked to sleep-related epilepsy alter synaptic balance in the murine prefrontal cortex.

Abstract book: pp. 54. 6th European Synapse Meeting, Milan, Italy.

Modena D [a], Meneghini S [b], Coatti A [b], Colombo G [b], Ascagni M [e], Madaschi L [e], Amadeo A [a] and Becchetti A [b] (2018)

Glutamatergic and cholinergic innervation in the prefrontal cortex of a murine model of Autosomal Dominant Nocturnal Frontal Lobe Epilepsy (ADNFLE).

11th FENS Forum of Neuroscience, Berlin, Germany.

Modena D [a], Meneghini S [b], Colombo G [b], Ascagni M [e], Amadeo A [a] and Becchetti A [b] (2019)

Characterization of two different GABAergic subpopulations in the prefrontal cortex layer V of a sleep-related epilepsy murine model.

48th Meeting of the European Brain Behavior Society, Prague, Czech Republic.

[a] *Department of Biosciences, University of Milano, Via Celoria, 26, 20133 Milano, Italy*
[b] *Department of Biotechnology and Biosciences, and NeuroMI-Milan Center of Neuroscience, University of Milano-Bicocca, Piazza della Scienza, 2, 20126 Milano, Italy*
[c] *Department of Experimental and Clinical Medicine, University of Florence, Largo Brambilla, 3, 50134 Firenze, Italy*
[d] *Dival Toscana Srl, Via Madonna del Piano, 6 – 50019 Sesto Fiorentino, Firenze, Italy*
[e] *Unitech NOLIMITS, University of Milan, Via Golgi 19, 20133 Milano, Italy*

ABSTRACT

Autosomal Dominant Nocturnal Frontal Lobe Epilepsy (ADNFLE) is a focal epilepsy characterized by hyperkinetic seizures frequently arising in the frontal lobe during sleep. ADNFLE tends to begin in childhood and cognitive and psychological alterations may be present. The ADNFLE families often bear mutations on genes coding for subunits of the nicotinic acetylcholine receptors (nAChRs), that in the central nervous system regulate excitability and neurotransmitters release. In layer V of prefrontal cortex (PFC), pyramidal cell activity is mainly controlled by parvalbumin-positive (PV+) fast-spiking (FS) cells and somatostatin-positive (SOM+) regular-spiking non-pyramidal (RSNP) cells. After an extensive morphological analysis of the PFC and its cholinergic and glutamatergic innervation, for which we found no significant differences, we focused our attention on the role of PV+ and SOM+ interneurons in a murine model of ADNFLE expressing the β2-V287L mutant nAChR subunit. We studied the spontaneous excitatory (EPSC) and inhibitory (IPSC) postsynaptic currents in the PFC layer V of adult mice, then we carried out an estimation of the number of both PV+ and SOM+ neurons and VGAT+ (vesicular GABA transporter) and VGLUT1+ (vesicular glutamate transporter 1) synaptic terminals contacting these neurons by immunohistochemical stainings. While in pyramidal neurons the basal ratio of the frequencies of EPSCs and IPSCs increased in mice expressing β2-V287L, an opposite tendency was observed in FS cells. In RSNP cells no significant difference was observed between control and β2-V287L mice. Regarding the estimation of synaptic terminals onto GABAergic interneurons cell bodies, we found a significant increase of VGLUT1+ terminals on PV+ cells, while data on SOM+ cells and of VGAT+ terminals on both SOM+ and PV+ neurons showed no significant differences in the PFC of β2-V287L mice. Our results indicate that β2-V287L increases excitability in layer V, by modifying the synaptic efficacy in both pyramidal and fast-spiking neurons.

INTRODUCTION

Epilepsy is a neurological disorder affecting approximately 50 million people worldwide (Ghasemi and Hadipour-Niktarash, 2015). It is usually caused by an imbalance between excitation and inhibition of neuronal networks, which can lead to an abnormal, excessive or hypersynchronous neuronal activity characteristic of epileptic seizures. Only 30% of the cases have an identifiable aetiology, such as tumors, trauma, infections and metabolic dysfunctions. In the remaining 70% the cause is unknown (Heron *et al.*, 2007). Some forms of epilepsy are due to a genetic predisposition and, especially, to mutations in genes encoding for ion channels and receptors; for this reason, these forms of the pathology are often considered as channelopathies. Autosomal Dominant Nocturnal Frontal Lobe Epilepsy (ADNFLE) is an example of the familial form of epilepsies and, in fact, it was the first epilepsy to be recognized as a channelopathy (Steinlein *et al.*, 1995). It is a focal epilepsy characterized by clusters of hyperkinetic seizures, often accompanied by sudden arousals, mostly occurring during stage 2 of NREM sleep. Attacks arise in the frontal lobe, tend to begin in childhood and cognitive and psychological alterations may be present, but the phenotypes associated with the disease are not uniform (Bertrand *et al.*, 2005). The association between seizures and NREM sleep stages suggests that sleep-controlling brain regions could be involved in the pathogenesis of ADNFLE (Noebels *et al.*, 2012). About 10-15% of the ADNFLE families bear mutations on genes coding for nicotinic acetylcholine receptor (nAChR) subunits and they are inherited as an autosomal dominant trait with penetrance ranging from 60% to 80% (Becchetti *et al.*, 2015; Ghasemi and Hadipour-Niktarash, 2015; Noebels *et al.*, 2012).

To better understand the mechanisms behind epileptogenesis, we studied a murine model of ADNFLE developed by Manfredi and colleagues in 2009. This FVB mouse model carries the V287L missense mutation in *CHRNB2*, the gene encoding for nAChR β2 subunit. Mice expressing these mutant nAChRs present a spontaneous epileptic phenotype during periods of increased delta wave electroencephalogram (EEG) activity, which generally characterizes the resting/sleeping phase in mice. Therefore, this model well reproduces the main features of human ADNFLE (Manfredi *et al.*, 2009). In these mice, β2-V287L needs to be expressed throughout brain development, until the end of the second postnatal week, for seizures to develop, indicating that critical stages of synaptic stabilization are implicated in the pathogenesis

of ADNFLE. These remarks led us to investigate whether expression of β2-V287L affected first of all the morphology of PFC, in addition to GABAergic, glutamatergic and cholinergic systems in mature stages.

The morphological characterization of the double-transgenic murine model showed no differences between control (CTRL) and double-transgenic (β2-V287L) mice regarding cortical thickness and neuronal volume. Similar results were found concerning the GABAergic system. From an electrophysiological standpoint, while in pyramidal neurons the basal ratio of the frequencies of EPSCs and IPSCs increased in mice expressing β2-V287L, an opposite tendency was observed in fast-spiking GABAergic interneurons. In regular-spiking non-pyramidal cells no significant difference was observed between control and β2-V287L mice. We then carried out an estimation of the number of both parvalbumin- (fast-spiking) and somatostatin-positive (regular-spiking non-pyramidal) neurons and VGAT+ and VGLUT1+ (vesicular GABA transporter and vesicular glutamate transporter 1) synaptic terminals contacting these neurons by immunohistochemical stainings, finding a significant increase of VGLUT1 terminals on parvalbumin-positive cells of β2-V287L mice. Our results indicate that β2-V287L increases excitability in layer V, by modifying the synaptic efficacy in both pyramidal and fast-spiking neurons.

EXPERIMENTAL PROCEDURES

Animals

Mice were housed in SPF conditions on a 12h light-dark cycle, at 21 ± 1°C, 55 ± 10% humidity and free access to food and water. Mice genotyping was carried out as previously described (Manfredi *et al.*, 2009). All procedures followed the Italian law (2014/26, implementing the 2010/63/UE) and were approved by the local Ethical Committees and the Italian Ministry of Health. For the different analyses we used FVB mice (Harlan) of either sex, at the postnatal (P) day 60 or 90. The transgenic strain we used was the S3 line of double-transgenic FVB (tTA:Chrnb2V287L) mice, which express β2-V287L under a tetracycline-controlled transcriptional activator (tTA). These mice were compared with their littermates not expressing β2-V287L, which were either WT or bearing TRE-Chrnb2V287L or PrnP-tTA genotypes (Manfredi *et al.*, 2009). For clarity, mice expressing the transgene are hereafter denoted as β2-V287L, while the control littermates are denoted as controls (CTRL). The analyses were carried out on at least 3 animals for each experimental group (CTRL and β2-V287L). Electrophysiological recordings were carried out on 15 CTRL (all PrnP-tTA) and 9 β2-V287L adult (P30) mice. No morphological or electrophysiological difference was observed between sexes.

Brain regions

For immunohistochemistry analyses, by PFC we refer to the entire secondary motor region (also known as M2, or Fr2) in the dorsomedial shoulder of the prefrontal cortex. According to Franklin and Paxinos (2008), coronal prefrontal sections were cut between +2.58 and -0.06 mm from bregma. For somatosensory cortex (SS), we sampled the extended SS region between +1.54 and -1.64 mm from bregma. For electrophysiological experiments, coronal PFC (Fr2) slices were cut between +2.68 mm and +2.10 mm from bregma.

Tissue preparation for immunohistochemistry

Adult mice were anesthetized with isoflurane and intraperitoneal 4% chloral hydrate (2 ml/100 g) and sacrificed by intracardiac perfusion as described (Aracri *et al.*, 2013). The brains were immersed in 4% paraformaldehyde in phosphate buffer (PB), for 24 h

at 4°C. Next, brains were stored in the same fresh fixative. Serial coronal brain sections (50 µm thick) were cut with a VT1000S vibratome (Leica Microsystems).

Primary antibodies

Anti-β2 nAChR: polyclonal, made in rabbit against the C-terminal 493-502 amino acids of nAChRs β2 subunit (Immunological Sciences; 1:200). Anti-SYN (synaptophysin): monoclonal, made in mouse against human protein (Dako; 1:100). Anti-ChAT (choline acetyltransferase): polyclonal, made in goat against against human placental enzyme (Millipore; 1:50). Anti-VAChT (vesicular ACh transporter): polyclonal, made in goat against C-terminal 475-530 amino acids of rat protein (Synaptic Systems; 1:300). Anti-PV (parvalbumin): polyclonal, made in rabbit against the rat muscular PV (Swant; 1:2000). Anti-SOM (somatostatin): monoclonal, made in mouse against amino acids 25-116 of human somatostatin (Santa Cruz; 1:200); anti-VGAT (vesicular GABA transporter): polyclonal, made in rabbit against the synthetic peptide corresponding to the N-terminal 75-87 amino acids of the rat protein (Synaptic Systems; 1:800). Anti-$GABA_A$ α1 subunit (Sigma): polyclonal, made in rabbit against the synthetic peptide corresponding to 28-43 amino acids of the protein (Sigma; 1:300). Anti-GAD67 (glutamic acid decarboxylase type 1/67kDa): polyclonal, made in goat against the human recombinant glutamic acid decarboxylase type 1, rhGAD1 (aa 2-97) derived from *E. coli* (R&D Systems; 1:300). Anti-VGLUT1 (vesicular glutamate transporter type 1): polyclonal, made in rabbit against Strep-TagR-fusion proteins containing the amino acid residues 456–560 of the rat VGLUT1/BNPI (brain-specific Na1-dependent inorganic phosphate transporter; Synaptic Systems; 1:500).

Immunoperoxidase histochemistry for light microscopy

The immunoreaction was carried out as previously reported (Aracri *et al.*, 2010), except that a mild pretreatment with ethanol (10%, 25%, 10% in phosphate buffered saline, PBS) was applied to increase the immunoreagent penetration. For SOM immunostaining a solution with nickel (Vector Laboratories) was added to improve reaction product visibility. Reaction specificity was assessed by negative controls, e.g. omission of primary antiserum. In these cases, no specific staining was observed. Briefly, sections were examined on a Leica DMRB microscope, and images were acquired using a Leica DCF 480 camera coupled to a personal computer or slide scanner Nanozoomer S60 (Hamamatsu), for densitometric immunoperoxidase

analysis. At least 3 mice were examined for each staining, with a maximum of 9 animals for VGLUT1 densitometric analysis. We analyzed at least 3-4 sections for each cortical region (PFC, SS).

Densitometric immunoperoxidase analysis

To perform a densitometric analysis on immunoperoxidase-stained sections, slices from P90 double-transgenic and control littermates, with layer II-III and V of the PFC and somatosensory cortex (SS) were chosen and the whole sections were acquired with the slide scanner Nanozoomer S60 (Hamamatsu). The images were magnified and saved at 10X with the software NDPview2 (Hamamatsu) to show only the supragranular or the infragranular layers from one region at once, and two different regions of interest (ROIs) were designed on ImageJ for PFC and SS. 3 slices for each animal were analyzed; from the first one (without the SS) 4 images were obtained, while from the other 2 sections 8 images (PFC II-III and V right and left hemisphere, SS II-III and V right and left hemisphere) were acquired, with a total of 20 cut images for each mouse. The images were then deconvoluted and spatially calibrated with ImageJ (NIH) software, and from each of them a mean intensity of the signal (in optical density; OD) of the pixels in the ROI was obtained and compared between controls and β2-V287L mice.

Immunofluorescence histochemistry

Sections were permeabilized and blocked as described for immunoperoxidase histochemistry. They were next incubated for two nights in a mixture of one/two primary antibodies, after staining with NeuroTrace™ (1:50, Molecular Probes) and/or before staining with Hoechst (Molecular Probes), as necessary for cytoarchitecture analysis and cell counting. For NeuroTrace™ staining, sections were treated as previously described (Aracri *et al.*, 2010). After washing the primary antibodies with PBS, sections were incubated in the following mixture of secondary fluorescent antibodies: Alexa Fluor™488 or CF™488A-conjugated donkey anti-rabbit IgG (Invitrogen and Biotium, respectively; 1:200), CF™568-conjugated donkey anti-mouse (Sigma; 1:200); Alexa Fluor™488-conjugated donkey anti-goat (Invitrogen; 1:200), for 75 min at room temperature. For anti-SOM and anti-β2 nAChR, biotinylated horse anti-mouse and biotinylated goat anti-rabbit (Vector Laboratories) were respectively used for 75 min at room temperature, followed by PBS rinsing and CF™568-conjugated or Alexa

Fluor™488-conjugated streptavidin incubation at room temperature for 2 hours. After rinsing, samples were mounted on coverslips (sometimes after nuclear staining with Hoechst) with PBS/glycerol (1:1 v/v) or Vectashield™ (Vector Laboratories) and inspected with a Leica TCS-NT or Nikon A1 laser scanning confocal microscope, to visualize double or triple fluorescent labeling.

Colocalization and densitometric analysis

Confocal micrographs were collected at 20X with a Leica SP2 or Nikon A1 laser scanning confocal microscope and analyzed with ImageJ for densitometric analysis. Identical parameters were used to acquire images for the same antigen, as previously described (Aracri *et al.*, 2013). In brief, nonoverlapping pictures were acquired in at least two different sections for neocortex, so that double immunolabeling was studied in 3 or 4 fields per region in each animal. For densitometric analysis, at least three/four distinct images of cortical layers with NeuroTrace™ and/or nuclear counterstaining were acquired to sample the different areas. For each animal, the mean fluorescence intensity of each image was sometimes divided by the number of neurons therein (counted with ImageJ), this normalization depended on the antigen distribution (somatodendritic or synaptic). The values thus obtained were averaged among animals before plotting. The degree of colocalization of different neuronal markers was calculated by comparing the Manders' coefficients, computed with the JACoP plug-in of ImageJ software (Bolte and Cordeliéres, 2006).

Stereological cell countings and cortical thickness measurement

Stereology is a methodology for the morphometric evaluation and for the cell counting in complex structures based on the technique known as Unbiased Optical Fractionator Stereology (Optical Dissector), that allows a three-dimensional interpretation of two-dimensional cross sections of materials or tissues. Stereology utilizes random, systematic sampling to provide unbiased and quantitative data. To obtain these data, the sections need to be equally distant from each other, spanning for the entire, or almost, volume of the target area. To quantify the number of PV+ and SOM+ neurons in the specific brain regions of immunoperoxidase-stained sections, stereological countings were carried out with the Optical Dissector workflow of StereoInvestigator 11 (MicroBrightField MBF Bioscience) software, wired to an optical microscope. Sections containing PFC, from 2.58 to 0.50 from bregma, and SS, from

1.54 to 0.02 from bregma, equally distant from each other, were chosen. With 4X objective, the regions were observed and the ROIs were defined. The workflow then applies a grid on the ROI. The grid is then divided in smaller areas called dissectors, that are equally distant from each other, and in which the count is carried out randomly and systematically. Each dissector has two green adjacent sides and two red adjacent sides. To standardize the count, only the cell bodies in the dissector and on the green sides were counted at 40X. For these counts, grids of 160x160 µm and 80x80 µm dissectors were chosen. In addition to the XY movement, the workflow allows the operator to investigate the whole thickness of the sections, thus obtaining an estimation of the counted cell number in the whole volume of the interested area.

For the measurement of cortical thickness, thionine-stained sections were chosen with a distance of 350 µm from +2.80 mm to 0.26 mm from bregma for the PFC, while for the SS the sections were chosen with a 750 µm distance from +1.98 mm to -1.82 mm from bregma. For each genotype and area, 30 different measurements of cortical thickness were performed with QCapture Pro 7 (QImaging) software.

Reconstruction and estimation of glutamatergic and GABAergic terminals

Analysis of double immunofluorescence for PV+, SOM+ and VGLUT1 and VGAT was carried out with ArivisVision4D software (Arivis AG, Munich, Germany). ArivisVision4D allows the three-dimensional reconstructions of cells, neurites and synapses with the creation of pipelines, that are sequences of operations performed on the images. The pipelines allow the identification and the following segmentation of objects based on one or more characteristics of them. After the reconstruction, it is possible to perform measurements, estimations and colocalization analysis. The analysis of the number of contacts between SOM+ or PV+ cell bodies with cholinergic (VAChT+), glutamatergic (VGLUT1+) and GABAergic (VGAT+) terminals was carried out on at least 20 neurons for each animal. The cells were acquired at the Nikon A1 confocal microscope, on their whole thickness at 60X with 1.6 zoom of the PFC layer V of 3 wt animals for VAChT and 3 CTRL and 3 β2-V287L mice for VGLUT1 and VGAT. After the automatic calibration of the images, a suitable pipeline for the identification and reconstruction of the VAChT+, VGLUT1+ and VGAT+ terminals was created and applied, by setting a signal intensity threshold and an object diameter appropriate to the stainings (800 nm). The cell bodies were identified and drawn manually on each optical plane. After the segmentation, a different pipeline was created, allowing the

counting of the target objects, the terminals contacting, respectively, SOM+ and PV+ cell bodies. The results were exported on Excel files and the terminals estimations were normalized on the neurons number. An analysis of distribution of terminals for each animal was also performed.

Whole-cell recordings in brain slices

PFC coronal sections were cut between +2.68 mm and +2.10 mm from bregma. During this procedure, brains (from P20-P50 mice) were placed in ice-cold solution containing (mM): 87 NaCl, 21 $NaHCO_3$, 1.25 NaH_2PO_4, 7 $MgCl_2$, 0.5 $CaCl_2$, 2.5 KCl, 25 D-glucose, 75 sucrose, 400 µM ascorbic acid, and aerated with 95% O_2 and 5% CO_2 (pH 7.4). Slices (300 µm thick) were cut with a VT1000S vibratome (Leica Microsystems), incubated at 32-33°C for 30 min in the above solution, and maintained at room temperature before being transferred to the recording chamber. Cells were examined with an Eclipse E600FN microscope, equipped with a water immersion differential interference contrast objective (Nikon Instruments), and an infrared digital CCD (C8484-05G01) equipped with HCImage Live acquisition software (Hamamatsu). Neurons were voltage- or current-clamped with a Multiclamp 700A (Molecular Devices), at 33-34°C. Micropipettes (2-3 MΩ) were pulled from borosilicate capillaries (Corning) with a P-97 Flaming/Brown Micropipette Puller (Sutter Instruments). The cell capacitance and series resistance (up to 75%) were always compensated. Series resistance was generally below 10 MΩ. Input resistance was usually close to 100 MΩ. Postsynaptic currents were low-pass filtered at 2 kHz and digitized at 5 kHz, with pClamp9/Digidata 1322A (Molecular Devices). Slices were perfused at 1.8 ml/min with ACSF, containing (mM): 135 NaCl, 21 $NaHCO_3$, 0.6 $CaCl_2$, 3 KCl, 1.25 NaH_2PO_4, 1.8 $MgSO_4$, 10 D-glucose, aerated with 95% O_2 and 5% CO_2 (pH 7.4). During EPSCs recordings, pipettes contained (mM): 140 K-gluconate, 5 KCl, 1 $MgCl_2$, 0.5 BAPTA, 2 Mg-ATP, 0.3 Na-GTP, 10 HEPES (pH 7.26). During IPSCs recordings in layer V pyramidal neurons, pipettes contained (mM): 140 Cs-gluconate, 2 $MgCl_2$, 0.5 BAPTA, 10 HEPES (pH 7.26). The tip of the pipettes was filled with an internal solution with the same composition of the one used for EPSCs experiments. This procedure allowed us to rapidly record the neuronal firing pattern, injecting steps of depolarizing current, during the first minutes after the whole-cell configuration achievement. During IPSCs recordings in layer V FS and RSNP neurons, pipettes contained (mM): 70 K-gluconate, 70 KCl, 2 $MgCl_2$, 0.5 BAPTA, 1 MgATP, 10 HEPES (pH 7.2). This procedure set the

chloride reversal potential around -16 mV, thus making IPSCs visible as inward positive currents with the membrane potential clamped at -70 mV. During these experiments, EPSCs were then abolished using saturating concentrations of glutamate receptors inhibitors (AP5 10 μM and CNQX 40 μM). Drugs were applied in the bath and their effects calculated at the steady-state (usually reached within 2-3 min). The resting membrane potential (Vrest) was measured in open circuit mode, soon after obtaining the whole-cell configuration. No correction was applied for liquid junction potentials. Stock solutions of (-)-nicotine hydrogen tartrate salt, dihydro beta erythroidine hydrobromide (DHβE) and [D(-)-2-amino-5phosphono-pentanoic acid] (AP5) were prepared in distilled water. Stock solutions of CNQX [6-cyano-7-nitroquinoxaline-2,3-dione] were prepared in dimethylsulfoxyde (20 mM). These solutions were dissolved in our standard extracellular solution and used at the indicated final concentration. Chemicals and drugs were purchased from Sigma-Aldrich Italy, except AP5 and CNQX (Tocris Bioscience). All the electrophysiological experiments were carried out in the laboratory of Professor Andrea Becchetti at the Department of Biotechnology and Biosciences and NeuroMI-Milan Center of Neuroscience of the University of Milano-Bicocca.

Statistical analysis

Data are given as mean values ± standard error of the mean. The number of experiments (n) is the number of tested mice or of tested neurons (in different slices for the electrophysiological recordings). Comparisons between two independent populations were carried out with unpaired Student's *t*-test, after testing for data normality (with a Kolmogorov-Smirnov test), and variance homogeneity (with F-test). In case of unequal variances, the Welch's correction was applied. In the figures, p values are indicated by * ($0.01 < p \leq 0.05$) or ** ($p \leq 0.01$). Unless otherwise indicated, detailed statistics are given in the figure legends.

RESULTS

Morphological characterization of the PFC of β2-V287L mouse model

Firstly, PFC and SS thionine-stained sections were analyzed (**Fig. 1**) to determine if the mutation altered cortical thickness. Thionine is a strongly staining metachromatic dye, which marks the nucleic acids, and thus nucleoplasm, cytoplasm and proximal extensions, of the majority of both glial and neuronal cells. It allows the identification of the different cortical layers by morphology and distribution observation. The data showed no significant differences between CTRL and β2-V287L mice.

Stereological counts of layer V neurons were carried out on thionine-stained sections (**Fig. 1A, B, C**). No significant differences were found between β2-V287L and their control littermates, but we could observe a slight decrease of both PFC and SS layer V neurons in the double-transgenic mice (**Fig. 2C, D**), in agreement with the results obtained with countings of NeuroTrace^{TM}+ cells using ImageJ software (**Fig. 2A, B).**

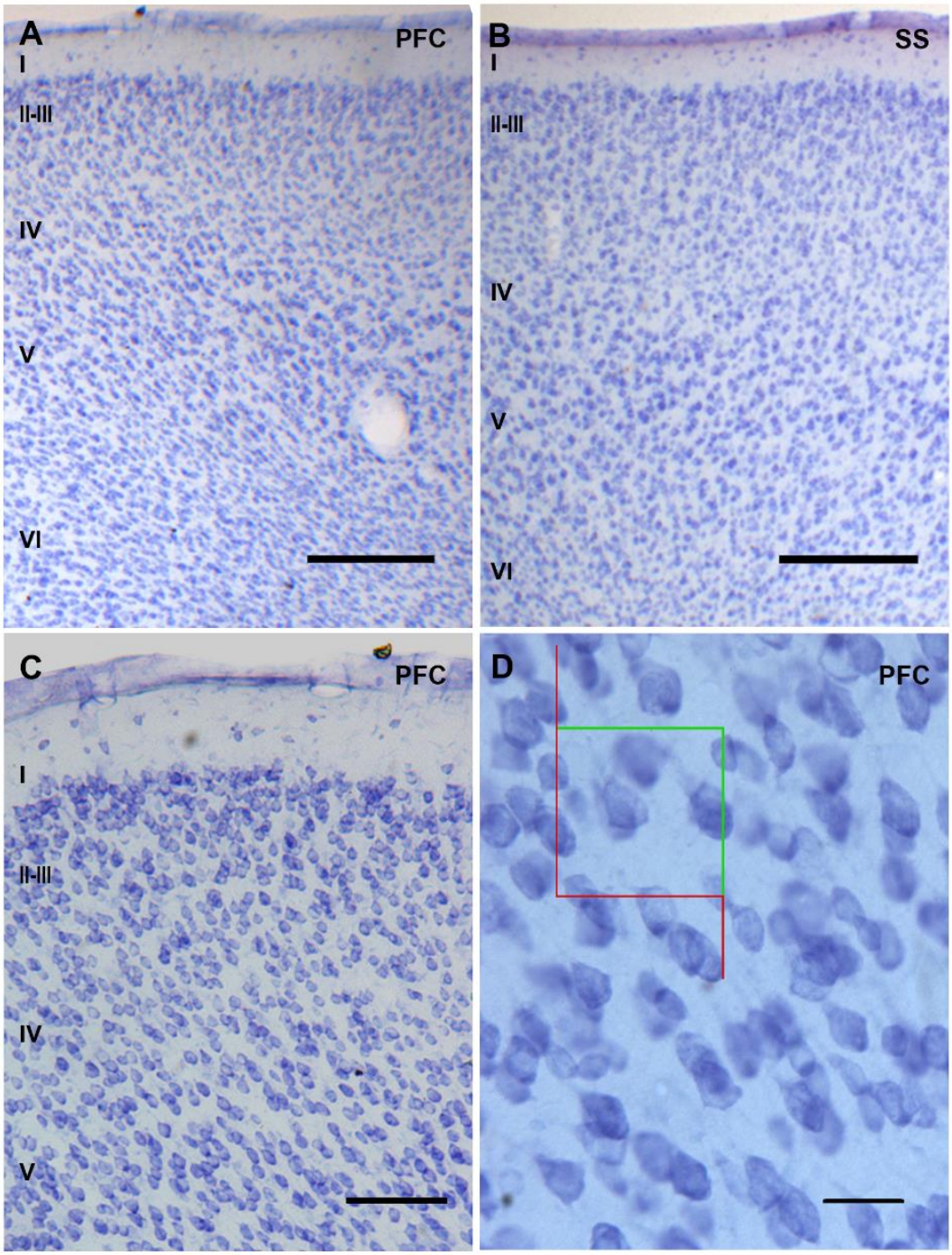

Fig. 1 Thionine-stained cortical coronal sections.
Thionine-stained sections of PFC (A, C, D) and SS (B) at low magnification (2.5X; A, B or 4X; C) and at higher magnification (40X; D). In D an optical dissector could be observed. Layer I is characterized by scarcity of cell bodies, while it is nearly impossible, in the mouse cortex, to distinguish layer II from layer III, that both contain small pyramidal neurons. Layer IV is characterized by radely packed small neurons. Layer V contains large pyramidal neurons, while layer VI is characterized by the presence of smaller and polymorphic neurons.
Mean cortical thickness: 1349.289 µm (PFC CTRL), 1293.703 µm (PFC β2-V287L), 1311.409 µm (SS CTRL), 1310.762 µm (SS β2-V287L).
(P60, n=5) Scale bars=250 µm (A, B), 100 µm (C) and 25 µm (D). For cortical thickness: p=0.364 (PFC); p=0.986 (SS).

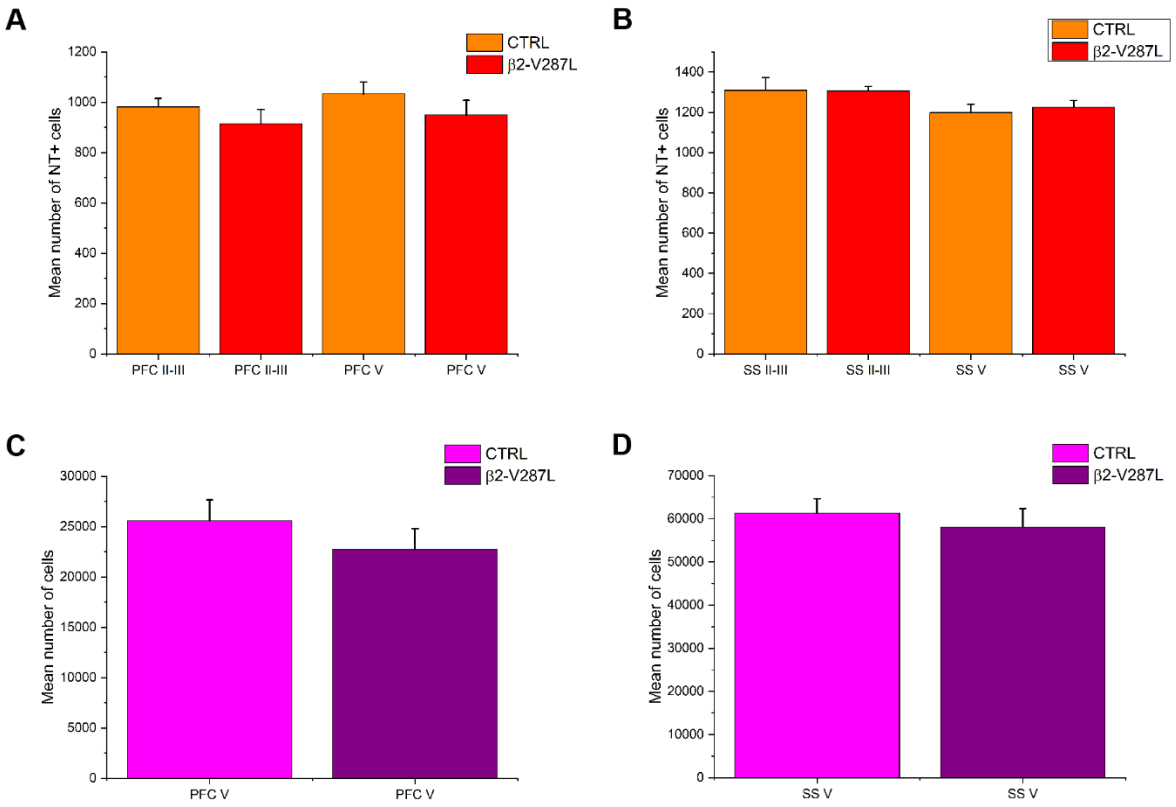

Fig. 2 Quantitative analysis of NeuroTrace™- or thionine-stained neurons.
Graphs depicting the results from the counts of NeuroTrace™- (A, B) and thionine-stained (C, D) neurons. Bars give average number of neurons. In A and B NeuroTrace™-stained neurons were acquired with a confocal microscope and counted with ImageJ in both layer II-III and V of PFC and SS (p=0.301 PFC layer II-III; p=0.056 PFC layer V; p=0.962 SS layer II-III; p=0.624 SS layer V). In C and D thionine-stained neurons of PFC and SS layer V were counted with the StereoInvestigator software. No significant differences were obtained in all the analyses. p=0.115 (PFC layer V); p=0.659 (SS layer V). (P60, n=5)

GABAergic populations in the PFC of WT and β2-V287L mice

Regarding the study of the GABAergic system, a quantitative analysis of parvalbumin- (PV+) and somatostatin-positive (SOM+) neurons was carried out in the neocortex. PV is a calcium-binding protein mainly expressed by fast-spiking GABAergic interneurons, that provide the main local inhibition source on pyramidal neurons with another class of GABAergic interneurons, the regular-spiking SOM-positive cells. Stereological counts of PV+ and SOM+ neurons were performed in PFC and SS. No significant differences were found between CTRL and β2-V287L for both PV and SOM. Interestingly, a larger number of PV+ cells was present in the SS compared to the PFC (**Fig. 3**). SOM+ neurons, in contrast, were more numerous in the PFC than in the SS (**Fig. 4**).

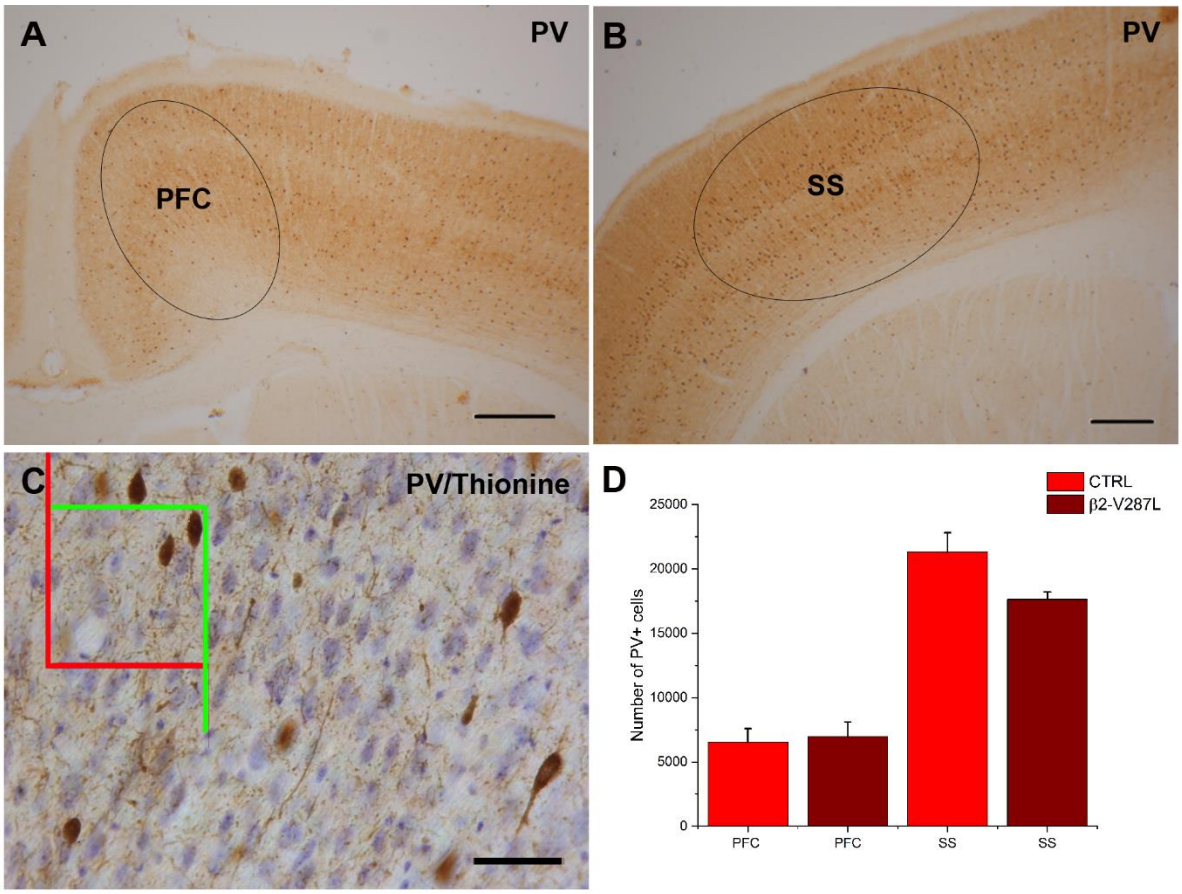

Fig. 3 Stereological counting of immunoperoxidase-stained parvalbumin neurons. *Coronal slices of murine brain immunolabeled against parvalbumin at low magnification (2.5X; A, B) and at high magnification (40X; C). In C, the section is counterstained with thionine and the dissector is present. The antibody against PV labels soma, dendrites and axons of a subgroup of GABAergic cortical interneurons. Stereological analysis of PV+ cells in the PFC and SS (D). Data are expressed as average number of PV+ neurons and were compared between CTRL and β2-V287L mice with Student's t-test. No significant differences were found between the genotypes, but a larger number of PV+ cells was present in the SS compared to the PFC. p=0,832 (PFC); p=0,798 (SS). (P90, n=3) Scale bars=250 µm (A, B); 25 µm (C).*

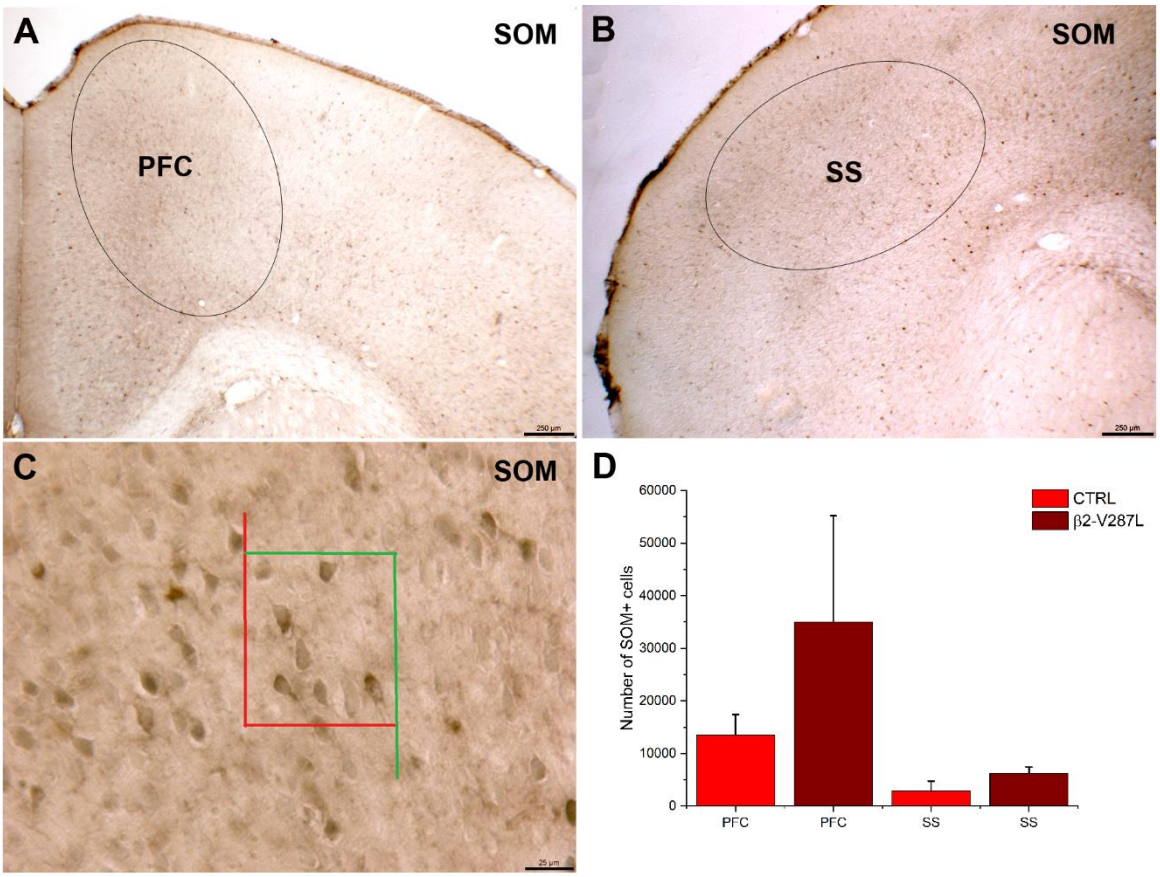

Fig. 4 Stereological counting of immunoperoxidase-stained somatostatin neurons. *Coronal slices of murine brain immunolabeled against somatostatin at low magnification (2.5X; A, B) and at high magnification (40X; E). Stereological analysis of SOM+ cells in the PFC and SS (D). Anti-SOM staining was intensified with nickel and labeled mainly cell bodies of RSNP GABAergic interneurons. Despite the high variability between the animals of the double-transgenic group, it seems that SOM+ neurons were more numerous in the PFC than in the SS. No differences were found between CTRL and β2-V287L mice. Data are expressed as average number of SOM+ neurons and were compared between CTRL and β2-V287L mice with Student's t-test. p=0,354 (PFC); p=0,203 (SS). (P90, n=3)*

Counts of PV+ and SOM+ neurons were performed also on immunofluorescence-labeled sections. Both antigens were detected simultaneously in the same slices by using secondary antibodies with different fluorochromes. Once again, no statistically significant differences were found, between β2-V287L and CTRL (**Fig. 5**).

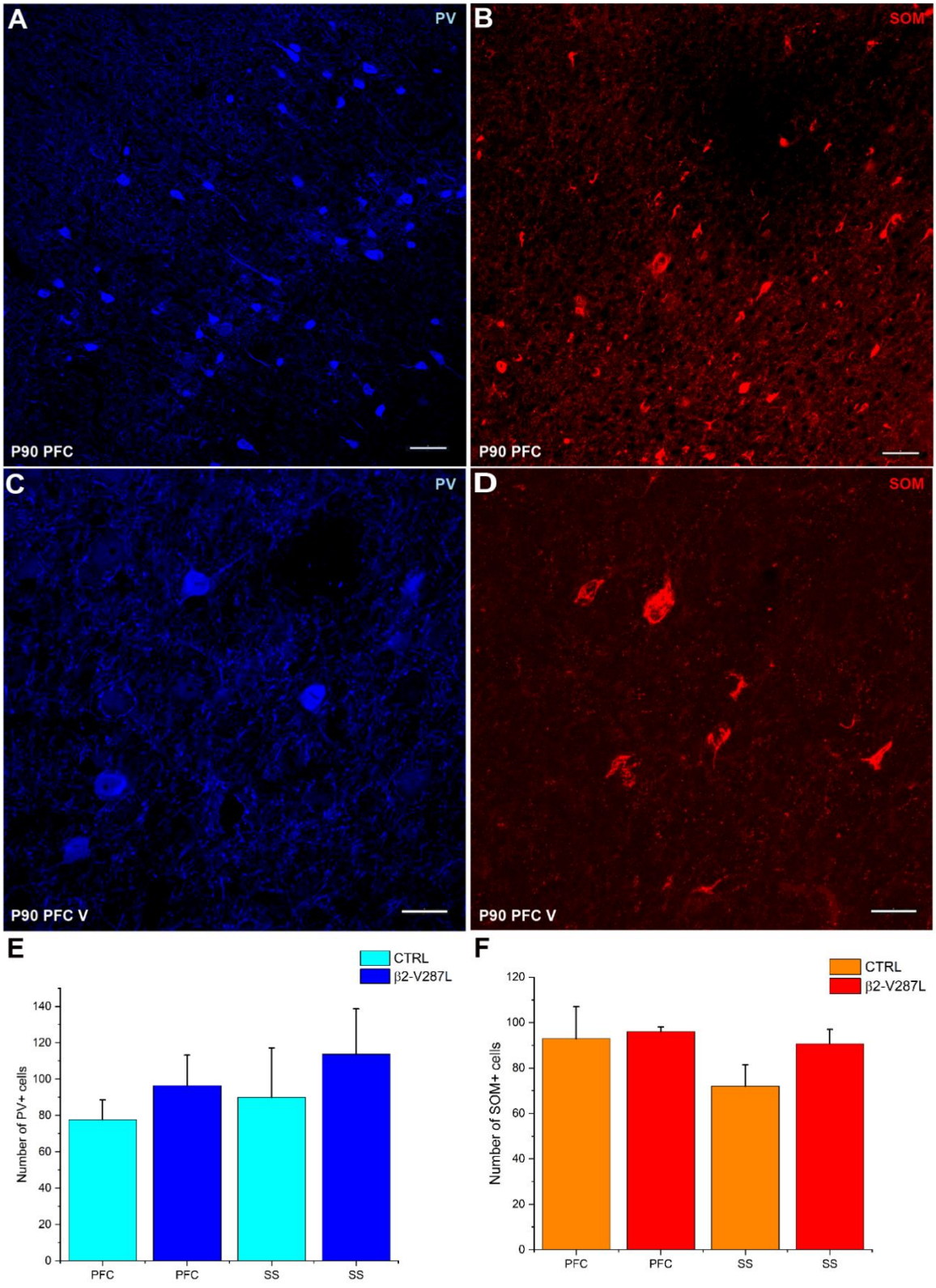

Fig. 5 Estimations of parvalbumin and somatostatin neurons in the neocortex.
Confocal microscope images of PV+ (A, C) and SOM+ cells (B, D). Analysis of the number of PV+ and SOM+ neurons (E, F, respectively). Data are expressed as estimated average number of neurons and were compared between CTRL and β2-V287L mice with Student's t-test. No statistically significant differences were found in both analyses between the genotypes. p=0,842 (PFC); p=0,176 (SS) for SOM+. p=0,404 (PFC); p=0,556 (SS) for PV+. (P90 N=3) Scale bars=50 μm (C, D) and 100 μm (A, B).

After the cell counting analyses, we focused on the study of different GABAergic markers. Glutamic acid decarboxylase (GAD) is the catalyzing enzyme of GABA biosynthesis. The antibody against GAD isoform 67 (GAD67) detects the majority of GABAergic cell bodies and is a good marker of different classes of GABAergic interneurons. Antibodies against α1 $GABA_A$ receptor subunit reveal a ubiquitous distribution of the staining in the neocortex, in particular in the neuropil. Vesicular GABA transporter (VGAT) is the marker of GABAergic presynaptic boutons.

For all the antibodies above, an immunofluorescence densitometric analysis was carried out. Data were expressed as mean grey value of fluorescence and normalized on the number of cells (stained with NeuroTrace™ or Hoechst) for GAD67 and α1 $GABA_AR$ and as number of spots for VGAT. Regarding GAD67, a slight increase in β2-V287L PFC layers II-II and V was found compared to CTRL (**Fig. 6**). Analogous result was observed from densitometric analysis of α1 $GABA_AR$ immunostaining in β2-V287L PFC layer II-II (**Fig. 7**). Concerning VGAT, similar levels of expression were found in all the regions of both experimental groups (**Fig. 8**).

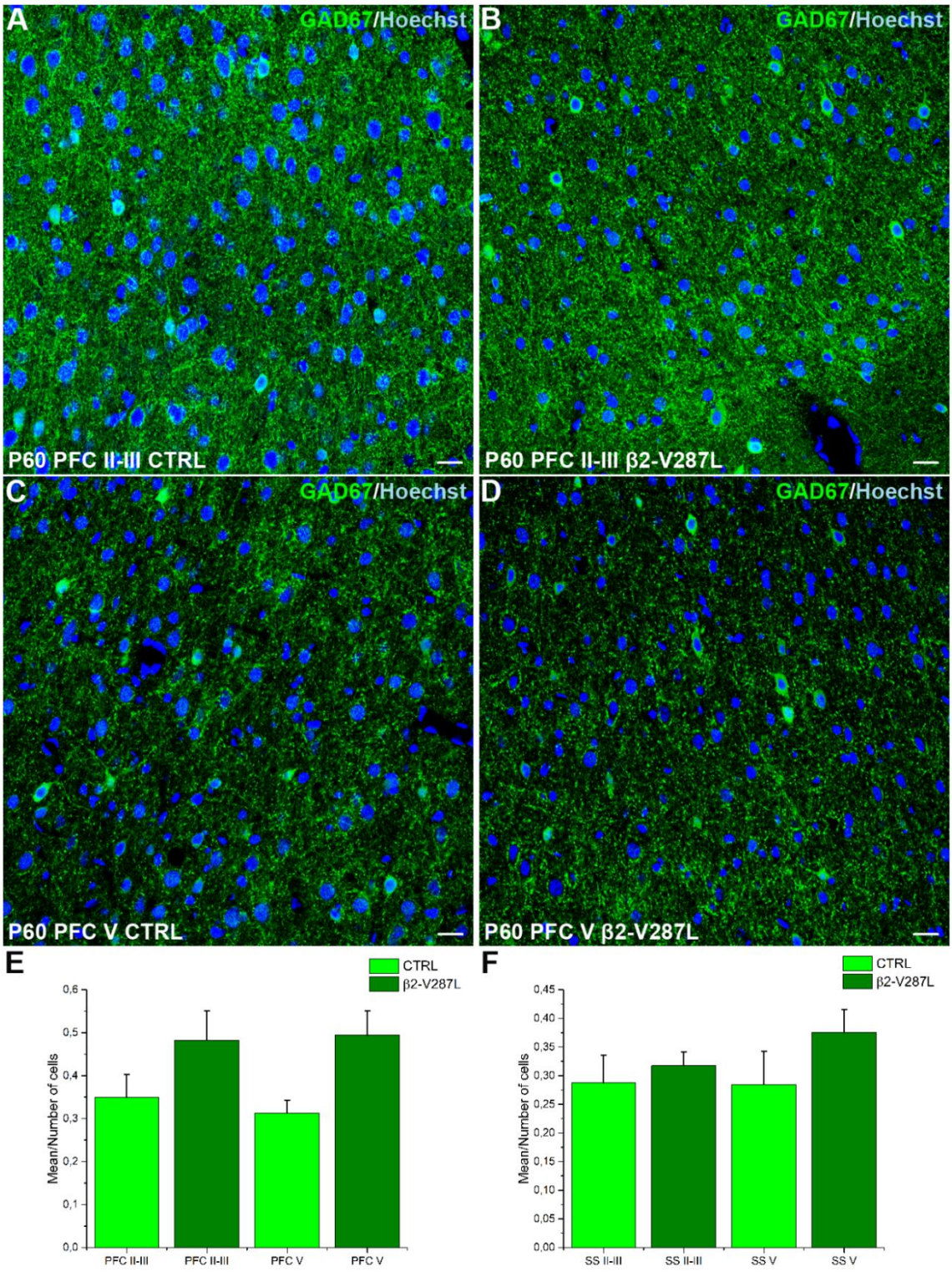

Fig. 6 Densitometric analysis of GAD67 immunofluorescence.
Confocal microscope images of GAD67 immunolabeling (green) in PFC (A-D) (Hoechst in blue). Results of the densitometric analysis of GAD67 (E, F). A slight increase of GAD67 expression in β2-V287L PFC layer II-II and layer V was observed compared to CTRL, but no significant differences were found. Data are expressed as mean grey value normalized on the number of cells and were compared between CTRL and β2-V287L mice with Student's t-test. p=0.261 (PFC II-III); p=0.098 (PFC V); p=0.573 (SS II-III); p=0.271 (SS V). (P60, n=3) Scale bar=20 μm.

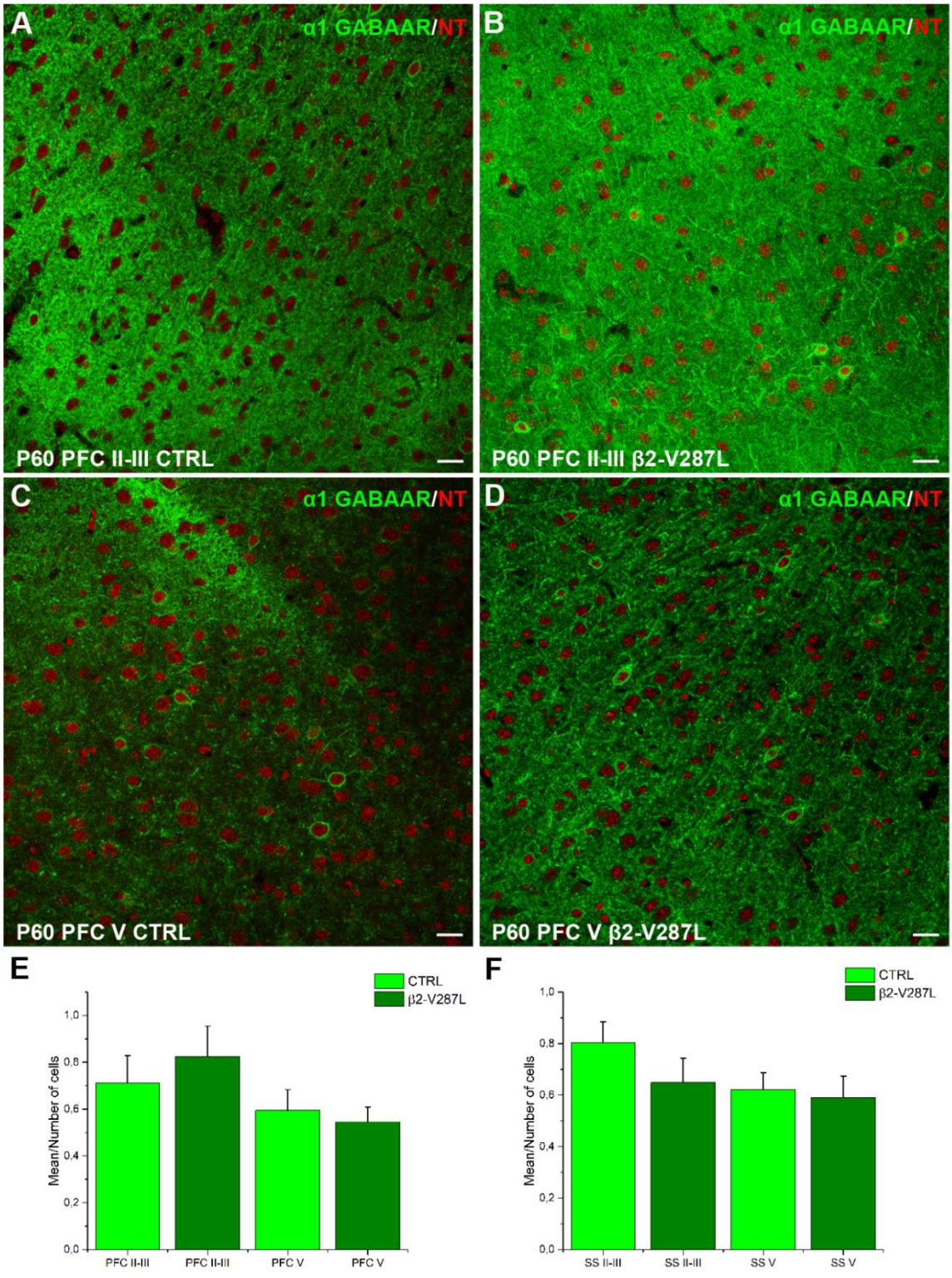

Fig. 7 Analysis of α1 $GABA_AR$ expression by immunofluorescence labeling.
Confocal microscope images of α1 $GABA_AR$ immunolabeling (green) in PFC (A-D) (NeuroTrace™ in red). Results of the densitometric analysis of α1 $GABA_AR$ (E, F). The level of the protein was slightly higher in β2-V287L PFC layer II-II was found compared to CTRL, but the result was not statistically significant. Data are expressed as mean grey value normalized on the number of cells and were compared between CTRL and β2-V287L mice with Student's t-test. p=0.535 (PFC II-III); p=0.668 (PFC V); p=0.243 (SS II-III); p=0.781 (SS V). (P60, n=5) Scale bar=20 μm.

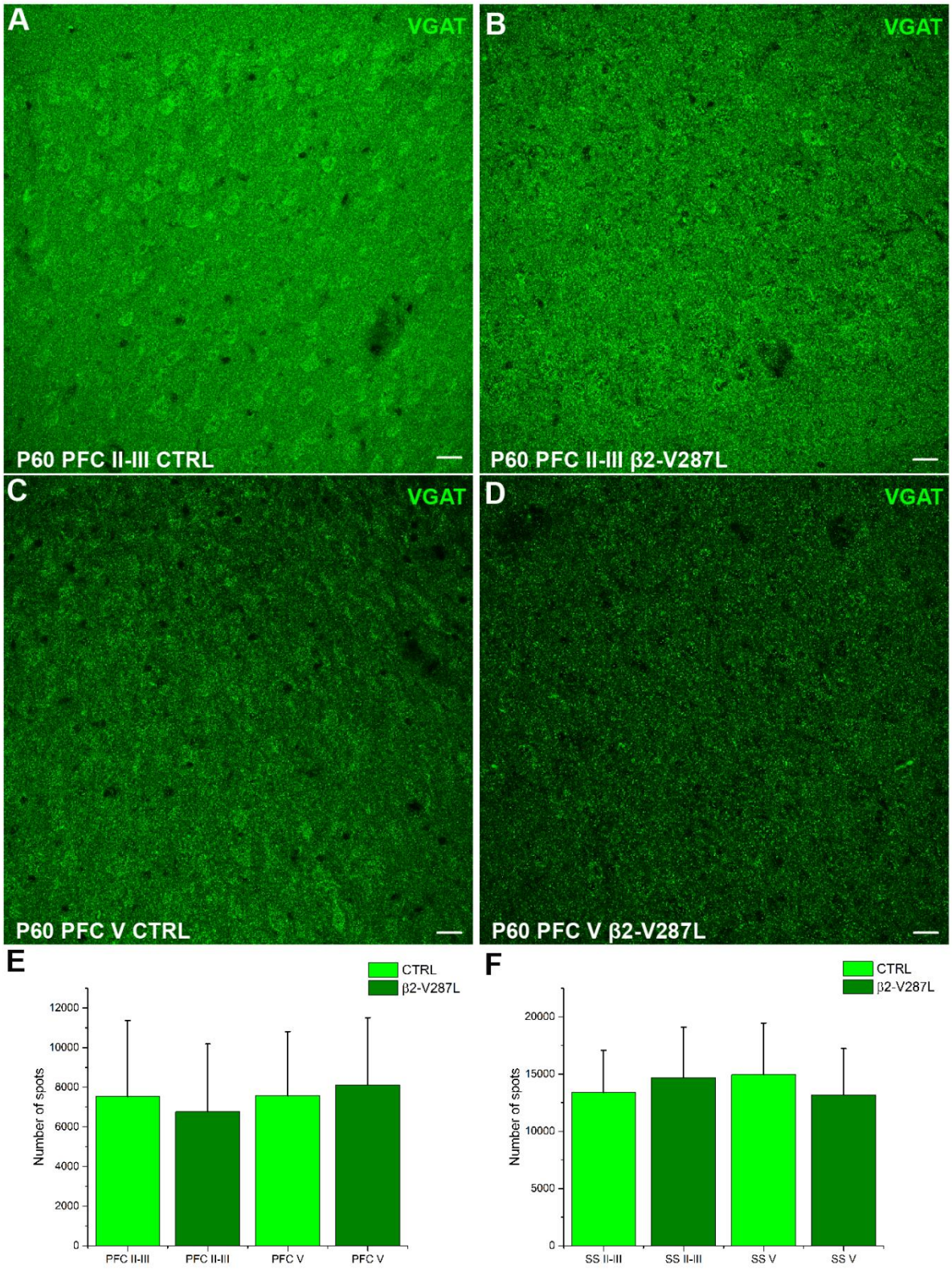

Fig. 8 Densitometric analysis of VGAT immunofluorescence.
Confocal microscope images of VGAT immunolabeling (green) in PFC (A-D). Results of the densitometric analysis of VGAT (E, F). The level of expression of VGAT was similar in all the examined layers and regions. Data are expressed as number of spots and were compared between CTRL and β2-V287L mice with Student's t-test. p=0.883 (PFC II-III); p=0.909 (PFC V); p=0.824 (SS II-III); p=0.775 (SS V). (P60, n=8) Scale bar=20 μm.

Electrophysiological analysis of PFC layer V neurons

After the preliminary morphological analysis and in parallel with the study of the GABAergic system, patch-clamp recordings were carried out in adult mice (P20-P50), to observe the spontaneous excitatory and inhibitory post-synaptic currents (EPSCs, IPSCs) in basal conditions in PFC layer V. A significant decrease of EPSC frequency was measured in fast-spiking (FS) cells (**Fig. 9C**), accompanied by a decrease of IPSC frequency in layer V pyramidal neurons (**Fig. 9B**). No significant difference was observed in the amplitude of synaptic events. In regular-spiking non-pyramidal cells (the other major population of GABAergic neurons in PFC layer V), no significant difference was observed between CTRL and β2-V287L mice (**Fig. 9D**). These data suggest that expression of β2-V287L causes, in the mature PFC network, a diminished efficacy of the negative feedback control exerted by FS interneurons onto pyramidal cells, which may be the cause of prefrontal hyperexcitability in mice carrying the mutant subunit.

To assess the impact of hyperfunctional heteromeric β2-V287L nAChRs activity on excitatory transmission we simulated an ACh upsurge in PFC brain slices. Nicotine was preferred to ACh, to avoid applying muscarinic receptors' inhibitors, which can affect nAChRs at relatively low concentrations (Zwart and Vijverberg, 1997). Nicotine was always applied in the bath at a concentration of 10 μM. This corresponds to the peak of the steady-state ("window") current for both α4β2 and α7 receptors (Aracri *et al.*, 2010), thus permitting to test the tonic contribution of both nAChR subtypes. **Fig. 9A** shows typical recordings in the indicated experimental conditions for tTA mice (upper panel) and β2-V287L mice (lower panel). In both control and double-transgenic mice, nicotine consistently increased the spontaneous EPSCs (**Fig. 9E**) frequency onto PFC layer V pyramidal neurons. Nicotine administration led to a potentiation of excitatory inputs onto FS cells in both CTRL and β2-V287L mice, but to a greater extent in the double-transgenic animals (**Fig. 9G, H**). Expression of β2-V287L decreased the efficacy of the excitatory input onto FS cells. The decrease in the inhibitory input that we observed on pyramidal neurons in basal conditions could be caused by the strong depression of the excitatory drive onto FS interneurons, that are known to be responsible for the feed-forward inhibition of PFC layer V pyramidal neurons. The results obtained from the basal spontaneous synaptic events suggest that seizures could be facilitated in β2-V287L mice by a decreased inhibitory feedback on pyramidal neurons, in conditions of low acetylcholine release, as it occurs during NREM sleep.

On the other hand, because nicotine administration makes the mutant synaptic responses more similar to the CTRL's, we hypothesize that the probability of developing seizures could decrease when ACh release is high, i.e. during wakefulness and REM sleep.

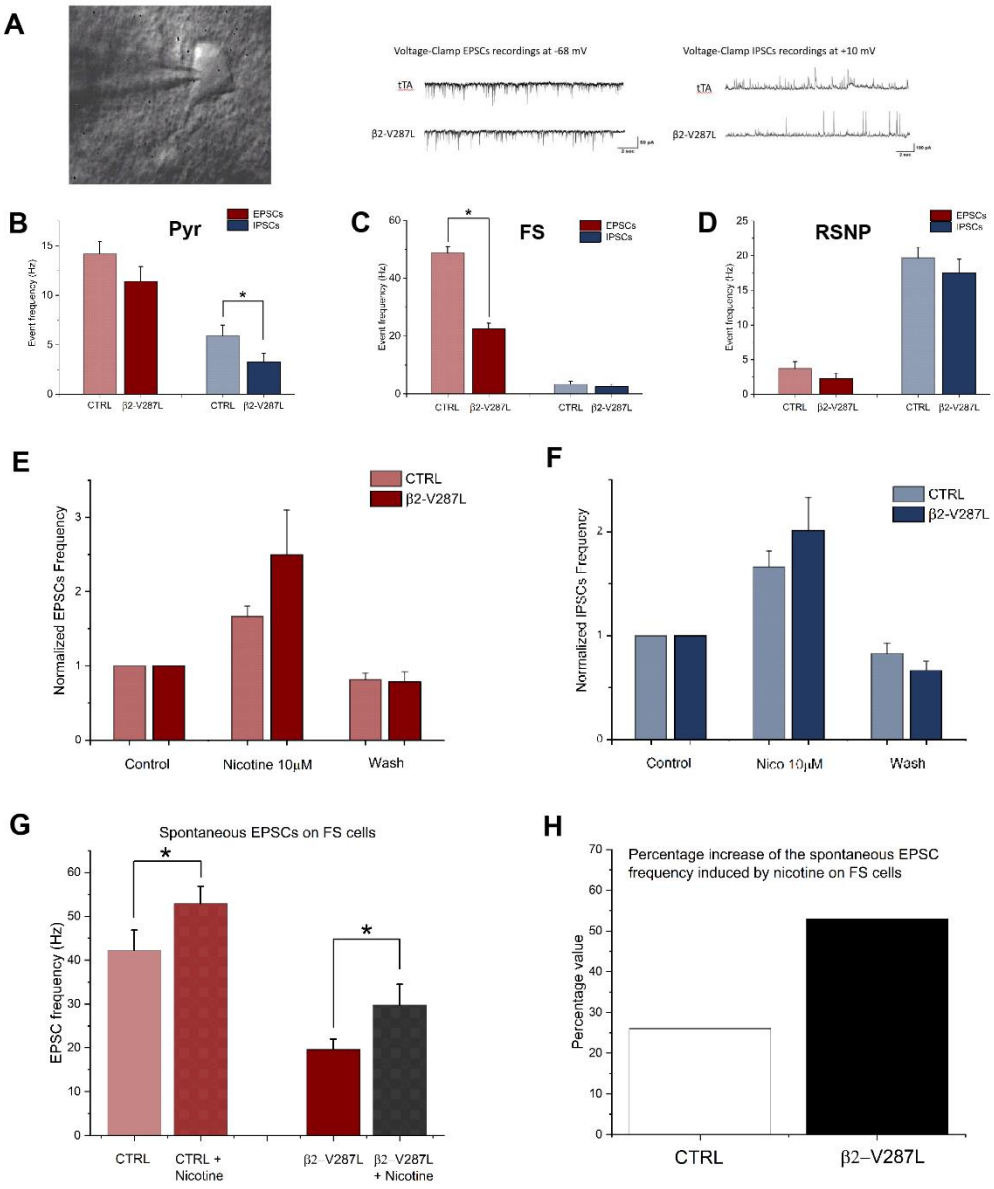

Fig. 9 Whole-cell recordings in PFC layer V neurons of CTRL and β2-V287L.
Typical recordings in the indicated experimental conditions for tTA mice (upper panel) and β2-V287L mice (lower panel) (A). Event frequency (in Hz) of EPSCs and IPSCs on pyramidal (B), fast-spiking (C) and regular-spiking non-pyramidal neurons (D). p=0.421 (EPSCs; Pyr), p=0.027 (IPSCs; Pyr); p=0.030 (EPSCs; FS), p=0.160 (IPSCs; FS); p=0.333 (EPSCs; RSNP), p=0.742 (IPSCs; RSNP). Nicotine stimulates glutamate release onto pyramidal neurons in both control and β2-V287L mice (E, F). E: average EPSCs frequencies recorded in tTA mice (n=9) were 14.20 ± 2.48 Hz (Control), 22.39 ± 3.74 Hz (Nicotine 10 μM), 11.61 ± 2.46 Hz (Washout of nicotine). Average EPSCs frequencies recorded in β2-V287L mice (n=12) were 11.40 ± 2.13 Hz (Control), 23.15 ± 4.41 Hz (Nicotine 10 μM), 8.38 ± 1.69 Hz (Washout of nicotine). F: average IPSCs frequencies recorded in tTA mice (n=8) were: 4.56 ± 0.30 Hz (Control), 7.60 ±

0.79 Hz (Nicotine 10 μM), 2.28 ± 0.41 Hz (Nicotine 10 μM + DHβE 1 μM), 3.91 ± 0.68 Hz (Washout of nicotine). Lower panel, Average IPSCs frequencies recorded in β2-V287L mice (n=8) were: 4.35 ± 0.86 Hz (Control), 7.32 ± 0.51 Hz (Nicotine 10 μM), 2.06 ± 0.28 Hz (Nicotine 10 μM + DHβE 1 μM), 2.75 ± 0.53 Hz (Washout of nicotine). Event frequency of EPSCs on FS cells in CTRL and β2-V287L mice following nicotine administration (G) and the percentage increase of the EPSC frequency induced by nicotine on FS cells (H). p=0.014 (CTRL); p=0.028 (β2-V287L). All the results were compared with Student's t-test.
Images by courtesy of Dr. Simone Meneghini, Department of Biotechnology and Biosciences and NeuroMI-Milan Center of Neuroscience, University of Milano-Bicocca.

Glutamatergic and cholinergic innervation in the PFC

In addition to the study of the GABAergic system, we focused our attention on the cholinergic characteristics of the model. Firstly, a detailed analysis of nAChRs β2 subunit was carried out, by means of densitometric analysis, to estimate its whole expression level, and colocalization with synaptophysin (SYN), to observe its expression at the presynaptic sites, where nAChRs mediate the release of various neurotransmitters. The antibody against β2 nAChR (Immunological Sciences) is specific for the C-terminus of the protein and not the mutation site, so both mutated and normal nAChRs are labeled, in the somatodendritic and synaptic regions of the neurons. The densitometric analysis of β2 nAChRs expression revealed no significant differences between the two genotypes in all the studied regions (**Fig. 10**), in agreement with previous experiments carried out with labeled epibatidine, which marks heteromeric nAChRs, by Manfredi and colleagues (2009).

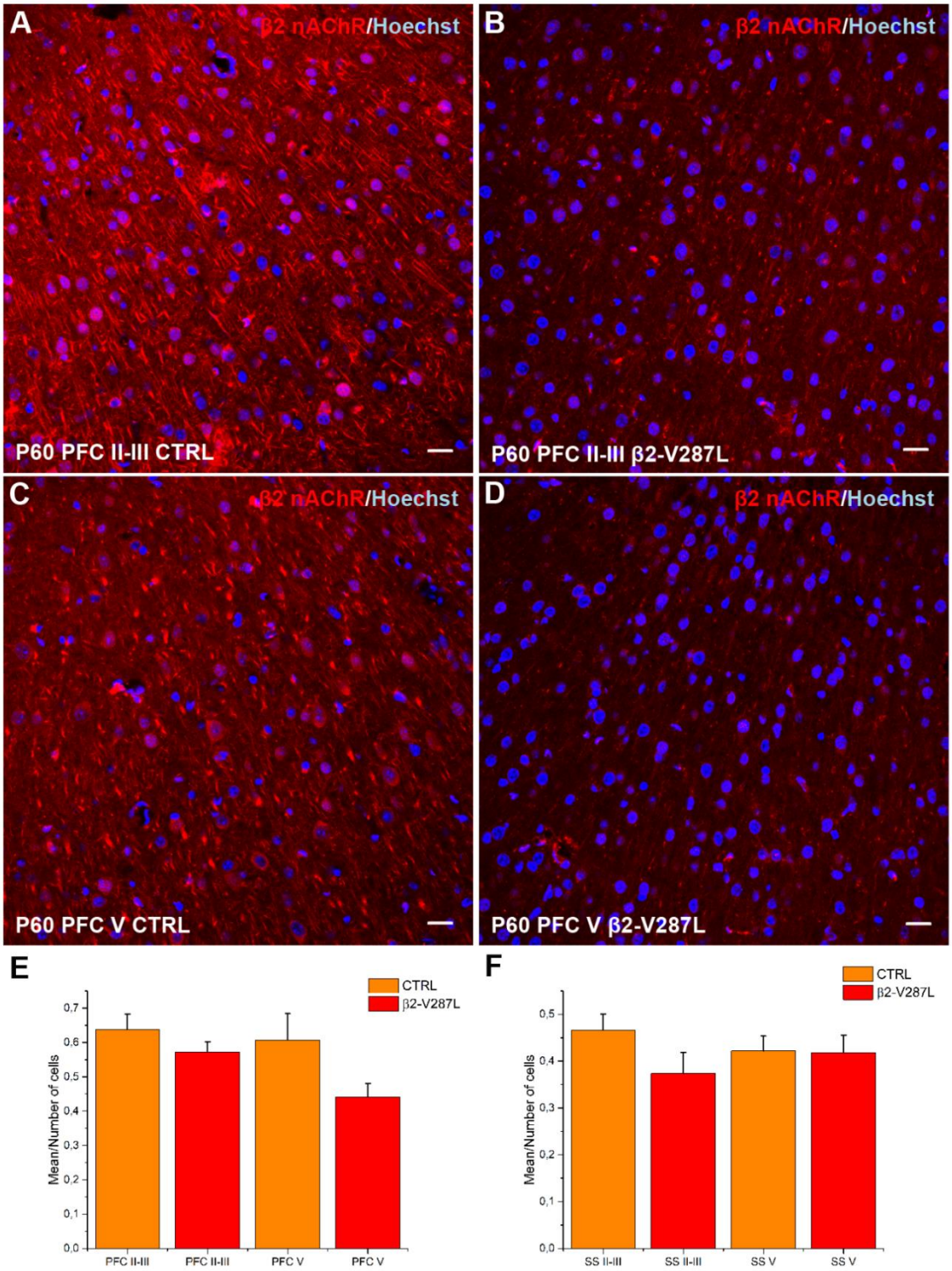

Fig. 10 Analysis of β2 nAChRs expression.
Confocal microscope images of β2 nAChR immunolabeling (red) in PFC (A-D) (Hoechst in blue). Results of the densitometric analysis (E, F). β2 nAChR staining was mainly observed in the neuropil and at the somatic level. Data are expressed as mean grey value normalized on the number of cells and were compared between CTRL and β2-V287L mice with Student's t-test. No significant differences were found. p=0.290 (PFC II-III); p=0.127 (PFC V); p=0.176 (SS II-III); p=0.947 (SS V). (P60, n=3) Scale bar=20 μm.

Synaptophysin (SYN) is a marker of synaptic vesicles and, in our study, was used mainly to evaluate β2 nAChRs expression at the presynaptic sites. In order to discard the hypothesis of an alteration of SYN expression, that could lead to a misinterpretation of the colocalization investigation, first of all, we performed a densitometric analysis of SYN. No statistically significant differences were found between β2-V287L and CTRL mice (**Fig. 11**).

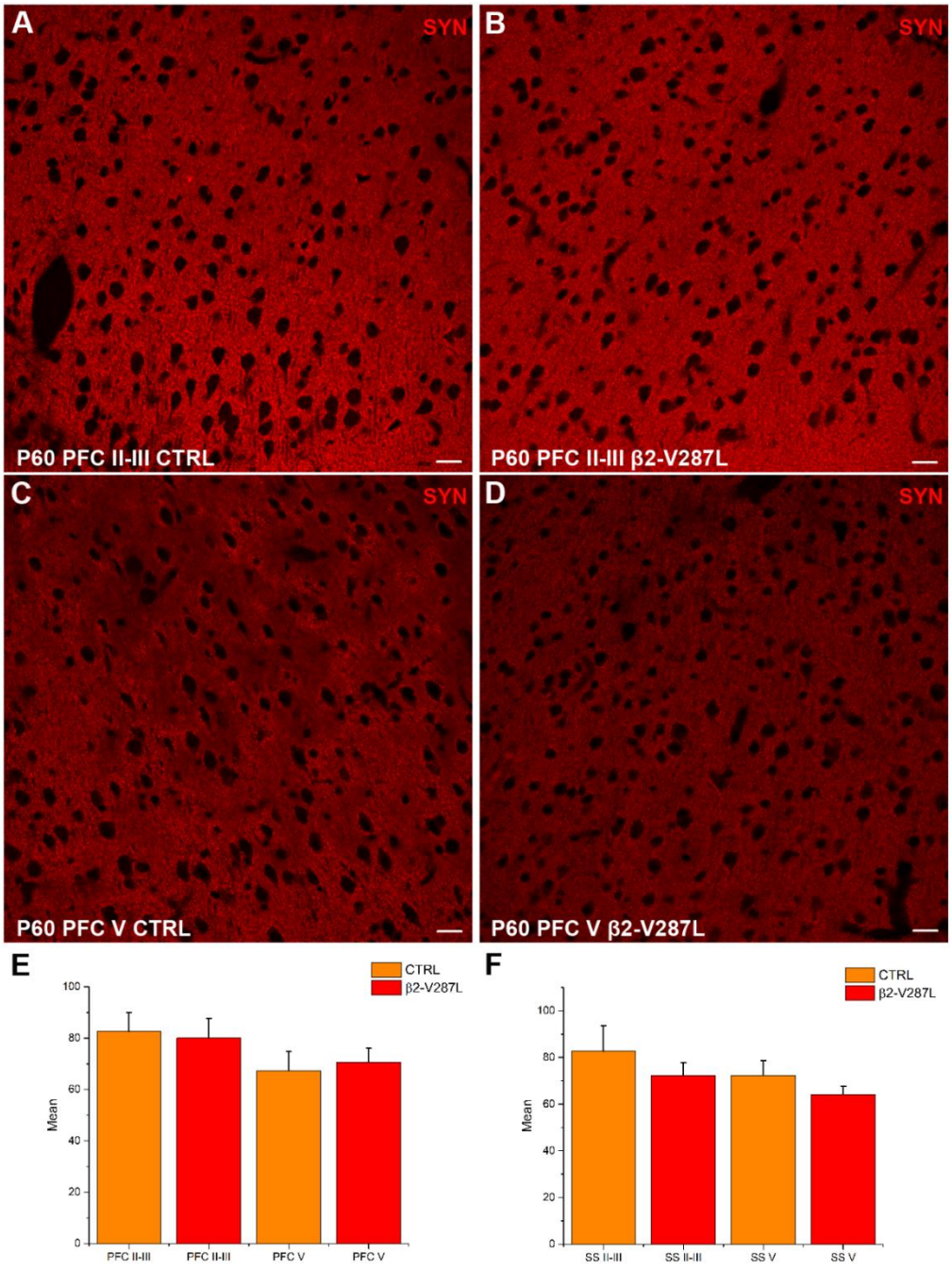

Fig. 11 Densitometric analysis of synaptophysin immunofluorescence.
Confocal microscope images of synaptophysin immunolabeling (red) in PFC (A-D). Results of the densitometric analysis (E, F). Data are expressed as mean grey value and were compared between CTRL and β2-V287L mice with Student's t-test. p=0.806 (PFC II-III); p=0.836 (PFC V); p=0.449 (SS II-III); p=0.318 (SS V). (P60, n=3) Scale bar=20 μm.

Regarding β2 nAChRs and SYN, qualitative colocalization was performed by Leica Confocal Software, that provided the cytofluorogram in **Fig. 12D**, while the quantitative colocalization was carried out with the ImageJ plugin JACoP. Only a slight decrease between the genotypes was found (**Fig. 12**).

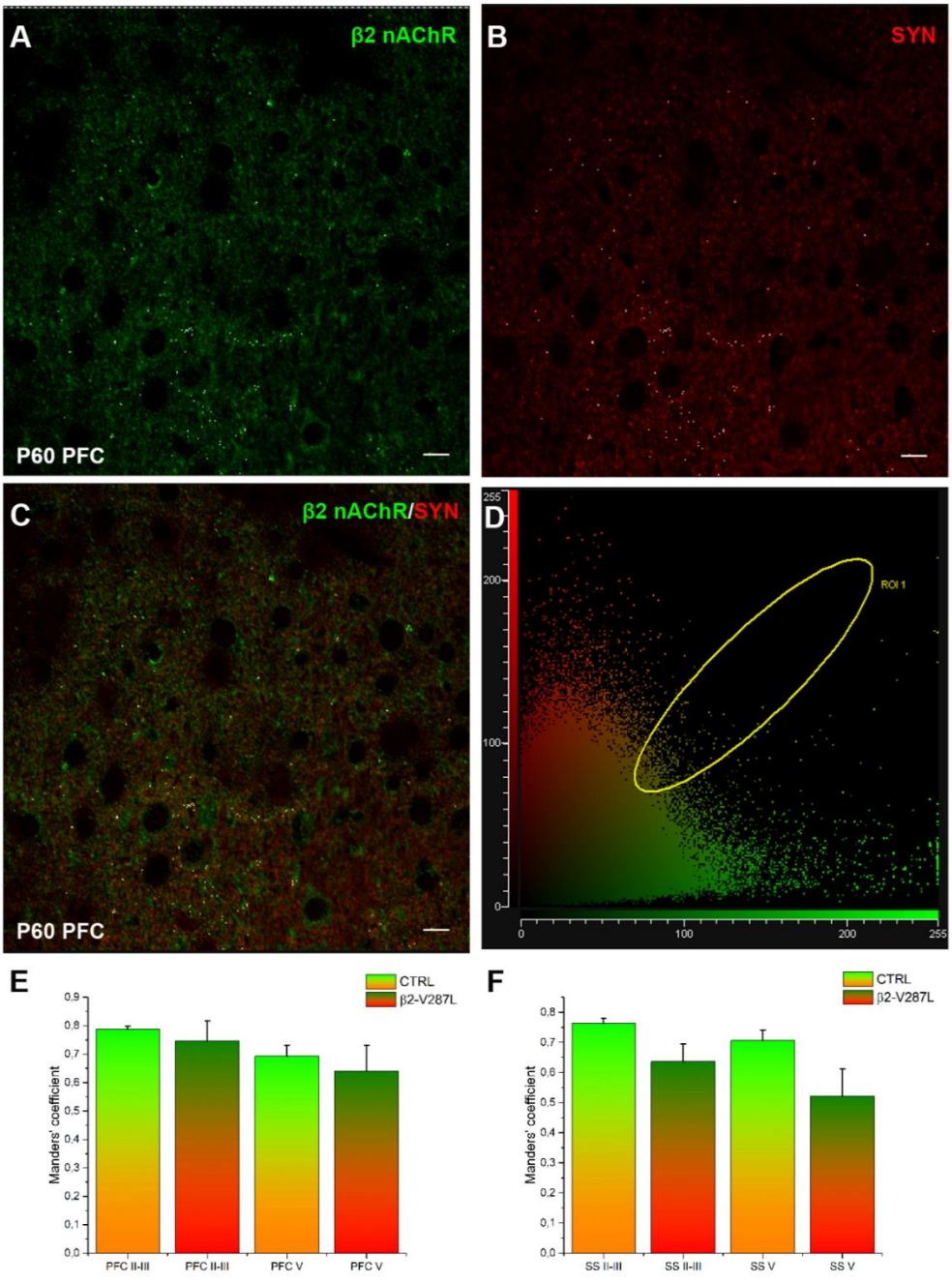

Fig. 12 Colocalization analysis of β2 nAChR and synaptophysin.
Confocal microscope images of β2 nAChR immunolabeling (green; A, C) and SYN (red; B, C) in PFC layer V. Cytofluorogram in D underlining the pixels in which the signal intensity is high for both channels, hence where β2 nAChR is expressed at the presynaptic level (showed in C as white pixels). Results of the colocalization analysis (E, F). Data are expressed as mean Manders' coefficient and were compared between CTRL and β2-V287L mice with Student's t-test. p=0.623 (PFC II-III); p=0.641 (PFC V); p=0.158 (SS II-III); p=0.168 (SS V). (P60, n=3) Scale bar=20 μm.

The following step was the study of cholinergic innervation in the neocortex. Cholinergic fibers were labeled by an immunoperoxidase staining for choline acetyltransferase (ChAT), and by an immunofluorescence staining for vesicular acetylcholine transporter (VAChT) (**Fig. 14**). Both these antibodies labeled soma and neurites with slight differences in the cortex. The reasons behind the choice of using two different techniques were mainly methodological, since in this way the antibodies worked better, with an improvement of the labeling and a reduction of the background, crucial for a densitometric investigation. Moreover, VAChT is more specific for the detection of cholinergic synaptic puncta and useful to confirm the preliminary densitometric analyses performed on immunoperoxidase-stained sections. No significant differences were found in both densitometric analyses, just a faint increment of the expression of ChAT in the PFC and SS of β2-V287L mice compared to the CTRL ones (**Fig. 13**).

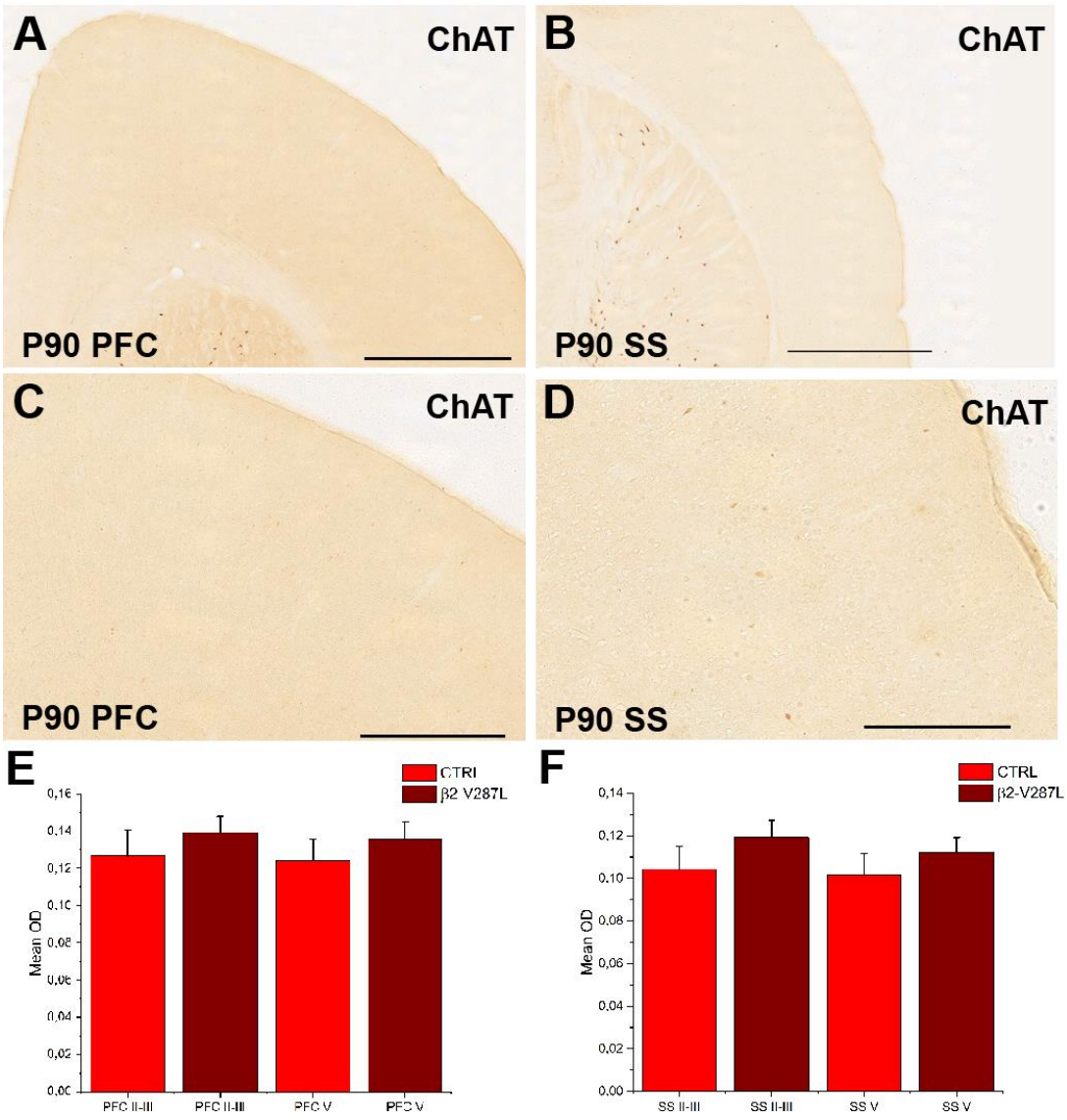

Fig. 13 Densitometric analysis of ChAT expression.
Optical microscope images of ChAT immunolabeling in PFC (A, C) and SS (B, D) at 2.5X (A, B) and 10X (B, C) magnification. Results of the densitometric analysis (E, F). The antibody mainly labeled cholinergic neurites, while the cholinergic cell bodies were scarcely stained in the cortices. In layers II-III and V of both PFC and SS a slight increment of ChAT level was observed in β2-V287L mice compared to CTRL ones. Data are expressed as mean optical density and were compared between CTRL and β2-V287L mice with Student's t-test. p=0.593 (PFC II-III); p=0.583 (PFC V); p=0.490 (SS II-III); p=0.554 (SS V). (P90, n=9) Scale bars=1 mm (A, C); 250 µm (B, D).

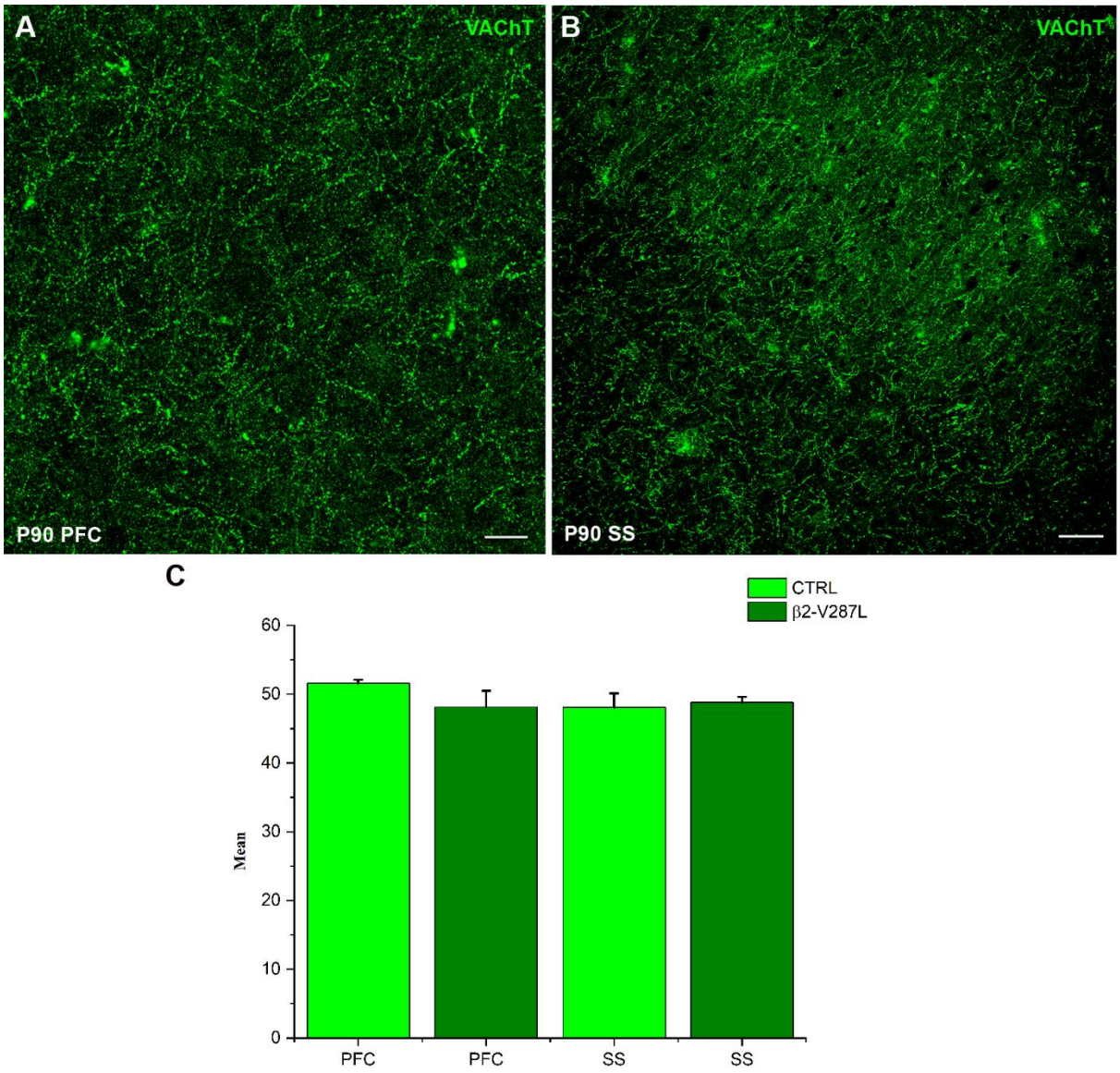

Fig. 14 Evaluation of VAChT expression by immunofluorescence.
Confocal microscope acquisitions of VAChT immunolabeling in PFC (A) and SS (B). Results of the densitometric analysis (E, F), that were similar in both PFC and SS of the different genotypes. Data are expressed as mean grey value and were compared between CTRL and β2-V287L mice with Student's t-test. p=0.227 (PFC); p=0.757 (SS). (P90, n=3) Scale bars=50 µm (A), 100 µm (B).

Since nAChRs modulate the release of different neurotransmitters, including glutamate, we studied if the mutation could lead to an alteration of the intrinsic glutamatergic innervation in the neocortex. Hence, the glutamatergic terminals were detected by an immunoperoxidase reaction against vesicular glutamate transporter 1 (VGLUT1), that is a specific marker of cortical glutamatergic terminals. A slight decrease of VGLUT1 expression was found in all the studied areas of the double-transgenic mice compared to the control littermates (**Fig. 15**).

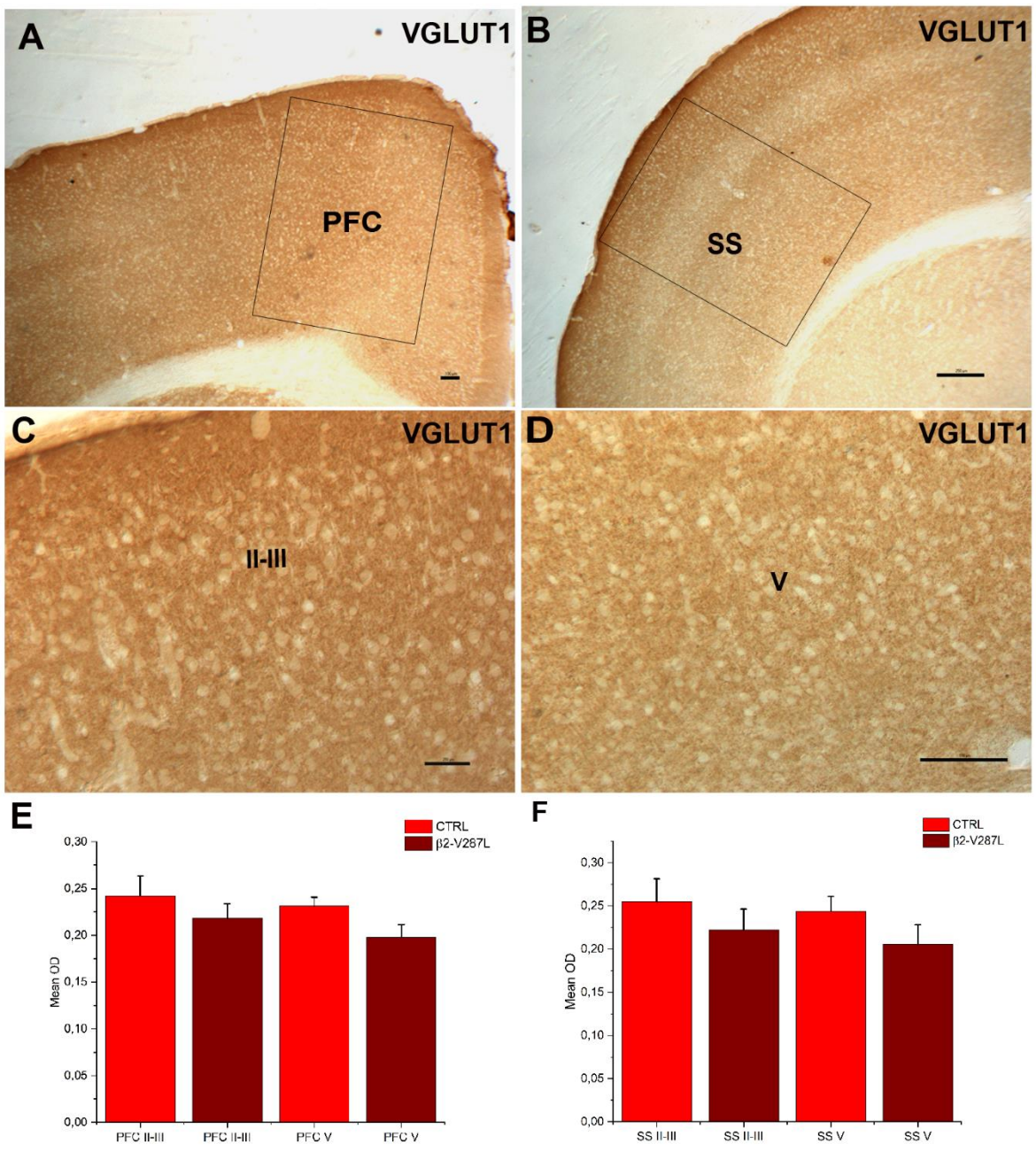

Fig. 15 Densitometric analysis of VGLUT1 expression.
Optical microscope images of VGLUT1 immunolabeling in PFC (A, C) and SS (B, D). Results of the densitometric analysis (E, F). No significant differences were found, only a slight decrease of VGLUT1 expression was observed in all the studied areas of the double-transgenic mice compared to the control littermates. Data are expressed as mean optical density and were compared between CTRL and β2-V287L mice with Student's t-test. p=0.355 (PFC II-III); p=0.732 (PFC V); p=0.532 (SS II-III); p=0.800 (SS V). (P90, n=9) Scale bars=100 µm (A, D); 250 µm (B, C).

Analysis of terminals onto the GABAergic interneurons in layer V of PFC

In the next step of our study, we focused our attention on the relationship between the two classes of GABAergic neurons, PV- and SOM-positive, the major sources of inhibition on pyramidal neurons, and the cholinergic innervation in PFC layer V of wild-type mice. The quantitative distribution of vesicular acetylcholine transporter (VAChT) onto the cell bodies of PV+ and SOM+ neurons was evaluated with ArivisVision4D software. From confocal microscope z-stacks of VAChT/PV/SOM immunofluorescence, the analysis of VAChT+ terminals contacting PV+ cell bodies showed an irregular distribution, since the average number of terminals was <100 for a single cell (**Fig. 16B**). Onto SOM+ cell bodies, the distribution of VAChT+ terminals was even more variable, but the average number was <50 (**Fig. 16D**). The normalization of the terminals estimation with the number of cells was in agreement with the distribution analysis (**Fig. 16F**), showing a slightly higher number of cholinergic contacts on PV+ neurons than on SOM+ cells.

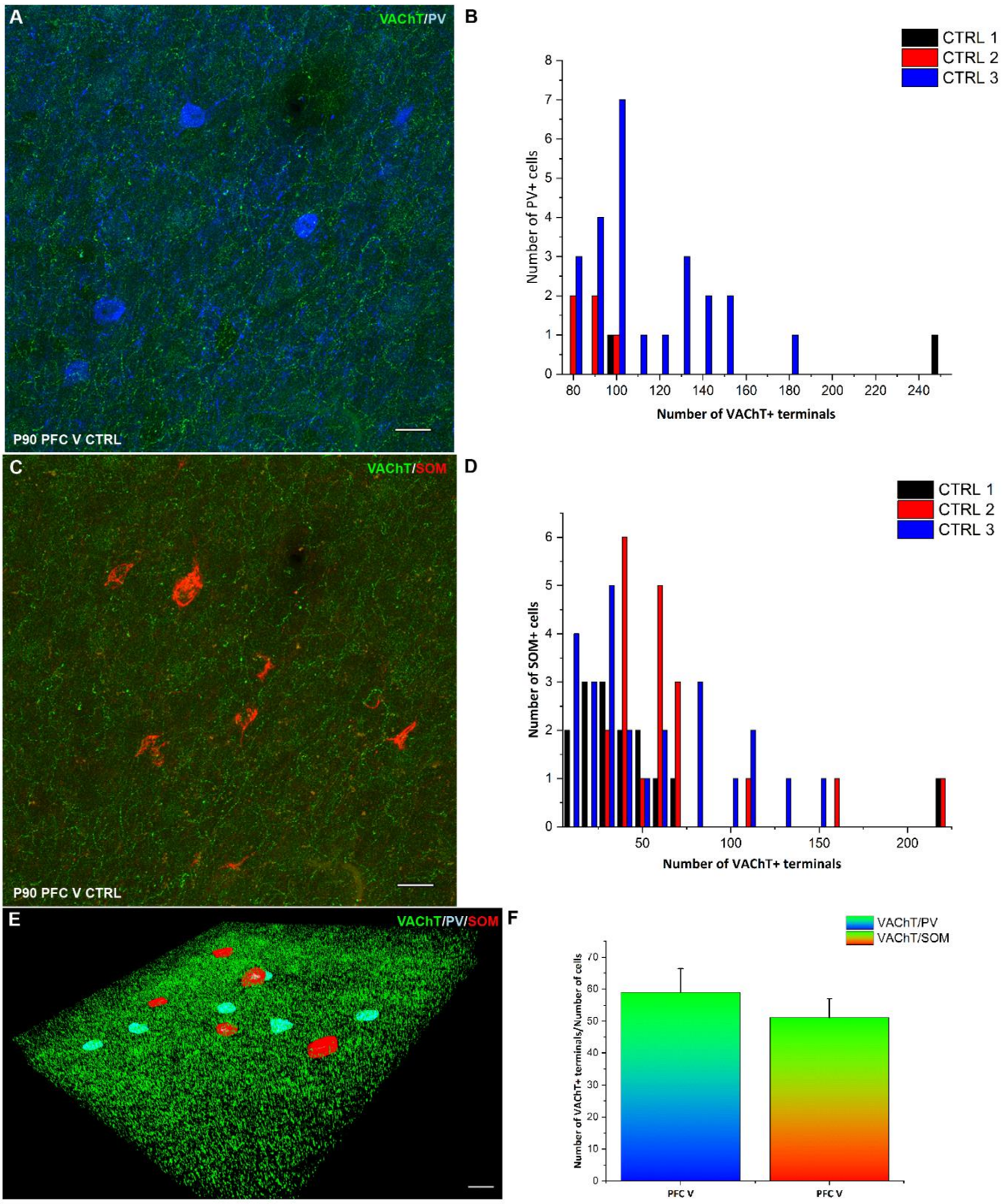

Fig. 16 Distribution analysis of VAChT+ terminals in wild-type mice.
Confocal microscope z-stacks of VAChT/PV (A) and VAChT/SOM (C) immunofluorescence in PFC layer V. Three-dimensional reconstruction of the triple VAChT/SOM/PV immunolabeling in PFC layer V using ArivisVision4D (E). Results of the distribution analysis for each animal (B, D) and the normalization on the number of cells (F) to compare PV+ and SOM+ cells. The average number of VAChT+ terminals contacting PV+ cell bodies was <100 for a single cell, while onto SOM+ cell bodies, the mean number was <50. The normalization of the terminals estimation with the number of cells was in agreement with the distribution analysis showing a slightly higher number of cholinergic contacts on PV+ neurons than on SOM+ cells. Data are expressed as number of terminals (B, D) and mean number of terminals divided for number of cells. The second results were compared between PV+ and SOM+ cells with Student's t-test. p=0.460. (P90, n=3) Scale bar=50 µm.

The same analyses were carried out on glutamatergic terminals but comparing CTRL and β2-V287L mice. In PFC layer V of double-transgenic mice the number of VGLUT1+ terminals contacting PV+ cell bodies was higher than in the CTRL littermates and the distribution was scattered (**Fig. 17C, D**). The normalization showed a statistically significant increase of VGLUT1+ terminals contacting PV+ soma in the double-transgenic mice compared to CTRL littermates (**p=0.008; **Fig. 17E**).

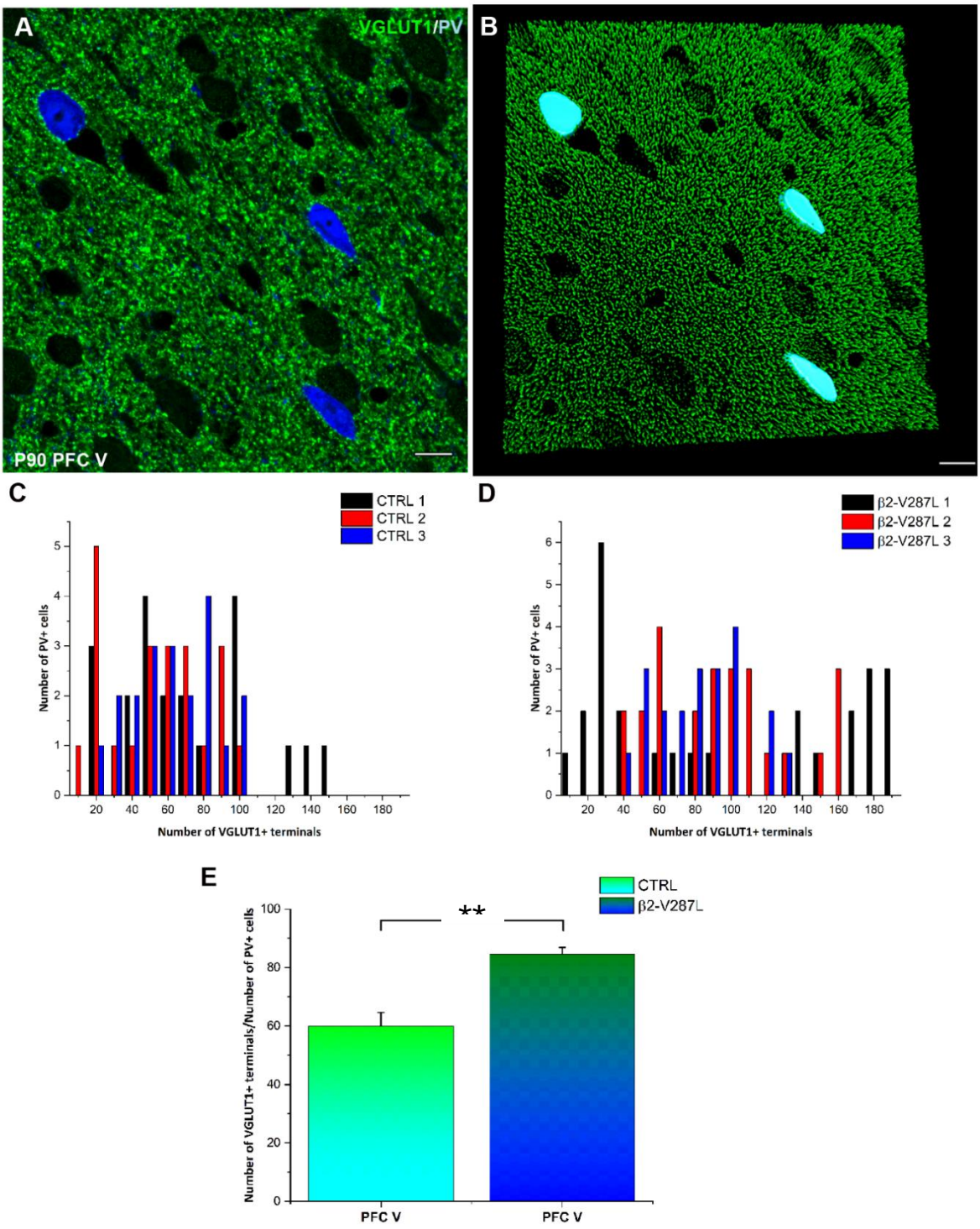

Fig. 17 Analysis of VGLUT1+ contacts on PV+ cells in CTRL and β2-V287L mice.
*Confocal microscope z-stacks of VGLUT1/PV (A) immunofluorescence in PFC layer V. Three-dimensional reconstruction of image in (A) using ArivisVision4D (B). Results of the distribution analysis for each animal (CTRL in C, β2-V287L in D) and the normalization on the number of cells (E) to compare CTRL and double-transgenic animals. The number of VGLUT1+ terminals contacting PV+ cell bodies was higher than in the CTRL littermates and the distribution was scattered. The normalization showed a statistically significant increase of glutamatergic terminals contacting PV+ soma in the double-transgenic mice compared to CTRL littermates. Data are expressed as number of terminals (C, D) and mean number of terminals divided for number of cells (E). The second results were compared with Student's t-test. **p=0.008. (P90, n=3) Scale bar=50 µm.*

Regarding the second class of inhibitory interneurons, the SOM+ ones, in PFC layer V of β2-V287L mice the average number of VGLUT1+ terminals contacting these cells was not different from the one observed in CTRL mice. VGLUT1+ distribution was similar in both β2-V287L and CTRL animals. The normalization showed no significant differences between the two genotypes (**Fig. 18**).

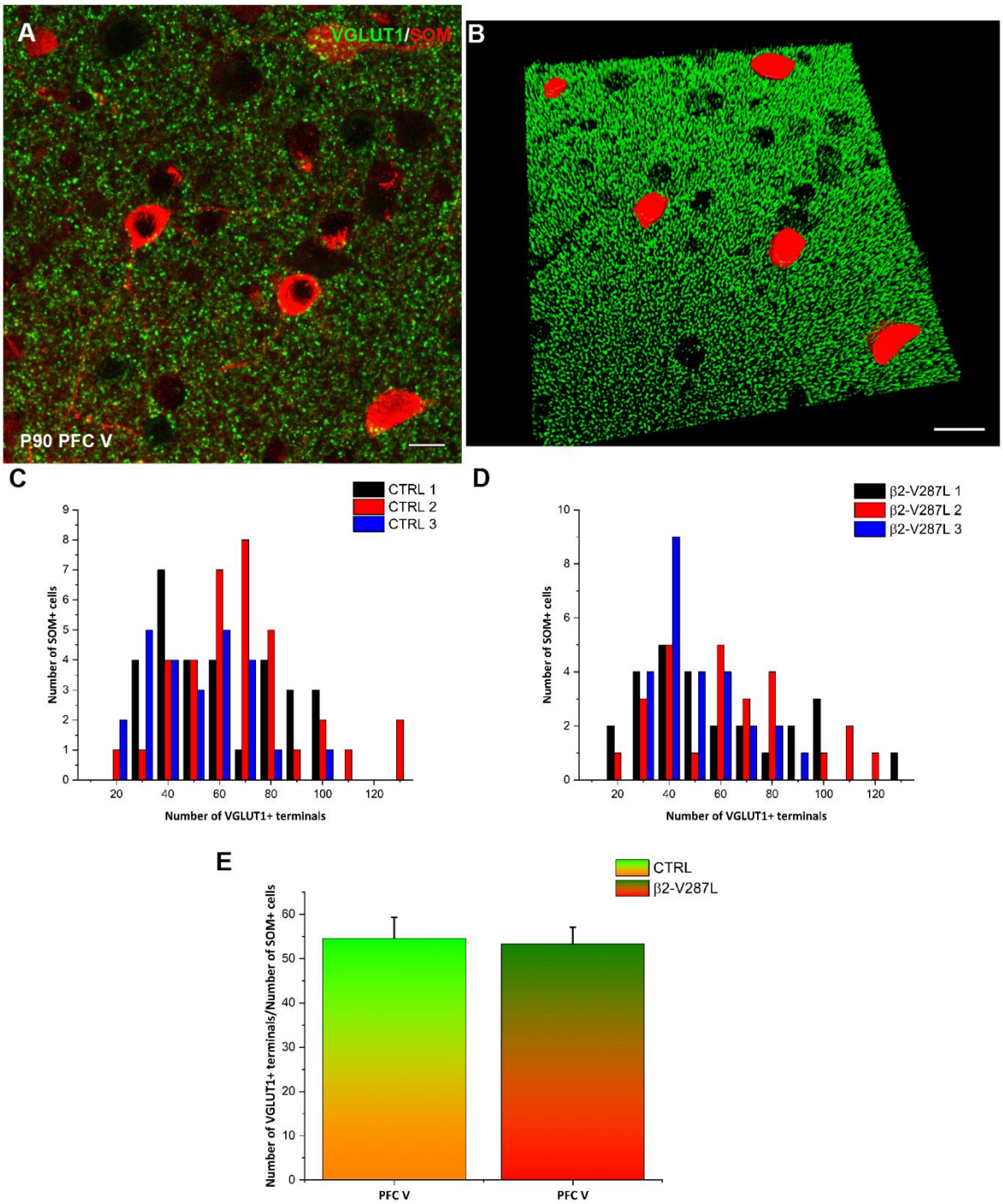

Fig. 18 Distribution analysis of VGLUT1+ terminals on SOM+ cells in CTRL and β2-V287L mice.

Confocal microscope z-stacks of VGLUT1/SOM (A) immunofluorescence in PFC layer V. Three-dimensional reconstruction of the image in (A) using ArivisVision4D (B). Results of the distribution analysis for each animal (CTRL in C, β2-V287L in D) and the normalization on the number of cells (E) to compare CTRL and double-transgenic animals. The results were similar between CTRL and β2-V287L mice. Data are expressed as number of terminals (C, D) and mean number of terminals divided for number of cells (E). The second results were compared with Student's t-test. p=0.850. Scale bar = 50 µm.

The analysis of GABAergic terminals was carried out with the aforementioned method, comparing CTRL and β2-V287L mice. In PFC layer V of double-transgenic mice the number of VGAT+ terminals contacting PV+ cell bodies was similar to the one of the CTRL littermates and the distributions of both CTRL and β2-V287L mice were quite uniform (**Fig. 19**).

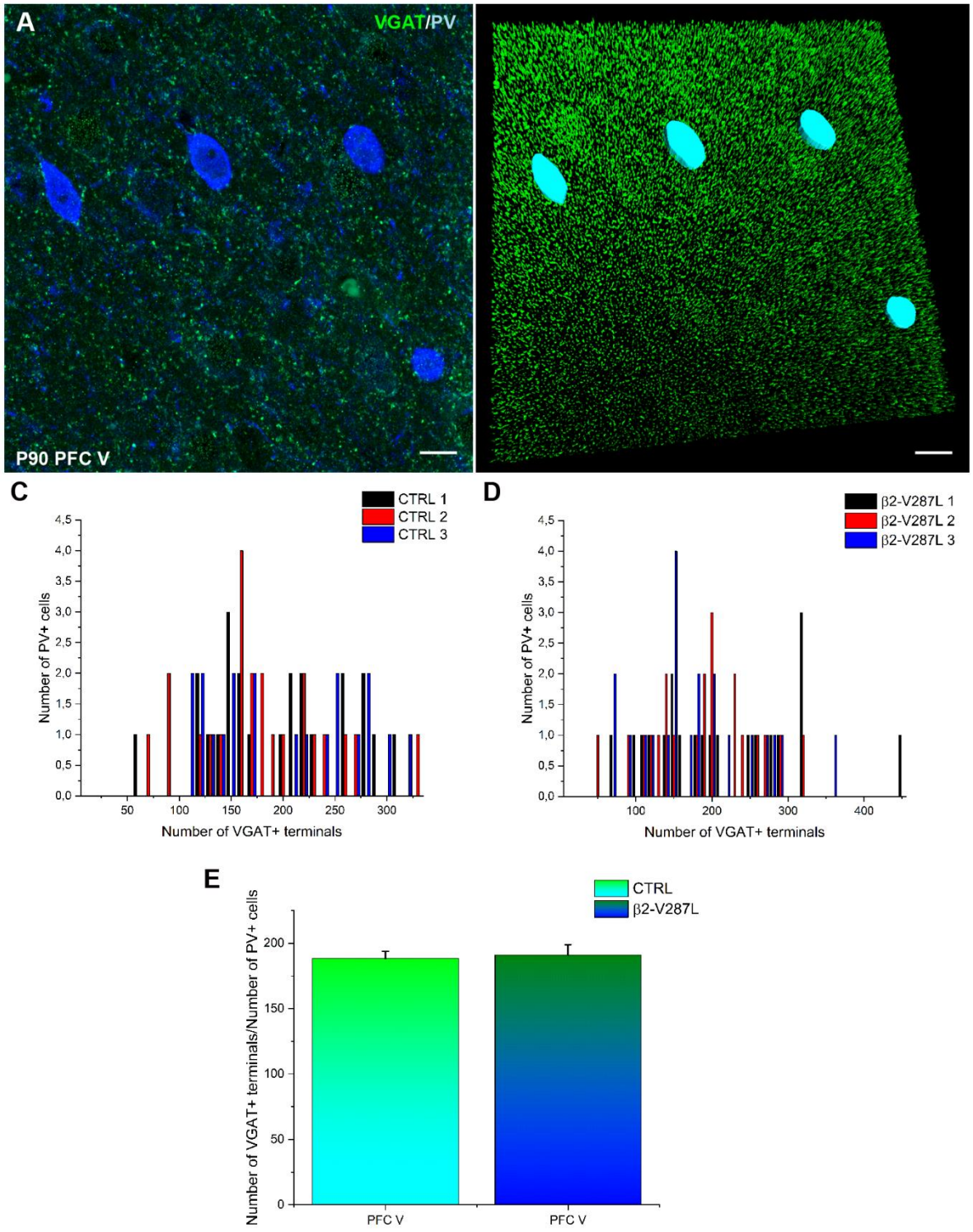

Fig. 19 Analysis of VGAT+ contacts on PV+ cells in CTRL and β2-V287L mice.
Confocal microscope z-stacks of VGAT/PV (A) immunofluorescence in PFC layer V. Three-dimensional reconstruction of image in (A) using ArivisVision4D (B). Results of the distribution analysis for each animal (CTRL in C, β2-V287L in D) and the normalization on the number of cells (E) to compare CTRL and double-transgenic animals. The number of VGAT+ terminals contacting PV+ cell bodies was similar to the one of the CTRL littermates and the distributions in both the genotypes were quite uniform. Data are expressed as number of terminals (C, D) and mean number of terminals divided for number of cells (E). The second results were compared with Student's t-test. p=0.794. (P90, n=3) Scale bar=50 µm.

Regarding the second class of inhibitory interneurons, the SOM+ ones, in PFC layer V of double-transgenic mice the number of VGAT+ terminals contacting these cells was slightly smaller than in the CTRL mice. VGAT+ distribution was homogeneous in β2-V287L, while in CTRL animals the distribution was similar to a normal distribution. The normalization showed no significant differences between the two genotypes (**Fig. 20**).

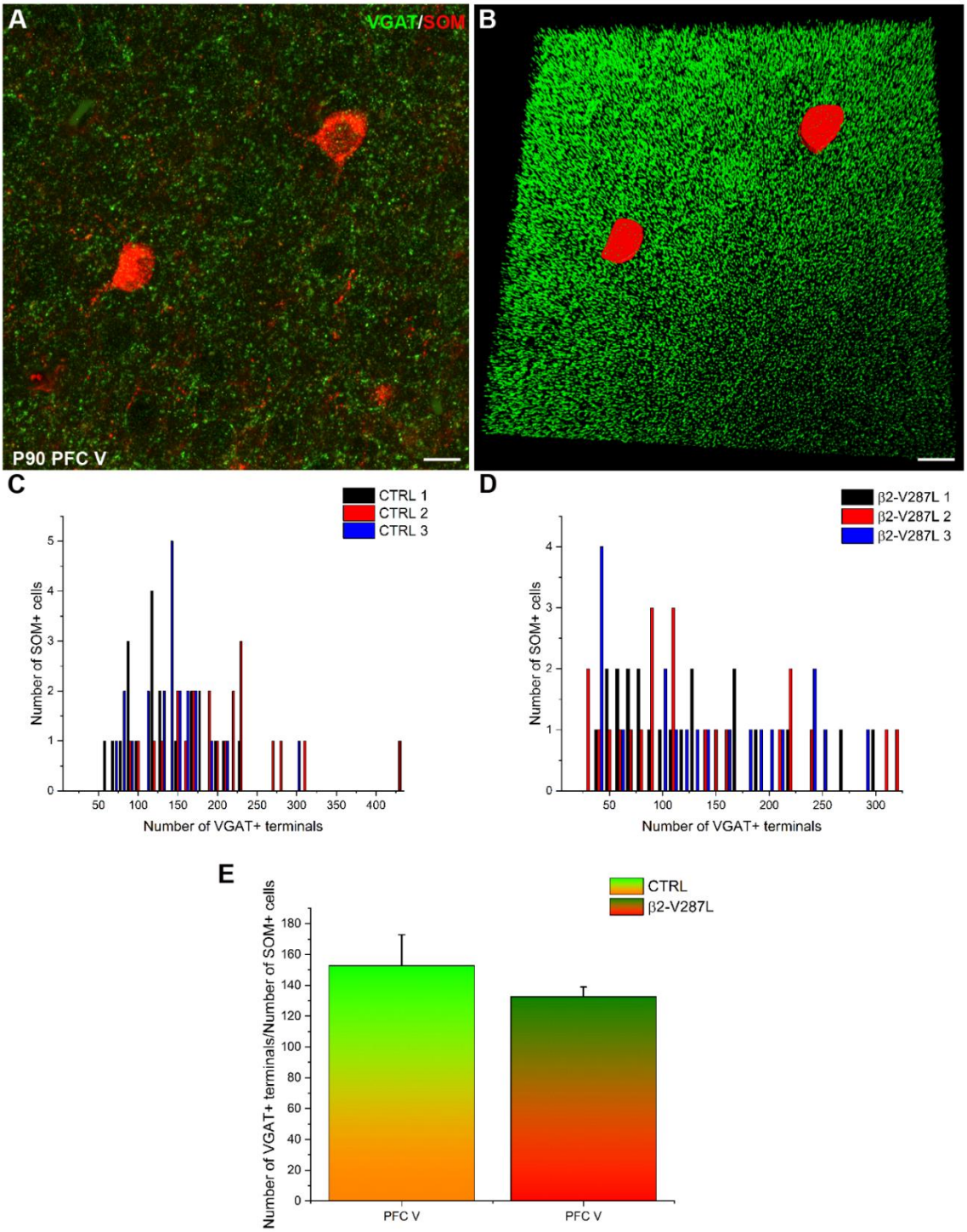

Fig. 20 Distribution analysis of VGAT+ terminals on SOM+ cells in CTRL and β2-V287L mice.

Confocal microscope z-stacks of VGAT/SOM (A) immunofluorescence in PFC layer V. Three-dimensional reconstruction of the image in (A) using ArivisVision4D (B). Results of the distribution analysis for each animal (CTRL in C, β2-V287L in D) and the normalization on the number of cells (E) to compare CTRL and double-transgenic animals. In β2-V287L mice layer V the number of VGAT+ terminals contacting SOM+ neurons was slightly smaller than in the CTRL mice. VGAT+ distribution was homogeneous in double-transgenic mice, while in CTRL animals the distribution was similar to a normal distribution. Data are expressed as number of terminals (C, D) and mean number of terminals divided for number of cells (E). The second results were compared with Student's t-test. p=0.394. Scale bar = 50 µm.

DISCUSSION

In human brain the prefrontal cortex (PFC) is an essential associative area for the integration of complex sensitive stimuli with emotional events and cognitive functions. Alteration of the synaptic balance in this region can lead to neurological disorders, such as epilepsy. In this study on transgenic mice carrying β2-V287L nicotinic acetylcholine receptors (nAChRs) mutation, we focused our attention on PFC, using the somatosensory cortex (SS) as a reference cortex, since, to the best of our knowledge, it's a good model of seizures foci in human frontal areas (Becchetti, 2015). Murine PFC, as the human one, is densely innervated by cholinergic fibers and the nAChRs are expressed throughout the cortical layers (Aracri *et al.*, 2010, 2013). nAChRs are involved in cortical circuits formation (Liu *et al.*, 2006) and the effect of acetylcholine (ACh) on these receptors modulates GABA, glutamate, dopamine, serotonin, adrenaline and ACh release. The study of nAChRs mutations in epilepsy aetiology is thus complex and the results are sometimes controversial. Mutation of β2 nAChRs subunit leads to a delay in the desensitization of the channel and an increase in the receptor sensitivity to the agonists (De Fusco *et al.*, 2000; Becchetti *et al.*, 2015). It is therefore possible that an alteration of neurotrasmitters release by ACh modulation could determine an excitation/inhibition imbalance that could ultimately lead to epileptiform events in the interested cortical area. In the neocortex, in addition, ACh action is more prolonged than in the peripheral synapses, since acetylcholinesterase (which degrades rapidly the neurotransmitter) localization does not completely overlap with cholinergic terminals (Dani and Bertrand, 2007).

Several works have characterized ADNFLE animal models (Fonck *et al.*, 2003, 2005; Klaassen *et al.*, 2006; Labarca *et al.*, 2001; Mann and Mody, 2008; Tapper *et al*., 2004; Teper *et al.*, 2007; Xu *et al*., 2011; Zhu *et al.*, 2008), nevertheless morphological and neurochemical data are scarce and fragmentary. Evidences regarding these aspects are provided by cortical cell counts after thionine-staining and mutated subunits expression analysis in different classes of neurons (Fonck *et al.*, 2003, 2005; Labarca *et al.*, 2001; Shiba *et al.*, 2015; Zhu *et al.*, 2008). The murine model generated by Manfredi and colleagues (2009) recapitulates several features of human pathological condition, since the epileptic seizures are spontaneous and occur during sleep. However, although gross anatomical and behavioral alterations are absent, thorough morphological studies of this model are still lacking. The aim of this work was to preliminarily characterize the PFC by means of immunohistochemistry and

electrophysiological recordings, with a focus on cholinergic, GABAergic and glutamatergic systems. The study was conducted on adult mice to observe the correlation between the epileptic phenotype and permanent alterations in the fully-developed cortical circuits.

Morphological aspects of the neocortex of β2-V287L mouse model

In different models of epilepsy, substantial morphological alterations have been found, caused by altered morphogenetic processes (Cipelletti *et al.*, 2002; Edwards *et al.*, 2000; Sisodiya, 2004). Nevertheless, in different models of ADNFLE no differences in cortical cytoarchitecture or apoptotic phenomena have been reported in adult animals (Fonck *et al.*, 2003, 2005; Shiba *et al.*, 2015; Tapper *et al.*, 2004; Zhu *et al.*, 2008). In our study, cortical thickness and number of both neurons and synapses are not dissimilar in double-transgenic and control mice, in agreement with the ADNFLE models. Further analyses on different developmental stages will be needed to rule out the presence of major morphological abnormalities in the model.

The GABAergic system in the adult PFC

Electrophysiological data on our model suggest that cortical hyperexcitability could be due to a decreased physiological feedback inhibition onto pyramidal neurons. Since GABA release is modulated by nAChRs (Aracri *et al.*, 2010; Liu *et al.*, 2006) and recalling that alterations in the GABAergic system were observed in different ADNFLE models (Klaassen *et al.*, 2006; Xu *et al.*, 2011; Zhu *et al.*, 2008) and in our previous work (Amadeo *et al.*, 2018; Chapter 2), our study was focused on the analysis of GABAergic system. We took into account, in particular, the two major classes of inhibitory neurons, respectively expressing parvalbumin (PV+) and somatostatin (SOM+). The first subgroup is formed by basket and chandelier cells that project their axons horizontally and form synapses onto perisomatic compartments and proximal part of axons of pyramidal neurons (Kawaguchi and Kubota, 1997; Kubota *et al.*, 2014). Martinotti and non-Martinotti cells are part of the SOM+ subgroup. These cells vertically project their axons towards supragranular cortical layers, forming synapses onto peripheral dendrites of pyramidal neurons, and are activated by synchronous discharges of pyramidal neurons themselves (Funk *et al.*, 2017). Both subpopulations are involved in the modulation of spontaneous epileptic discharges in genetic models (Bohannon and Hablitz, 2018; Calin *et al.*, 2019; Tai *et al.*, 2018). Our data show that

PV+ and SOM+ neurons present a tendency in upregulation in the PFC of double-transgenic mice, from the results of immunofluorescence and immunoperoxidase. This tendency could be due to the relative increase of one or both subpopulations. This evidence could be interpreted in different ways, since ADNFLE experimental models provided controversial data regarding the role of the GABA in different species (rat and mouse) and different murine strains (Klaassen *et al.*, 2006; Shiba *et al.*, 2015; Teper *et al.*, 2007; Zhu *et al.*, 2008). Hence, one could assume that the GABAergic system, after alterations in the GABAergic switch (Amadeo *et al.*, 2018; Chapter 2) and/or in the synaptogenesis during the development, might be upregulated in adult stages as a compensatory mechanism to counterbalance cortical hyperexcitability.

Effect of β2-V287L mutation on PFC innervation and glutamatergic and GABAergic terminals expression in the mouse model

Heteromeric nAChRs could influence the development of glutamatergic system (Molas and Dierssen, 2014), by directly affecting neurotransmitter release: presynaptic nAChRs have been found to promote the release of both glutamate and GABA on PFC layer V pyramidal neurons (Aracri *et al.*, 2010, 2013). nAChRs located on presynaptic glutamatergic terminals are known to facilitate the release of glutamate that help to convert “silent” synapses to functional ones in developing hippocampal and cortical neurons (Molas and Dierssen, 2014). Conversion of silent synapses into functional ones constitutes an efficient mechanism for enhancing synaptic efficacy in the immature brain. Nicotine administration has been found to elicit persistent changes in synaptic efficacy in immature glutamatergic synapses (Maggi *et al.*, 2003) and nAChRs activation can also affect the localization of glutamatergic synapses (Lozada *et al.*, 2012). Mutations in genes encoding nAChRs subunits could alter glutamatergic release and cause an excitation/inhibition imbalance that might lead to epileptogenesis during the development (Molas and Dierssen, 2014). On the other hand, several studies have showed alterations in glutamatergic markers expression in both genetic and pilocarpine-induced animal models of epilepsy, especially in neurotransmitter reuptake and/or in the expression of specific vesicular transporters (Touret *et al.*, 2007; Zubareva *et al.*, 2018). Since alteration of glutamate vesicular transporters could affect the amount of released glutamate, it might be related to different pathologic processes (Liguz-Lecznar and Skangiel-Kramska, 2007). We considered the expression of vesicular glutamate transporter 1 (VGLUT1), specific of intracortical synapses, in PFC

layer V of β2-V287L murine model. The density of intracortical glutamatergic innervation was not different in the two genotypes. The analysis of VGLUT1+ terminals contacting PV+ and SOM+ cells revealed a statistically significant increment of VGLUT1/PV contacts in β2-V287L compared to CTRL animals, while the same analysis on SOM+ cells showed no significant differences. It is necessary to emphasize that SOM+ neurons, receiving a large amount of pyramidal glutamatergic terminals, seem to exert a global antiepileptic effect in some experimental models (Yavorska and Wehr, 2016). On the other hand, PV+ neurons have a central role in cortical synchronization mechanisms (Bohannon and Hablitz, 2018) and in epileptic discharges suppression (Calin *et al.*, 2018). Nevertheless, electrophysiological data on our model show a decrement of excitatory inputs on fast-spiking PV+ neurons in double-transgenic mice compared to the control littermates. The difference between morphological and electrophysiological data could be due to the different ages of animals and, in particular, to the fact that the recorded mice were younger (P20-P50) than the ones analyzed in the morphological study (P90). This evidence could suggest the presence of a partial compensatory mechanism capable of sustaining the feedback inhibition provided by PV+ cells towards pyramidal neurons in P90 adult mice. This mechanism might explain why some cases of partial remission were found in ADNFLE adult patients (Combi *et al.*, 2004; Steinlein *et al.*, 1997). In addition, it is interesting to take into account that the progressive increase of input onto GABAergic interneurons could be a proepileptic effect *per se*, as showed in different experimental models. For instance, the optogenetic activation of PV+ neurons in the CA3 region of the hippocampus and in the visual cortex just before an epileptic discharge induces a briefer seizure event, but photo-stimulating PV+ cells 2 seconds after the beginning of the epileptic discharge leads to the opposite effect (Ellender *et al.*, 2014; Magloire *et al.*, 2019). KCC2 cotransporter overexpression in pyramidal neurons located near the epileptogenic site prevents the effect of the “delayed” photo-stimulation of PV+ cells (Magloire *et al.*, 2019). These effects were not produced by stimulating SOM+ neurons (Magloire *et al.*, 2019). The involvement of chloride cotransporters could suggest their crucial role in Cl^- intracellular accumulation-induced epileptogenesis (Raimondo and Dulla, 2019). Bohannon and colleagues, in addition, showed the contribution of SOM+ and PV+ in the generation of synchronous long-lasting aberrant discharges in the sensorimotor murine cortex by means of optogenetics (Bohannon and Hablitz, 2018).

Conclusion

Our data suggest an alteration of PFC layer V microcircuits in the studied model of ADNFLE. Despite the absence of gross GABAergic or cholinergic abnormalities, KCC2 expression is altered in the PFC both in postnatal development and in adult stages (Amadeo *et al.*, 2018; Chapter 2). This evidence, along with the results of this work, suggests the establishment of particular adaptation mechanisms of thalamocortical and corticocortical circuits, aimed to counteract the propagation of epileptic events. It would be useful to carry out further analyses of SOM+ and PV+ GABAergic subpopulations and their glutamatergic and GABAergic afferences at different developmental stages, when an alteration of GABAergic and glutamatergic release by nicotinic receptors could be present. This study could be performed along with a thorough investigation of terminals contacting PFC layer V pyramidal neurons and of different GABAergic subpopulations, as neurons expressing vasointestinal peptide (VIP+). Onto VIP+ neurons many cholinergic afferences are present (Kamigaki, 2018; Wall *et al.*, 2016) and these cells can exert an inhibitory effect on SOM+ and PV+ neurons (Parrish *et al.*, 2019; Pfeffer *et al.*, 2013). The global interpretation of these data and the ones present in the literature suggests a non-straightforward perspective, but nuanced, multi-faceted and far from being completely understood, of mechanisms regulating cortical microcircuits, especially in pathological conditions and in relationship to GABAergic subpopulations. Further experiments will be necessary to shed light on these mechanisms and on the role of mutated nAChRs in ADNFLE pathogenesis.

REFERENCES

Amadeo A, Coatti A, Aracri P, Ascagni M, Iannantuoni D, Modena D, Carraresi L, Brusco S, Meneghini S, Arcangeli M, Pasini ME and Becchetti A (2018) *Postnatal Changes in K^+/Cl^- Cotransporter-2 Expression in the Forebrain of Mice Bearing a Mutant Nicotinic Subunit Linked to Sleep-Related Epilepsy*. Neuroscience 386:91-107.

Aracri P, Consonni S, Morini R, Perrella M, Rodighiero S, Amadeo A and Becchetti A (2010) *Tonic modulation of GABA release by nicotinic acetylcholine receptors in layer V of the murine prefrontal cortex.* Cerebral Cortex 20: 1539-1555.

Aracri P, Amadeo A, Pasini ME, Fascio U, and Becchetti A (2013) *Regulation of glutamate release by heteromeric nicotinic receptors in layer V of the secondary motor region (Fr2) in the dorsomedial shoulder of prefrontal cortex in mouse.* Synapse 67, 338-357.

Aracri P, Meneghini S, Coatti A, Amadeo A and Becchetti A (2017) *α4β2* nicotinic receptors stimulate GABA release onto fast-spiking cells in layer V of mouse prefrontal (Fr2) cortex.* Neuroscience. 340: 48-61.

Becchetti A, Aracri P, Meneghini S, Brusco S and Amadeo A (2015) *The role of nicotinic acetylcholine receptors in autosomal dominant nocturnal frontal lobe epilepsy.* Frontiers in Physiology. 6(22):1-12.

Bertrand D, Elmslie F, Hughes E, Trounce J, Sander T, Bertrand S and Steinlein OK (2005) *The CHRNB2 mutation I312M is associated with epilepsy and distinct memory deficits.* Neurobiol. Dis. 20 (3): 799-804.

Bohannon AS and Hablitz JJ (2018) *Optogenetic dissection of roles of specific cortical interneuron subtypes in GABAergic network synchronization.* J Physiol. 596(5):901-919.

Bolte S and Cordelières FP (2006) *A guided tour into subcellular colocalization analysis in light microscopy.* J Microsc 224:213-232.

Calin A, Stancu M, Zagrean A, Jefferys JGR, Ilie AS and Akerman CJ (2019) *Chemogenetic Recruitment of Specific Interneurons Suppresses Seizure Activity.* Front. Cell. Neurosci. 12:293.

Cipelletti B, Avanzini G, Vitellaro-Zuccarello L, Franceschetti S, Sancini G, Lavazza T, Acampora D, Simeone A, Spreafico R and Frassoni C (2002) *Morphological organization of somatosensory cortex in $Otx1^{-/-}$ mice.* Neuroscience 115, no. 3: 657-667.

Combi R, Dalpra L, Tenchini ML and Ferrini-Strambi L (2004) *Autosomal dominant noctunal frontal lobe epilepsy- A critical overview.* Journal of Neurology 251 (8): 923-934.

Dani JA and Bertrand D (2007) *Nicotinic Acetylcholine Receptors and Nicotinic Cholinergic Mechanisms of the Central Nervous System*. Annu. Rev. Pharmacol. Toxicol. 47: 699-729.

De Fusco M, Becchetti A, Patrignani A, Annesi G, Gambardella A, Quattrone A, Ballabio A, Wanke E and Casari G (2000) *The nicotinic receptor beta2 subunit is mutant in nocturnal frontal lobe epilepsy.* Nature Genetics 26 (3), 275-276.

Edwards JC, Wyllie E, Ruggeri PM, Bingaman W, Lüders H, Kotagal P, Dinner DS, Morris HH, Prayson RA and Comair YG (2000) *Seizure outcome after surgery for epilepsy due to malformation of cortical development.* Neurology 55, no. 8 1110-1114.

Ellender TJ, Raimondo JV, Irkle A, Lamsa KP and Akerman CJ (2014) *Excitatory effects of parvalbumin-expressing interneurons maintain hippocampal epileptiform activity via synchronous afterdischarges.* J. Neurosci. 34(46):15208-22.

Fonck C, Nashmi R, Deshpande P, Damaj MI, Marks MJ, Riedel A, Schwarz J, Collins AC, Labarca C and Lester HA (2003) *Increased sensitivity to agonist-induced seizures, Straub tail, and hippocampal theta rhythm in knock-in mice carrying hypersensitive α4 nicotinic receptors.* The Journal of neuroscience 23, no. 7 25822590.

Fonck C, Cohen BN, Nashmi R, Whiteaker P, Wagenaar DA, Rodrigues-Pinguet N, Deshpande P *et al.* (2005) *Novel seizure phenotype and sleep disruptions in knock-in mice with hypersensitive α4* nicotinic receptors.* The Journal of neuroscience 25, no. 49 11396-11411.

Funk CM, Peelman K, Bellesi M, Marshall W, Cirelli C and Tononi G (2017) *Role of Somatostatin-Positive Cortical Interneurons in the Generation of Sleep Slow Waves.* The Journal of Neuroscience 37(38):9132-9148.

Ghasemi M and Hadipour-Niktarash A (2015) *Pathologic role of neuronal nicotinic acetylcholine receptors in epileptic disorders: implication for pharmacological interventions.* Reviews in the Neurosciences. 26(2), 199-223.

Heron SE, Scheffer IE, Berkovic SF, Dibbens LM and Mulley JC (2007) *Channelopathies in idiopathic epilepsy.* Neurotherapeutics. 4: 295-304.

Kamigaki T (2019) *Prefrontal circuit organization for executive control.* Neurosci. Res.140:23-36.

Kawaguchi Y and Kubota Y (1997) *GABAergic cell subtypes and their synaptic connections in rat frontal cortex.* Cereb. Cortex 7, 476-486.

Klaassen A, Glykys J, Maguire J, Labarca C, Mody I and Boulter J (2006). *Seizures and enhanced cortical GABAergic inhibition in two mouse models of human autosomal dominant nocturnal frontal lobe epilepsy.* Proc. Natl. Acad. Sci. U.S.A. 103, 19152-19157.

Kubota Y (2014) *Untangling GABAergic wiring in the cortical microcircuit.* Curr. Opin. Neurobiol. 26, 7-14.

Labarca C, Schwarz J, Deshpande P, Schwarz S, Nowak MW, Fonck C and Nashmi R (2001) *Point mutant mice with hypersensitive α4 nicotinic receptors show dopaminergic deficits and increased anxiety.* Proceedings of the National Academy of Sciences 98, no. 5 2786-2791.

Liguz-Lecznar M and Skangiel-Kramska J (2007) *Vesicular glutamate transporters (VGLUTs): the three musketeers of glutamatergic system.* Acta Neurobiol Exp (Wars). 67(3):207-18.

Liu Z, Neff RA and Berg DK (2006) *Sequential interplay of nicotinic and GABAergic signaling guides neuronal development.* Science 314, 1610-1613.

Lozada AF, Wang X, Gounko NV, Massey KA, Duan J, Liu Z and Berg DK (2012) *Induction of dendritic spines by β2-containing nicotinic receptors.* The Journal of Neuroscience 32: 8391-8400.

Maggi L, Le Magueresse C, Changeux JP and Cherubini E (2003) *Nicotine activates immature "silent" connections in the developing hippocampus.* Proceedings of the National Academy of Sciences 100: 2059-2064.

Magloire V, Cornford J, Lieb A, Kullmann DM, Pavlov I (2019) *KCC2 overexpression prevents the paradoxical seizure-promoting action of somatic inhibition.* Nat. Commun. 10(1):1225.

Manfredi I, Zani AD, Rampoldi L, Pegorini S, Bernascone I, Moretti M *et al.* (2009) *Expression of mutant β2 nicotinic receptors during development is crucial for epileptogenesis.* Hum. Mol. Genet. 18, 1075-1088.

Mann EO and Mody I (2008) *The multifaceted role of inhibition in epilepsy: seizure-genesis through excessive GABAergic inhibition in autosomal dominant nocturnal frontal lobe epilepsy.* Curr. Opin. Neurol. 21, 155-160.

Molas S and Dierssen M (2014) *The role of nicotinic receptors in shaping and functioning of the glutamatergic system: A window into cognitive pathology.* Neuroscience & Biobehavioral Reviews 46: 315-325.

Noebels JL, Avoli M, Rogawski MA *et al.* (2012) *Jasper's Basic Mechanisms of the Epilepsies.* 4th edition. National Center for Biotechnology Information (US).

Parrish RR, Codadu NK, Mackenzie-Gray Scott C and Trevelyan AJ (2019) *Feedforward inhibition ahead of ictal wavefronts is provided by both parvalbumin- and somatostatin-expressing interneurons.* J. Physiol. 2019 597(8):2297-2314.

Pfeffer CK, Xue M, He M, Huang ZJ and Scanziani M (2013) *Inhibition of inhibition in visual cortex: the logic of connections between molecularly distinct interneurons.* Nat. Neurosci. 16, 1068-1076.

Raimondo JV and Dulla C (2019) *When a Good Cop Turns Bad: The Pro-Ictal Action of Parvalbumin Expressing Interneurons During Seizures.* Epilepsy Curr. (4):256-257.

Shiba Y, Mori F, Yamada J, Migita K, Nikaido Y, Wakabayashi K, Kaneko S, Okada M, Hirose S and Ueno S (2005) *Spontaneous epileptic seizures in transgenic rats harboring a human ADNFLE missense mutation in the β2subunit of the nicotinic acetylcholine receptor.* Neuroscience research 100: 46-54.

Sisodiya SM (2004) *Malformations of cortical development: burdens and insights from important causes of human epilepsy.* The Lancet Neurology 3, no. 1 29-38.

Steinlein OK, Mulley JC, Propping P, Wallace RH, Phillips HA, Sutherland GR, Sheffer IE and Berkovic SF (1995) *A missense mutation in the neuronal nicotinic acetylcholine receptor alpha 4 subunit is associated with autosomal dominant nocturnal frontal lobe epilepsy.* Nature Genetics 11 (2): 201-203.

Steinlein OK, Magnusson A, Stoodt J, Bertrand S, Weiland S, Berkovic SF, Nakken KO, Propping P and Bertrand D (1997). *An insertion mutation of the CHRNA4 gene in a family with autosomal dominant nocturnal frontal lobe epilepsy.* Hum. Mol. Genet. 6: 943-947.

Tai C, Abe Y, Westenbroek RE, Scheuer T and Catterall WA (2014) *Impaired excitability of somatostatin- and parvalbumin-expressing cortical interneurons in a mouse model of Dravet syndrome.* PNAS E3139–E3148.

Tapper AR, McKinney SL, Nashmi R, Schwarz J, Deshpande P, Labarca C, Whiteaker P, Marks MJ, Collins AC and Lester HA (2004) *Nicotine activation of α4* receptors: sufficient for reward, tolerance, and sensitization.* Science 306, no. 5698 1029-1032.

Teper Y, Whyte D, Cahir E, Lester HA, Grady SR, Marks MJ *et al.* (2007*) Nicotine-induced dystonic arousal complex in a mouse line harboring a human autosomal-dominant nocturnal frontal lobe epilepsy mutation.* J. Neurosci. 27, 10128-10142.

Touret M, Parrot S, Denoroy L, Belin M and Didier-Bazes M (2007) *Glutamatergic alterations in the cortex of genetic absence epilepsy rats.* BMC Neuroscience 8:69.

Wall NR, De La Parra M, Sorokin JM, Taniguchi H, Huang ZJ and Callaway EM (2016) *Brain-Wide Maps of Synaptic Input to Cortical Interneurons.* J Neurosci. 36(14):4000-9.

Xu J, Cohen BN, Zhu Y, Dziewczapolski G, Panda S, Lester HA *et al.* (2011) *Altered activity-rest patterns in mice with a human autosomal dominant nocturnal frontal lobe epilepsy mutation in the β2 nicotinic receptor.* Mol. Psychiatry 16, 1048-1061.

Yavorska I and Wehr M (2016) *Somatostatin-Expressing Inhibitory Interneurons in Cortical Circuits.* Front. Neural Circuits 10:76.

Zhu G, Okada M, Yoshida S, Ueno S, Mori F, Takahara T *et al.* (2008) *Rats harboring S284L Chrna4 mutation show attenuation of synaptic and extrasynaptic GABAergic transmission and exhibit the nocturnal frontal lobe epilepsy phenotype.* J. Neurosci. 28, 12465-12476.

Zubareva OE, Kovalenko AA, Kalemenev SV, Schwarz AP, Karyakin VB and Zaitsev AV (2018) *Alterations in mRNA expression of glutamate receptor subunits and excitatory amino acid transporters following pilocarpine-induced seizures in rats.* Neuroscience Letters 686: 94-100.

Zwart R and Vijverberg HP (1997) *Potentiation and inhibition of neuronal nicotinic receptors by atropine: competitive and noncompetitive effects.* Molecular Pharmacology 52, 886-895.

Chapter 4

The Expression of Mutant β2-V287L Nicotinic Receptor Does Not Affect Cholinergic Nuclei and Different Neuronal and Synaptic Markers in the Thalamus

Meneghini S [b], Brusco S [b], Coatti A [b], Aracri P [b], Modena D [a], Carraresi L [d], Arcangeli A [c], Amadeo A [a] and Becchetti A [b] (2017) *The role of neuronal nicotinic receptors in the pathogenesis of Autosomal Dominant Nocturnal Frontal Lobe Epilepsy: a study on wild-type and conditional transgenic mice expressing the β2-V287L subunit.* Abstract book: pp. 30, #93. XIX Scientific Convention Telethon, Riva del Garda, Italy.

Modena D [a], Ascagni M [e], Iannantuoni D [a], Donati CE [a], Franquesa Puig E [a], Becchetti A [b] and Amadeo A [a] (2017) *Morphological characterization of a murine model of Autosomal Dominant Nocturnal Frontal Lobe Epilepsy (ADNFLE)*. Abstract book "Facciamo rete in Neuronest - 1° meeting traslazionale del gruppo di ricerca strategico in neuroscienze de "La Statale"": P.11. Neuronest, Milan, Italy.

[a] *Department of Biosciences, University of Milano, Via Celoria, 26, 20133 Milano, Italy*
[b] *Department of Biotechnology and Biosciences, and NeuroMI-Milan Center of Neuroscience, University of Milano-Bicocca, Piazza della Scienza, 2, 20126 Milano, Italy*
[c] *Department of Experimental and Clinical Medicine, University of Florence, Largo Brambilla, 3, 50134 Firenze, Italy*
[d] *Dival Toscana Srl, Via Madonna del Piano, 6 – 50019 Sesto Fiorentino, Firenze, Italy*
[e] *Unitech NOLIMITS, University of Milan, Via Golgi 19, 20133 Milano, Italy*

ABSTRACT

Cerebral cholinergic system is involved in many cognitive processes, such as attention, memory and sleep-wake cycle regulation. nAChRs have a crucial role in cellular proliferation and survival, in formation and maturation of the synapses, in neuronal differentiation and neurotransmitters release. Mutations in genes encoding nAChRs subunits are related to some forms of epilepsy, as Autosomal Dominant Nocturnal Frontal Lobe Epilepsy (ADNFLE). In this study, we took advantage of β2-V287L murine model to analyse the main cerebral cholinergic nuclei and the thalamic reticular nucleus, since, even though the epileptic foci are in the cerebral cortex, this area seems to be involved in epileptogenesis, directly acting on cortical activity and on sleep-wake cycle. The analyses revealed no significant differences in the expression of several cholinergic and GABAergic markers in the thalamus and in the number of cerebral cholinergic nuclei neurons.

INTRODUCTION

In the somatosensory regions of the thalamus, inputs are processed by a network of thalamocortical neurons, mutually interconnected in the ventrobasal nucleus (VB) and in the thalamic reticular nucleus (RT). Thalamic modulation of stimuli is determined by complex close and open circuits that connect mainly the cortical and thalamocortical glutamatergic neurons with the RT GABAergic cells (Pita-Almenar *et al.*, 2014). On these circuits modulatory cholinergic afferences arrive from the ascending reticular activating system (ARAS), in particular from the laterodorsal tegmental nucleus (LDT) and the peduncolopontine tegmental nucleus (PPT), that form synapses with several nuclei of dorsal thalamus, including VB and RT (Beierlein, 2014; Picard and de Saint Martin, 2003). RT, in particular, receives cholinergic projections even from the forebrain *nucleus basalis magnocellularis* (nBM) (Beierlein, 2014; Heckers *et al.*, 1992; Mitchell *et al.*, 2002; Sun *et al.*, 2013). In RT both muscarinic and nicotinic receptors are present, the formers induce hyperpolarization, while the latters determine the excitation of RT neurons. Hence, even if the major effect of cholinergic stimulation of RT seems to induce an inhibition of thalamocortical relay cells (Holmstrand and Sesack, 2011; Pita-Almenar *et al.*, 2014), the global picture is more complex, due to the neurochemical and electrophysiological properties of this nucleus. RT is formed by GABAergic neurons, it determines a strong inhibitory input on thalamic relay cells (Nanobashvili *et al.*, 2012; Sokhadze *et al.*, 2018) and is located between the dorsal thalamus and the cerebral cortex, receiving glutamatergic inputs from the collateral axons of thalamocortical (TC) neurons and layer VI corticothalamic (CT) cells (Beierlein, 2014). RT efferents project to TC neurons, that send glutamatergic inputs to the RT and the cerebral cortex (Jones, 2007). Therefore, RT is largely involved in the control of sensory elaboration and in the generation of rhythmic activity in the TC system (Beierlein, 2014). The nucleus does not project directly to the cortex, but modulates TC neurons in order to select the information (Pratt and Morris, 2015). The circuits are made even more complex by the presence of intrinsic GABAergic synapses in RT that are depolarizing. RT neurons maintain a low concentration of cloride cotransporter KCC2, whose expression increases during the development (Amadeo *et al.*, 2018; Chapter 2). These intrinsic GABAergic inputs can activate low-threshold Ca^{2+} type-T channels, that, after depolarization, determine the action potentials occurrence in RT neurons and the generation of strong inhibitory inputs on thalamic relay cells

(Sun *et al.*, 2012). In addition, RT is the responsible of the generation of the sleep spindles, synchronous TC oscillations that characterize the stage 2 of NREM sleep (Sun *et al.*, 2012). The role of the cholinergic system in RT is still controversial. Recent studies showed that optogenetic stimulation of cholinergic inputs to RT determined the local GABAergic RT neurons activation to promote sleep, shortening the transition between wakefulness and sleep and inducing NREM-related spindles (Ni *et al.*, 2016). Ni and colleagues (2016) also noted that cholinergic neurons promoted NREM stages in sleeping mice. On the other hand, previous studies showed that, in the ferret, the activation of RT cells by ACh could be able to contribute to sleep spindles shutdown at the time of awakening, increasing intrareticular GABAergic activity (Lee and McCormick, 1995). ACh release in the thalamus during NREM sleep induces, through nicotinic acetylcholine receptors (nAChRs), the activity of inhibitory intrareticular synapses and de-synchronizes TC activity, leading to awakening. Some authors hypothesized that an altered nAChRs sensitivity could prevent sleep spindles shutdown, leading to pathological oscillations and epilepic discharges (Picard and de Saint Martin, 2003). nAChRs sensitivity could be altered by mutations in genes encoding for their subunits. These mutations are the culprits of particular forms of epilepsies, as Autosomal Dominant Nocturnal Frontal Lobe Epilepsy (ADNFLE). In ADNFLE nAChRs alteration seems to determine a chronic hyperactivation of the ARAS, especially LDT, which releases ACh in the thalamus during NREM sleep before the awakening, and of the mediodorsal thalamus (Picard *et al.*, 2006). The resulting excitation induces epileptic events in the frontal lobe (Halasz and Szűcs, 2018). In other studies, nAChRs containing β2 subunit have been found as important mediator of NREM sleep stability (Becchetti *et al.*, 2015).

As observed in the work of Clemente-Perez and colleagues (2017), in RT several GABAergic subpopulations are present. These subgroups are characterized by different morphological and electrophysiological properties and connections, and might have different functional roles. Only the GABAergic interneurons that express parvalbumin (PV) seem to be rhythmogenic, while neurons expressing somatostatin (SOM) seem to be involved in the modulation of the limbic system. Hence, alterations of PV+ subgroup might be implicated in epilepsies, while SOM+ neurons could be altered in psychiatric disorders (Clemente-Perez *et al.*, 2017; Crabtree, 2018; Pinault, 2004).

To better understand the relationship between RT and nAChRs in both physiological and pathological conditions, and the possible alterations of the cholinergic nuclei due to a nAChRs subunit mutation found in ADNFLE patients, we studied a murine model of ADNFLE developed by Manfredi and colleagues in 2009, that well reproduces the main features of the human pathology (Manfredi *et al.*, 2009). In these mice, β2-V287L needs to be expressed throughout brain development, until the end of the second postnatal week, for seizures to develop, indicating that critical stages of synaptic stabilization are implicated in the pathogenesis of ADNFLE. As shown in Chapter 2, the mutation induced an altered expression of the chloride cotransporter KCC2, the responsible of the “switch of the GABA”, in the thalamic reticular nucleus (RT) in adulthood. These remarks led us to investigate whether the expression of β2-V287L affected the GABAergic and cholinergic systems in RT and the main cerebral cholinergic nuclei. Regarding cholinergic and GABAergic markers in the thalamus, no significant differences were found between control and double-transgenic (β2-V287L) mice. The number of neurons in the cholinergic nuclei was similar in the two experimental groups. Our results indicate that β2-V287L mutation seems to affect only the expression of KCC2 in the thalamic reticular nucleus of adult mice.

EXPERIMENTAL PROCEDURES

Animals

Mice were housed in SPF conditions on a 12h light-dark cycle, at 21 ± 1°C, 55 ± 10% humidity and free access to food and water. Mice genotyping was carried out as previously described (Manfredi *et al.*, 2009). All procedures followed the Italian law (2014/26, implementing the 2010/63/UE) and were approved by the local Ethical Committees and the Italian Ministry of Health. For the different analyses we used FVB mice (Harlan) of either sex, at the postnatal (P) day 90. The transgenic strain we used was the S3 line of double-transgenic FVB (tTA:Chrnb2V287L) mice, which express β2-V287L under a tetracycline-controlled transcriptional activator (tTA). These mice were compared with their littermates not expressing β2-V287L, which were either WT or bearing TRE-Chrnb2V287L or PrnP-tTA genotypes (Manfredi *et al.*, 2009). For clarity, mice expressing the transgene are hereafter denoted as β2-V287L, while the control littermates are denoted as controls (CTRL). The analyses were carried out on at least 3 animals for each experimental group (CTRL and β2-V287L). No morphological difference was observed between sexes.

Brain regions

For stereological cell countings, slices between -5.02 and -4.36 mm from bregma for laterodorsal tegmental (LDT) and pedunculopontine tegmental (PPT) nuclei and between -0.34 and -0.82 mm from bregma for *nucleus basalis magnocellularis* (nBM) were chosen. For immunohistochemistry and densitometric analyses, sections for reticular (RT) and ventrobasal (VB) thalamic nuclei were prepared between -0,58 and -1,82 mm from bregma, according to Franklin and Paxinos (2008).

Tissue preparation for immunohistochemistry

Adult mice were anesthetized with isoflurane and intraperitoneal 4% chloral hydrate (2 ml/100 g) and sacrificed by intracardiac perfusion as previously described (Aracri *et al.*, 2013). The brains were immersed in 4% paraformaldehyde in phosphate buffer (PB), for 24 h at 4°C. Next, brains were stored in the same fresh fixative. Serial coronal brain sections (50 µm thick) were cut with a VT1000S vibratome (Leica Microsystems).

Primary antibodies

Anti-ChAT (choline acetyltransferase): polyclonal, made in goat against human placental enzyme (Millipore; 1:50); anti-VAChT (vesicular ACh transporter): polyclonal, made in goat against C-terminal 475-530 amino acids of rat protein (Synaptic Systems; 1:300); anti-α4 nAChR: polyclonal, made in rabbit against the synthetic peptide corresponding to human nAChR alpha 4/CHRNA4 aa 620-627 (C terminal) conjugated to keyhole limpet haemocyanin (Cysteine residue) (Immunological Sciences; 1:200). Anti-SYN (synaptophysin): polyclonal, made in guinea pig against the synthetic peptide corresponding to aa 301-313 of human synaptophysin 1 (Synaptic Systems; 1:400). Anti-PV (parvalbumin): polyclonal, made in rabbit against the rat muscular PV (Swant; 1:2000); anti-SOM (somatostatin): monoclonal, made in mouse against amino acids 25-116 of human somatostatin (Santa Cruz; 1:200); anti-$GABA_A$ α1 subunit (Sigma): polyclonal, made in rabbit against the synthetic peptide corresponding to 28-43 amino acids of the protein (Sigma; 1:300); anti-GAD67 (glutamic acid decarboxylase type 1/67kDa): polyclonal, made in goat against the human recombinant glutamic acid decarboxylase type 1, rhGAD1 (aa 2-97) derived from *E. coli* (R&D Systems; 1:300).

Immunoperoxidase histochemistry for light microscopy

The immunoreaction was carried out as reported (Aracri *et al.*, 2010), except that a mild pretreatment with ethanol (10%, 25%, 10% in phosphate buffered saline, PBS) was applied to increase the immunoreagent penetration. Reaction specificity was assessed by negative controls, e.g. omission of primary antiserum. In these cases, no specific staining was observed. Briefly, sections were examined on a Leica DMRB microscope, and images were acquired using a Leica DCF 480 camera coupled to a personal computer or slide scanner Nanozoomer S60 (Hamamatsu), for densitometric immunoperoxidase analysis. At least 3 mice were examined for each staining, with a maximum of 9 animals for ChAT densitometric analysis. We analyzed at least 5-6 sections representative of the whole rostro-caudal thalamic extension. Several images were acquired per section.

Densitometric immunoperoxidase analysis

To perform a densitometric analysis of cholinergic fibers on immunoperoxidase-stained sections, slices from P90 double-transgenic and control littermates, with reticular and ventrobasal thalamic nuclei (RT and VB) were chosen. Cholinergic fibers

were marked with anti-ChAT antibody and the whole sections were acquired with the slide scanner Nanozoomer S60 (Hamamatsu). The images were then magnified and saved at 10X with the software NDPview2 (Hamamatsu) to show only the single nucleus, and two different regions of interest (ROIs) were designed on ImageJ for RT and VB. For RT 8 images at 10X for each hemisphere were cut (16 for each animal), while for VB 5 images at 10X for each hemisphere (10 for each animal) were chosen. The images were then deconvoluted and spatially calibrated with ImageJ (NIH) software, and from each of them a mean intensity of the signal (in optical density; OD) of the pixels in the ROI was obtained and compared between controls and β2-V287L mice.

Immunofluorescence histochemistry

Sections were permeabilized and blocked as described for immunoperoxidase histochemistry. They were next incubated for two nights in a mixture of one/two primary antibodies. After washing the primary antibodies with PBS, sections were incubated in the following mixture of secondary fluorescent antibodies: Cy5-conjugated donkey anti-rabbit IgG (Jackson; 1:200), Alexa Fluor^{TM}488-conjugated donkey anti-goat (Invitrogen; 1:200), CF^{TM}568-conjugated donkey anti-guinea pig (Biotium; 1:200) for 75 min at room temperature. For anti-SOM, biotinylated horse anti-mouse (Vector Laboratories) was used for 75 min at room temperature, followed by PBS rinsing and rhodamine RedX^{TM}-conjugated streptavidin (ThermoFisher) incubation at room temperature for 2 hours. After rinsing, samples were mounted on coverslips with PBS/glycerol (1:1 v/v) and inspected with a Nikon A1 laser scanning confocal microscope, to visualize double or triple fluorescent labeling.

Colocalization and densitometric analysis

Confocal micrographs were collected at 20X with a Nikon A1 laser scanning confocal microscope and analyzed with ImageJ for densitometric analysis. Identical parameters were used to acquire images for the same antigen, as previously described (Aracri *et al.*, 2013). In brief, nonoverlapping pictures were acquired in at least three different sections for the thalamus, so that double immunolabeling was studied in 5 or 6 fields per region in each animal. For densitometric analysis, at least 5/6 distinct images of the thalamus were acquired. The values thus obtained were averaged among animals before plotting. The degree of colocalization of different neuronal

markers was calculated by comparing the Manders' coefficients, computed with the JACoP plug-in of ImageJ software (Bolte and Cordeliéres, 2006).

Stereological counts

To quantify the number of ChAT+ neurons in the specific brain regions of immunoperoxidase-stained sections, stereological cell countings were carried out with the Optical Dissector workflow of StereoInvestigator 11 (MicroBrightField MBF Bioscience) software, as previously described in Chapter 3. Sections containing LDT and PPT, from -5.02 to -4.36 mm, and nBM from -0.34 to -0.82 mm from bregma, equally distant from each other, were chosen. For these counts, grids of 100x100 µm and 50x50 µm dissectors were chosen.

Statistical analysis

Data are given as mean values ± standard error of the mean. The number of experiments (n) is the number of tested mice. Comparisons between two independent populations were carried out with unpaired Student's *t*-test, after testing for data normality (with a Kolmogorov-Smirnov test), and variance homogeneity (with F-test). In case of unequal variances, the Welch's correction was applied. In the figures, p values are indicated by * ($0.01 < p \leq 0.05$) or ** ($p \leq 0.01$). Unless otherwise indicated, detailed statistics are given in the figure legends.

RESULTS

Stereological cell countings of cholinergic neurons in LDT, PPT and nBM of CTRL and double-transgenic mice

ChAT is the biosynthetic enzyme of ACh and a marker of cholinergic neurons and fibers. Firstly, a quantitative analysis of ChAT+ neurons had been performed in the main mesopontine cholinergic nuclei, the pedunculopontine tegmental (PPT; **Fig. 1A**) and the laterodorsal tegmental nucleus (LDT; **Fig. 1B**). These nuclei are involved in the sleep-wake cycle regulation and from them the majority of cholinergic afferents arrive at the thalamus. Stereological cell count of ChAT+ neurons stained with immunoperoxidase method using StereoInvestigator software had been followed by statistical analysis of the results. No significant differences were found between CTRL and β2-V287L animals, even if in the double-transgenic mice the number of ChAT+ cells was higher in both PPT and LDT (**Fig. 1C**).

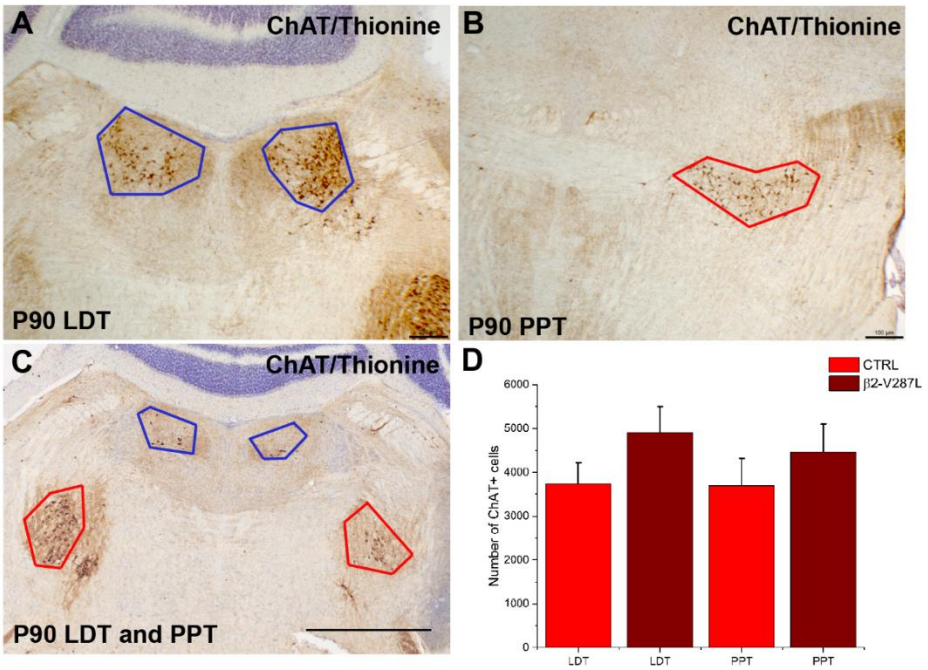

Fig. 1 Stereological cell countings of ChAT+ neurons in LDT and PPT.

Coronal murine brain sections stained for ChAT with immunoperoxidase method in LDT (A, C in blue) and in PPT (B, C in red) and stereological cell count analysis (D). Anti-ChAT labels cell bodies and neurites of cholinergic neurons. Even if in the double-transgenic mice the number of cholinergic neurons was higher in both PPT and LDT compared to CTRL animals, no significant differences were found. Data are expressed as average number of ChAT+ cells in the two areas by using StereoInvestigator software and compared between CTRL and β2-V287L mice with Student's t-test. p=0.145 (LDT); p=0.407 (PPT). (P90, n=9) Scale bars=250 μm (A); 100 μm (B); 1 mm (C).

Nucleus basalis magnocellularis (nBM) was studied with the same methodology used for PPT and LDT. From nBM many cholinergic afferents project to the prefrontal cortex (PFC). These afferents, interacting with pyramidal and GABAergic neurons, determine the elaboration of information to the neocortex. From the stereological cell count of ChAT+ cells in this nucleus, no significant difference was observed between the two genotypes, even if an increase in the number of ChAT+ neurons in β2-V287L mice was present (**Fig. 2**).

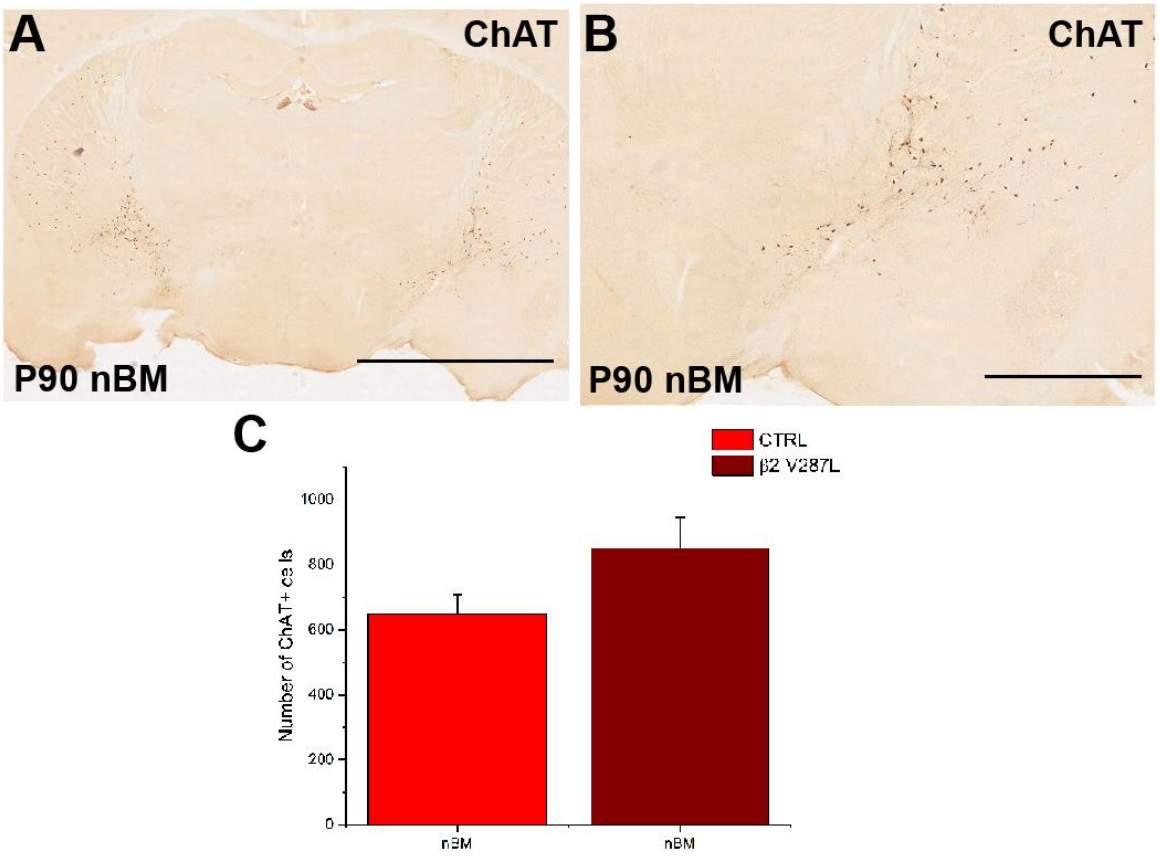

Fig. 2 Analysis of the number of ChAT+ neurons in nBM.
Coronal murine brain sections stained for ChAT with immunoperoxidase method in nBM at different magnifications (A, B) and stereological cell count analysis (D). Similarly to the results obtained from mesopontine nuclei, the number of ChAT+ neurons in β2-V287L mice was slightly higher than in the CTRL littermates, but the difference was not statistically significant. Data are expressed as average number of ChAT+ cells in the nucleus by using StereoInvestigator software and compared between CTRL and β2-V287L mice with Student's t-test. p=0.089. (P90, n=9) Scale bars=2.50 mm (A); 1mm (B).

Cholinergic innervation in the thalamus of WT and β2-V287L mice

Cortical activity is modulated by thalamocortical projections; in particular, the thalamic reticular nucleus (RT) exerts an indirect modulation of afferent information in the cortex, acting like a pacemaker of several thalamic nuclei activity, that project directly to the cortex. In addition to this role, RT receives cholinergic afferents from PPT and LDT, that can modulate RT activity. Alteration of RT activity could ultimately lead to modifications of cortical activity. On these bases, a preliminary densitometric analysis of cholinergic innervation in RT was performed, by using ventrobasal complex (VB) as a reference thalamic nucleus, that receives both cholinergic and somatosensory projections. After immunoperoxidase staining with anti-ChAT antibody, densitometric analysis with ImageJ software was carried out. Only a slight increase of ChAT expression was noticed in both RT and VB of β2-V287L mice (**Fig. 3**).

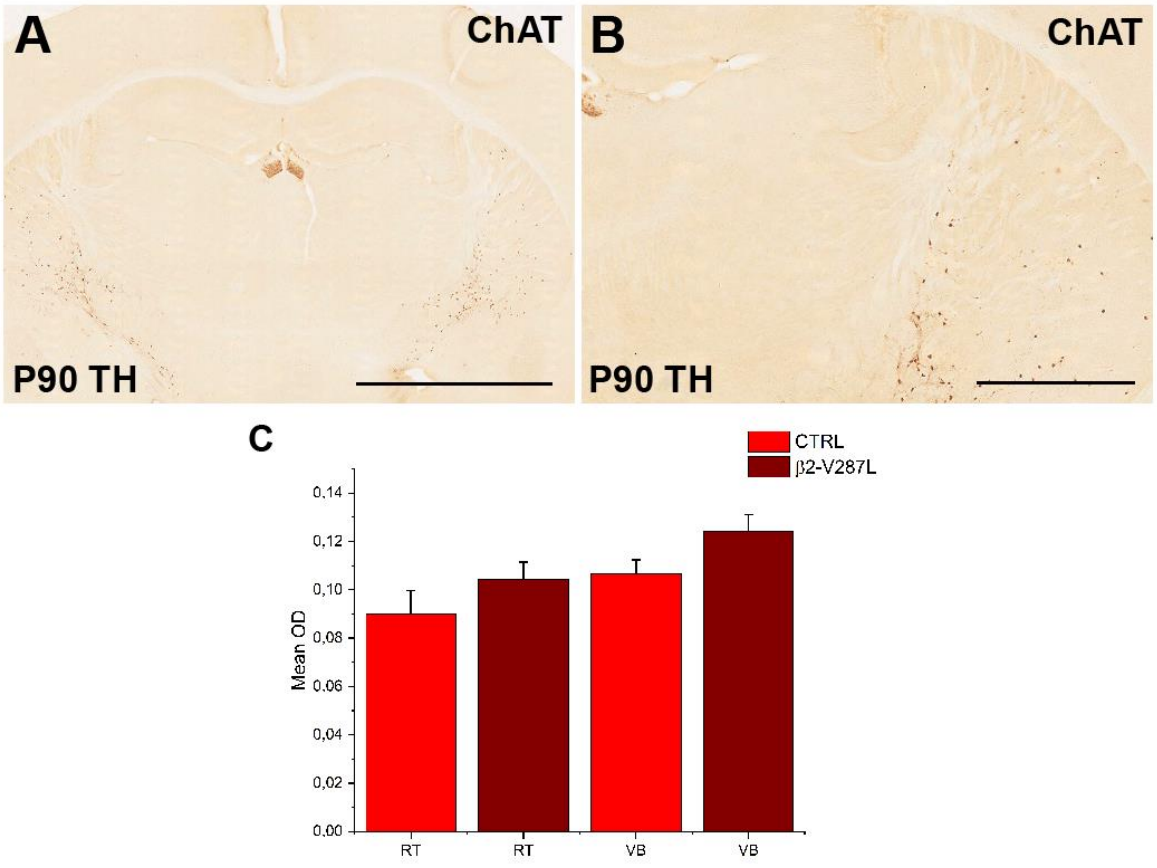

Fig. 3 Densitometric analysis of ChAT expression.
Optical microscope images of ChAT immunolabeling in the thalamus at 1.25X (A) and 2.5X (B). Results of the densitometric analysis (C). Since this antibody labels both soma and neurites of cholinergic neurons, cholinergic innervation was estimated by a preliminary densitometric analysis. No significant differences were found. Data are expressed as mean optical density and were compared between CTRL and β2-V287L mice with Student's t-test. p=0.242 (RT); p=0.069 (VB). (P90, n=9) Scale bars=2.5 mm (A); 1 mm (B).

In addition to the previous analysis, a densitometric study of the cholinergic innervation by means of vesicular ACh transporter (VAChT) immunofluorescence was performed with a focus in RT. Statistical analysis of the results showed no significant differences between the two genotypes (**Fig. 4.5 B**). This data confirmed the results obtained with the densitometric analysis of immunoperoxidase-stained sections for ChAT.

After that, a colocalization analysis was carried out on slices labeled with antibodies against ChAT, synaptophysin (SYN), a marker of synapses, and the subunit α4 of nAChRs (**Fig. 4E**) in RT. By SYN/ChAT colocalization it was possible to quantify the cholinergic synaptic amount. No significant differences were found between CTRL and β2-V287L mice; in both genotypes, the colocalization rate between ChAT and SYN was very similar (about 60%; ChAT on the total amount of the synapses) (**Fig. 4D**).

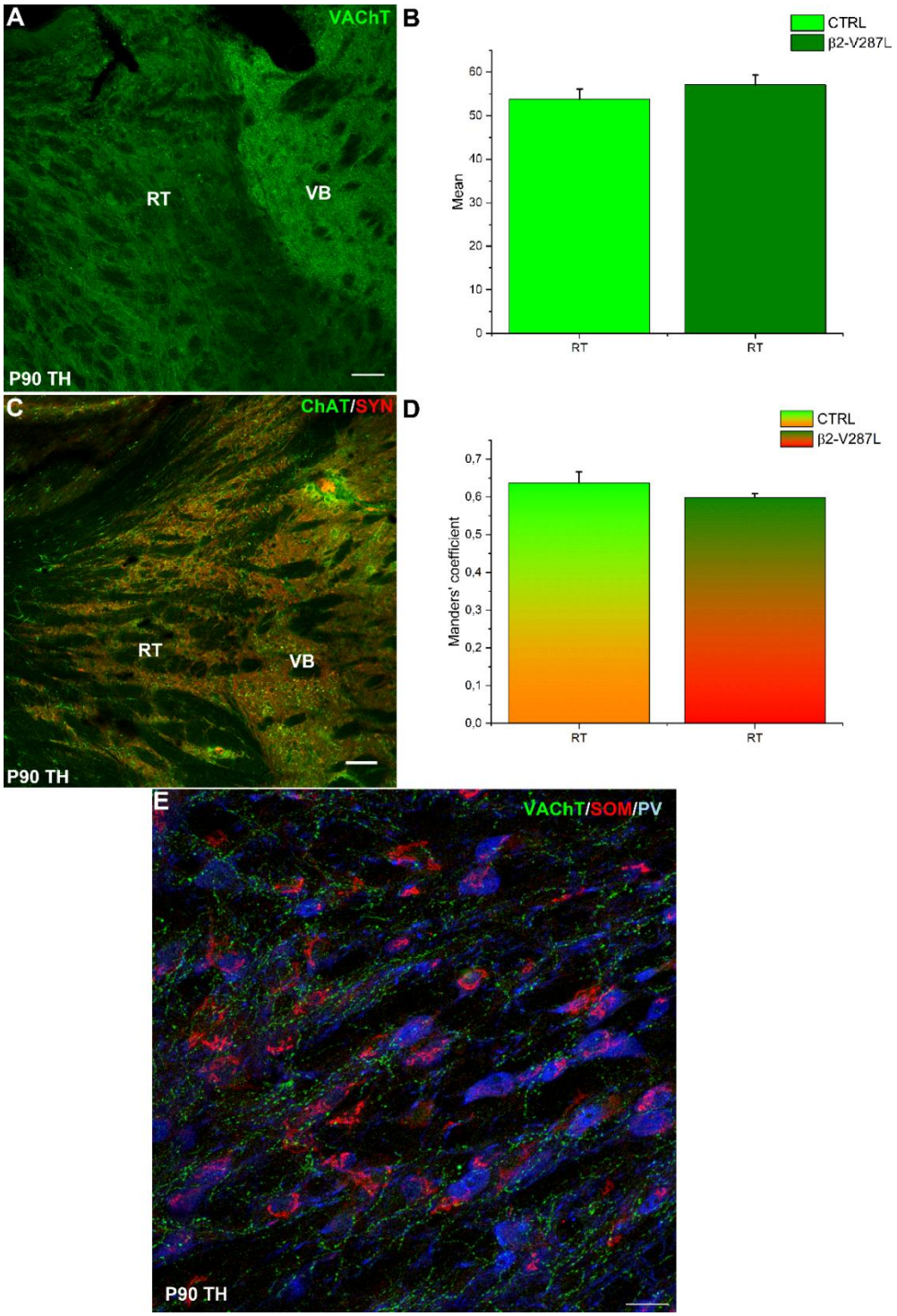

Fig. 4 Densitometric analysis of VAChT and colocalization analysis of ChAT and synaptophysin in RT.

Confocal microscope images of VAChT immunolabeling (green; A), SYN/ChAT (red and green, respectively; C) and VAChT/SOM/PV (green, red and blue, respectively; E) in RT and VB at 20X (A, C) and 60X (E). Results of VAChT densitometric analysis (B) and SYN/ChAT colocalization analysis (D). As it emerges from the confocal microscope images, cholinergic innervation is broadly present in RT and VB (A, C) and both PV+ and SOM+ neurons in RT are interspersed in a cholinergic network (E). The results were similar in both genotypes. Data are expressed as mean grey value (B) and Manders' coefficient and were compared between CTRL and β2-V287L mice with Student's t-test. p=0.361 (VAChT); p=0.290 (SYN/ChAT). (P90, n=3) Scale bars=50 μm (A, C) and 10 μm (E).

To study more thoroughly the cholinergic system in RT, a densitometric analysis of α4 nAChRs was carried out (**Fig. 5A**). α4β2 nAChR subtype is the most expressed in both cerebral cortex and thalamus. Results showed no significant differences between the genotypes (**Fig. 5B**) and confirmed the data obtained with different approaches, since this mutation does not alter heteromeric nicotinic acetylcholine receptors expression (Manfredi *et al.*, 2009). No significant differences were also found after SYN/α4 nAChRs colocalization analysis (**Figura 5C**), that revealed the amount of presynaptic α4-containing nAChRs localization. The percentage of SYN+ terminals on α4 nAChRs+ synapses was about 80% in both CTRL and β2-V287L mice (**Fig. 5D**). Hence, no differences were observed regarding the cholinergic system between the model and the control animals, and the study was then focused on the GABAergic system in RT.

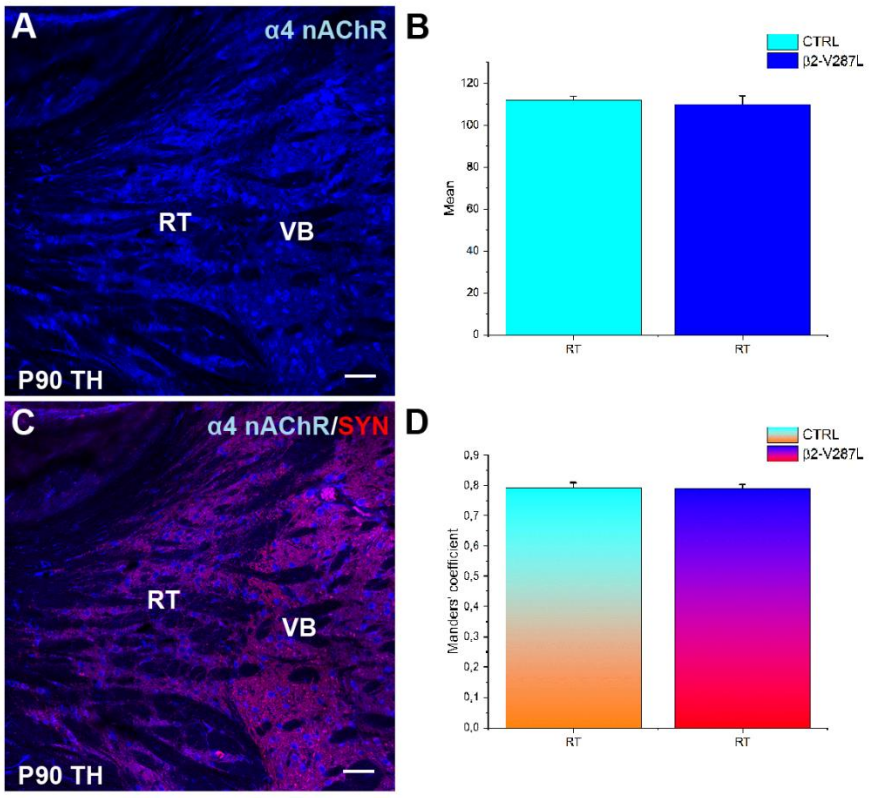

Fig. 5 Densitometric analysis of α4 nAChR and colocalization analysis of α4 nAChR and synaptophysin in RT.
Confocal microscope images of α4 nAChR immunolabeling (blue; A), SYN/α4 nAChR (red and blue, respectively; C) in RT and VB at 20X. Results of α4 nAChR densitometric analysis (B) and SYN/ α4 nAChR colocalization analysis (D). α4 subunit is expressed throughout the thalamus, indicating the extensive presence of heteromeric nAChRs in this area. No significant differences were found regarding α4 nAChR level of expression and colocalization index of α4 nAChR and synaptophysin in RT between β2-V287L and CTRL mice. Data are expressed as mean grey value (B) and Manders' coefficient and were compared between CTRL and β2-V287L mice with Student's t-test. p=0.644 (α4 nAChR), p=0.886 (SIN/α4 nAChR). (P90, n=3) Scale bar=50 μm (A, C).

GABAergic populations in the thalamic reticular nucleus of WT and β-2V287L mice

As shown in the work of Clemente-Perez and colleagues (2017), in RT several GABAergic subpopulations are present. These subgroups are characterized by different morphological and electrophysiological properties, and might have different postsynaptic targets and functional roles. The GABAergic interneurons that express parvalbumin (PV) seem to be the most preponderant and the only rhythmogenic ones, while neurons expressing somatostatin (SOM) seem to be involved in the modulation of the limbic system and are present in a smaller amount. Neurons that express both SOM and PV seem to be present (**Fig. 6E**). On these bases, countings of PV+, SOM+ or double- positive (PV+/SOM+) neurons were carried out on confocal microscope acquisitions of sections stained for PV, SOM and VAChT. From these analyses no significant differences were found regarding neurons labeled for PV (**Fig. 6B**), for SOM (**Fig. 6D**) and double-labeled for PV and SOM (**Fig. 6F**), even if in all cases a faint increment of the number of cells was present in β2-V287L mice respect to CTRL animals. It is important to take into account that the recognition of single SOM+ and, to a greater extent, double-positive cells was troublesome, due to the fact that anti-SOM antibody does not stain the whole cell body (as the anti-PV one), but distinct compartments of it or the neurites, since peptides are often dislocated away from the soma. It will be useful to perform stereological cell countings to discriminate and better evaluate the number of these GABAergic subpopulations of neurons.

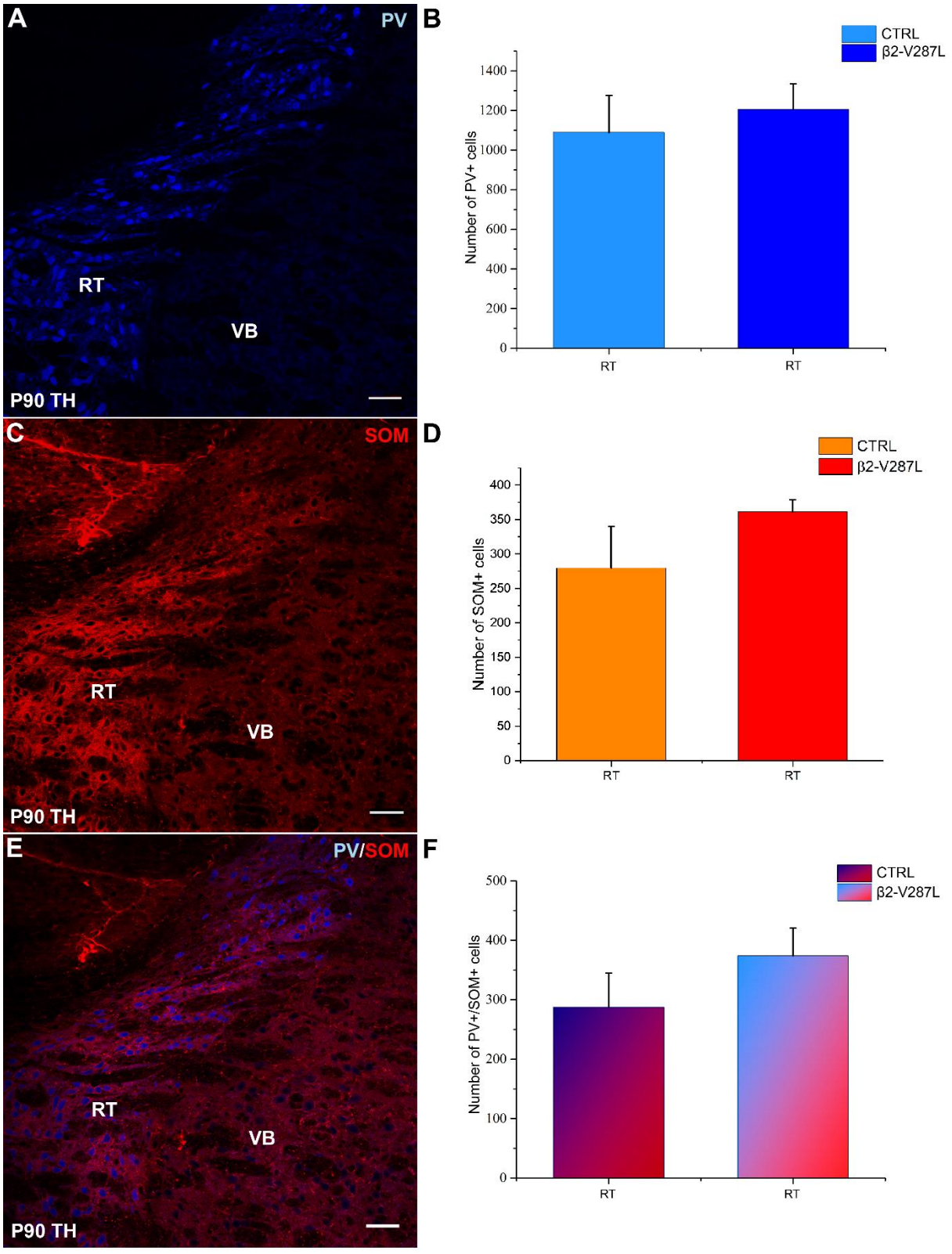

Fig. 6 Cell countings of PV+, SOM+ and PV+/SOM+ neurons in RT.
Confocal microscope acquisitions of PV (A), SOM (C) and PV/SOM (E) immunolabeling in RT and VB of CTRL and β2-V287L P90 transgenic mice (PV in blue; SOM in red) at 20X. Results of the cell counting (B, D, F). No significant differences were found in all the analyses between the two genotypes. Data are expressed as the number of counted cells and were compared between CTRL and β2-V287L mice with Student t-test. p=0.634 (PV+); p=0.263 (SOM+); p=0.308 (PV+/SOM+). (P90, n=3) Scale bar=50 µm (A, C, E).

GABAergic terminals and receptors in the thalamic reticular nucleus of the mouse model

In the last part of the work, we focused our attention on the intrareticular inhibitory terminals. From the literature, nAChRs are known to have a morphogenetic role during development and, since β2 subunit is mutated in the considered mouse model, we studied the possible presence of alterations of GABAergic synapses and receptors. For this aim, an immunofluorescence labeling for GAD1, synaptophysin and α1 subunit of $GABA_A$ receptor was carried out. Firstly, a densitometric analysis of GAD1 was performed (**Fig. 7A**). GAD1 expression levels were not significantly different between the two genotypes (**Fig. 7B**). Secondly, a colocalization analysis of GAD1 and synaptophysin was made in order to evaluate the intrareticular inhibitory synaptic terminals (**Fig. 7C**). GAD1 signal seemed to be overlapped for about 65% in the CTRL animals and about 60% in the double-transgenic mice and the difference was not significant (**Fig. 7D**).

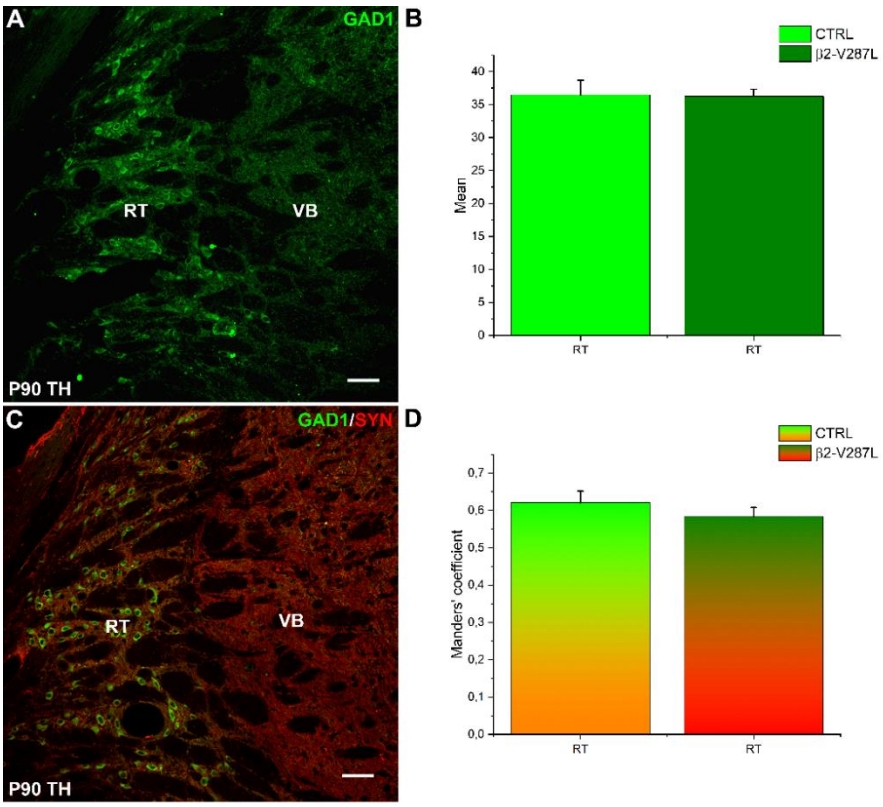

Fig. 7 Densitometric analysis of GAD1 and colocalization analysis of GAD1 and synaptophysin in RT.
Confocal microscope images of GAD1 immunolabeling (green; A), SYN/GAD1 (red and green, respectively; C) in RT and VB at 20X. Results of GAD1 densitometric analysis (B) and SYN/GAD1 colocalization analysis (D). The obtained results were very similar in double-transgenic and CTRL mice. Data are expressed as mean grey value (B) and Manders' coefficient and were compared between CTRL and β2-V287L mice with Student's t-test. p=0.938 (GAD1), p=0.393 (SYN/GAD1). (P90, n=3) Scale bar=50 μm (A, C).

$GABA_A$ receptor is a pre- and postsynaptic chloride channel present in several neurons. We analyzed the expression of its α1 subunit alone and colocalized with synaptophysin in the RT of β2-V287L mouse model. The densitometric analysis showed no significant difference between the experimental groups (**Fig. 8B).** Regarding the colocalization, a similar Manders' coefficient was found for double-transgenic and CTRL mice (**Fig. 8D**).

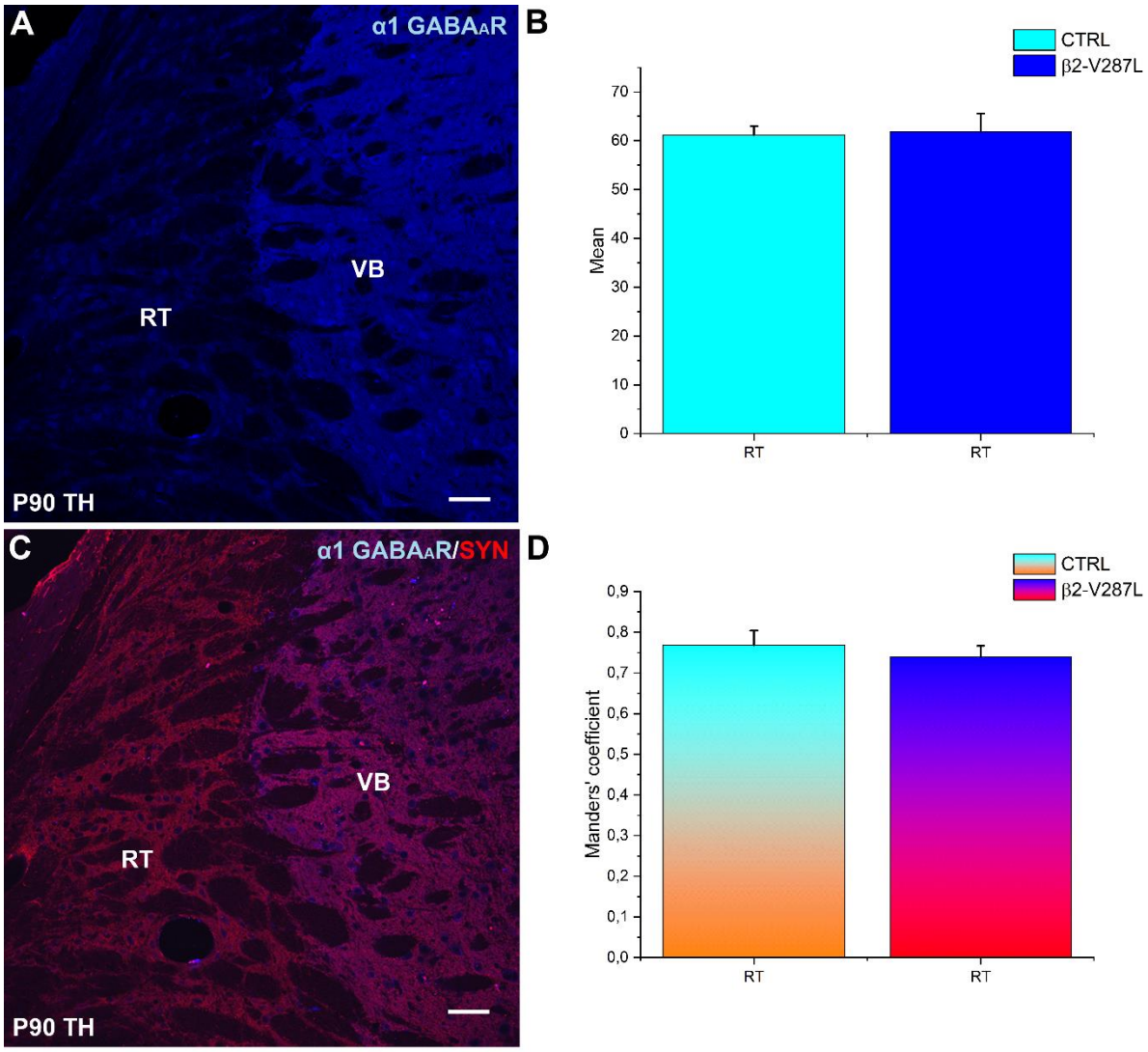

Fig. 8 Densitometric analysis of α1 $GABA_AR$ and colocalization analysis of the receptor and synaptophysin in RT.
Confocal microscope images of α1 $GABA_AR$ immunolabeling (blue; A), SYN/α1 $GABA_AR$ (red and blue, respectively; C) in RT and VB at 20X. Results of densitometric analysis (B) and colocalization analysis (D). The obtained results were very similar in double-transgenic and CTRL mice. Data are expressed as mean grey value (B) and Manders' coefficient and were compared between CTRL and β2-V287L mice with Student's t-test. p=0.876 (α1 $GABA_AR$), p=0.561 (SIN/ α1 $GABA_AR$). (P90, n=3) Scale bar=50 μm (A, C).

DISCUSSION

The cholinergic system represents one of the main modulators of the mammalian brain. Several studies highlighted its involvement both in physiological processes, as sleep-wake cycle (Saper *et al.*, 2005) and in the pathogenesis of some neurological disorders, such as epilepsies (Friedman *et al.*, 2007; Wang *et al.*, 2017). On these bases, the study of the cholinergic system would be very useful. Hence, we focused our attention on the mesopontine and basal forebrain cholinergic nuclei and on the cholinergic innervation in one of the areas of projection, the thalamus. The role of the thalamus in the epileptogenesis, although subject of extensive studies (Li *et al.*, 2014; Ni *et al.*, 2016; Pita-Almenar *et al.*, 2014) is still unclear, due to its structural and network complexity. On the other hand, cholinergic system analysis at molecular and cellular level allowed the identification of mutations in genes encoding for cholinergic receptors as the cause of different form of epilepsies. The murine model we took advantage of represents an excellent tool of analysis for the study of epileptogenic mechanisms. Hence, in the first instance, a thorough analysis of the cholinergic system was carried out to verify the possible presence of morphological alterations due to V287L mutation of β2 subunit, whose morphogenetic role during the development is well known (Molas and Dierssen, 2014). In the second instance, an accurate study of the circuits in RT was performed. RT has a key-role in thalamocortical oscillations during sleep and in discharges that lead to epileptic seizures (Chang *et al.*, 2017; Ferrarelli and Tononi, 2011; Magdaleno-Madrigal *et al.*, 2019; Picard and de Saint Martin, 2003; Ritter-Makinson *et al.*, 2019). Regarding the cholinergic system, the results showed no significant alterations in all the studied areas, even if a constant tendency to increase of the number of cholinergic neurons and of innervation density in thalamic projection areas was noted. The detailed analysis of RT revealed no significant modifications in the expression of synaptic markers and in the cell countings.

The cholinergic system in the thalamic nuclei of β2-V287L mouse

Immunoperoxidase-staining with an antibody against ChAT allowed the localization of both cholinergic neurons in mesopontine nuclei LDT and PPT and *nucleus basalis magnocellularis* (nBM) and the distribution of cholinergic innervation in the thalamus. The cell countings were performed with a reliable stereological method, since it provides the estimation of the whole cholinergic population in each nucleus. The

densitometric analysis of cholinergic fibers on immunoperoxidase-stained sections is useful for preliminary investigations, before focusing on specific areas. ChAT localization in both mesopontine and forebrain nuclei is similar to the one showed by different authors with the same methodology (Amadeo *et al.*, 2005, 2007; Hallanger *et al.*, 1987; Mechawar *et al.*, 2000). On the other hand, the experimental groups were large in this analysis (n=9), since a remarkable variability between the different litters was observed, that, at the beginning of the study, suggested an actual increase of cholinergic innervation in the thalamic nuclei RT and VB. All the data showed a constant tendency to increment, that, due to the neurochemical and electrophysiological properties of cholinergic system and of projection neurons, could lead to an imbalance of the delicate excitation/inhibition equilibrium (Sun *et al.*, 2013). Hence, it is possible that even a slight increment of ACh release, prompted by mutated receptors during the development, could lead to destabilizing effects in both thalamic and cortical microcircuits, causing the typical epileptic hyper-synchronization (Ritter-Makinson *et al.*, 2019; Sun *et al.*, 2012). On the other hand, it is known that small optogenetic stimulations or lesions in the cholinergic nuclei that project to the cortex and the thalamus could cause different effects, as REM sleep induction (Van Dort *et al.*, 2015), alterations of sleep-wake transition (Petrovic *et al.*, 2013) or modifications of EEG in epileptic models (Furman *et al.*, 2015). It is interesting to notice that impairments of cholinergic neurons numbers were not detected, in agreement with our analysis, while a recent study showed a significant alteration of the dimensions of PPT neurons in a kainic acid-induced model of epilepsy (Soares *et al.*, 2018).

The interplay between GABAergic neurons and cholinergic terminals in the thalamic reticular nucleus

As mentioned before, one of the key aspects of the central nervous system is the balance between excitation and inhibition, that is often altered in epileptic models (Briggs and Galanopoulou, 2011). Therefore, the previous work of our laboratory (Amadeo *et al.*, 2018; Chapter 2) on the murine model developed by Manfredi and colleagues (2009) was focused on the analysis of variation in the chloride cotranporters NKKC1 and KCC2 expression. These cotransporters are the responsible of the “switch of the GABA” during the postnatal development; hence, alterations of NKCC1 and KCC2 could lead to modifications of the networks and ultimately cause epileptic disorders (Ben-Ari, 2002). The data highlighted a delay of the “switch of the GABA” at

the end of the first postnatal week, along with a decrease of KCC2 level in PFC layer V, while in adult mice a significant increment in PFC layer V and a significant decrement in RT of KCC2 expression were found (Amadeo *et al.*, 2018; Chapter 2). In physiological conditions in RT, responsible of the generation of sleep spindles that characterize stage 2 of NREM sleep, KCC2 distribution is heterogeneous in adulthood (Barthó *et al.*, 2004) and during the development (Amadeo *et al.*, 2016). This evidence, in agreement with Barthó and colleagues (2004), could be related to the role of RT as a thalamic "pacemaker". This nucleus regulates thalamocortical activity, generating rhythmic discharges towards other thalamic nuclei when the cholinergic stimulation is low, as during NREM sleep. This property could be related to physiological characteristics of RT neurons and to its intrareticular GABAergic connections. RT cells are characterized by an intense "burst-firing" activity, that derives from the hyperpolarized state; these neurons induce a long-lasting inhibition on the thalamic nuclei and generate a rhythmic activity that modulates thalamocortical system (Sun *et al.*, 2013). It is not know whether the murine model of ADNFLE studied in this work presents epileptic seizures during postnatal development or not (Manfredi *et al.*, 2009), but, since in human the epileptic onset is in childhood, one can hypothesize that KCC2 expression level at P60 in RT could be attributed to compensatory mechanisms as a result of postnatal epileptic seizures. The significant decrease of KCC2 in RT could be interpreted as an attempt to limit RT neurons sensibility to hyperpolarization to avoid anomalous discharges (Astori *et al.*, 2013) directed to thalamocortical neurons, that are responsible of sleep spindles generation (Lüthi, 2013), maintaining high concentrations of intracellular chloride ions, to avoid the entrance in the "burst firing" activity. On these bases, we focused our attention on RT to detect the eventual alterations in this nucleus, that has been identified as a possible target of therapeutic intervents, as deep cerebral stimulation (Magdaleno-Madrigal *et al.*, 2019). By means of immunofluorescence stainings, it was possible to study the interactions among cholinergic afferents, RT neuronal populations and expressions of heteromeric nAChRs and $GABA_A$ receptor. In agreement with the previous densitometric immunoperoxidase analysis for ChAT, cholinergic innervation detected with VAChT immunolabeling in RT was similar in the two experimental groups. The eventual variation could have been important because it has been recently highlighted the "*en passant*" ACh release in the RT and its effect on both muscarinic and nicotinic receptors, even at presynaptic level (Beierlein, 2014). For this reason, α4 nAChRs

subunit expression, alone and in the synaptic compartment, was observed, but no significant differences were found between CTRL and double-transgenic mice, in agreement with the results of Manfredi and colleagues (2009). On the bases of intrareticular GABAergic activity in thalamocortical synchronization mechanisms and in the sleep spindles (Lüthi, 2013; Ritter-Makinson *et al.*, 2019, Sun *et al.*, 2012) a further analysis of GABAergic synapses was carried out in RT, using anti-GAD1 and α1 $GABA_AR$ markers, but no significant differences were found. Finally, RT neuronal PV+ and SOM+ subpopulations were analysed. For PV+, SOM+ and SOM+/PV+ cells no significant differences were found. It is necessary to take into account that these data are not comparable with the ones of Clemente-Perez and colleagues (2017), since in their work SOM+ subgroup was identified by gene-reporter transgenic animals and this method tends to the overestimation of cellular populations. Hence, even though the peptide localization in the neurons is hard to find and often non-homogeneous, since peptides are frequently dislocated in the neurites, immunohistochemical technique appears more reliable.

Conclusion

The data suggest that the thalamic reticular nucleus could play a minor role in the manifestation of nocturnal epileptic seizures in ADNFLE. Even though no significant alterations of GABAergic and cholinergic systems have been found, the expression of KCC2 cotransporter was altered in the RT of adult β2-V287L mice (Amadeo *et al.*, 2018; Chapter 2). This result, along with the data obtained in the cortex (Chapter 2 and 3), suggests the establishment of adaptative mechanisms of the thalamocortical circuits against the propagation of cortical epileptic events. Further analyses of RT and its glutamatergic afferents could be useful for the global picture and to clarify the possible involvement of RT in the epileptogenesis. It would be interesting to analyze thoroughly the distribution of glutamatergic receptors and muscarinic ACh receptors, since recent studies highlighted the complex interaction between these two systems in the modulation of thalamocortical circuits (Beierlein, 2014; Sun *et al.*, 2016). Further studies of different thalamic nuclei, as the mediodorsal one, could be useful to clarify the role of the thalamus in the epileptogenesis, since, at the best of our knowledge, this is one of the few works focusing on the thalamus of a transgenic murine model of epilepsy.

REFERENCES

Amadeo A, Guerneri S, Consonni S and Becchetti A (2005) *Expression of cholinergic markers in the developing murine thalamus.* P.174, Abstracts SINS, Ischia, Napoli.

Amadeo A, Gandelli P, Leone S, Consonni S and Becchetti A (2007) *Transient cholinergic innervation of the developing somatosensory murine thalamus.* FRI-34, Abstract SINS, Verona.

Amadeo A, Aracri P, Mattevi F *et al.* (2016) *Developmental expression of the K+/Cl- cotransporter KCC2 in forebrain of wild type and transgenic mice expressing mutant nicotinic receptors.* International Society Developmental Neuroscience (ISDN), Juan Les Pins (Francia).

Amadeo A, Coatti A, Aracri P, Ascagni M, Iannantuoni D, Modena D, Carraresi L, Brusco S, Meneghini S, Arcangeli M, Pasini ME and Becchetti A (2018) *Postnatal Changes in K^+/Cl^- Cotransporter-2 Expression in the Forebrain of Mice Bearing a Mutant Nicotinic Subunit Linked to Sleep-Related Epilepsy.* Neuroscience 386:91-107.

Astori S, Wimmer RD and Lüthi A (2013) *Manipulating of sleep spindles- expanding views on sleep, memory and disease.* Trend of Neurosci 36(12)738-748.

Barthó P, Payne JA, Freund TF and Acsády L (2004) *Differential distribution of the KCl cotransporter KCC2 in Thalamic relay and reticular nuclei*. European Journal of Neuroscience 20:965-975.

Becchetti A, Aracri P, Meneghini S, Brusco S and Amadeo A (2015) *The role of nicotinic acetylcholine receptors in autosomal dominant nocturnal frontal lobe epilepsy.* Frontiers in Physiology. 6(22):1-12.

Beierlein M (2014) *Synaptic mechanisms underlying cholinergic control of thalamic reticular nucleus neurons.* J Physiol pp 4137-4145.

Ben-Ari Y (2002) *Excitatory actions of GABA during development: the nature of the nurture.* Nat Rev Neurosci. 3(9):728-39.

Bolte S and Cordelières FP (2006) *A guided tour into subcellular colocalization analysis in light microscopy.* J Microsc 224:213-232.

Briggs SW and Galanopoulou AS (2011) *Altered GABA signaling in early life epilepsies.* Neural Plast. 2011:527605.

Chang WJ, Chang WP and Shyu BC (2017) *Suppression of cortical seizures by optic stimulation of the reticular thalamus in PV-mhChR2-YFP BAC transgenic mice.* Molecular Brain 2;10(1):42.

Clemente-Perez A, Makinson SR, Higashikubo B, Paz JT *et al.* (2017) *Distinct Thalamic Reticular Cell Types Differentially Modulate Normal and Pathological Cortical Rhythms.* Cell Reports 19:2130-2142.

Crabtree JW (2018) *Functional Diversity of Thalamic Reticular Subnetworks.* Front Syst Neurosci. 12:41.

Ferrarelli F and Tononi G (2011) *The Thalamic Reticular Nucleus and Schizophrenia.* Schizophrenia Bulletin 37:306–315.

Friedman A, Behrens CJ and Heinemann U (2007) *Cholinergic Dysfunction in Temporal Lobe Epilepsy. Pathophysiology of Chronic Epilepsy.* Blackwell Publishing, Inc. 48(5):126-130.

Furman M, Zhan Q, McCafferty C, Lerner BA, Motelow JE, Meng J, Ma C, Buchanan GF, Witten IB, Deisseroth K, Cardin JA and Blumenfeld H (2015) *Optogenetic stimulation of cholinergic brainstem neurons during focal limbic seizures: Effects on cortical physiology.* Epilepsia 56(12):e198-e202.

Halász P and Szűcs A (2018) *Sleep, epilepsies, and cognitive impairment.* Academic Press, Elsevier pp 56-60.

Hallanger AE, Levey AI, Lee HJ, Rye DB and Wainer BH (1987) *The origins of cholinergic and other subcortical afferents to the thalamus in the rat.* J. Comp. Neurol. 262: 105-124.

Heckers S, Geula C and Mesulam MM (1992) *Cholinergic innervation of the human thalamus: dual origin and differential nuclear distribution.* J Comp Neurol. 325(1):68-82.

Holmstrand EC and Sesack SR (2011) *Projections from the rat pedunculopontine and laterodorsal tegmental nuclei to the anterior thalamus and ventral tegmental area arise from largely separate populations of neurons.* Brain Struct Funct 216:331-345.

Jones EG (2007) *The Thalamus.* Cambridge: Cambridge University Press.

Lee KH and McCormick DA (1995) *Acetylcholine excites GABAergic neurons of the ferret perigeniculate nucleus through nicotinic receptors.* J Neurophysiol. 73(5):2123-8.

Li YH, Li JJ, Lu QC, Gong HQ, Liang PJ and Zhang PM (2014) *Involvement of Thalamus in Initiation of Epileptic Seizures Induced by Pilocarpine in Mice.* Hindawi Publishing Corporation. Neural Plasticity 2014:675128.

Lüthi A (2014) *Sleep spindles: where they come from, what they do.* Neuroscientist 20, 243-256.

Magdaleno-Madrigal VM, Contreras-Murillo G, Valdés-Cruz A, Martinez-Vargas D, Martinez A, Villasana-Salazar B and Almazàn-Alvarado S (2019) *Effects of High- and Low-Frequency Stimulation of the Thalamic Reticular Nucleus on Pentylentetrazole-Induced Seizures in Rats.* Neuromodulation 22(4):425-434.

Manfredi I, Zani AD, Rampoldi L, Pegorini S, Bernascone I, Moretti M *et al.* (2009) *Expression of mutant β2 nicotinic receptors during development is crucial for epileptogenesis.* Hum. Mol. Genet. 18, 1075-1088.

Mechawar N, Watkins KC and Descarries L (2002) *Ultrastructural features of the acetylcholine innervation in the developing parietal cortex of rat.* The Journal of Comparative Neurology 443: 250-258.

Mitchell AS, Dalrymple-Alford JC and Christie MA (2002) *Spatial working memory and the brainstem cholinergic innervation to the anterior thalamus.* J Neurosci 22(5):1922-8.

Molas S and Dierssen M (2014) *The role of nicotinic receptors in shaping and functioning of the glutamatergic system: A window into cognitive pathology.* Neuroscience & Biobehavioral Reviews 46: 315-325.

Nanobashvili ZI, Surmava AG, Bilanishvili IG, Barbaqadze MG, Mariamidze MD and Khizanishvili NA (2012) *Significance of the Thalamic Reticular Nucleus GABAergic Neurons in Normal and Pathological Activity of the Brain.* Journal of Behavioral and Brain Science 436-444.

Ni KM, Hou XJ,Yang CH, Dong P, Li Y, Zhang Y, Jiang P, Berg DK, Duan S and Li XM (2016) *Selectively driving cholinergic fibers optically in the thalamic reticular nucleus promotes sleep.* e-LIFE 1-17.

Petrovic J, Ciric J, Lazic K, Kalauzi A and Saponjic J (2013) *Lesion of the pedunculopontine tegmental nucleus in rat augments cortical activation and disturbs sleep/wake state transitions structure.* Experimental Neurology 247:562-571.

Picard F and de Saint Martin A (2003) *Natural history of frontal lobe epilepsies.* Cap. 6 in Frontal lobe seizures and epilepsies in children. Beaumanoir A, Andermann F, Chauvel P, Mira L, Zifkin B. Mariani Foundation Paediatric Neurology. John Libbey Eurotext.

Picard F, Bruel D, Servant D, Saba W, Fruchart-Gaillard C, Schöllhorn-Peyronneau MA, Roumenov D *et al.* (2006) *Alteration of the in vivo nicotinic receptor density in ADNFLE patients: a PET study.* Brain 129, 8: 2047-2060.

Pinault D (2004) *The thalamic reticular nucleus: structure, function and concept.* Brain Research Reviews 46:1-31.

Pita-Almenar JD, Yu D, Lu HC and Beierlein M (2014) *Mechanisms Underlying Desynchronization of Cholinergic-Evoked Thalamic Network Activity.* The Journal of Neuroscience 34(43):14463-14474.

Pratt JA and Morris BJ (2015) *The thalamic reticular nucleus: a functional hub for thalamocortical network dysfunction in schizophrenia and a target for drug discovery.* J Psychopharmacol. 29(2):127-37.

Ritter-Makinson S, Clemente-Perez A, Higashikubo B, Cilio MR, Delord B and Paz JT (2019) *Augmented Reticular Thalamic Bursting and Seizures in Scn1a-Dravet Syndrome.* Cell Reports 26(4):1071.

Saper CB, Scammell TE and Lu J (2005) *Hypothalamic regulation of sleep and circadian rhythms.* Nature 437(7063):1257-1263.

Soares JI, Afonso AR, Maia GH and Lukoyanov NV (2018) *The pedunculopontine and laterodorsal tegmental nuclei in the kainite model of epilepsy.* Neuroscience Letters 672:90-95.

Sokhadze G, Campbell PW and Guido W (2018) *Postnatal development of cholinergic input to the thalamic reticular nucleus of the mouse.* European Journal of Neuroscience pp. 1-12.

Sun YG, Wu CS, Renger JJ, Uebele VN, Lu HC and Beierlein M (2012) *GABAergic Synaptic Transmission Triggers Action Potentials in Thalamic Reticular Nucleus Neurons.* The Journal of Neuroscience 32(23):7782-7790.

Sun YG, Pita-Almenar JD, Wu CS, Renger JJ, Uebele VN, Lu HC and Beierlein M (2013) *Biphasic cholinergic synaptic transmission controls action potential activity in thalamic reticular nucleus neurons.* J Neurosci 33: 2048-2059.

Sun YG, Rupprecht V, Zhou L, Dasgupta R, Seibt F and Beierlein M (2016) *mGluR1 and mGluR5 Synergistically Control Cholinergic Synaptic Transmission in the Thalamic Reticular Nucleus.* The Journal of Neuroscience 36(30):7886.7896.

Van Dort CJ, Zachs DP, Kenny JD, Zheng S, Goldblum RR, Gelwan NA, Ramos DM, Nolan MA, Wang K, Weng FJ, Lin Y, Wilson MA and Brown EN (2015) *Optogenetic activation of cholinergic neurons in the PPT or LDT induces REM sleep.* PNAS 112(2):584-9.

Wang Y, Wang Y and Chen Z (2017) *The role of central cholinergic system in epilepsy.* J Zhejiang Univ (Med Sci) 46(1):15-21.

Chapter 5

α-Synuclein Imbalance as a Potential Histopathological Marker in Frontal Lobe Epilepsy: a Pilot Study in a Murine Model of Human Genetic Sleep-Related Epilepsy

Calogero AM [a], Cantele F [a], Mazzetti S [b], Modena D [a], Pizzi S [a], Tarantino D [a], Onelli E [a], Moscatelli A [a], Gagliardi G [a], Giaccone G [b], Pezzoli G [b], Arnal I [c], Amadeo A [a] and Cappelletti G [ab] (2018) *The interplay between α-synuclein and tubulin in health and disease: from pure protein to human brain.* Neuronest Milan, Italy.

[a] *Department of Biosciences, University of Milano, Via Celoria, 26, 20133 Milano, Italy*
[b] *Fondazione Grigioni per il Morbo di Parkinson, Via Zuretti 35, 20125 Milano, Italy*
[c] *GIN, Inserm 1216, Univ. Grenoble Alpes, 38000, Grenoble, France*

ABSTRACT

α-Synuclein is a protein widely expressed in brain tissue, mainly at the level of presynaptic terminals, where it is implicated in synaptic vesicle function and recycling. Despite decades of intensive investigation, the physiological role of α-Synuclein remains elusive and, consequently, its contribution to pathologies, such as Parkinson's disease (PD) and dementia with Lewy bodies (DLB), was not well cleared up. Both PD and DLB, besides α-Synuclein accumulation, showed sleep dysfunction and EEG alterations, which in DLB became frequently epileptic seizures. This is very interesting as recent studies, focused on the neuropathological features and the proteomic profiling of epileptic tissues, unraveled the presence of lipofuscin and tau aggregates other than the alteration of α-synuclein expression both in human and in animal model epileptic brains. Moreover, further works highlighted the interplay between α-synuclein and synaptic neuronal activity, in particular its role in the modulation of cholinergic signaling through interaction with nicotinic acetylcholine receptors (nAChRs). On these bases, unraveling the involvement of α-synuclein imbalance in the pathogenesis of epilepsy is a challenge. Our aim was to analyze α-synuclein cellular and neuroanatomical distribution in, preliminarily, wild-type mice; then we started to analyze synaptic expression of α-synuclein in a murine model bearing a mutant nicotinic subunit linked to a sleep-related epilepsy, the Autosomal Dominant Nocturnal Frontal Lobe Epilepsy (ADNFLE). Therefore, we pointed our attention on quantifying α-synuclein presence in specific areas of non-epileptic (CTRL) and epileptic adult mice, using immunoperoxidase and immunofluorescence methods against α-synuclein, focusing the preliminary analyses on the *corpus striatum* (CS) and on the somatosensory cortex (SS). Moreover, a colocalization analysis was performed for GABA and glutamate vesicular transporters with α-synuclein in the same areas to assess whether the colocalization index was altered in epileptic mice. The results showed a significant decrease of α-synuclein expression in the dorsolateral CS of the epileptic mice, and an increase of the colocalization ratio in GABAergic synapses of the dorsomedial CS. These results may help to begin further studies regarding the relationship between α-synuclein and epilepsy in other areas of central nervous system and more widely in different animal models and human brains.

INTRODUCTION

α-Synuclein started to be interesting for the scientific community in the 1997, when a mutation in the *SNCA* gene was discovered in some families with hereditary Parkinson's disease (PD) and when it was discovered that it is the major constituent of the histopathological lesions present in some specific neurodegenerative disorders (Polymeropoulos *et al.*, 1997; Spillantini *et al.*, 1998). For this reason, these diseases were classified as synucleinopathies and comprise three main disorders: PD, dementia with Lewy bodies (DLB) and multiple system atrophy (MSA). Also, rare disorders like neuroaxonal dystrophies present synuclein pathologies (Goedert *et al.*, 2017). Synucleinopathies are characterized by an abnormal accumulation of α-Synuclein aggregates in neurons and nerve fibers. Anyway, around 10% of neurologically normal elder people above 60 years of age present also an abnormal accumulation of the protein in the nervous system, but their levels are much lower (McCann *et al.*, 2013). All these disorders share the following symptoms: parkinsonism (syndrome characterized by tremor, rigidity, postural instability and bradykinesia, slow initiation of voluntary movement with a progressive loss in speed and range of repeated actions), impaired cognition, sleep disorders and visual hallucinations. Sometimes, synucleinopathies can overlap with tauopathies, and it has been found a possible interaction between α-synuclein and tau proteins (Delenclos *et al.*, 2014; Sánchez *et al.*, 2018). The presence of sleep dysfunction and electroencephalogram alterations are also common in synuclein pathologies and the former can precede the onset of parkinsonism by many years (McDowell *et al.*, 2014). Indeed, an excessive day-time sleepiness and REM behavioural disorder have been linked to an increased risk of developing PD (Abbott *et al.*, 2005; Arnulf *et al.*, 2002). Moreover, in DLB sleep dysfunction and EEG alterations became frequently epileptic seizures (McDowell *et al.*, 2014; Morris *et al.*, 2015) and recent studies highlighted the interplay between α-synuclein and synaptic transmission (Yamada and Iwatsubo, 2017). In particular, α-synuclein role in the modulation of cholinergic signaling through interaction with nicotinic acetylcholine receptors was pointed out (Liu *et al.*, 2013; nAChRs). Interestingly, in PD and other neurodegenerative disorders, the cholinergic system appears to show more alterations in comparison with other regulatory systems (Oda, 1999). The nAChRs are very important in regulating dopamine release in the nigrostriatal pathway through α6β3β2 and α4β2 nicotinic receptors (Champtiaux *et al.*,

2003; Quik and Kulak, 2002). In rodent and monkey models of PD, there is a selective decrease in the number of α6, α4 and β2 containing receptors as detected by means of specific ligand binding or immunoprecipitation experiments (Champtiaux *et al.*, 2003, Lai *et al.*, 2004; Quik *et al.*, 2004). Moreover, a decrease in nAChRs has been found in the cerebral cortex of Parkinson's disease patients, which is mainly due to a decrease in α4 and α7 containing receptors (Burghaus *et al.*, 2003). Recent works have also underlined that nAChR mutations in Autosomal Dominant Nocturnal Frontal Lobe Epilepsy (ADNFLE) families not only cause a sleep-related epilepsy but can also be associated with additional neurological or psychiatric features (Cho *et al.*, 2003; Hirose *et al.*, 1999; Magnusson *et al.*, 2003). Furthermore, recent studies, focused on the neuropathological features and the proteomic profiling of epileptic tissues, unraveled the presence of lipofuscin and tau aggregates (Liu *et al.*, 2016; Sànchez *et al.*, 2018) other than the alteration of α-synuclein expression both in human and in animal model epileptic brains (Hu *et al.*, 2015; Li *et al.*, 2010; Yang *et al.*, 2006).

On these bases, the main goals of this study were characterizing α-synuclein distribution in some brain regions of wild-type (WT) mice, analyzing the possible involvement of α-synuclein imbalance in the pathogenesis of the epileptic brain and detecting possible α-synuclein alterations on specific synapses. Therefore, we focused our attention, firstly, on an extensive immunoperoxidase and ultrastructural observation of the protein in WT C57BL/6J adult mice, in view of future investigations on animal models of PD. α-Synuclein was mainly present at the neuropilar level and had a region-dependent distribution in the different areas. Subsequently, we quantified α-synuclein presence in specific regions of non-epileptic (CTRL) and epileptic adult mice, using immunoperoxidase and immunofluorescence methods against α-synuclein, focusing our preliminary analyses on the *corpus striatum* (CS) and on the somatosensory cortex (SS). CS is one of the areas typically studied in synucleinopathies models and it presents a high expression of α-synuclein physiologically. Furthermore, this region is involved in the signal transmission from the neocortex and receives afferent pathways from the *substantia nigra*, giving it a crucial role in studies concerning PD. On the other hand, the SS cortex is the reference cortex for investigations on epilepsy. For this reason, as a pilot study, the work was preliminarily focused on the SS cortex before moving on to the analysis of the prefrontal cortex, which is known to be directly involved in ADNFLE. Finally, a colocalization

evaluation was carried out for GABA and glutamate vesicular transporters with α-synuclein in the same areas to assess whether the colocalization coefficient was altered in epileptic mice. The data showed a significant decrease of α-synuclein expression in the dorsolateral CS of the epileptic mice, and an increase of the colocalization ratio in GABAergic synapses of the dorsomedial CS.

EXPERIMENTAL PROCEDURES

Animals

Mice were kept in pathogen-free conditions, with a 12 h light-dark cycle, and free access to water and food. All procedures followed the Italian law (2014/26, implementing the 2010/63/UE) and were approved by the local Ethical Committees and the Italian Ministry of Health. For the preliminary morphological analyses of wild-type (WT) mice, we used 6 animals at postnatal day 60 (P60) with C57BL/6J strain (3 for immunoperoxidase stainings alone, 3 for ultrastructural analysis), which shows a high sensitivity to develop experimental dopaminergic denervation, that makes this strain an ideal candidate to dissect the pattern of α-synuclein localization by using a validated immunohistochemical approach (Vivacqua *et al.*, 2011). Regarding the study on the epileptic mice, we took advantage of the S3 line of double-transgenic FVB (tTA:Chrnb2V287L) mice, which express β2-V287L under a tetracycline-controlled transcriptional activator (tTA). These mice were compared with their littermates not expressing β2-V287L, which were either WT or bearing TRE-Chrnb2V287L or PrnP-tTA genotypes (Manfredi *et al.*, 2009). For clarity, mice expressing the transgene are hereafter denoted as β2-V287L, while the control littermates are denoted as controls (CTRL). The morphological analysis was carried out on 3 animals of either sex for each experimental group (CTRL and β2-V287L), at P90.

Brain regions

For immunohistochemistry and densitometric analyses, by PFC we refer to the entire secondary motor region (also known as M2, or Fr2) in the dorsomedial shoulder of prefrontal cortex. According to Franklin and Paxinos (2008), coronal prefrontal sections were cut between +2.58 and +1.14 mm from bregma. For somatosensory cortex (SS) and *corpus striatum* (CS), we chose sections in proximity to -0.34 mm from bregma. Regarding *substantia nigra,* slices at -3.64 mm from bregma were chosen, and sections at -3.16 mm from bregma were used for the entorhinal cortex and the hippocampus.

Tissue preparation for immunohistochemistry

Adult mice were anesthetized with isoflurane and intraperitoneal 4% chloral hydrate (2 ml/100 g) and sacrificed by intracardiac perfusion as previously described (Aracri *et*

al., 2013). The brains were immersed in 4% paraformaldehyde in phosphate buffer (PB), for 24 h at 4°C. Next, brains were stored in the same fresh fixative. Serial coronal brain sections (50 µm thick) were cut with a VT1000S vibratome (Leica Microsystems).

Primary antibodies

Anti α-synuclein (S3062, Sigma-Aldrich): polyclonal, made in rabbit against synthetic peptide corresponding to a sequence near the C-terminus of human α-Synuclein (amino acids 111-132 with C-terminally added lysine) (1:1500) used for immunoperoxidase and immunogold histochemistry on WT mice; anti α-synuclein (clone 42; BD Biosciences): monoclonal antibody made in mouse against 15-123 amino acids of the rat protein (1:500 for immunoperoxidase, 1:200 for colocalization analyses). Anti-VGAT (vesicular GABA transporter): polyclonal, made in rabbit against the synthetic peptide corresponding to the N-terminal 75-87 amino acids of the rat protein (Synaptic Systems; 1:800). Anti-VGLUT1 (vesicular glutamate transporter type 1): polyclonal, made in rabbit against Strep-TagR-fusion proteins containing the amino acid residues 456–560 of the rat VGLUT1/BNPI (brain-specific Na1-dependent inorganic phosphate transporter; Synaptic Systems; 1:500).

Immunoperoxidase histochemistry for light and electron microscopy

After aldehyde quenching with NH_4Cl (0.05M in phosphate buffered saline, PBS) for 30 min and inactivation of endogenous peroxidases with 1% H_2O_2 (in PBS) for 30 minutes, sections were permeabilized with a mild pretreatment with ethanol (10%, 25%, 10% in PBS) to increase the immunoreagent penetration. The blocking solution constituted by 0.2% Triton X-100 in 1% bovine serum albumin (BSA; in PBS) was then applied for 30 minutes. Next, the slices were incubated overnight with the primary antibody diluted in 0.1% BSA, at room temperature. This procedure was followed by incubation with biotinylated goat anti-rabbit or biotinylated horse anti-mouse (1:200; Vector Laboratories), for 75 min. After washing, sections were treated with the avidin-biotin complex (ABC kit; Vector; diluted 1:100) and then with a freshly prepared solution (0.075%) of 3-3'-diaminobenzidine tetrahydrochloride and 0.002% H_2O_2. Finally, sections were mounted, dehydrated with ethanol (75%, 96% and 100% for 5 minutes each), immersed in xylene for 10 minutes and laid on coverslips with Eukitt® (O. Kindler GmbH & Co.). The specificity of primary antibodies was assessed by negative controls, e.g. omission of primary antiserum. In these cases, no specific staining was

ever observed. Sections were examined on a Leica DMRB microscope, and images were acquired using a Leica DCF 480 camera coupled to a personal computer or slide scanner Nanozoomer S60 (Hamamatsu), for densitometric immunoperoxidase analysis. We analyzed at least 3-4 images for each area.

Immunogold electron microscopy

To preserve the ultrastructure of the tissues, 3 C57BL/6J WT mice at P60 were perfused with 4 % paraformaldehyde and 0.2% glutaraldehyde in phosphate buffer (PB 0.1 M). Sections with PFC, CS and SNpc were selected for immunoperoxidase or immunogold pre-embedding immunohistochemistry reaction. After aldehyde quenching with 0.2% $NaBH_4$ (in phosphate buffered saline, PBS 0.01 M) for 30 minutes, sections were permeabilized with a mild treatment with ethanol (10%, 25%, 10% in PBS), rinsed with PBS and treated to block the unspecific interaction sites for 30 min with bovine serum albumine (BSA; 1% in PBS; Aurion). Next, they were incubated overnight with the primary antibody anti-α-synuclein S3062 (Sigma-Aldrich) diluted 1:500 in 1% BSA, at room temperature. This procedure was followed by rinsing with PBS and, after that, incubation with biotinylated goat anti-rabbit secondary antibody (Vector Laboratories; diluted 1:100 in 0.1% BSA in PBS) for 4 hours. After washing, sections were treated overnight with streptavidin-Gold 6 nm (Aurion; diluted 1:10 in 0.1% BSA in PBS). The next day, slices were washed with PBS and PB 0.1 M and then transferred in new glass boxes and rinsed with double-distilled water. After the washes, immunogold reaction was intensified with silver enhancement, by using R-GENT SE-EM kit (Aurion). Following rinsing with double-distilled water and PB 0.1 M, the sections were post-fixed with 1% glutaraldehyde in PB. Finally, the slices were osmicated and epoxy-embedded. After polymerization, small areas from PFC, CS and *substantia nigra pars compacta* (SNpc) were cut with a razor blade and glued to blank resin blocks for sectioning with a Reichert ultramicrotome. Ultrathin sections (50–70 nm) collected on Cu/Rh grids were counterstained with lead citrate, or left unstained, and examined with a Zeiss LEO912AB electron microscope.

Densitometric immunoperoxidase analysis

To perform a densitometric analysis of α-synuclein on immunoperoxidase-stained sections, slices from P60 WT C57BL/6J mice and P90 β2-V287L and their control littermates were chosen. The whole sections were acquired with the slide scanner

Nanozoomer S60 (Hamamatsu). The images were then magnified and saved at 20X with the software NDPview2 (Hamamatsu) to show only the considered area, and different regions of interest (ROIs) were designed on ImageJ for each region. For WT mice 2 images at 20X for each hemisphere were cut (4 for each animal), and the following areas were analyzed: prefrontal cortex, primary motor cortex, somatosensory cortex, dorsomedial, dorsolateral and ventral corpus striatum, dentate gyrus, *cornu Ammonis* region 3, entorhinal cortex, *substantia nigra pars compacta* and *reticulata*. For β2-V287L mice and their control littermates 6 images at 20X for each hemisphere (12 for each animal) were chosen. The images were then deconvoluted and spatially calibrated with ImageJ (NIH) software, and from each of them a mean intensity of the signal (in optical density; OD) of the pixels in the ROI was obtained and compared between the different areas for WT mice or between controls and β2-V287L mice.

Immunofluorescence histochemistry

Sections were permeabilized and blocked as described for immunoperoxidase histochemistry. They were next incubated for two nights in a mixture of one/two primary antibodies, before staining with Hoechst (Molecular Probes), as necessary for cytoarchitecture analysis. After washing the primary antibodies with PBS, sections were incubated with a biotinylated horse anti-mouse secondary antibody (Vector Laboratories) for 75 min at room temperature, followed by PBS rinsing and CF^{TM}488-conjugated streptavidin and Cy3^{TM}-conjugated donkey anti-rabbit incubation at room temperature for 2 hours. After rinsing, samples were mounted on coverslips with Vectashield^{TM} (Vector Laboratories) and inspected with a Nikon A1 laser scanning confocal microscope, to visualize double fluorescent labeling.

Colocalization and densitometric analysis

Confocal micrographs were collected at 40X with a Nikon A1 laser scanning confocal microscope and analyzed with Fiji, a by-product of ImageJ. Identical parameters were used to acquire images for the same antigen, as previously described (Aracri *et al.*, 2013). In brief, nonoverlapping pictures were acquired in at least two different sections, so that double immunolabeling was studied in 3 or 4 fields per region in each animal. The degree of colocalization of different neuronal markers was calculated by comparing the Manders' coefficients, computed with the JACoP plug-in of ImageJ software (Bolte and Cordeliéres, 2006). The plug-in merges the confocal

images and gives different correlation coefficients. For this study, only Manders' coefficients M1 and M2 together with Pearson's coefficient were used. M1 is defined as the ratio of the "summed intensities of pixels from the green image for which the intensity in the red channel is above zero" to the "total intensity in the green channel". M1 is a good indicator of the proportion of the green signal (α-synuclein) coincident with a signal in the red channel (vesicular transporter) over its total intensity (Manders *et al.*, 1992).

Statistical analysis

Data are given as mean values ± standard error of the mean. The number of experiments (n) is the number of tested mice. Comparisons between two independent populations were carried out with unpaired Student's *t*-test, after testing for data normality (with a Kolmogorov-Smirnov test), and variance homogeneity (with F-test). Data obtained from WT mice were compared with one-way Analysis of Variance (ANOVA), using Bonferroni post-hoc test. In the figures, p values are indicated by * ($0.01 < p \leq 0.05$) or ** ($p \leq 0.01$). Unless otherwise indicated, detailed statistics are given in the figure legends.

RESULTS

Distribution of α-synuclein in different regions of WT mice

Immunoperoxidase labeling of α-synuclein in WT mice showed a diffuse and punctiform staining, mainly neuropilar, with no labeling of the cell bodies (**Fig. 1A-E**), in agreement with the prevalent localization at the presynaptic sites reported in the literature. Nevertheless, in the *substantia nigra pars compacta* (SNpc), the labeled puncta appeared scarce and the product of the reaction was detected in the soma of few neurons (**Fig. 1F**). Interestingly, a more intense staining between granule cells layer and molecular layer of dentate gyrus (DG; **Fig. 1C**) and between pyramidal cells layer and molecular layer of CA3 stratum oriens (**Fig. 1D**) could be observed. The densitometric analysis, performed on several brain areas to evaluate the expression level of the protein in central nervous system, highlighted a quantitative region-dependent distribution of α-synuclein. As it could be seen in **Fig. 1G**, the expression level of the protein in SNpc appeared significantly lower than the ones detected in the somatosensory cortex (SS), in the hippocampus (DG and CA3) and in the entorhinal cortex (Ent). In addition, in Ent α-synuclein level was significantly higher than in the dorsolateral *corpus striatum* (CS DL).

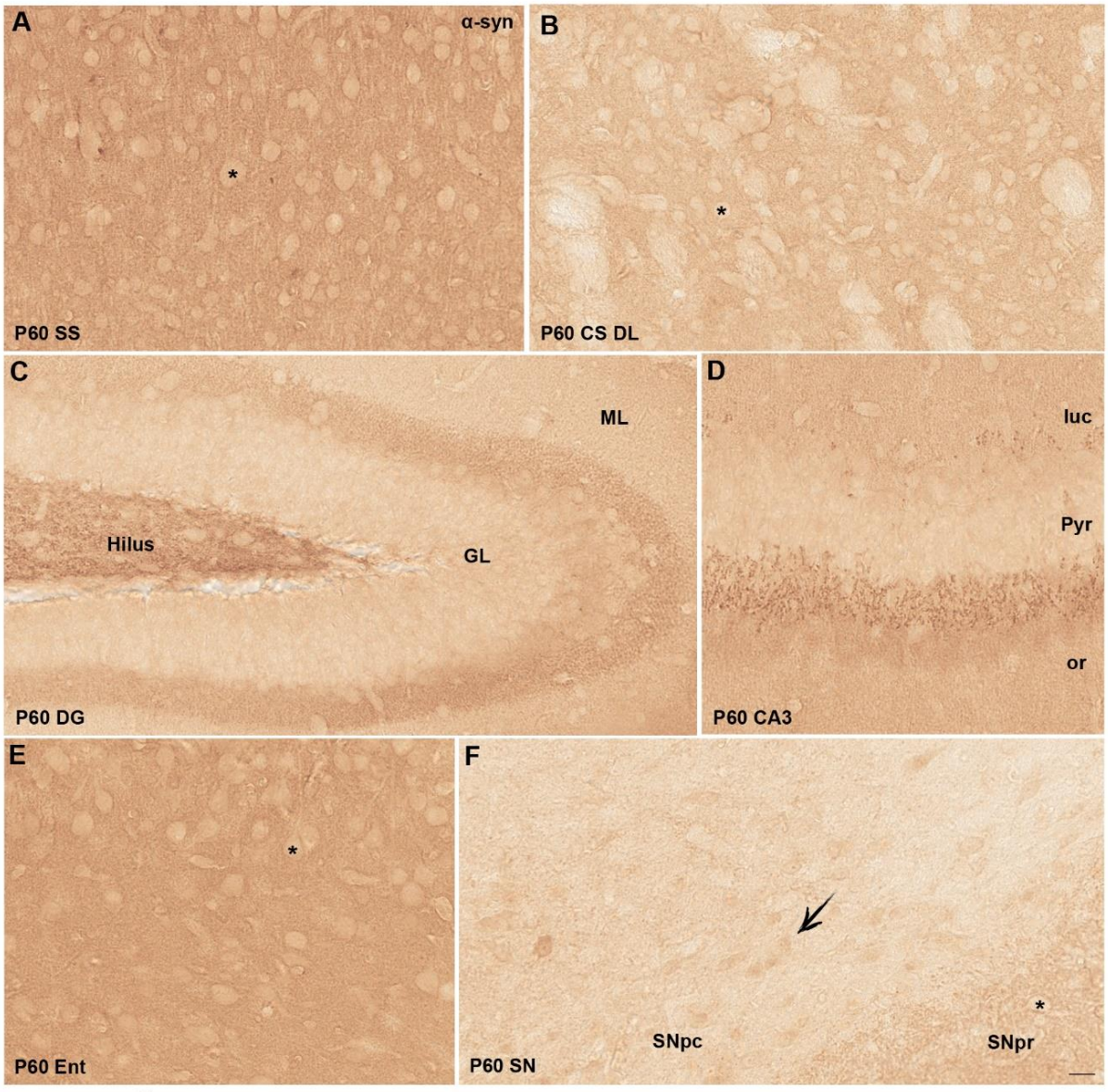
A
α-syn
*
P60 SS
B
*
P60 CS DL
C
ML
Hilus
GL
P60 DG
D
luc
Pyr
or
P60 CA3
E
*
P60 Ent
F
*
SNpc
SNpr
P60 SN

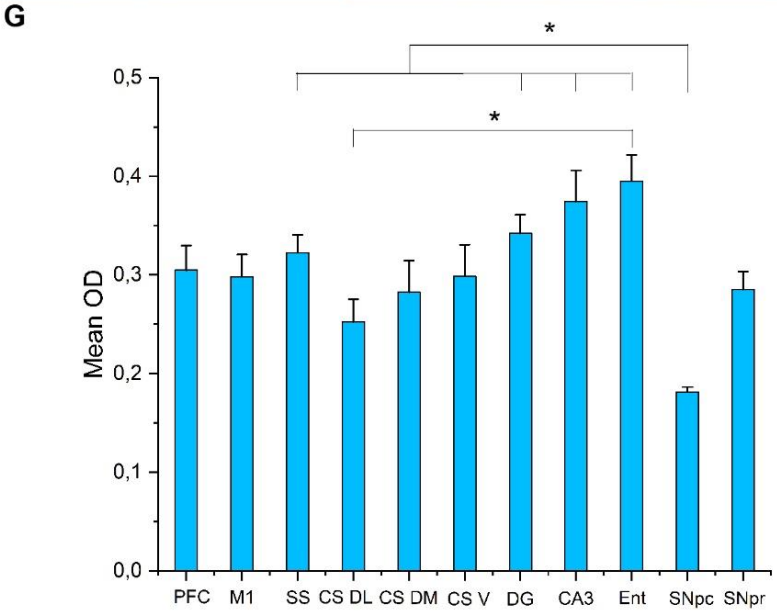
G
*
*
0,5
0,4
0,3
0,2
0,1
0,0
Mean OD
PFC
M1
SS
CS DL
CS DM
CS V
DG
CA3
Ent
SNpc
SNpr

Fig.1 α-Synuclein immunoperoxidase staining and densitometric analysis in coronal sections of WT mice brain.

*Optical microscope images of α-synuclein immunolabeling in SS (A), CS DL (B), DG (C), CA3 (D), Ent (E) and SNpc (F). Results of the densitometric analysis (G). α-synuclein staining is punctiform and mainly neuropilar. The asterisks showed that the cell bodies are not labeled, except in the SNpc (arrow). Data are expressed as mean optical density and were compared among the different areas with ANOVA; Bonferroni post-hoc test. *p<0.05. (P60, n=3) Scale bar=20 µm.*

PFC=prefrontal cortex; M1=primary motor cortex; SS=somatosensory cortex; CS DM=dorsomedial corpus striatum; CS DL=dorsolateral corpus striatum; CS V=ventral corpus striatum; DG=dentate gyrus; CA3=cornu Ammonis region 3; Ent=entorhinal cortex; SNpc and SNpr=substantia nigra pars compacta and reticulata, respectively. ML=molecular layer; GL=granule cell layer; luc=stratum lucidum; Pyr=pyramidal neuron layer; or=stratum oriens.

Ultrastructural analysis of α-synuclein in WT mice

Firstly, we wanted to see if the anti-α-synuclein antibody confirmed the presynaptic localization of the protein as the predominant one by means of ultrastructural analysis. The study was carried out on PFC-, CS- and SNpc-containing slices of WT mice. The labeling consisted in an immunoperoxidase staining in pre-embedding. Oxidation product of diaminobenzidine (DAB) precipitates in proximity of the antigen and after osmication could be detected at transmission electron microscope (TEM), due to its elevate electron density, allowing the discrimination of cellular compartment in which the protein is located. In the three examined regions the labeling was mainly at presynaptic level in association with synaptic vesicles (**Fig. 2A-C**). Not all the synaptic boutons appeared to be stained (**Fig. 2B**, **Fig. 3A**). α-Synuclein-positive synaptic terminals contacted different structures, mainly dendritic shafts and dendritic spines. The presence of both symmetric, generally inhibitory, and asymmetric, generally excitatory, synapses, could be observed. In addition, immunoperoxidase reaction product was present even in the dendritic (**Fig. 3A**) and in the axonal (**Fig. 3A-D**) compartments. The staining was present in myelinic fibers of large caliber (**Fig. 3A, C**), in partially myelinated axons (**Fig. 3D**) and in amyelinic fibers of small caliber (**Fig. 3B, C**).

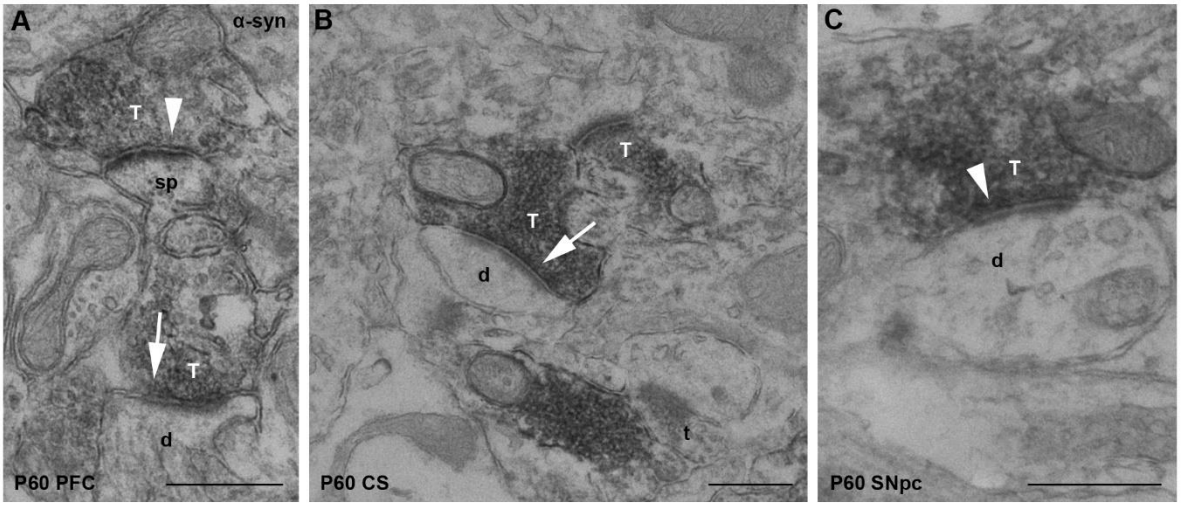

Fig.2 Immunoperoxidase electron microscopy for α-synuclein in WT mice PFC, CS and SNpc.

In all the studied regions the labeling was mainly at presynaptic level in association with synaptic vesicles (A-C), but not all the synaptic boutons appeared to be stained (B). α-Synuclein-positive synaptic terminals contacted mainly dendritic shafts and dendritic spines. The presence of both symmetric (white arrows) and asymmetric (white arrowheads) synapses could be observed.

PFC=prefrontal cortex (A), CS=corpus striatum (B) and SNpc=substantia nigra pars compacta (C); labeled synaptic terminal=T; non-labeled synaptic terminal=t; dendritic spine=sp; dendrite=d. Scale bar=500 nm.

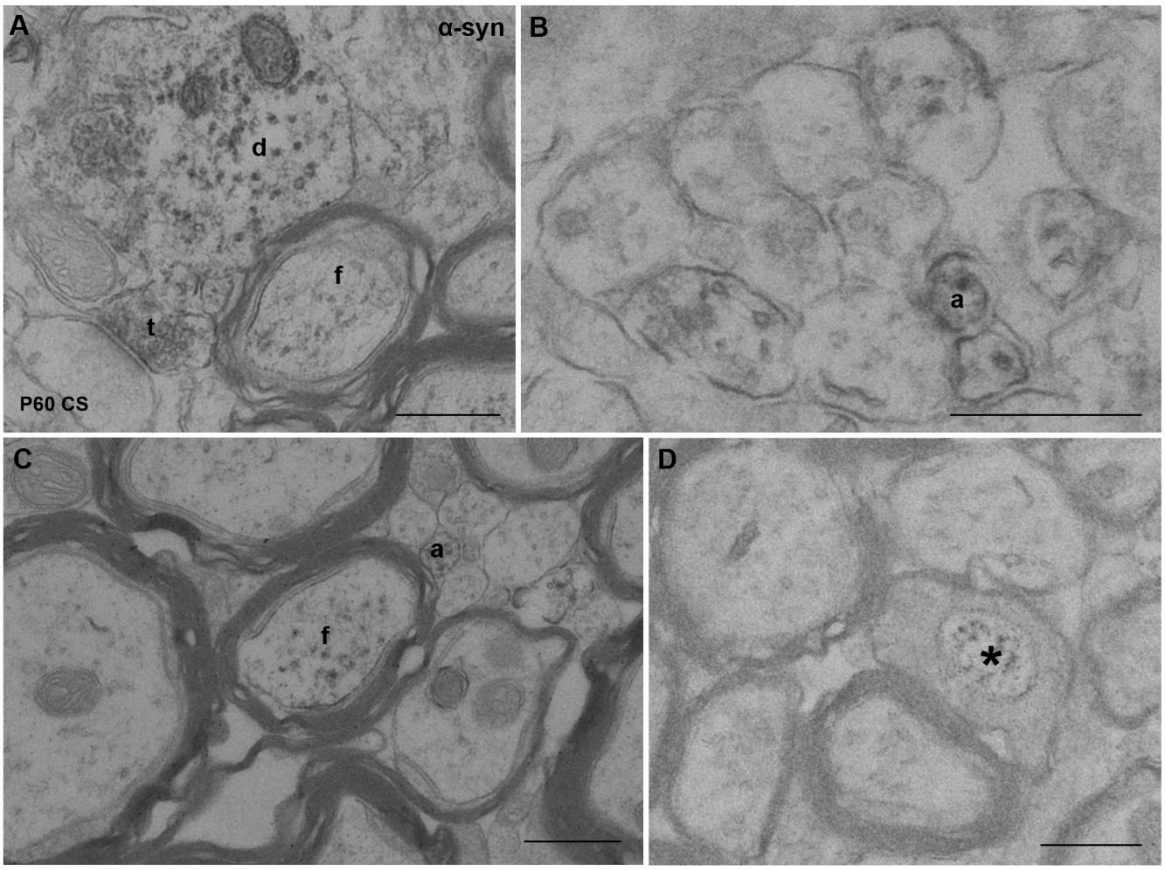

Fig.3 Electron micrographs of α-synuclein expression in CS of WT mice.
*As it emerges from the images, immunoperoxidase reaction product was present even in the dendritic (A) and in the axonal (Fig. 3A-D) compartments. Myelinic fibers of large caliber (A, C), partially myelinated axons (D) and amyelinic fibers of small caliber (B, C) were labeled. CS=corpus striatum; d=dendrites; f=axons; a=amyelinic small caliber axon; *=partially myelinated axon; t=non-labeled synaptic terminal. Scale bar=500 nm.*

The subcellular localization by immunoperoxidase electron method was confirmed with immunogold reaction in pre-embedding (**Fig. 4**). The staining, electron dense particles labeling the antigen, was as expected and α-synuclein was found in both neurites and terminals full of vesicles (**Fig. 4**).

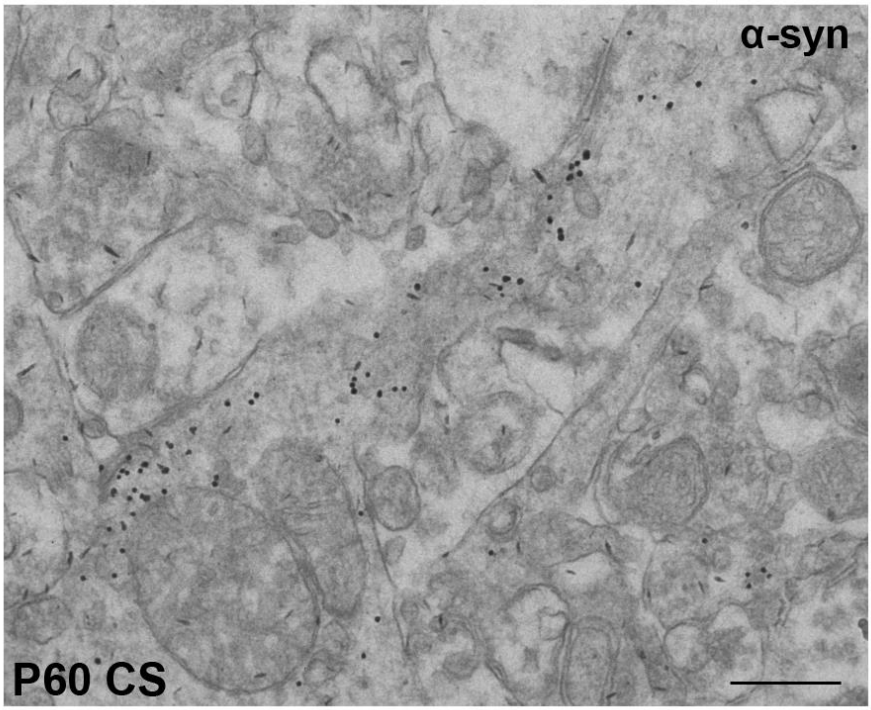

Fig. 4 Immunogold staining of α-synuclein in CS of WT mice.
The pattern of α-synuclein staining, represented as well-defined small electron dense nanoparticles of gold was, as expected, mainly found in both terminals and neurites.
Scale bar=500 nm.

Distribution of α-synuclein in β2-V287L mice

The experiments were carried out on the bases of previous studies that described the distribution of α-synuclein throughout the murine brain (Taguchi *et al.*, 2016). Here, the potential difference that could exist between ADNFLE and healthy brains in the protein abundance was tested. In order to assess it, two different densitometric analyses were performed, by immunoperoxidase method and by immunofluorescence. The number of animals for each experimental group was 3 (n=3) at postnatal day 90 (P90). The signal obtained with this method was particularly strong, and the distribution was quite uniform (**Fig. 5A, B, C**). It could be possible to observe the differences between various areas of the murine brain. No significant differences were found in the expression level of α-synuclein after the immunoperoxidase densitometric analysis in the examined regions (**Fig. 5D, E**).

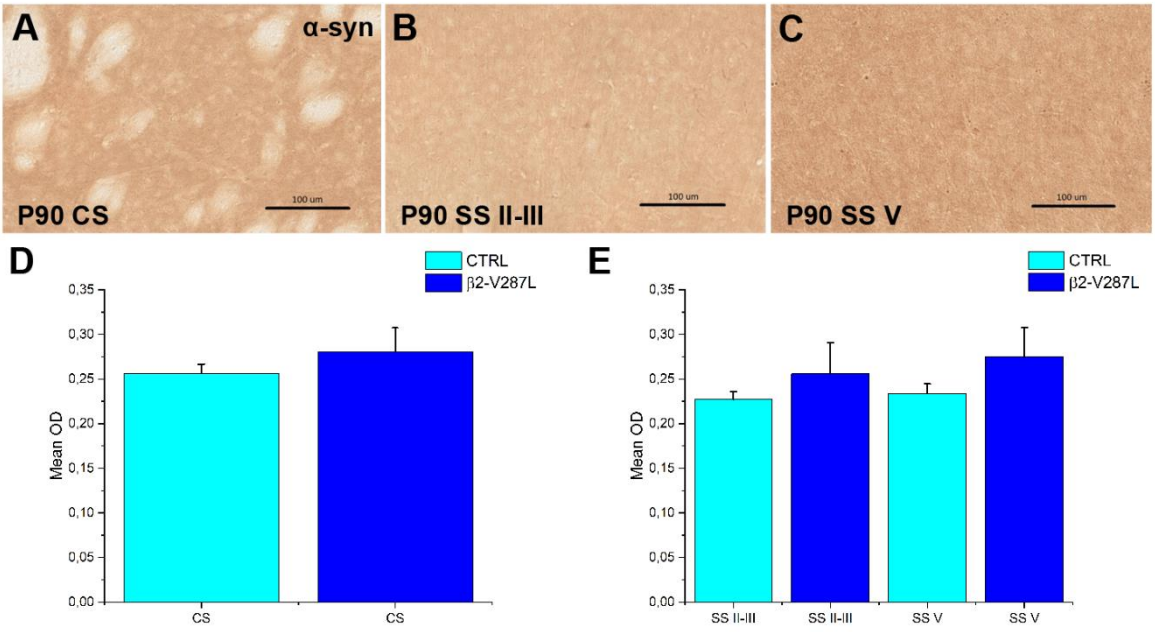

Fig.5 α-Synuclein immunolocalization with immunoperoxidase method on β2-V287L and CTRL mice.
Optical images of coronal slices containing the areas of the study: CS (A) SS layer II-III (B), SS layer V (C) at 20X. CS=corpus striatum; SS II-III=somatosensory cortex layer II-III; SS V=somatosensory cortex layer V. As seen in the WT mice, α-synuclein staining is predominantly neuropilar in CS and SS. Histograms resulting from the statistical analysis (D, E) are displayed to show the results of the t-Student hypothesis testing. No significant differences were found in all the examined regions. Data are expressed as mean optical density and were compared between CTRL and β2-V287L mice. p=0.443 (CS); p=0.470 (SS II-III); p=0.303 (SS V). (P90, n=3) Scale bar=100 µm.

However, the densitometric analysis was also carried out by means of α-synuclein immunofluorescence. The studied regions were the same, but the CS was separated in dorsolateral (DL) and dorsomedial (DM). These acquisitions were also used for the following colocalization analyses. The final number of images analyzed was 24 for each of the examined area. The results in this analysis showed significant differences between CTRL and double-transgenic mice only in the DL striatum (**Fig. 6C**), where it has been found a decrease of α-synuclein density. In the other regions, no significant differences were statistically detected.

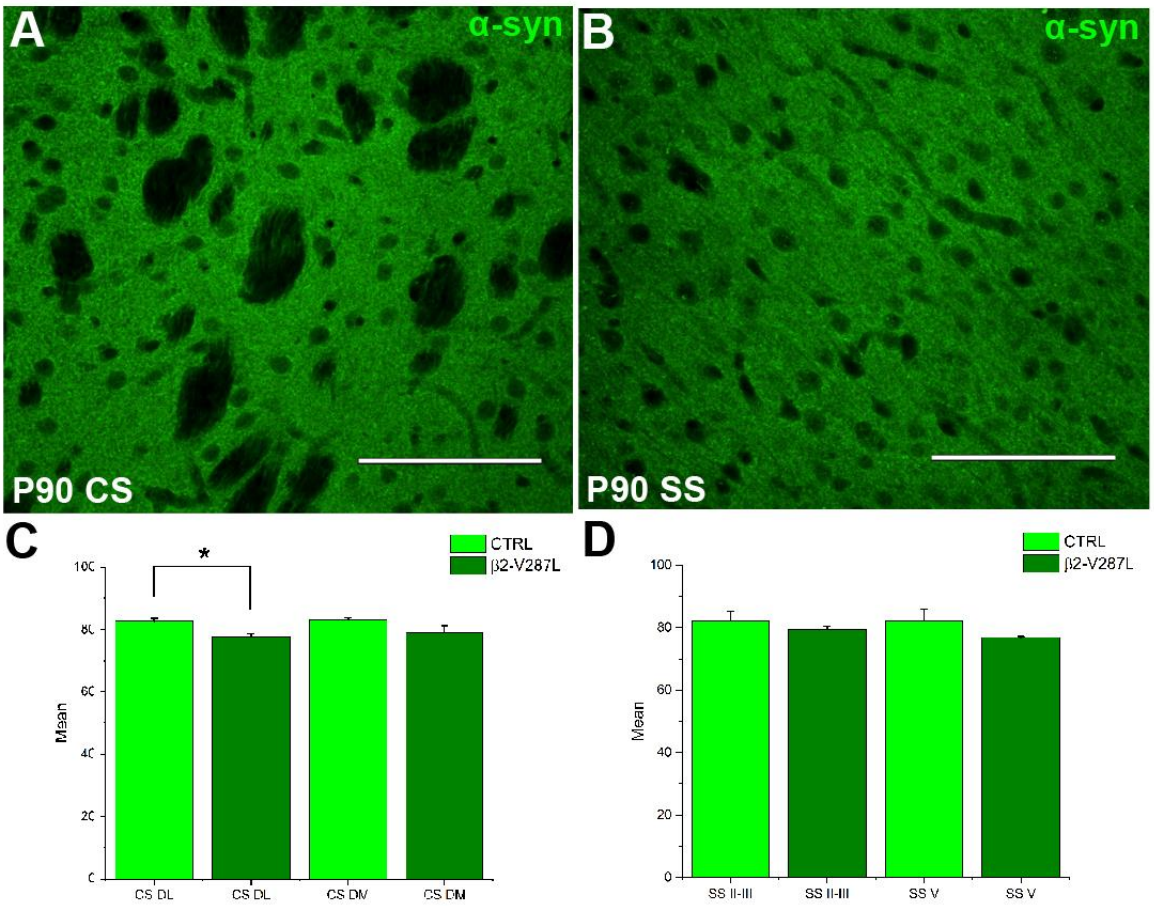

Fig. 6: Densitometric analyses of α-synuclein on immunofluorescence images. *Examples of images used for the analysis are shown at 40x magnification (A, B). Graphics displayed the results of the analysis (C, D). α-synuclein immunolabeling is similar to the one obtained by immunoperoxidase method. A statistically significant decrease of α-synuclein density was found in the DL striatum of double-transgenic mice compared to the CTRL littermates. In the other regions, no significant differences were statistically detected. Data are expressed as means of the intensity of the fluorescent signal depending on the zone and the genotype and were compared between CTRL and β2-V287L mice with Student's t-test. *p=0.018 (CS DL); p=0.114 (CS DM); p=0.420 (SS II-III); p=0.233 (SS V). (P90, n=3) Scale bar=100 µm.*

The interplay between α-synuclein and glutamatergic and GABAergic synapses in WT and β2-V287L mice

This analysis was carried out to assess if there were differences between CTRL and β2-V387L mice in the expression of α-synuclein in different kinds of synapses. The transporters used to select specific synapses were vesicular glutamate transporter 1 (VGLUT1) and vesicular GABA transporter (VGAT), to study excitatory and inhibitory synapses, respectively. The CS was again separated in DL and DM and the somatosensory cortex in layers II-III and V.

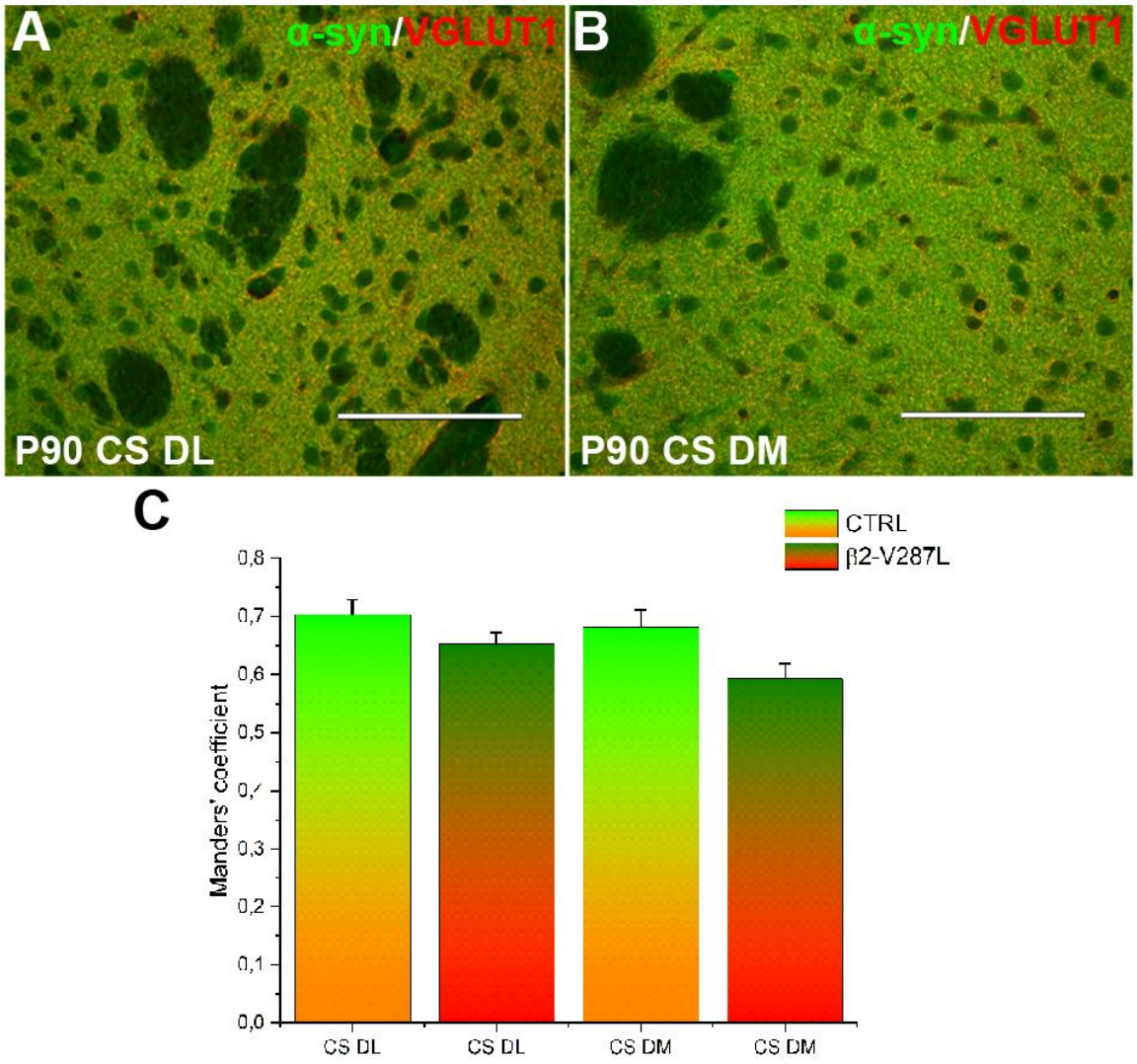

Figure 7: Colocalization analysis for α-synuclein and VGLUT1 in the CS.
Confocal images from the DL and the DM CS showing α-synuclein (in green) and VGLUT1 (in red) (A, B). The resulting graphic from statistical analysis is displayed in C. No significant differences were noticed in the different areas. Data are expressed as mean Manders' coefficient and were compared between CTRL and β2-V287L mice with Student's t-test. p=0.192 (CS DL); p=0.086 (CS DM). (P90, n=3) Scale bar=100 µm.

The number of images was the same as for the immunoperoxidase densitometric analysis (12 for the DM CS, 12 for the DL CS, 12 for the SS II-III, and 12 for the SS V). Manders' coefficient M1 was the colocalization coefficient indicating the signal colocalization percentage of both fluorochromes over α-synuclein total signal. For α-synuclein and VGLUT1 analyses all graphics and images are shown in **Fig. 7** and **Fig. 8**. In the striatum no significant differences were found for α-syn/VGLUT1

colocalization. The analyses on somatosensory cortex did not show any difference between the two genotypes for both the vesicular transporters.

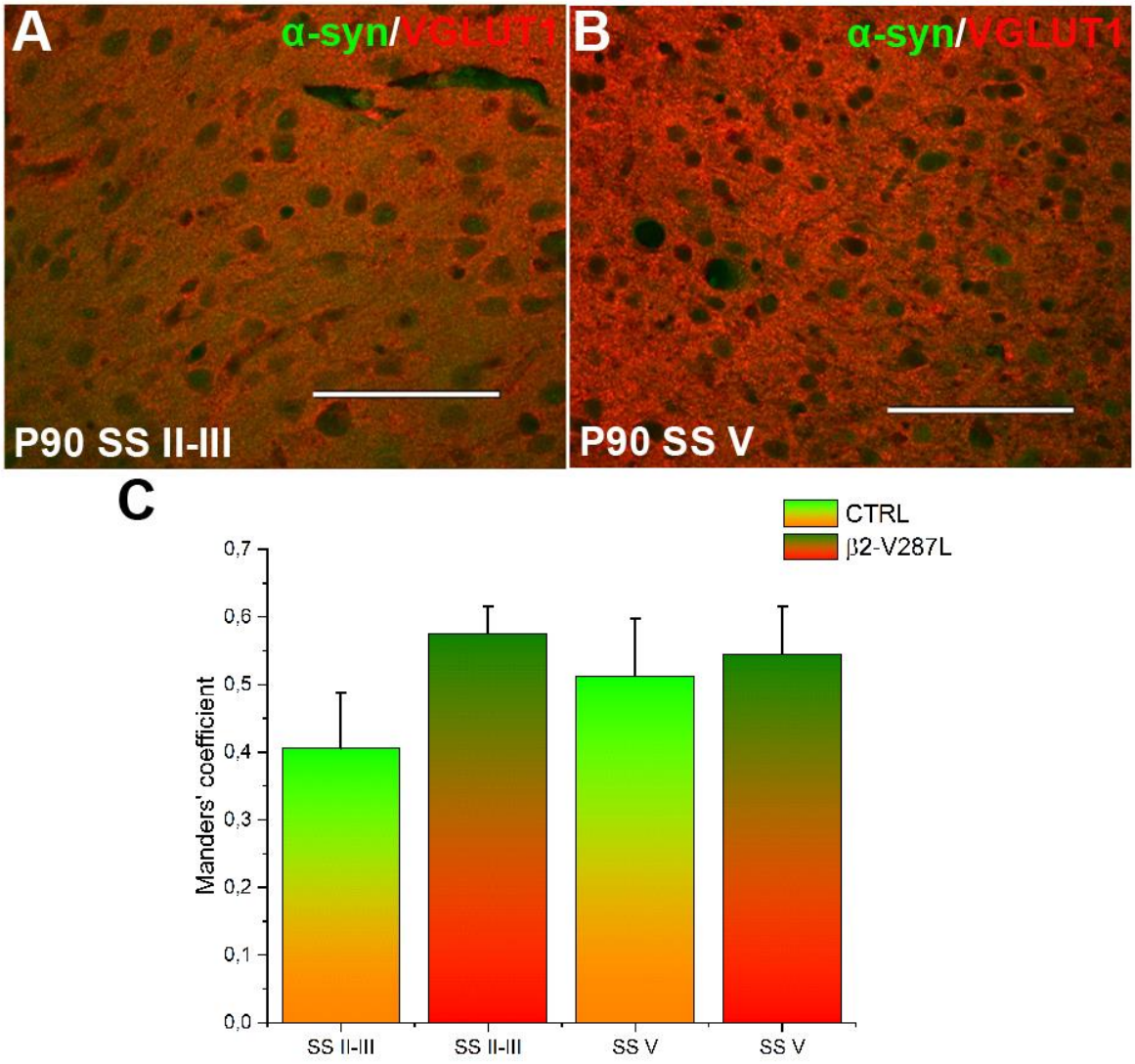

Fig. 8 Colocalization analysis for α-synuclein and VGLUT1 in the SS.
Confocal acquisitions from the layer II-III (A) and the layer V (B) of the somatosensory cortex showing α-synuclein (in green) and VGLUT1 (in red). The resulting histogram from statistical analysis is shown in picture C. Data are expressed as mean Manders' coefficient and were compared between CTRL and β2-V287L mice with Student's t-test. p=0.140 (SS II-III); p=0.784 (SS V). (P90, n=3) Scale bar=100 µm.

Regarding the colocalization with VGAT, the DL striatum did not show significant differences. On the contrary, the CS DM was the only region that displayed significant differences between the genotypes, as shown in **Fig. 9**. In this area β2-V287L mice showed an increase of the M1 coefficient compared to the CTRL littermates.

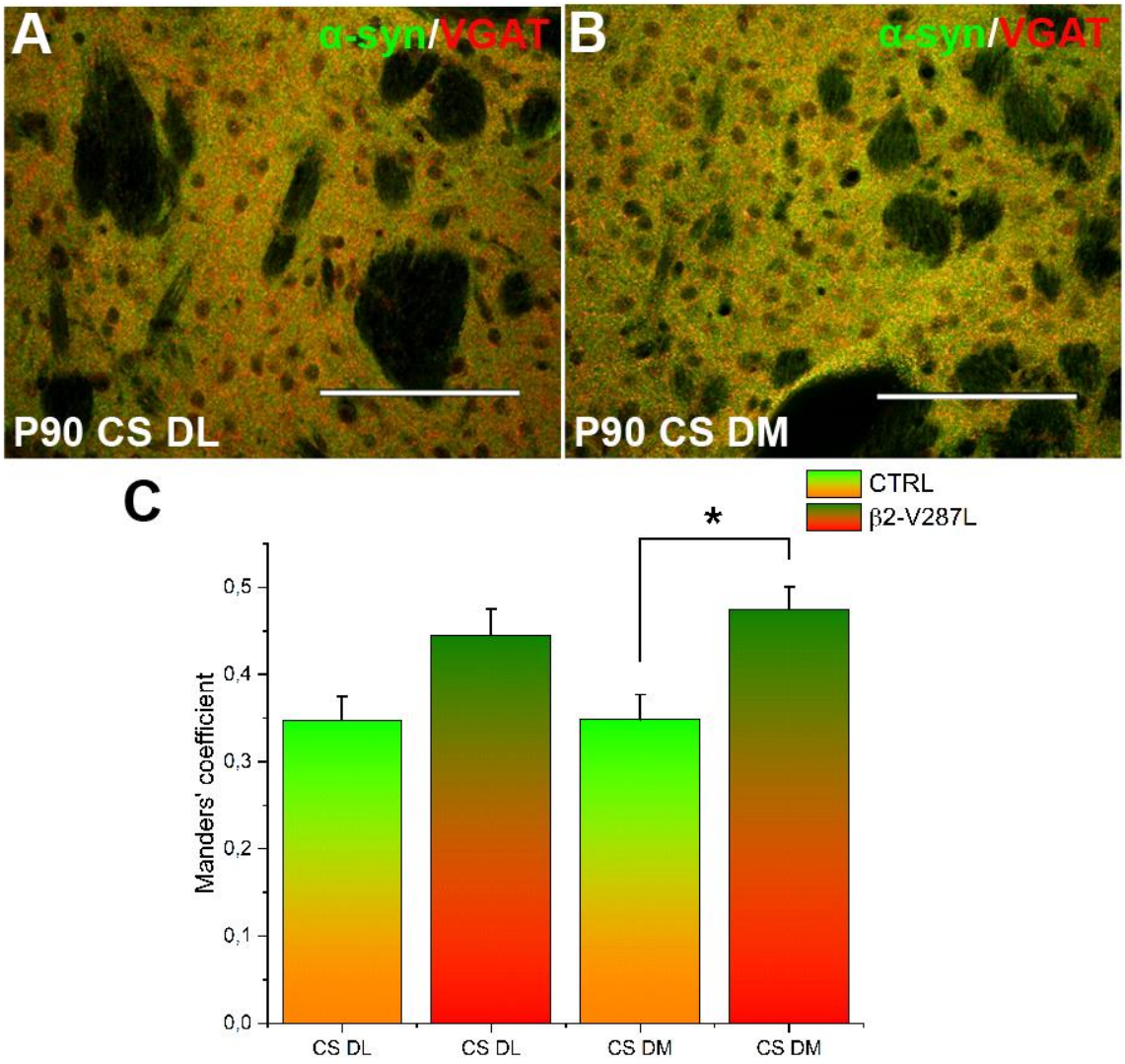

Fig. 9 Colocalization analysis of α-synuclein and VGAT in the CS.
*Images from the DL (A) and the DM (B) striatum showing α-synuclein (in green) and VGAT (in red). Regarding the colocalization with VGAT, in CS DM β2-V287L mice showed an increase of the M1 coefficient compared to the CTRL littermates. The DL CS did not show significant differences. The resulting histogram from statistical analysis is displayed in picture C. Data are expressed as mean Manders' coefficient and were compared between CTRL and β2-V287L mice with Student's t-test. p=0.075 (CS DL); *p=0.030 (CS DM). (P90, n=3) Scale bar=100 μm.*

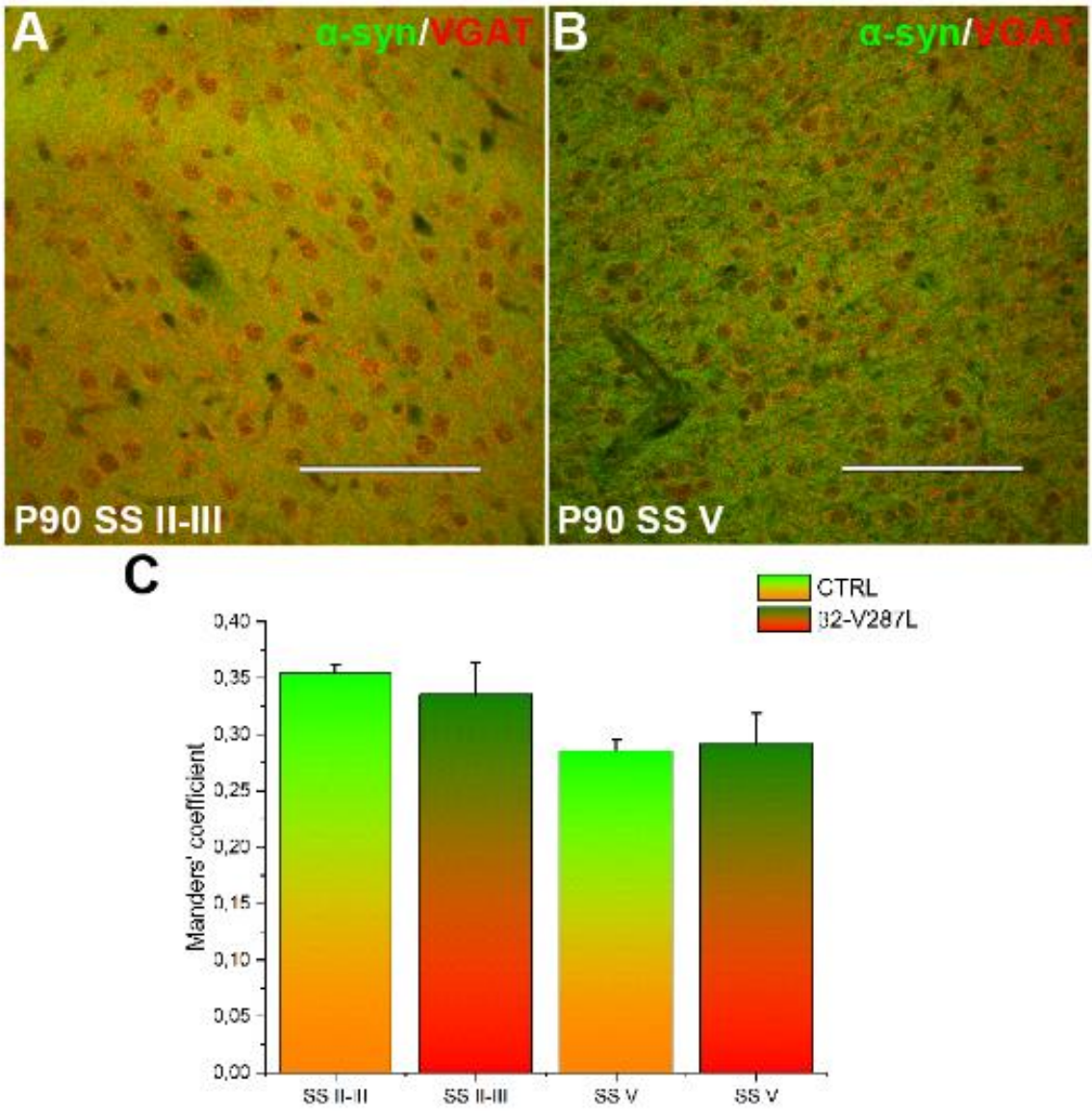

Fig. 10 Colocalization analysis for α-synuclein and VGAT in the SS.
Immunofluorescence images from the layer II-III (A) and the layer V (B) of the somatosensory cortex showing α-synuclein (in green) and VGAT (in red). The graph with the results from statistical analysis is displayed in C. Data are expressed as mean Manders' coefficient and were compared between CTRL and β2-V287L mice with Student's t-test. p=0.549 (SS II-III); p=0.859 (SS V). (P90, n=3) Scale bar=100 µm.

DISCUSSION

Differential expression of α-synuclein in the CNS of WT mice

Regarding α-synuclein distribution in wild-type murine brain, the densitometric analysis highlighted differences in the expression levels of the protein among the studied regions. In particular, *substantia nigra pars compacta* appeared to be one of the least labeled areas. This result was obtained previously also by Taguchi and colleagues (2016) on C57BL/6N 10-15-week-old wild-type mice. However, in their study, the authors showed only a semiquantitative evaluation of the protein expression levels, while our data show quantitative results on α-synuclein distribution. Our observations are partially in agreement with the literature data, reported mainly in mice by Taguchi and colleagues (2016; 2019) and also in rat brain by Andringa *et al.* (2003). In these two studies the monoclonal antibody Syn-1 (BD Biosciences) was used, even if its specificity is doubtful (Perrin *et al.*, 2003). Polyclonal antibody S3062 (Sigma-Aldrich) is highly specific, as it recognizes a single band of 19 kDa in Western blotting method. In the work of Andringa and colleagues (2003), the somatic neuronal staining is present in the somatosensory cortex, dentate gyrus, CA3, entorhinal cortex, *substantia nigra pars compacta* and in other neuronal populations prone to develop Lewy pathology in human. By using S3062 antibody it is possible to detect somatic α-synuclein only in the *substantia nigra pars compacta*, confirming the specificity of this localization. Since the high expression of α-synuclein is considered a key risk factor for the development of Parkinson's disease, as showed by the presence of genetic multiplications in the patients, the particular enrichment of the protein in the cell body of dopaminergic neurons of *substantia nigra pars compacta* could provide a possible explanation of specific neurodegenerative vulnerability of these neurons.

Ultrastructural analysis allowed the thorough investigation of α-synuclein distribution in the different cellular compartments. From our study it appeared that the protein is expressed in terminals with different synaptic specialization. These results are in agreement with the ones presented by Totterdell and colleagues in 2004 and 2005. In particular, it was observed that in the *corpus striatum* α-synuclein is mainly expressed in asymmetric synapses, generally excitatory (Totterdell *et al.*, 2004). This evidence justifies the high grade of colocalization between α-synuclein and VGLUT1 (marker of glutamatergic terminals) and a low colocalization with GAD (marker of GABAergic terminals) detected by Taguchi and colleagues (2016). Moreover, we

observed that the protein is present in axons with different myelinization level. Braak and Del Tredici (2004) highlighted the importance of myelinization level, caliber and axonal length in determining the vulnerability to degeneration in some neuronal populations. *Substantia nigra pars compacta* dopaminergic neurons possess long projective axons of small caliber, property that correlates with the neurodegenerative susceptibility. As it appears from our study, in the *corpus striatum* fibers with these aforementioned properties are present, they mainly constitute the nigrostriatal pathway and are positive for α-synuclein. Using neuronal tracers, it was showed the presence of α-synuclein in both corticostriatal and nigrostriatal pathway terminals (Totterdell and Meredith, 2005). Globally, these studies lay the foundation for further analyses designed to better understand α-synuclein expression in neuronal populations that possess different neurochemical properties. The obtained data, in addition, could be useful to provide possible explanations regarding the specific vulnerability of some neuronal populations to degenerate during Parkinson's disease progression, since, in neuronal coltures, also a physiological expression of α-synuclein is sufficient to sustain protein aggregation (Volpicelli-Daley *et al.*, 2011).

Imbalance of α-synuclein in mutant β2-V287L mice

α-Synuclein aggregation, alterations and mutations are classically related to Parkinson's disease, since 1997, when a mutation in the gene encoding for the protein was associated to the pathology (Polymeropoulos *et al.*, 1997). This discovery represented an inflection point in our knowledge on α-synuclein, because many investigators focused on elucidating its genetics and dynamics to better understand its physiology and implications on PD (Davidson *et al.*, 1998; Narhi *et al.*, 1999; Spillantini *et al.*, 1998). After many years of investigation, recent studies have found an implication for α-synuclein overexpression in different diseases, calling them synucleinopathies. It has been proven that α-synuclein overexpression could cause neurotransmission dysfunctions due to its role in neurotransmitter release in the synaptic terminals (Hassink *et al.*, 2018; Hunn *et al.*, 2015). Recent studies have indicated a new target for α-synuclein, the nicotinic acetylcholine receptors (nAChRs, Liu *et al.*, 2013). It is known that mutations in subunits of the neuronal nAChRs cause epileptic phenotypes (Manfredi *et al.*, 2009), and their implications in Autosomal Dominant Nocturnal Frontal Lobe Epilepsy (ADNFLE) have been demonstrated (Becchetti *et al.*, 2015; Ghasemi and Hadipour-Niktarash, 2015). In this kind of

disorder, the epileptic seizures arise from the prefrontal cortex (PFC), in the frontal lobe. Moreover, further studies have linked nAChRs to the regulation of GABAergic and glutamatergic synapses in the PFC (Aracri *et al.*, 2010; 2013). Therefore, it would be interesting to study whether nAChRs mutations in the ADNFLE model could alter α-synuclein expression. Studies on the hippocampus of epileptic mice have found a relationship between the decrease of physiological filamentous α-synuclein and microtubular-associated proteins, inducing synaptic deficit and cytoskeletal abnormalities (Yang *et al.*, 2006). Other studies regarding epilepsy have noticed an increase of α-synuclein in different brain regions, such as the dentate gyrus, linked to a synaptic dysfunction in epileptic mice (Li *et al.*, 2010). Moreover, α-Synuclein presence has been recently found abnormally high in the serum of patients with untreatable epilepsy (Rong *et al.*, 2015). These last results show that abnormal α-synuclein does not affect only the regions where its overexpression is present, but it also spreads through the plasma and the cerebrospinal fluid (Hong *et al.*, 2010). On these bases, unraveling the involvement of α-synuclein imbalance in the pathogenesis of epilepsy is a challenge. Our aim has been to analyze the protein expression in a murine model bearing a mutant nicotinic subunit linked to ADNFLE. Furthermore, it was also hypothesized a change of α-synuclein presence in different kind of synapses. In this pilot study, we focused our experiments on the *corpus striatum* (CS) and on the somatosensory cortex (SS). The CS is a common studied area in neurodegenerative disorders and synucleinopathies research because it is one of the most affected regions. On the other hand, the SS cortex was also added to this study because it is the reference cortex for studies on epileptogenesis. The densitometric analysis on immunoperoxidase-stained sections carried out to compare the abundance of α-synuclein between control and ADNFLE mice did not show any significant difference. Nevertheless, α-synuclein immunofluorescence images revealed a significant decrease of the protein expression in DL CS. Results from immunofluorescence analysis are more reliable because the number of images used for each experimental condition was higher than the number of acquisitions considered from the immunoperoxidase method and the fluorescence intensity is stoichiometrically proportional to the level of expression of the protein. Previous studies found a high colocalization ratio between glutamatergic terminals and α-synuclein aggregates in hippocampal cell cultures of normal mice (Taguchi *et al.*, 2014). Therefore, when the CS was analyzed under the same conditions, a high colocalization coefficient was also

observed. In layer V of the cerebral cortex, the colocalization coefficient between VGLUT1 and α-synuclein resulted high (Taguchi *et al.*, 2016). Anyway, our results have shown no difference between CTRL and β2-V287L mice in VGLUT1 colocalization with α-synuclein in the CS and SS. A similar morphological study showed different results in mice with dysfunctional SNARE complex assembly. The mutation caused synaptic transmission impairment, due to excessive accumulation of presynaptic vesicles and enlargement of the VGLUT1-positive nerve terminals, which presented an aggregation of α-synuclein (Nakata *et al.*, 2012). The results we obtained showed instead that the GABAergic synapses of the DM CS have a higher expression of α-synuclein in ADNFLE mice, whereas the DL CS presented greater values in ADNFLE mice but the results in this case were not statistically significant. In wild-type mice, recent studies found a low colocalization ratio between α-synuclein and glutamate acid decarboxylase (GAD) in the majority of the brain areas (Taguchi *et al.*, 2019). Our results regarding VGAT suggest an increase of the vesicle pool in GABAergic nerve terminals of the CS like those found previously for glutamatergic terminals by Nakata et al. (2012). Moreover, studies on the PFC in mice overexpressing α-synuclein have displayed an important decrease of GABAergic activity (Ito *et al.*, 2012). From these data, it seems that the relationship between GABAergic system and α-synuclein expression could be altered in epilepsy.

Conclusion

Summarizing the results, this preliminary study seems to be an interesting perspective approach on α-synuclein expression alterations in the *corpus striatum* of ADNFLE mice. Densitometric analysis has shown that in the *corpus striatum* the expression of α-synuclein is altered, at least in the dorsolateral part. Further studies on a bigger sample size could confirm the alteration of α-synuclein expression in the dorsal *corpus striatum*. In addition, our results suggest a relationship between α-synuclein and GABAergic synapses in the *corpus striatum*, at least in the dorsomedial zone, where the presence of the protein in these nerve terminals was increased. Thus, abnormalities of α-synuclein expression in the *corpus striatum* could lead to an alteration of the inhibitory control of the afferent projections, possibly related to the presence of epileptic seizures. Further studies focused on the effect of α-synuclein accumulation onto the GABAergic and glutamatergic synapses of the prefrontal cortex would help to clarify the mechanisms of the epileptic seizures in ADNFLE. Moreover,

the investigation of other systems, like the dopaminergic one, would be an interesting approach to find possible alterations of the nigrostriatal pathway control by GABAergic neurons. Finally, developmental studies would help to clarify if neuronal circuits are altered during the crucial period of synaptogenesis, generally occurring in rodent second postnatal week.

REFERENCES

Abbott, RD, Ross GW, White LR, Tanner CM, Masaki KH, Nelson JS *et al.* (2005) *Excessive daytime sleepiness and subsequent development of Parkinson's disease.* Neurology, 65(9), 1442-1446.

Andringa G, Du F, Chase TN and Bennett MC (2003) *Mapping of rat brain using the Synuclein-1 monoclonal antibody reveals somatodendritic expression of alpha-synuclein in populations of neurons homologous to those vulnerable to Lewy body formation in human synucleopathies.* J Neuropathol Exp Neurol. 62(10):1060-75.

Aracri P, Consonni S, Morini R, Perrella M, Rodighiero S, Amadeo A and Becchetti A (2010) *Tonic modulation of GABA release by nicotinic acetylcholine receptors in layer V of the murine prefrontal cortex.* Cerebral Cortex 20: 1539-1555.

Aracri P, Amadeo A, Pasini ME, Fascio U, and Becchetti A (2013) *Regulation of glutamate release by heteromeric nicotinic receptors in layer V of the secondary motor region (Fr2) in the dorsomedial shoulder of prefrontal cortex in mouse.* Synapse 67, 338-357.

Arnulf I, Konofal E, Merino-Andreu M, Houeto JL, Mesnage V, Welter ML *et al.* (2002). *Parkinson's disease and sleepiness: an integral part of PD.* Neurology, 58(7), 1019-1024.

Becchetti A, Aracri P, Meneghini S, Brusco S and Amadeo A (2015) *The role of nicotinic acetylcholine receptors in autosomal dominant nocturnal frontal lobe epilepsy.* Frontiers in Physiology. 6(22):1-12.

Bolte S and Cordelières FP (2006) *A guided tour into subcellular colocalization analysis in light microscopy.* J Microsc 224:213-232.

Burghaus L, Schutz U, Krempel U, Lindstrom J, Schroder H (2003) *Loss of nicotinic acetylcholine receptor subunits alpha4 and alpha7 in the cerebral cortex of Parkinson patients*. Parkinsonism. Relat. Disord. 9: 243-246.

Champtiaux N, Gotti C, Cordero-ErausquinM, David DJ, Przybylski C, Lena C, Clementi F, Moretti M, Rossi FM, Le Novere N, McIntosh JM, Gardier AM and Changeux JP (2003) *Subunit composition of functional nicotinic receptors in dopaminergic neurons investigated with knock-out mice*. J. Neurosci. 23: 7820-7829.

Cho YW, Motamedi GK, Laufenberg I, Sohn SI, Lim JG, Lee H, Yi SD, Lee JH, Kim DK, Reba R, Gaillard WD, Theodore WH, Lesser RP and Steinlein OK (2003) *Korean kindred with autosomal dominant nocturnal frontal lobe epilepsy and mental retardation.* Archives of Neurology 60 (11): 1625-1632.

Davidson WS, Jonas A, Clayton DF and George JM (1998) *Stabilization of Synuclein secondary structure upon binding to synthetic membranes.* Journal of Biological Chemistry, 273(16), 9443-9449.

Delenclos, M, Ross OA, Jones DR, Moussaud S, McLean PJ and MoussaudLamodière EL (2014) *Alpha-Synuclein and Tau: Teammates in Neurodegeneration?* Molecular Neurodegeneration, 9(1), 43.

Ghasemi M and Hadipour-Niktarash A (2015) *Pathologic role of neuronal nicotinic acetylcholine receptors in epileptic disorders: implication for pharmacological interventions.* Reviews in the Neurosciences. 26(2), 199-223.

Goedert, M, Jakes, R and Spillantini, MG (2017) *The Synucleinopathies: Twenty Years on.* Journal of Parkinson's Disease, 7(s1), S53–S71.

Hassink GC, Raiss CC, Segers-Nolten IMJ, Van Wezel RJA, Subramaniam V, Le Feber J and Claessens MMAE (2018) *Exogenous α-synuclein hinders synaptic communication in cultured cortical primary rat neurons.* PLoS ONE, 13(3), 1-21.

Hirose S, Iwata H, Akiyoshi H, Kobayashi K, Ito M, Wada K, Kaneko S and Mitsudome A (1999) *A novel mutation of CHRNA4 responsible for autosomal dominant nocturnal frontal lobe epilepsy.* Neurology 53 (8): 1749-1753.

Hong Z, Shi M, Chung KA, Quinn JF, Peskind ER, Galasko D *et al.* (2010) *DJ-1 and α-synuclein in human cerebrospinal fluid as biomarkers of Parkinson's disease.* Brain, 133(3), 713-726.

Hu R, Luo J, Wang W, Wang X, Xi Z (2015) *Alpha-Synuclein Is A Potential Biomarker In The Serum And Csf Of Patients With Intractable Epilepsy.* Seizure, 27: 6-9.

Hunn BHM, Cragg SJ, Bolam JP, Spillantini MG and Wade-Martins R (2015) *Impaired intracellular trafficking defines early Parkinson's disease. Trends* in Neurosciences, 38(3), 178-188.

Ito H, Nakayama K, Jin C, Suzuki Y and Yazawa I (2012) *α-Synuclein accumulation reduces GABAergic inhibitory transmission in a model of multiple system atrophy.* Biochemical and Biophysical Research Communications, 428(3), 348-353.

Lai A, Sum J, Fan H, McIntosh JM, Quik M (2004) *Selective recovery of striatal 125I-alpha-conotoxinmii nicotinic receptors after nigrostriatal damage in monkeys.* Neuroscience 127:399-408.

Li A, Choi YS, Dziema H, Cao R, Cho HY, Jung YJ, Obrietan K (2010) *Proteomic Profiling Of The Epileptic Dentate Gyrus.* Brain Pathol. 20(6):1077-89.

Liu Q, Emadi S, Shen JX, Sierks MR, Wu J (2013) *Human α4β2 Nicotinic Acetylcholine Receptor As A Novel Target Of Oligomeric α-Synuclein.* Plos One. 8(2):E55886.

Liu JY, Reeves C, Diehl B, Coppola A, Al-Hajri A, Hoskote C, Mughairy SA,Tachrount M, Groves M, Michalak Z, Mills K, Mcevoy AW, Miserocchi A, Sisodiya SM, Thom M (2016) *Early Lipofuscin Accumulation In Frontal Lobe Epilepsy.* Ann Neurol. 80(6):882-895.

Magnusson A, Stordal E, Brodtkorb E and Steinlein O (2003) *Schizophrenia, psychotic illness and other psychiatric symptoms in families with autosomal dominant nocturnal frontal lobe epilepsy caused by different mutations.* Psychiatric Genetics 13 (2): 91-95.

Manders EM, Stap J, Brakenhoff GJ, van Driel R and Aten JA (1992) *Dynamics of three-dimensional replication patterns during the S-phase, analysed by double labelling of DNA and confocal microscopy.* Journal of Cell Science, 103 (Pt 3), 857- 862.

Manfredi I, Zani AD, Rampoldi L, Pegorini S, Bernascone I, Moretti M *et al.* (2009) *Expression of mutant β2 nicotinic receptors during development is crucial for epileptogenesis.* Hum. Mol. Genet. 18, 1075-1088.

McCann H, Stevens CH, Cartwright H and Halliday GM (2013) *α-Synucleinopathy phenotypes.* Parkinsonism Relat Disord. 20 Suppl 1:S62-7.

McDowell KA, Shin D, Roos KP and Chesselet MF (2014) *Sleep dysfunction and EEG alterations in mice overexpressing alpha-synuclein.* J Parkinsons Dis. 4(3):531-539.

Morris M, Sanchez PE, Verret L, Beagle AJ, Guo W, Dubal D, Ranasinghe KG, Koyama A, Ho K, Yu GQ, Vossel KQ, Mucke L (2015) *Network Dysfunction In α-Synuclein Transgenic Mice And Human Lewy Body Dementia.* Ann Clin Transl Neurol. 2(11):1012-28.

Narhi L, Wood SJ, Jiang Y, Wu GM, Kaufman SA, Martin F *et al.* (1999) *Both familial Parkinson's disease mutations accelerate alpha-synuclein aggregation.* 274(14), 9843-9846.

Nakata Y, Yasuda T, Fukaya M, Yamamori S, Itakura M, Nihira T *et al.* (2012) *Accumulation of α-Synuclein Triggered by Presynaptic Dysfunction.* Journal of Neuroscience, 32(48), 17186-17196.

Oda Y (1999) *Choline acetyltransferase: the structure, distribution and pathologic changes in the central nervous system.* Pathology International 49: 921-937.

Perrin RJ, Payton JE, Barnett DH, Wraight CL, Woods WS, Ye L and George JM (2003) *Epitope mapping and specificity of the anti-alpha-synuclein monoclonal antibody Syn-1 in mouse brain and cultured cell lines.* Neurosci Lett. 349(2):133-5.

Polymeropoulos MH, Lavedan C, Leroy E, Ide SE, Dehejia A, Dutra A, Pike B, Root H, Rubenstein J, Boyer R, Stenroos ES, Chandrasekharappa S, Athanassiadou A, Papapetropoulos T, Johnson WG, Lazzarini AM, Duvoisin RC, Di Iorio G, Golbe LI and Nussbaum RL (1997) *Mutation in the alpha-synuclein gene identified in families with Parkinson's disease.* Science. 276(5321):2045-2047.

Quik M and Kulak JM (2002) *Nicotine and nicotinic receptors; relevance to Parkinson's disease*. Neurotoxicology 23: 581-594.

Quik M, Bordia T, Forno L, McIntosh JM (2004) *Loss of alphaconotoxinMII- and A85380-sensitive nicotinic receptors in Parkinson's disease striatum.* J. Neurochem. 88: 668–679.

Rong H, Jin L, Wei W, Wang X and Xi Z (2015) *Alpha-synuclein is a potential biomarker in the serum and CSF of patients with intractable epilepsy.* Seizure, 27, 6-9.

Sánchez MP, García-Cabrero AM, Sánchez-Elexpuru G, Burgos Df, Serratosa JM (2018) *Tau-Induced Pathology In Epilepsy And Dementia: Notions From Patients And Animal Models.* Int J Mol Sci. 19(4).

Spillantini MG, Crowther RA, Jakes R, Hasegawa M and Goedert M (1998) *Synuclein in filamentous inclusions of Lewy bodies from Parkinson's disease and dementia with Lewy bodies.* Proceedings of the National Academy of Sciences, 95(11), 6469-6473.

Taguchi K, Watanabe Y, Tsujimura A and Tanaka M (2016) *Brain region-dependent differential expression of alpha-synuclein.* Journal of Comparative Neurology, 524(6), 1236-1258.

Taguchi K, Watanabe Y, Tsujimura A and Tanaka M (2019) *Expression of synuclein is regulated in a neuronal cell type-dependent manner.* Anatomical Science International, 94(1), 11-22.

Totterdell S, Hanger D and Meredith GE (2004) *The ultrastructural distribution of alpha-synuclein-like protein in normal mouse brain.* Brain Res. 1004(1-2):61-72.

Totterdell S and Meredith GE (2005) *Localization of alpha-synuclein to identified fibers and synapses in the normal mouse brain.* Neuroscience. 135(3):907-13.

Vivacqua G, Casini A, Vaccaro R, Fornai F, Yu S, D'Este L (2011) *Different sub-cellular localization of alpha-synuclein in the C57BL\6J mouse's central nervous system by two novel monoclonal antibodies.* J Chem Neuroanat. 2011 Mar;41(2):97-110.

Volpicelli-Daley LA, Luk KC, Patel TP, Tanik SA, Riddle DM, Stieber A, Meaney DF, Trojanowski JQ and Lee VM (2011) *Exogenous α-synuclein fibrils induce Lewy body pathology leading to synaptic dysfunction and neuron death.* Neuron. 72(1):57-71.

Yamada K and Iwatsubo T (2018) *Extracellular α-Synuclein Levels Are Regulated By Neuronal Activity.* Mol Neurodegener. 22;13(1):9.

Yang JW, Czech T, Felizardo M, Baumgartner C and Lubec G (2006) *Aberrant Expression Of Cytoskeleton Proteins In Hippocampus From Patients With Mesial Temporal Lobe Epilepsy.* Amino Acids. 30(4):477-93.

Overview, conclusions and future perspectives

Our work was focused on a murine model of Autosomal Dominant Nocturnal Frontal Lobe Epilepsy (ADNFLE) bearing the mutation V287L in the gene encoding for the β2 subunit of the neuronal nicotinic acetylcholine receptors (nAChRs). Previous studies on this conditional murine model of ADNFLE suggest that the transgene could exert its effects during synaptogenesis. Hence, we investigated the possible alterations led by the mutation primarily in adulthood. In the first study, we have analyzed the distribution of chloride cotransporters NKCC1 and KCC2 in the murine neocortex and in the thalamus, also at different developmental stages. The main finding was that mice carrying the mutant nAChR subunit β2-V287L displayed a delayed expression of KCC2 (but not NKCC1) in prefrontal cortex layer V, during the first postnatal weeks. This led to a transient decrease in the ratio between KCC2 and NKCC1, which was accompanied by a delayed "switch of the GABA". Moreover, expression of β2-V287L was also correlated to changes in KCC2 expression in adult prefrontal cortex and in reticular thalamic nucleus. The retardation of the GABAergic switch we observed in the prefrontal cortex of mice carrying β2-V287L suggests that the pathogenetic mechanism in ADNFLE comprises physiological alterations during synaptogenesis that are likely to depend on the integrity of GABAergic signaling. In the adult, complex alterations of KCC2 expression were observed in both prefrontal cortex and reticular thalamic nucleus of mice expressing the transgene. Understanding the precise functional meaning of these alterations will require deeper studies on the thalamocortical excitability of these mice. Nonetheless, the fact that no such alteration was observed in the somatosensory cortex and in other thalamic nuclei is consistent with the hypothesis that the effect of β2-V287L is specifically related to frontal hyperexcitability during sleep (**Chapter 2**).

The morphological characterization of the double-transgenic murine model, however, showed no differences between control and double-transgenic mice regarding cortical thickness and neuronal volume, and same results were found about the GABAergic system. Concerning the electrophysiological standpoint, whole-cell recordings on slices showed that while in pyramidal neurons the basal ratio of the frequencies of EPSCs and IPSCs increased in mice expressing β2-V287L, an opposite tendency was observed in fast-spiking GABAergic parvalbumin-positive (PV+)

interneurons. In regular-spiking non-pyramidal cells (somatostatin-positive, SOM+) no significant difference was observed between control and β2-V287L mice. The estimation of the number of both PV+ and SOM+ neurons and VGAT+ and VGLUT1+ (vesicular GABA and glutamate transporter, respectively) synaptic terminals contacting these neurons by immunohistochemical stainings, revealed a significant increase of VGLUT1 terminals on parvalbumin-positive cells of β2-V287L mice. Our results indicate that β2-V287L augments excitability in layer V, by modifying the synaptic efficacy in both pyramidal and fast-spiking neurons. Our data suggest an alteration of prefrontal cortex layer V microcircuits in the studied model of ADNFLE and the establishment of particular adaptation mechanisms of thalamocortical and corticocortical circuits, aimed to counteract the propagation of epileptic events. It would be useful to carry out further analyses of SOM+ and PV+ GABAergic subpopulations and their glutamatergic and GABAergic afferences in different developmental stages, when it could be present an alteration of GABAergic and glutamatergic release modulated by mutant nicotinic receptors. This study could be performed along with a thorough investigation of terminals contacting prefrontal cortex layer V pyramidal neurons and of different GABAergic subpopulations, as neurons expressing vasointestinal peptide (VIP+). Onto VIP+ neurons many cholinergic afferences are present and these cells can exert an inhibitory effect on SOM+ and PV+ neurons (**Chapter 3**).

We then pointed our attention on the cholinergic nuclei of the ascending reticular activating system (ARAS) and on the reticular thalamic nucleus. Regarding cholinergic and GABAergic markers in the thalamus, no significant differences were found between control and double-transgenic mice. The number of neurons in the cholinergic nuclei was similar in the two experimental groups. Our results thus indicate that β2-V287L mutation seems to affect only the expression of KCC2 in the reticular thalamic nucleus of adult mice. The data suggest that the reticular thalamic nucleus could play a minor role in the manifestation of nocturnal epileptic seizures in ADNFLE. Further analyses of the reticular thalamic nucleus and its glutamatergic afferents could be useful for the global picture and to clarify the possible involvement of this area in the epileptogenesis since, at the best of our knowledge, this is one of the few works focusing on the thalamus of a transgenic murine model of epilepsy. It would be

interesting to thoroughly analyze the distribution of glutamatergic and muscarinic acetylcholine receptors, in addition to different thalamic nuclei (**Chapter 4**).

In relation to another project and taking advantage of both wild-type and β2-V287L mice, we then studied α-synuclein distribution and its expression in specific synaptic terminals, since its role is not well clarified even in physiological conditions. Moreover, recent studies highlighted its relationship with nAChRs and its possible involvement in epilepsy. On these bases, the main goals of this last part of experiments were characterizing α-synuclein distribution in several brain regions of wild-type mice, subsequently analyzing the possible involvement of α-synuclein imbalance in the pathogenesis of the epileptic brain and detecting eventual α-synuclein alterations in specific synapses. α-Synuclein was mainly present at the neuropilar level and had a region-dependent distribution in the different areas. The data on the somatosensory cortex and the *corpus striatum* of β2-V287L showed a significant decrease of α-synuclein expression in the dorsolateral *corpus striatum* of the epileptic mice, and an increase of the colocalization ratio in GABAergic synapses of the dorsomedial *corpus striatum*. Thus, abnormalities of α-synuclein expression in the *corpus striatum* could lead to an alteration of the inhibitory control of the afferent projections, possibly related to the presence of epileptic seizures. Further studies focused on the effect of α-synuclein accumulation onto the GABAergic and glutamatergic synapses of the prefrontal cortex would help to clarify the mechanisms of the epileptic seizures in ADNFLE. Finally, developmental studies would be useful to understand if neuronal circuits are altered during the crucial period of synaptogenesis (**Chapter 5**).

The global interpretation of these data and the ones present in the literature suggests a non-straightforward perspective, but nuanced, multi-faceted and far from being completely understood, of mechanisms regulating microcircuits of the central nervous system, especially in pathological conditions and in relationship to GABAergic subpopulations. Further experiments will be necessary to shed light on these mechanisms and on the role of mutated nAChRs in ADNFLE pathogenesis.